

THE CONNECTIONS WITHIN:

PEDIATRIC POPULATION-BASED
NEUROIMAGING OF BRAIN DEVELOPMENT



Ryan Muetzel

ISBN: 978-94-6233-419-9

© Ryan Muetzel, 2016

For all articles published, the copyright has been transferred to the respective publisher. No part of this thesis may be reproduced, stored in a retrieval system, or transmitted in any form or by any means, without written permission from the author or, when appropriate, from the publisher.

Cover / Designs: Miranda Dood, Mirakels Ontwerp, Nijmegen, the Netherlands

Layout: Gildeprint (Nicole Nijhuis), Enschede, the Netherlands

Printing: Gildeprint, Enschede, the Netherlands

The Connections Within:

Pediatric population-based neuroimaging of brain development

De verbindingen van binnen:
pediatrische populatie-gebaseerde beeldvorming van de ontwikkeling
van het brein

Proefschrift

ter verkrijging van de graad van doctor aan de
Erasmus Universiteit Rotterdam
op gezag van de
rector magnificus

Prof.dr. H.A.P. Pols

en volgens besluit van het College voor Promoties.
De openbare verdediging zal plaatsvinden op

woensdag 9 november 2016 om 13.30 uur

door

Ryan Lee Muetzel

geboren te Marshall, Verenigde Staten van Amerika

Erasmus University Rotterdam



PROMOTIECOMMISSIE

Promotoren Prof.dr. H.W. Tiemeier
 Prof.dr. F.C. Verhulst

Overige leden Prof.dr. W.J. Niessen
 Prof.dr. E.A.M. Crone
 dr. P. Shaw

Copromotor dr. T.J.H. White

Paranimfen Laura Blanken
 Eirini Pappa

TABLE OF CONTENTS

Part I

Chapter 1	General Introduction	11
-----------	----------------------	----

Part II **Pediatric Structural Neuroimaging: Applications in typical brain development and child behavioral problems**

Chapter 2	The development of corpus callosum microstructure and associations with bimanual task performance in healthy adolescents	25
Chapter 3	White matter integrity and cognitive performance in school-age children: A population-based neuroimaging study	45
Chapter 4	White matter microstructure and autistic traits	71
Chapter 5	Childhood psychiatric symptoms and differential white matter development: A longitudinal population-based neuroimaging study	91

Part III **Intrinsic Functional Connectivity During Childhood**

Chapter 6	Resting-state networks in 6-to-10 year-old children	115
Chapter 7	From connectivity to connectopathy: a pediatric population-based resting-state study of connectivity dynamics in typical development and autistic traits	145

Part IV

Chapter 8	General Discussion	181
Chapter 9	Summary / Samenvatting	201
Appendix	Acknowledgements	211
	Author Affiliations	213
	Publications	215
	Portfolio	221
	Words of Gratitude / Dankwoord	225

MANUSCRIPTS THAT FORM THE BASIS OF THIS THESIS

Muetzel, R.L., Collins, P.F., Mueller, B.A., Schissel, A.M., Lim, K.O., Luciana, M. (2008). The development of corpus callosum microstructure and associations with bimanual task performance in healthy adolescents. *NeuroImage*, 39(4). (Chapter 2)

Muetzel, R.L., Mous, S.E., van der Ende, J., Blanken, L.M.E., van der Lugt, A., Jaddoe, V.W.V., Verhulst, F.C., Tiemeier, H., White, T. (2015). White matter integrity and cognitive performance in school-age children: A population-based neuroimaging study. *NeuroImage*, 119. (Chapter 3)

Blanken, L.M.E., **Muetzel, R.L.**, Jaddoe, V.W.V., Verhulst, F.C., van der Lugt, A., Tiemeier, H., White, T. White matter microstructure in children with autistic traits. Manuscript submitted for publication. (Chapter 4)

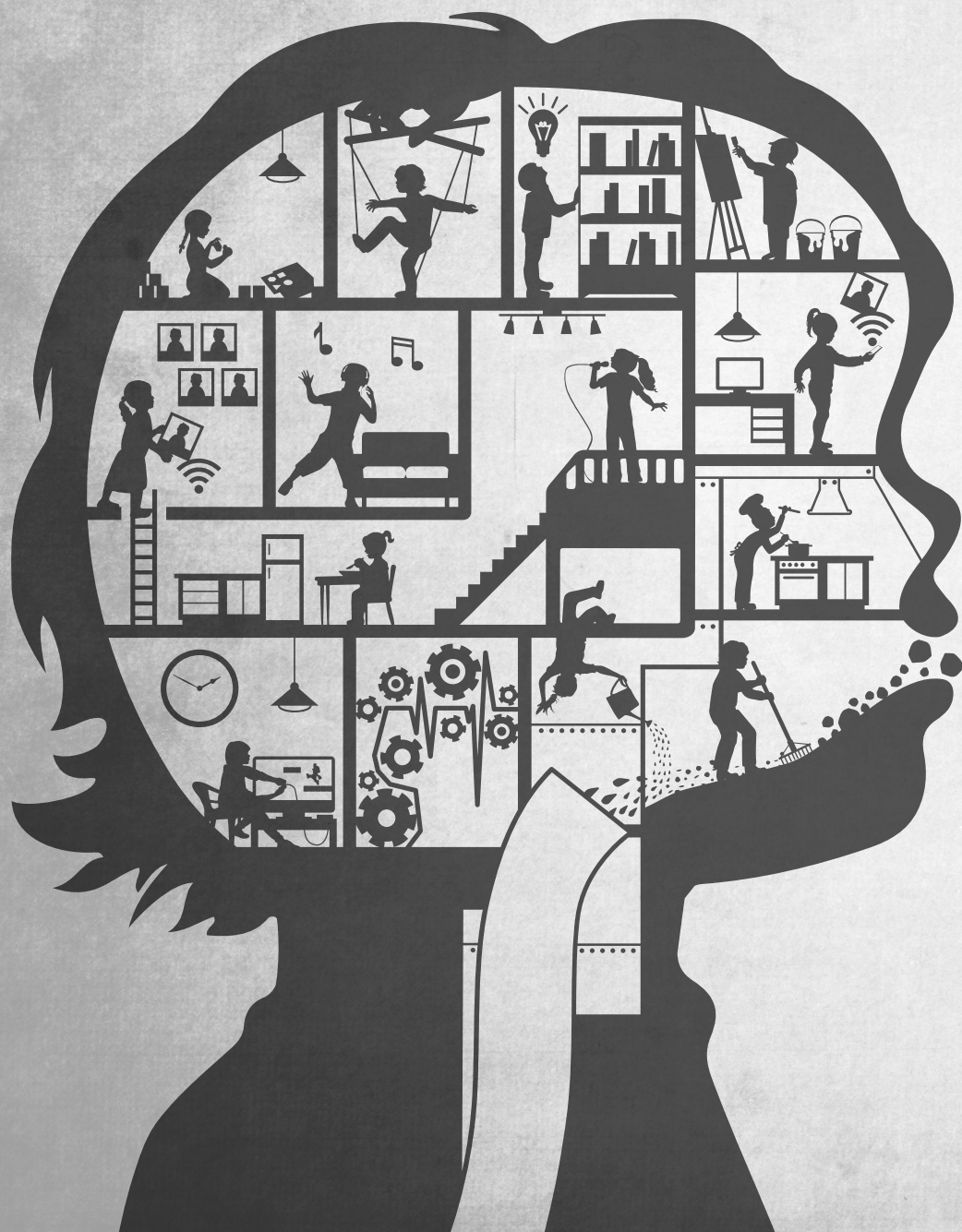
Muetzel, R.L., Blanken, L.M.E., van der Ende, J., El Marroun, H., van der Lugt, A., Jaddoe, V., Verhulst, F.C., Tiemeier, H., White, T. Childhood psychiatric symptoms and white matter development: A longitudinal population-based neuroimaging study. Manuscript in revision, American Journal of Psychiatry. (Chapter 5)

Muetzel, R.L., Blanken, L.M.E., Thijssen, S., van der Lugt, A., Jaddoe, V.W.V., Verhulst, F.C., Tiemeier, H., White, T. (2016) Resting-state networks in 6-to-10 year-old children. *Human Brain Mapping*, in press. (Chapter 6)

Muetzel, R.L.*, Blanken, L.M.E.*, Rashid, B.*, Miller, R., Damaraju, E., Arbabshirani, M.R., Erhardt, E.B., Verhulst, F.C., van der Lugt, A., Jaddoe, V.W.V., Tiemeier, H., White, T., Calhoun, V. From Chronnectivity To Chronnectopathy: Connectivity Dynamics of Typical Development And Autistic Traits. Manuscript submitted for publication. (Chapter 7)

PART





CHAPTER

1

General Introduction

INTRODUCTION

Over the past twenty years, novel *in vivo* neuroimaging techniques have led to a surge in readily available information on the living brain. In the year 2015 alone, there were nearly 13,000 brain imaging studies published; almost triple the number of reports in the year 2000. However, given the complexity and substantial financial cost of the work, a non-trivial proportion of this literature is based on relatively small, cross-sectional samples. Against this backdrop, there has been a paradigm shift towards ‘population neuroscience’; simply put, adding an epidemiological perspective to the field of neuroscience to improve our understanding of the human brain (Paus 2010, White 2015). This was recently evidenced by a number of large cohort studies collecting neuroimaging data, even in young children (White et al. 2013, Satterthwaite et al. 2014). The implications of this transition for the field of neuroscience and, in particular, child psychiatry are far reaching, granting scientists the ability to ask questions previously only discussed as limitations in the extant literature. For instance, understanding the various facets of neurodevelopment at the population level will allow for the identification of abnormal neurobiological processes in child psychopathology. Uncovering such biomarkers invigorates the possibility for improved clinical care through various means, including early identification, subtyping, and ultimately treatment response prediction.

White matter, neurodevelopment and cognition

In tandem with the introduction of safe, high-resolution neuroimaging techniques, such as magnetic resonance imaging (MRI), a number of studies began examining morphological refinements of the brain during childhood and adolescence (Lenroot and Giedd 2006). The general consensus from these *in vivo* data largely confirmed earlier postmortem work demonstrating that white matter develops throughout childhood into young adulthood (Yakovlev and Lecours 1967, Giedd et al. 1999). Shortly after these detailed ‘macrostructural’ observations were made using traditional MRI methods, a new technique called diffusion tensor imaging (DTI) was introduced to examine white matter on a ‘microstructural’ level (Schmithorst et al. 2002). DTI exploits features of Brownian motion of cellular water, specifically the idea that the diffusion profile in white matter is distinct from that in other neuronal tissues (Basser 1995). Two general factors are thought to be responsible for this unique diffusion profile in white matter: The lipid-rich, wrapped layer of myelin that encapsulates axons and gives white matter its characteristic name, and the highly organized, densely packed structure of axons in large fiber bundles (Paus 2010). Given its high lipid content, myelin is hydrophobic, thereby facilitating water diffusion parallel to the axon and preventing water from diffusing perpendicular to the axon. Further, white matter fiber bundles (or, tracts) are often densely packed collections of axons, which intuitively suggests

the diffusion profile also likely arises from trapped intra- and extracellular water that diffuses preferentially along the length of the axons. DTI expands upon traditional diffusion weighted images by measuring diffusion along at least 6 (preferably more) non-collinear directions, and reconstructing mathematical models of the water diffusion as ellipsoids (Pierpaoli et al. 1996). These mathematical models allow for the quantification of both the magnitude and direction of water diffusion. This derived information can then be used to examine features of white matter microstructure, such as fractional anisotropy (FA) and mean diffusivity (MD) (Le Bihan et al. 2001), or to reconstruct representations of white matter anatomy (i.e., tracts) using the directional information (“Tractography”, Mori and van Zijl 2002, Behrens et al. 2007).

In the context of typical brain development, a number of cross-sectional studies have shown age-related associations with DTI metrics that suggest relatively linear increases in FA through childhood into young adulthood (Schmithorst and Yuan 2010). This pattern has been substantiated with longitudinal data, though only through a limited number of studies (Giorgio et al. 2009). Tracking along with *in vivo*-measured developmental remodeling, changes in behavior and cognition are also apparent in children. For instance, improvements in decision making (Crone and van der Molen 2007), motor and visuospatial ability (Mous et al. 2016), and executive functioning (Luciana et al. 2009) have been demonstrated during childhood. Thus, one natural extension to examining the neurobiological features of white matter development is to identify so-called “structure-function” associations, where cognitive performance (measured outside of the MR-environment) is correlated with measures of white matter microstructure. Such intuitive associations, where brain structure predicts performance on neuropsychological tests, have been explored previously (Schmithorst et al. 2005, Fryer et al. 2008, Olson et al. 2009, Navas-Sanchez et al. 2014), though arguably under-represented in the literature, especially in typically developing children. Understanding the neurotypical pattern of white matter development lays the crucial foundation for which abnormal features can be observed in childhood psychopathology.

Structural connectivity and childhood psychopathology

The same measures of white matter microstructural integrity described above have also been implicated in a broader context referred to as structural connectivity; the status of neural architecture supporting fast and efficient communication between different cortical regions. Disruptions in white matter, at the macro- or microstructural level, are believed to affect connectivity between distant neuronal regions that rely on this communication bridge. For instance, in certain types of psychopathology known as internalizing disorders (e.g., depression and anxiety), it is thought that aberrant connectivity between primitive regions of the brain underlying emotion (e.g., the amygdala) and higher-level emotional regulation areas (i.e., the frontal cortex) may form the basis of some of the symptomatology

(Heller 2016). Such abnormalities in structural connectivity have already been demonstrated in clinical depression (Cullen et al. 2010). However, despite a large number of neuropsychiatric imaging studies, there are a relatively small number of replicated features of structural connectivity that have been identified in common childhood and adolescent psychiatric disorders such as autism, attention deficit/hyperactivity disorder and major depression. Interestingly, in studies examining children with autism, nearly all include results demonstrating an effect with structural connectivity in autism, though there is a relatively high level of variability in the spatial localization of these findings (Ameis and Catani 2015). In addition to considerable heterogeneity in findings across reports, a number of studies show higher-order interaction effects (e.g., group-by-age), suggesting a potential developmental aspect. This heterogeneity in findings (and potential publication bias) is likely the product of a complex array of factors, including small sample sizes, heterogeneity in the disorders, and differences in methodology. Another interesting potential source of heterogeneity is the type of psychiatric classification employed, which is most often a traditional Diagnostic and Statistical Manual (DSM) diagnosis. In contrast to this diagnostic approach, for many decades behavior and psychopathology have also been characterized dimensionally; rather than using a simple “present” or “absent” classification, the traits of interest are estimated along a continuum (Hathaway and McKinley 1943, Achenbach 1991). Support for dimensional approaches in psychopathology is growing (Garvey et al. 2016), and there is an expanding body of evidence that structural brain features vary with behavioral characteristics along a continuum (Urosevic et al. 2012, Ducharme et al. 2014, Mous et al. 2014, Blanken et al. 2015, Thijssen et al. 2015). However, literature examining psychiatric problems along a continuum in association with structural connectivity in children is limited.

Functional Connectivity, neurodevelopment and psychopathology

Distinct from structural connectivity, which focuses on the interconnecting architecture of white matter, functional connectivity examines correlation in temporal fluctuations of neuronal-related activity. While also measured with other neuroimaging techniques (e.g., EEG, MEG), functional connectivity has primarily been studied with resting-state functional MRI (RS-fMRI). This type of neuroimaging is identical to traditional functional MRI, in that it measures fluctuations in the oxygenation status of hemoglobin (BOLD), except that it is performed in the absence of a task (i.e., during ‘rest’). For a number of both practical and scientific reasons, this particular method has been widely used. For instance, the demands placed on participants are relatively low; there is no requirement they understand a task or particular instruction set, the scans are relatively short in duration, and data can even be collected independent of cognitive ‘state’ (e.g., under sedation, and varying levels of consciousness). Further, RS-fMRI measures intrinsic neuronal activity (activity that is not evoked by an external stimulus), which has been shown to account for a substantial portion

of the brain's metabolic demand (Raichle 2006). Numerous statistical methods have been developed to quantify functional connectivity, including the use of independent component analyses to separate temporally and spatially distinct signals. In general, RS-fMRI studies have shown age-related associations with functional connectivity that suggest a transition from highly diffuse to spatially distinct, focal activity with age (Fair et al. 2009). Interestingly, this general pattern resembles previous work in task-based functional MRI studies showing evoked activation becomes less diffuse with age (Durstun et al. 2006). A number of studies have also examined functional connectivity in child psychopathology (Uddin et al. 2013, Di Martino et al. 2014), though there is considerable heterogeneity in reports. For instance, in children with autism, some groups demonstrate stronger functional connectivity between certain regions while others show weaker connectivity (Uddin, Supekar et al. 2013). Further, all studies of functional connectivity in childhood psychopathology operate under the assumption that the correlation structure is stationary throughout the measurement period, which has been shown to be a potentially inaccurate and limiting assumption (Allen et al. 2014). Finally, similar to what is described above regarding structural connectivity, most functional connectivity studies in child and adolescent psychiatry conceptualize psychopathology dichotomously rather than along a continuum.

AIMS

This thesis aims to apply advanced neuroimaging techniques to the study of the developing brain. Using data from both community-based (i.e., focused recruitment from the community) and population-based (i.e., broad inclusion from a large catchment area) samples, the studies described in this thesis examine age-related neuroimaging features of white matter and functional connectivity. Expanding upon features of neurotypical brain development, both structural and functional connectivity are examined in the context of psychopathology along a continuum. Specifically, Part I of this thesis examines structural connectivity using diffusion tensor imaging, where data on structure-function associations (Chapters 2 and 3) and psychopathology (Chapters 4 and 5) are presented. Part II of this thesis applies functional connectivity to the study of brain development (Chapter 6) and autism (Chapter 7). Chapter 8 concludes this thesis with a general discussion of the research findings, methodological considerations, clinical implications, and future directions.

SETTING

The studies described in this thesis are large, community- or population-based neuroimaging samples of child brain development. Data presented in Chapter 2 are part of a large, longitudinal study of adolescent brain development housed at the University of Minnesota's Department of Psychology (Luciana et al. 2013). The remaining chapters are studies embedded in the Generation R Study, a population-based birth cohort in Rotterdam, the Netherlands (Jaddoe et al. 2012). All pregnant women in the Rotterdam area with an expected delivery date between 2002 and 2006 were invited to participate in the study. Detailed behavioral assessments were conducted when the children were 5-to-8 years of age (Tiemeier et al. 2012). In 2009, a sub-study was initiated where children were invited to undergo a comprehensive neuroimaging and neuropsychological assessment (White, El Marroun et al. 2013). This sub-study, consisting of over 1000 children 6-to-10 years of age, is the basis for the majority of the studies presented in this thesis.

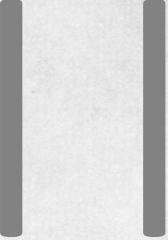
REFERENCES

- Achenbach, T. M. (1991). Manual for the revised child behavior checklist. Burlington, VT, University of Vermont Department of Psychiatry.
- Allen, E. A., E. Damaraju, S. M. Plis, E. B. Erhardt, T. Eichele and V. D. Calhoun (2014). Tracking whole-brain connectivity dynamics in the resting state. *Cereb Cortex* **24**(3): 663-676.
- Ameis, S. H. and M. Catani (2015). Altered white matter connectivity as a neural substrate for social impairment in Autism Spectrum Disorder. *Cortex* **62**: 158-181.
- Basser, P. J. (1995). Inferring microstructural features and the physiological state of tissues from diffusion-weighted images. *NMR Biomed* **8**(7-8): 333-344.
- Behrens, T. E., H. J. Berg, S. Jbabdi, M. F. Rushworth and M. W. Woolrich (2007). Probabilistic diffusion tractography with multiple fibre orientations: What can we gain? *Neuroimage* **34**(1): 144-155.
- Blanken, L. M., S. E. Mous, A. Ghassabian, R. L. Muetzel, N. K. Schoemaker, H. El Marroun, A. van der Lugt, V. W. Jaddoe, A. Hofman, F. C. Verhulst, H. Tiemeier and T. White (2015). Cortical morphology in 6- to 10-year old children with autistic traits: a population-based neuroimaging study. *Am J Psychiatry* **172**(5): 479-486.
- Crone, E. A. and M. W. van der Molen (2007). Development of decision making in school-aged children and adolescents: evidence from heart rate and skin conductance analysis. *Child Dev* **78**(4): 1288-1301.
- Cullen, K. R., B. Klimes-Dougan, R. Muetzel, B. A. Mueller, J. Camchong, A. Hour, S. Kurma and K. O. Lim (2010). Altered white matter microstructure in adolescents with major depression: a preliminary study. *J Am Acad Child Adolesc Psychiatry* **49**(2): 173-183 e171.
- Di Martino, A., D. A. Fair, C. Kelly, T. D. Satterthwaite, F. X. Castellanos, M. E. Thomason, R. C. Craddock, B. Luna, B. L. Leventhal, X. N. Zuo and M. P. Milham (2014). Unraveling the miswired connectome: a developmental perspective. *Neuron* **83**(6): 1335-1353.
- Ducharme, S., M. D. Albaugh, J. J. Hudziak, K. N. Botteron, T. V. Nguyen, C. Truong, A. C. Evans, S. Karama and G. Brain Development Cooperative (2014). Anxious/depressed symptoms are linked to right ventromedial prefrontal cortical thickness maturation in healthy children and young adults. *Cereb Cortex* **24**(11): 2941-2950.
- Durston, S., M. C. Davidson, N. Tottenham, A. Galvan, J. Spicer, J. A. Fossella and B. J. Casey (2006). A shift from diffuse to focal cortical activity with development. *Developmental Science* **9**(1): 1-8.
- Fair, D. A., A. L. Cohen, J. D. Power, N. U. Dosenbach, J. A. Church, F. M. Miezin, B. L. Schlaggar and S. E. Petersen (2009). Functional brain networks develop from a "local to distributed" organization. *PLoS computational biology* **5**(5): e1000381.
- Fryer, S. L., L. R. Frank, A. D. Spadoni, R. J. Theilmann, B. J. Nagel, A. D. Schweinsburg and S. F. Tapert (2008). Microstructural integrity of the corpus callosum linked with neuropsychological performance in adolescents. *Brain Cogn* **67**(2): 225-233.
- Garvey, M., S. Avenevoli and K. Anderson (2016). The National Institute of Mental Health Research Domain Criteria and Clinical Research in Child and Adolescent Psychiatry. *J Am Acad Child Adolesc Psychiatry* **55**(2): 93-98.
- Giedd, J. N., J. Blumenthal, N. O. Jeffries, F. X. Castellanos, H. Liu, A. Zijdenbos, T. Paus, A. C. Evans and J. L. Rapoport (1999). Brain development during childhood and adolescence: a longitudinal MRI study. *Nat Neurosci* **2**(10): 861-863.
- Giorgio, A., K. E. Watkins, M. Chadwick, S. James, L. Winmill, G. Douaud, N. De Stefano, P. M. Matthews, S. M. Smith, H. Johansen-Berg and A. C. James (2009). Longitudinal changes in grey and white matter during adolescence. *Neuroimage*.
- Hathaway, S. R. and J. C. McKinley (1943). Manual for the Minesota Multiphasic Personality Inventory. New York, Psychological Cooperation.

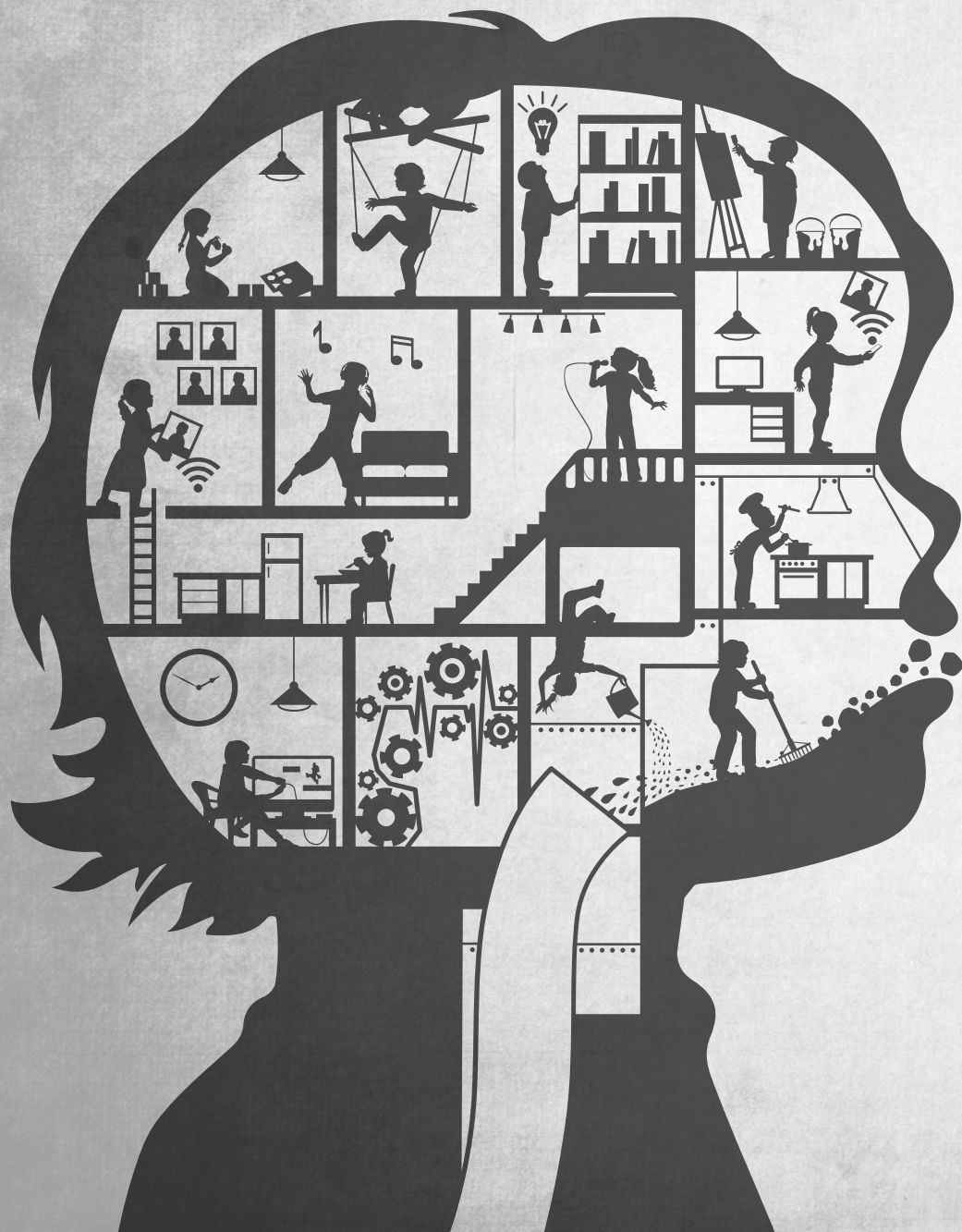
- Heller, A. S. (2016). Cortical-Subcortical Interactions in Depression: From Animal Models to Human Psychopathology. *Front Syst Neurosci* **10**: 20.
- Jaddoe, V. W., C. M. van Duijn, O. H. Franco, A. J. van der Heijden, M. H. van Iizendoorn, J. C. de Jongste, A. van der Lugt, J. P. Mackenbach, H. A. Moll, H. Raat, F. Rivadeneira, E. A. Steegers, H. Tiemeier, A. G. Uitterlinden, F. C. Verhulst and A. Hofman (2012). The Generation R Study: design and cohort update 2012. *European journal of epidemiology* **27**(9): 739-756.
- Le Bihan, D., J. F. Mangin, C. Poupon, C. A. Clark, S. Pappata, N. Molko and H. Chabriet (2001). Diffusion tensor imaging: concepts and applications. *J Magn Reson Imaging* **13**(4): 534-546.
- Lenroot, R. K. and J. N. Giedd (2006). Brain development in children and adolescents: insights from anatomical magnetic resonance imaging. *Neurosci Biobehav Rev* **30**(6): 718-729.
- Luciana, M., P. F. Collins, R. L. Muetzel and K. O. Lim (2013). Effects of alcohol use initiation on brain structure in typically developing adolescents. *Am J Drug Alcohol Abuse* **39**(6): 345-355.
- Luciana, M., P. F. Collins, E. A. Olson and A. M. Schissel (2009). Tower of London performance in healthy adolescents: the development of planning skills and associations with self-reported inattention and impulsivity. *Dev Neuropsychol* **34**(4): 461-475.
- Mori, S. and P. C. van Zijl (2002). Fiber tracking: principles and strategies - a technical review. *NMR Biomed* **15**(7-8): 468-480.
- Mous, S. E., R. L. Muetzel, H. El Marroun, T. J. C. Polderman, V. W. Jaddoe, A. Hofman, F. Verhulst, H. Tiemeier, D. Posthuma and T. White (2014). Cortical Thickness and Inattention/Hyperactivity Symptoms in Young Children: a population-based study. *Psychological Medicine* **in press**.
- Mous, S. E., N. K. Schoemaker, L. M. Blanken, S. Thijssen, J. van der Ende, T. J. Polderman, V. W. Jaddoe, A. Hofman, F. C. Verhulst, H. Tiemeier and T. White (2016). The association of gender, age, and intelligence with neuropsychological functioning in young typically developing children: The Generation R study. *Appl Neuropsychol Child*: 1-19.
- Navas-Sanchez, F. J., Y. Aleman-Gomez, J. Sanchez-Gonzalez, J. A. Guzman-De-Villoria, C. Franco, O. Robles, C. Arango and M. Desco (2014). White matter microstructure correlates of mathematical giftedness and intelligence quotient. *Hum Brain Mapp* **35**(6): 2619-2631.
- Olson, E. A., P. F. Collins, C. J. Hooper, R. Muetzel, K. O. Lim and M. Luciana (2009). White matter integrity predicts delay discounting behavior in 9- to 23-year-olds: a diffusion tensor imaging study. *J Cogn Neurosci* **21**(7): 1406-1421.
- Paus, T. (2010). Growth of white matter in the adolescent brain: myelin or axon? *Brain Cogn* **72**(1): 26-35.
- Paus, T. (2010). Population neuroscience: why and how. *Hum Brain Mapp* **31**(6): 891-903.
- Pierpaoli, C., P. Jezzard, P. J. Basser, A. Barnett and G. Di Chiro (1996). Diffusion tensor MR imaging of the human brain. *Radiology* **201**(3): 637-648.
- Raichle, M. E. (2006). Neuroscience. The brain's dark energy. *Science* **314**(5803): 1249-1250.
- Satterthwaite, T. D., M. A. Elliott, K. Ruparel, J. Loughhead, K. Prabhakaran, M. E. Calkins, R. Hopson, C. Jackson, J. Keefe, M. Riley, F. D. Mentch, P. Sleiman, R. Verma, C. Davatzikos, H. Hakonarson, R. C. Gur and R. E. Gur (2014). Neuroimaging of the Philadelphia neurodevelopmental cohort. *Neuroimage* **86**: 544-553.
- Schmithorst, V. J., M. Wilke, B. J. Dardzinski and S. K. Holland (2002). Correlation of white matter diffusivity and anisotropy with age during childhood and adolescence: a cross-sectional diffusion-tensor MR imaging study. *Radiology* **222**(1): 212-218.
- Schmithorst, V. J., M. Wilke, B. J. Dardzinski and S. K. Holland (2005). Cognitive functions correlate with white matter architecture in a normal pediatric population: a diffusion tensor MRI study. *Hum Brain Mapp* **26**(2): 139-147.
- Schmithorst, V. J. and W. Yuan (2010). White matter development during adolescence as shown by diffusion MRI. *Brain Cogn* **72**(1): 16-25.

- Thijssen, S., A. Wildeboer, R. L. Muetzel, M. J. Bakermans-Kranenburg, H. El Marroun, A. Hofman, V. W. Jaddoe, A. van der Lugt, F. C. Verhulst, H. Tiemeier, I. M. H. van and T. White (2015). Cortical thickness and prosocial behavior in school-age children: A population-based MRI study. *Soc Neurosci*: 1-12.
- Tiemeier, H., F. P. Velders, E. Szekely, S. J. Roza, G. Dieleman, V. W. Jaddoe, A. G. Uitterlinden, T. J. White, M. J. Bakermans-Kranenburg, A. Hofman, M. H. Van Ijzendoorn, J. J. Hudziak and F. C. Verhulst (2012). The Generation R Study: A review of design, findings to date, and a study of the 5-HTTLPR by environmental interaction from fetal life onward. *Journal of the American Academy of Child and Adolescent Psychiatry* **51**(11): 1119-1135 e1117.
- Uddin, L. Q., K. Supekar and V. Menon (2013). Reconceptualizing functional brain connectivity in autism from a developmental perspective. *Front Hum Neurosci* **7**: 458.
- Urošević, S., P. Collins, R. Muetzel, K. Lim and M. Luciana (2012). Longitudinal changes in behavioral approach system sensitivity and brain structures involved in reward processing during adolescence. *Dev Psychol* **48**(5): 1488-1500.
- White, T. (2015). Subclinical psychiatric symptoms and the brain: what can developmental population neuroimaging bring to the table? *J Am Acad Child Adolesc Psychiatry* **54**(10): 797-798.
- White, T., H. El Marroun, I. Nijs, M. Schmidt, A. van der Lugt, P. A. Wielopolski, V. W. Jaddoe, A. Hofman, G. P. Krestin, H. Tiemeier and F. C. Verhulst (2013). Pediatric population-based neuroimaging and the Generation R Study: the intersection of developmental neuroscience and epidemiology. *European journal of epidemiology* **28**(1): 99-111.
- Yakovlev, P. I. and A. R. Lecours, Eds. (1967). The myelogenetic cycles of regional maturation of the brain. *Regional Development of the Brain in Early Life*. Boston, Blackwell Scientific Publications.

PART



**Pediatric Structural Neuroimaging:
Applications in typical brain development
and child behavioral problems**



CHAPTER

2

The development of corpus callosum microstructure and associations with bimanual task performance in healthy adolescents

Ryan L. Muetzel, Paul F. Collins, Bryon A. Mueller, Ann M. Schissel,
Kelvin O. Lim and Monica Luciana

NeuroImage, 2008, 39(4):1918-25

ABSTRACT

Cross-sectional and longitudinal volumetric studies suggest that the corpus callosum (CC) continues to mature structurally from infancy to adulthood. Diffusion tensor imaging (DTI) provides in vivo information about the directional organization of white matter microstructure and shows potential for elucidating even more subtle brain changes during adolescent development. We used DTI to examine CC microstructure in healthy right-handed adolescents (n=92, ages 9-23 years) and correlated the imaging data with motor task performance. The primary DTI variable was fractional anisotropy (FA), which reflects the degree of white matter's directional organization. Participants completed an alternating finger tapping test to assess interhemispheric transfer and motor speed. Task performance was significantly correlated with age. Analyses of variance indicated that 9-11 year-olds generally performed worse than each of the older groups. Males outperformed females. Significant positive correlations between age and FA were observed in the splenium of the CC, which interconnects posterior cortical regions. Analyses of variance indicated that individuals older than 18 years had significantly higher FA than 9-11 year-olds. FA levels in the genu and splenium correlated significantly with task performance. Regression analyses indicated that bimanual coordination was significantly predicted by age, gender, and splenium FA. Decreases in alternating finger tapping time and increases in FA likely reflect increased myelination in the CC and more efficient neuronal signal transmission. These findings expand upon existing neuroimaging reports of CC development by showing associations between bimanual coordination and white matter microstructural organization in an adolescent sample.

INTRODUCTION

The corpus callosum (CC) is the primary connection between cerebral hemispheres, allowing for the interhemispheric integration of sensory, motor, and cognitive processes. The CC is composed of densely packed, myelinated axons and is commonly partitioned into regions based on anatomical and functional connectivity with cortical regions. It contains interhemispheric projections that terminate in cortical layer IV (Schmahmann and Pandya 2006). The structure and function of the CC has been studied extensively in callosotomy patients, through post-mortem studies, and through the use of in vivo brain imaging. Despite the vast literature regarding its structure and function, little has been reported on the development of the CC during childhood and adolescence. Although available reports are somewhat inconsistent, both cross-sectional and longitudinal studies (described below) suggest that the CC continues to mature structurally from infancy to adulthood. Whether these structural changes support behavioral changes has not been extensively studied.

Conventional magnetic resonance imaging (MRI) methods have yielded morphological information about the CC in relation to age, gender and pathology. In a large study of children ages 2-15 and adults ages 16-79 years, Allen et al. (1991) showed through midsagittal tracings of the CC that its area increased with age, reached a plateau in the group of children then decreased steadily with advancing age in the adults. The study also revealed gender differences in the morphology of the CC, with females exhibiting a bulbous shaped splenium compared to what was described as a more tubular shaped splenium in males. Pujol et al. (1993) conducted a longitudinal study of individuals 11-61 years old and found increases in CC area up to roughly the third decade of life. Males and females did not differ in total CC area, however males did show an increased rate of CC development compared to females. Regional distinctions in CC development have also been reported. In a large longitudinal study of 139 individuals ages 4-18, Giedd et al. (1999) examined CC volume and found evidence of CC development through adolescence, even after correcting for total cerebral volume. The study showed a significant age-related increase in area of the posterior portion of the CC, especially in the splenium. The authors interpreted this pattern as possibly being indicative of an anterior-to-posterior gradient in CC development, where anterior regions were presumed to have reached adult sizes earlier in development. Similarly, Thompson et al. (2000) showed sharp increases in area of the posterior portion of the CC (isthmus and splenium) with age in normally developing children and adolescents from ages 6-15 years. This group also reported that children ages 3-6 years showed marked increases in anterior CC area, which, in part, corroborates the findings and hypotheses of Giedd et al. (1999). In contrast, Paus et al. (1999) studied individuals ages 4-17 using modified segmentation output from structural MRI scans and did not report any age-related differences in CC white matter density.

Conventional imaging methods can assess developmental trends in brain tissue macrostructure during childhood and adolescence, but they cannot provide specific information about microstructure, such as axonal organization and orientation. Diffusion tensor imaging (DTI) is an in vivo approach to examining white matter microstructure that has demonstrated sensitivity to both developmental and degenerative age-related changes in tissue integrity (Barnea-Goraly et al. 2005, Sullivan and Pfefferbaum 2006, Wozniak and Lim 2006, Bonekamp et al. 2007). DTI provides information about the magnitude and direction of water diffusion within tissue (Basser and Pierpaoli 1996). Myelin, a lipid and protein rich axonal covering, restricts water diffusion in white matter. Intracellular water within myelinated axons diffuses in a more directional manner compared to diffusion in unmyelinated axons. Mean diffusivity (MD) and fractional anisotropy (FA) are two commonly derived scalar measures of DTI. MD describes the degree of diffusion in all directions, whereas FA describes the directional portion of diffusion. High MD corresponds to relatively unimpeded water diffusion and indicates regions of low tissue organization, while high FA corresponds to preferential diffusion along one direction, indicating a high level of tissue organization. Developmental studies utilizing DTI have shown age-related changes in microstructural development in the CC using both region of interest (ROI) and voxel-based analyses (Li and Noseworthy 2002, Barnea-Goraly, Menon et al. 2005, Ashtari et al. 2007, Bonekamp, Nagae et al. 2007, Snook et al. 2007). Li & Noseworthy (2002) revealed increases in FA and volume in the splenium with age in a sample of healthy 10-40 year-olds. Also, histograms that were generated suggested that development peaked at some point in the second decade of life and then declined with increasing age. In a study of forty individuals ages 5-19, Bonekamp et al. (2007) showed age-related decreases in the apparent diffusion coefficient (a measure similar to MD) of the splenium, but not the genu. Barnea-Goraly (2005) reported age-related increases in FA and white matter density in the body of the CC using voxel based analyses. More recently, Ashtari et al. (2007) studied twenty-four healthy males, ages 10-20 and found that the older males had significantly higher FA in the splenium compared to younger males.

Although the imaging methods discussed thus far reveal a great deal about the CC's structural maturation, they lack direct information about how these structural refinements relate to the behavioral changes that accompany normal development. Numerous neuropsychological methods have been developed to assess the level of function in various brain regions, including the CC. A fundamental role of the CC, interhemispheric transfer of information, can be assessed in a number of different ways, from simple finger tapping exercises to complex visual hemifield stimulation. It has been suggested that there is both a clear increase in CC utilization throughout development and also increased utilization in children only, based on these behavioral measures (Banich et al. 2000, Marion et al. 2003). It has not been customary to examine the relationship between task performance and

brain microstructure in normal development, however some studies have examined these associations in older individuals (Sullivan et al. 2001, Roebuck et al. 2002, Baird et al. 2005, Johansen-Berg et al. 2007). For example, Sullivan et al. (2001) reported correlations between FA and alternating finger tapping performance in a cross-sectional analysis of healthy adults. The group also reported regression analyses in which task performance was predicted by FA and age. In a study of ten healthy adults, Johansen-Berg et al. (2007) found relationships between bimanual coordination and FA of the CC midbody.

The current study uses DTI to investigate white matter changes with age using a cross sectional cohort of preadolescents, adolescents, and young adults. Regions of interest (ROI) were used to evaluate changes in CC white matter microstructure with age and whether these changes were associated with improved motor skills. Gender differences were examined in both task performance and DTI measures. Finally, regression analyses were performed to determine whether task performance could be predicted by age, gender and DTI values that showed age-related maturational changes. It was hypothesized that FA in multiple regions of the CC would correlate positively with age and that finger tapping performance would also improve with increased age. We also expected FA to correlate with bimanual finger tapping performance. We anticipated that MD would show similar, inverse relationships with age and task performance.

MATERIALS AND METHODS

Participants

Ninety-two right-handed adolescents and young adults (47 male and 45 female, aged 9-23 years) were recruited (see Table 1). Two methods for recruiting participants 17-years-old and under were utilized. The first method involved contacting potentially interested families through a participant database maintained by the University of Minnesota's Institute of Child Development (ICD). Participant lists from the ICD are created by sending postcards to families in the Twin Cities metro area after the birth of a child. These postcards ask families if they would be interested in having their child participate in future research studies at the University of Minnesota. Interested families return these postcards with necessary contact information. Their names and contact information are maintained in a database for use by researchers affiliated with the ICD. Our lab has recruited families to participate in previous studies of adolescent development (Hooper et al. 2004). The second method for recruiting minors involved sending postcards to University of Minnesota employees who may have had children in the desired age range. Interested families were directed to call our lab. Young adult participants, aged 18 years and above, were recruited through the use of flyers posted on the University of Minnesota campus.

Table 1. Sample Characteristics

	Age (years)				
	9-11	12-14	15-17	18-20	21-24
Total (n = 92)	18	14	20	27	13
Females (n = 45)	10	5	9	16	5
Males (n = 47)	8	9	11	11	8
Mean (SD) task and DTI values ^a					
Full scale IQ	124.06 (10.87)	110.57 (7.86)	113.30 (11.22)	115.96 (9.07)	115.15 (6.68)
AFT right-hand	5813.30 (801.06)	5180.07 (749.90)	4799.37 (782.85)	4925.09 (785.07)	4672.46 (721.81)
AFT left-hand	6666.68 (940.92)	6014.62 (1395.95)	5519.63 (864.26)	5344.91 (789.14)	4956.85 (610.82)
AFT alternating	4458.26 (1017.36)	3933.00 (763.41)	4019.83 (1199.09)	3521.07 (759.12)	3444.41 (539.70)
Laterality score	-853.39 (759.72)	-834.55 (966.89)	-720.27 (585.99)	-419.82 (386.99)	-284.39 (418.78)
Splenium FA (x 10 ⁻³)	775.73 (59.73)	793.05 (59.97)	794.30 (80.37)	841.39 (55.17)	831.94 (47.50)
Splenium MD (x 10 ⁻⁶ mm ² /s)	808.92 (93.66)	759.26 (96.22)	776.16 (128.83)	713.41 (86.14)	723.02 (82.36)

^a AFT values in milliseconds

After briefly explaining the study to potential participants, interested individuals completed a brief phone screening to ascertain eligibility. Exclusion criteria included major physical, neurological, or psychiatric illnesses, alcohol or drug abuse, head injuries resulting in loss of consciousness, mental retardation, learning disabilities, current or past use of psychoactive medications, non-native English speaking, vision and hearing that were not normal or corrected to normal, and MRI contraindications (e.g. metallic implants, severe claustrophobia, braces, etc). All procedures were approved by the University of Minnesota's Institutional Review Board.

Diagnostic Interview

After the successful completion of this phone interview, participants were invited to an in person screening session to verify information that was presented over the phone. The Kiddie Schedule for Affective Disorders and Schizophrenia Present and Lifetime Version (K-SADS-PL) was used to assess for any current or past history of DSM-IV axis I disorder (Kaufman et al. 1997). The presence or absence of DSM-IV disorders was determined later by consensus meetings among trained project staff members, including a clinical psychologist (P.F.C.). General intellectual functioning was assessed with the Wechsler Abbreviated Scale of Intelligence (Wechsler 1999). Additionally, handedness was assessed using the Edinburgh Handedness Inventory (Oldfield 1971). Participants who were strongly right-handed were selected for participation.

Behavioral testing

If participants were found eligible after the in person screening session, they were invited to complete an MRI scan and behavioral testing. Behavioral testing was conducted at the University of Minnesota's Center for Neurobehavioral Development and included an alternating finger tapping task (AFT). Other cognitive and personality measures were included in the battery but are not reported upon here.

The AFT was derived from a task previously used by other groups in studies of CC function (Pelletier et al. 1993, Sullivan, Adalsteinsson et al. 2001). In the current study, the AFT was programmed in E-Prime (Psychology Software Tools, www.psnet.com). Three conditions were administered. In the first condition, participants were presented with a screen directing them to use their right index finger to press a response key 30 times as quickly as possible. After the completion of 30 responses, the elapsed time was shown on the computer screen. The second condition was identical, except participants were instructed to press the button with their left index finger. The third condition directed participants to alternate between pressing two different buttons, one with their right index finger and the other with their left index finger. Again, when 30 taps had passed, the elapsed time was presented on the computer screen. These three conditions were presented three times in this order, for a

total of nine trials. E-Prime measured and recorded reaction times in milliseconds. Average completion times and standard deviations across the three trials in each condition were computed. A laterality index was calculated by subtracting the average elapsed time for the left hand condition from the average elapsed time for the right hand condition. Consequently, a high score would reflect a large difference in performance between the two hands, suggesting a more lateralized pattern of performance.

MRI data acquisition

Imaging data were acquired on a Siemens 3 Tesla Trio scanner (Erlangen, Germany) at the University of Minnesota's Center for Magnetic Resonance Research. DTI data were acquired axially using a dual spin echo, single shot, pulsed gradient, echo planar imaging (EPI) sequence (TR=12.5s, TE=98ms, 64 slices, voxel size=2x2x2mm, 0mm skip, FOV=256mm, 2 averages, b value=1000s/mm²). Thirteen unique volumes were collected to compute the tensor: a b=0 s/mm² image and 12 images with diffusion gradients applied in 12 non-collinear directions: (G_x,G_y,G_z) = [1.0,0.0,0.5], [0.0,0.5,1.0], [0.5,1.0,0.0], [1.0,0.5,0.0], [0.0,1.0,0.5], [0.5,0.0,1.0], [1.0, 0.0,-0.5], [0.0,-0.5, 1.0], [-0.5, 1.0, 0.0], [1.0,-0.5, 0.0], [0.0, 1.0,-0.5], [-0.5, 0.0, 1.0]. Field maps were acquired and used to correct the DTI data for geometric distortion (TR=700ms, TE=4.62ms/7.08ms, flip angle=90 degrees, voxel parameters identical to the DTI, magnitude and phase difference contrasts).

DTI data processing

The diffusion tensor was computed using the Diffusion Toolbox (FDT) from the FMRIB software library (Smith et al. 2004) (FSL, <http://www.fmrib.ox.ac.uk/>). Each diffusion weighted volume was aligned to the b=0 image using an affine transformation to correct for the distortions caused by eddy currents (Haselgrove and Moore 1996). The diffusion tensor was derived from the b=0 image and the twelve aligned, eddy current corrected diffusion weighted images. Fractional anisotropy (FA) and mean diffusivity (MD) maps were created from the eigenvalue maps. The DTI b=0 image and the MD and FA maps were corrected for the geometric distortion caused by magnetic field inhomogeneity using FUGUE (FMRIB).

Regions of Interest

The DTI b=0 image was registered to standard space (Montreal Neurological Institute-152 brain) using a 6 parameter (rigid body) fit using FLIRT with trilinear interpolation. The FA and MD maps were subsequently registered to standard space using the same transformation obtained from the previously described step. Six circular regions of interest (13-mm² area) were manually defined on the mid-sagittal slice of the aligned b=0 image; these ROIs included the genu, rostral body, anterior midbody, posterior midbody, isthmus, and splenium of the CC (Witelson 1989). Figure 1 presents a schematic of these regions. ROIs were placed in

the center of each callosal region to minimize partial volume effects. Mean FA and MD values were obtained from each ROI using a custom IDL-based program (IDL version 6.0, ITT Visual Information Solutions, Boulder, Colorado). Each ROI was defined by a single trained rater (R.L.M.). Twenty cases were defined twice, and intrarater reliability was found to be acceptable (genu, $r=0.95$; rostral body, $r=0.84$; anterior midbody, $r=0.82$; posterior midbody $r=0.67$; isthmus, $r=0.73$; splenium, $r=0.90$).

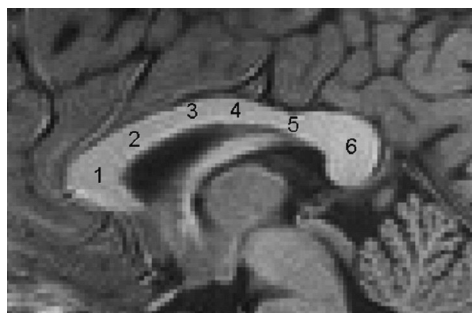


Figure 1.

The corpus callosum divided into six subregions. A T1 image is used for illustration only. Actual ROIs were defined on the $b = 0$ image. (1) genu; (2) rostral body; (3) anterior midbody; (4) posterior midbody; (5) isthmus; (6) splenium.

Statistical Approach

Data were analyzed using the Statistical Package for the Social Sciences, version 12.0 (SPSS for Windows 2003). Relationships between age, task performance, and DTI measures in each callosal ROI were examined by calculating Pearson correlations. Because the literature is inconsistent regarding the relationship between gender and CC development, correlations were computed for the entire sample, as well as for males and females separately. In addition to examining age as a continuous variable, univariate analyses of variance (ANOVA) were used to assess performance differences between discrete age and gender groups (presented in Table 1) as well as gender differences in DTI measures in each callosal ROI. ROIs showing significant correlations with age were further evaluated between the age and gender groups described above with univariate ANOVAs. Finally, hierarchical regression analyses were also conducted to assess the contributions of age, gender and FA to task performance, using variables that were significantly correlated with age. An alpha level of .05 was used for all statistical tests.

RESULTS

Sample Demographic characteristics

Table 1 presents the demographic characteristics of the sample. In addition to examining the whole sample, age groups were created that were approximately equivalent in size (ages 9-11, 12-14, 15-17, 18-20, and 21-23). These groups did not differ in gender distribution [χ^2 (4, N=92)=3.14, $p > 0.05$]. Mean full scale IQ (FSIQ) was examined between age and gender groups, revealing a main effect of age group [$F(4,82)=4.35$, $p<0.01$] but not gender [$F(1, 82)=0.21$, ns] and no interaction between age group and gender [$F(4,82)=0.92$, ns]. Least significant difference (LSD) post hoc tests indicated that 9-11 year-olds obtained higher IQ scores than every other group. There were no other IQ differences between groups.

Alternated Finger Tapping (AFT)

As shown in Table 2, average elapsed times for the alternating condition and both of the unilateral conditions correlated significantly with age, with average elapsed times decreasing with age. These age-related changes in performance were significant for both males and females. In males, the laterality score also correlated with age, demonstrating that younger males have a greater difference between their right and left-hand completion times. In females, the laterality score was unrelated to age. Table 3 presents means and standard deviations for task performance in males versus females.

Table 2. Pearson correlations between age and alternating finger tapping task performance

	Total sample (n = 92)		Males (n = 47)		Females (n = 45)	
	r	p	r	p	r	p
Right-hand	-0.423	< 0.0001	-0.433	0.002	-0.448	0.002
Left-hand	-0.523	< 0.0001	-0.597	< 0.0001	-0.496	0.001
Alternating	-0.382	0.0001	-0.441	0.002	-0.369	0.01
Laterality score ^a	0.306	0.003	0.391	0.007	0.233	0.12

^aThe laterality score is the left-hand–right-hand difference, as described in the text.

Table 3. Gender differences in AFT task performance

	Males (n = 47)		Females (n = 45)		Group effects	
	Mean (ms)	SD	Mean (ms)	SD	F(df)	p
Right-hand	4800.84	703.6	5360.6	909.1	10.881 (1,82)	0.001
Left-hand	5392.65	910.9	5997.66	1149	10.934 (1,82)	0.001
Alternating	3559.86	764.5	4183.12	1039.3	11.038 (1,82)	0.001
Laterality score	591.81	611.3	637.05	701	0.635 (1,82)	0.428

A univariate ANOVA to examine group differences in performance on the alternating condition revealed a main effect of age group [$F(4,82)=4.07$, $p<0.01$] and a main effect of gender [$F(1,82)=11.04$, $p=0.001$], but no interaction between age group and gender [$F(4,82)=0.01$, ns]. LSD post hoc analyses showed differences were between the 9-11 year-olds and the 18-20 year-olds and 21-23 year-olds, with the youngest group performing slower. Similarly, on the right-hand condition, there was a main effect of age group [$F(4,82)=5.72$, $p<0.001$], a main effect of gender [$F(1,82)=10.88$, $p=0.001$], but no interaction between age group and gender [$F(4,82)=0.11$, ns]. LSD post hoc tests indicated the 9-11 year-olds performed slower than every other group. For the left-hand condition, there was also a main effect of age group [$F(4,82)=9.04$, $p<0.001$], a main effect of gender [$F(1,82)=10.92$, $p=0.001$], but no interaction between the two [$F(4,82)=0.56$, ns]. Again, LSD post hoc tests showed the 9-11 year-olds performed slower than every other group and that the 12-14 year-olds performed slower than the 18-20 and 21-23 year-olds. Males outperformed females with significantly faster completion times in each of the three conditions. No differences were observed between males and females for the laterality score (see Table 3), however there was a main effect of age group [$F(4,82)=3.13$, $p<0.05$]. LSD post hoc analyses showed the differences were between the 9-11 year-olds and the 18-20 and 21-23 year-olds, and also between the 12-14 year-olds and the 18-20 and 21-23 year-olds. Because there were age group differences in FSIQ, these analyses were re-done entering FSIQ as a covariate. The pattern of significant findings was unchanged when covarying for FSIQ.

DTI Findings

Correlation coefficients were computed to associate age with FA in each ROI. A significant positive correlation was observed between age and FA in the splenium, suggesting an age related increase in white matter development of the splenium in young children and adolescents (see Figure 2). A similar (but negative) relationship was observed between mean MD in the splenium and age. Correlational analyses with age did not change in terms of the overall pattern of significant findings when males and females were analyzed separately. Mean FA and MD in the other regions of the CC did not correlate significantly with age (see Table 4). Because age and splenium FA and MD were found to be significantly related, group differences were further examined. Univariate tests showed a main effect of age group for FA in the splenium [$F(4,82)=3.656$, $p<0.01$]. LSD post hoc tests showed the differences were between the 9-11 year-olds and the 18-20 and 21-23 year-olds, the 12-14 year-olds and the 18-20 year-olds, and the 15-17 year-olds and the 18-20 year-olds. There was no main effect of gender or interaction between age group and gender. Similar effects were observed with MD in the splenium. Patterns of overall significance did not change with FSIQ entered as a covariate. No differences in FA or MD were found between males and females in any region of interest.

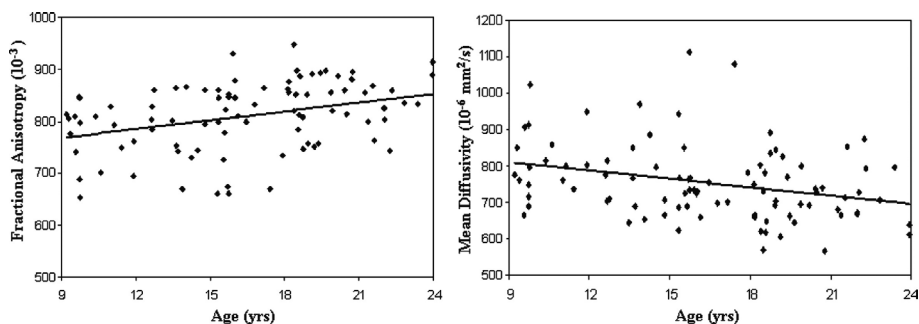


Figure 2. Scatter plots showing the relationships between age and mean FA and MD as measured in the splenium.

Table 4. Pearson correlations between age and DTI measures of corpus callosum ROIs

Region of interest	All (n = 92)		Males (n = 47)		Females (n = 45)	
	r	p	r	p	r	p
<i>Fractional anisotropy</i>						
Genu	0.097	0.36	0.005	0.97	0.207	0.17
Rostral body	0.002	0.99	-0.008	0.96	0.004	0.98
Anterior midbody	0.001	0.99	0.03	0.84	-0.043	0.78
Posterior midbody	0.05	0.64	0.019	0.9	0.084	0.58
Isthmus	-0.072	0.49	-0.109	0.47	-0.024	0.88
Splenium	0.348	0.001	0.362	0.013	0.345	0.02
<i>Mean diffusivity</i>						
Genu	-0.068	0.52	-0.004	0.98	-0.137	0.37
Rostral body	-0.049	0.64	0.035	0.82	-0.121	0.43
Anterior midbody	-0.007	0.95	0.007	0.96	-0.014	0.93
Posterior midbody	-0.015	0.89	0.012	0.93	-0.04	0.8
Isthmus	0.042	0.69	0.056	0.71	0.023	0.88
Splenium	-0.305	0.003	-0.36	0.013	-0.253	0.094

DTI & Task Performance

Next, we considered whether age-related changes in CC FA and MD were associated with AFT performance. Mean FA in the splenium showed significant negative correlations with the left-hand and alternating elapsed time conditions of the AFT task. Higher FA was associated with faster left-handed and alternating performance (see Table 5). Similar correlations were observed with MD in the splenium. Neither right-hand performance nor the laterality score correlated significantly with DTI measures in any region of the CC. No other regions of the corpus callosum showed a significant relationship between FA or

MD and performance on the AFT task, when examining both males and females together. Separate correlational analyses for males and females revealed significant relationships that were not present in the full sample. For example, correlations observed in the full sample were generally stronger in males only and were reduced or absent in females. Additionally, left-hand, right-hand, and alternating performance on the AFT correlated significantly with FA and MD in the genu of males, but showed no significant correlations in females.

Table 5. Pearson correlations between task performance and FA of corpus callosum ROIs

	Total (n = 92)		Males (n = 47)		Females (n = 45)	
	r	p	r	p	r	p
<i>Right-hand</i>						
Genu	-0.156	0.14	-0.377	0.009	0.095	0.536
Rostral body	-0.137	0.19	-0.248	0.092	0.045	0.771
A. Midbody	-0.188	0.07	-0.303	0.039	0.004	0.98
P. Midbody	-0.009	0.93	-0.044	0.767	0.068	0.658
Isthmus	0.046	0.66	0.061	0.684	-0.078	0.612
Splenium	-0.154	0.14	-0.281	0.056	-0.131	0.39
<i>Left-hand</i>						
Genu	-0.15	0.15	-0.428	0.003	0.164	0.281
Rostral body	-0.113	0.28	-0.346	0.017	0.168	0.269
A. Midbody	-0.189	0.072	-0.315	0.031	0.008	0.958
P. Midbody	-0.008	0.94	-0.085	0.57	0.105	0.491
Isthmus	0.007	0.94	0.036	0.809	-0.122	0.425
Splenium	-0.211	0.043	-0.385	0.008	-0.134	0.38
<i>Alternating</i>						
Genu	-0.231	0.027	-0.436	0.002	-0.024	0.877
Rostral body	-0.234	0.025	-0.189	0.203	-0.203	0.181
A. Midbody	-0.264	0.011	-0.295	0.044	-0.181	0.233
P. Midbody	-0.075	0.479	-0.145	0.329	0.02	0.894
Isthmus	-0.076	0.473	-0.163	0.275	-0.126	0.411
Splenium	-0.336	0.001	-0.409	0.004	-0.391	0.008

Regressions

Because of the apparent impact of gender on task performance, multiple linear regression analyses were conducted to isolate the individual contributions of age, gender and FA to task performance. Hierarchical regressions were run with AFT task variables that were strongly correlated with CC FA. The AFT conditions were entered as the dependent variables. Predictors included age entered in the first step, gender added in the second step, and FA for each CC ROI in the final step. The right hand and left hand performance variables

were not predicted by this model. However, the alternating condition of the AFT was predicted significantly by age, gender and splenium FA (see Table 6). This model accounted overall for 32% of the variance in performance.

Table 6. Summary of hierarchical regression analysis for variables predicting the alternating condition of the AFT (n = 92)

Step and variable	B	SE	β	<i>p</i>
<i>Step 1</i>				
Age	-89.32	22.79	-0.382	< 0.001
<i>Step 2</i>				
Age	-87.56	21.52	-0.374	< 0.001
Gender	606.45	175.16	0.319	< 0.001
<i>Step 3</i>				
Age	-65.17	22.109	-0.279	0.004
Gender	662.13	169.52	0.348	< 0.001
Splenium FA	-3.95	1.37	-0.273	0.005

$R^2 = 0.146$ for step 1 ($p < 0.001$); $\Delta R^2 = 0.101$ for step 2 ($p = 0.001$); and $\Delta R^2 = 0.065$ ($p = 0.005$) for step 3. The total R^2 was 0.312.

DISCUSSION

The current study examined white matter microstructural development of the corpus callosum in healthy children, adolescents and young adults using diffusion tensor imaging. Relationships between measures of white matter microstructure, age, gender and behavioral performance on a bimanual finger tapping task were investigated. These relationships were further evaluated with hierarchical regression analyses using age, gender and FA to predict bimanual task performance. Negative correlations between age and unilateral and bimanual finger tapping were observed, with younger participants performing significantly slower than older participants. Non-dominant (left-hand) performance exhibited stronger relationships with age, compared to both dominant-hand and alternating performance. The age-performance relationships found in this study have been attributed to maturation of the CC in previous behavioral studies (Marion, Kilian et al. 2003). The stronger relationship between non-dominant-hand performance and age has been previously explained by increased non-dominant hemisphere involvement in generating motor responses. It has been proposed that left-hand innervations in right-handed individuals require additional motor signaling from the left hemisphere, thereby potentially increasing the amount of interhemispheric communication between the left and right motor cortices (Marion, Kilian et al. 2003). In our dataset, these findings were also confirmed by univariate ANOVAs that indicated as asymptote in right-handed and alternating performance after age 11 but

continued development of left-handed performance until at least age 15. This continued development also impacted the laterality score, which similarly showed evidence of development until age 15.

Age was correlated with white matter microstructure, with older individuals showing increased white matter integrity in the splenium. Our between-groups comparisons suggested that white matter integrity in the splenium continues to develop until 18 years of age. Similar age-related changes in human splenium composition have been reported elsewhere, in terms of both area (Giedd, Blumenthal et al. 1999, Thompson, Giedd et al. 2000) and microstructural integrity (Li and Noseworthy 2002, Bonekamp, Nagae et al. 2007, Snook, Plewes et al. 2007). Increases in midsagittal area of the CC seems to be related more to increased myelination rather than increased axonal density (LaMantia and Rakic 1990, Aboitiz et al. 1992). Increased axonal myelin in the splenium is consistent with findings of increased splenium white matter volume in conventional MRI studies and increased splenium FA in DTI studies. Topographical studies of the CC have shown that the splenium is primarily responsible for the transmission of interhemispheric signals from the occipital lobes, and to a lesser extent the temporal and parietal lobes (Schmahmann and Pandya 2006). The developmental relationship between age and FA of the splenium, but not other CC regions, is thus somewhat surprising, given that the occipital lobes have been reported to be nearly developed early in childhood (Huttenlocher 1990, Lippe et al. 2007).

FA in the splenium in both males and females correlated significantly with alternating-hands performance, and also with left-hand performance in males only. Subsequent regression analyses indicated that when age and gender were controlled, alternating-hands performance was predicted significantly by splenium FA, indicating that individual differences in splenium white matter structure directly influenced the speed of bimanual motor coordination. The midbody of the CC has been shown to topographically interconnect cortical regions involved in motor innervation (Barnea-Goraly, Menon et al. 2005, Johansen-Berg, Della-Maggiore et al. 2007), and the present study found moderate correlations between bimanual task performance and anterior midbody white matter microstructure, in males only. Males also showed a significant correlation between genu FA and performance in all three finger tapping conditions. Although no overall gender differences were observed in FA or MD of the CC, males and females differed significantly in task performance as well as in the strength of associations between task performance and FA. It is possible these differences are driven by gender differences in pubertal timing, with females (who tend to show earlier pubertal timing as compared to males) showing earlier development of the anterior CC.

Although it is possible to view excitatory and inhibitory actions at the neural level within the CC, these actions can also be viewed at the functional level (Bloom and Hynd 2005). Increased interhemispheric signaling has been thought of as being either constructive (excitatory), when both hemispheres collaborate on specific goals or destructive (inhibitory), when hemispheric dominance is apparent. Inhibitory regulation mediated by transcallosal fibers can benefit from increased callosal size (Muller-Oehring et al. 2007) and it may also be the case that increased microstructural integrity in the CC enhances these inhibitory effects. Meaningful inhibitory controls likely require competent cortical systems to initiate the signal as well as an intact CC to propagate the signal to the contralateral hemisphere. A structurally defective or immature CC may create a bottleneck for interhemispheric information transfer, leading to dysregulated patterns of communication with the contralateral hemisphere. Callosal inhibitory control in the developing brain may be of particular interest when evaluating performance on various behavioral measures in relation to CC integrity. Although the task used in the current study was not designed to interpret inhibitory functions of the CC, our age-related findings demonstrate that care must be exercised when interpreting developmental behavioral and brain changes in the context of CC inhibitory control.

This study adds to the current literature in two distinct ways: 1) it examined a large sample with ages 9-23 all being well represented and 2) it examined relationships between task performance and white matter microstructure. With the large sample in this study, it was possible to examine age relationships in a continuous fashion with FA and MD of the CC. Previous literature has provided detailed developmental analyses of white matter microstructure and performance on fine motor tasks within separate neuroimaging and behavioral studies, whereas the current study demonstrated direct relationships between CC white matter microstructure development and fine motor skills in childhood and adolescence. To our knowledge, this is the largest DTI study in this age range that shows developmental trends in CC microstructure, and the first to show bimanual task performance correlates of CC microstructure in children and adolescents. The ability to demonstrate relationships between task performance and underlying white matter microstructure has expanded the utility of diffusion tensor imaging however this utility has been taken one step further, with the incorporation of task, DTI and fMRI all in the same session. Baird et al. (2005) used both DTI and fMRI to assess cortical connectivity in fifteen adults. Regions of interest in left and right parietal and frontal cortices were defined and the group was able to show that both a decrease in blood oxygenated level dependent (BOLD) response within the cortical ROIs and faster reaction times on a picture recognition task were associated with higher FA in the splenium of the CC. Moreover, higher BOLD response in the same ROIs and longer reaction times were associated with increased FA in the genu of the CC. These results suggest longer compute time is associated with higher activation in frontal cortices, as well

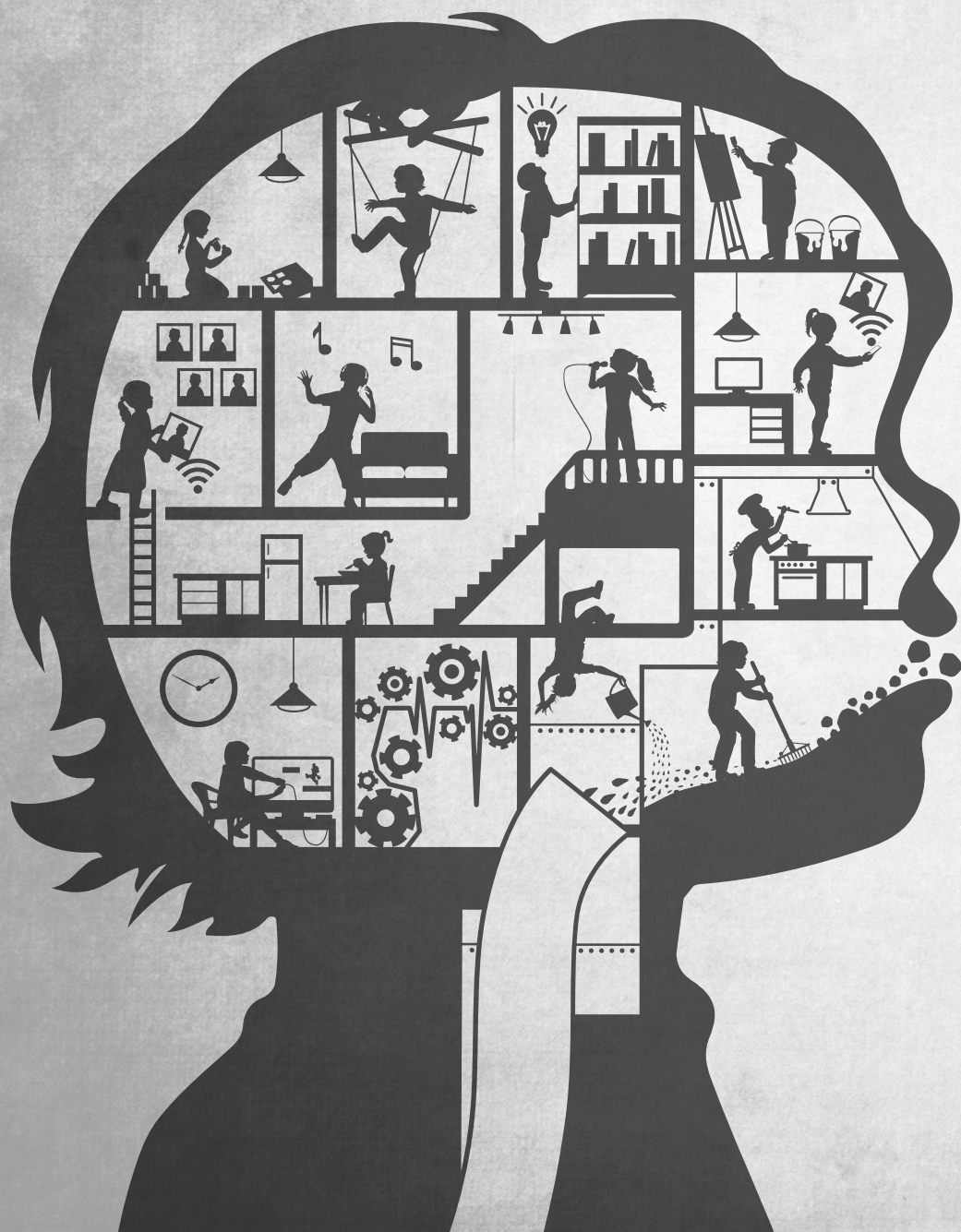
as stronger connectivity between these frontal cortices. Similarly, shorter compute time and decreased cortical activation is linked to stronger connectivity between the association areas. This concomitant use of DTI and fMRI will undoubtedly provide additional insight into the underlying changes associated with adolescent brain development.

The developmental findings reported here are limited by the use of a cross-sectional dataset for age analyses. Additionally, other reports have suggested that the CC continues to develop into the third decade of life (Pujol, Vendrell et al. 1993), indicating the need for a more comprehensive age sampling than we have accomplished to date. However, we are retesting all participants in this study two years after their initial enrollment, and by combining longitudinal and cross-sectional designs we will achieve a more comprehensive understanding of white matter development and its effects on behavior.

REFERENCES

- Aboitiz, F., A. B. Scheibel, R. S. Fisher and E. Zaidel (1992). Fiber composition of the human corpus callosum. *Brain Res* **598**(1-2): 143-153.
- Allen, L. S., M. F. Richey, Y. M. Chai and R. A. Gorski (1991). Sex differences in the corpus callosum of the living human being. *J Neurosci* **11**(4): 933-942.
- Ashtari, M., K. L. Cervellione, K. M. Hasan, J. Wu, C. McIlree, H. Kester, B. A. Ardekani, D. Roofeh, P. R. Szeszko and S. Kumra (2007). White matter development during late adolescence in healthy males: a cross-sectional diffusion tensor imaging study. *Neuroimage* **35**(2): 501-510.
- Baird, A. A., M. K. Colvin, J. D. Vanhorn, S. Inati and M. S. Gazzaniga (2005). Functional connectivity: integrating behavioral, diffusion tensor imaging, and functional magnetic resonance imaging data sets. *J Cogn Neurosci* **17**(4): 687-693.
- Banich, M. T., A. M. Passarotti and D. Janes (2000). Interhemispheric interaction during childhood: I. Neurologically intact children. *Dev Neuropsychol* **18**(1): 33-51.
- Barnea-Goraly, N., V. Menon, M. Eckert, L. Tamm, R. Bammer, A. Karchemskiy, C. C. Dant and A. L. Reiss (2005). White matter development during childhood and adolescence: a cross-sectional diffusion tensor imaging study. *Cereb Cortex* **15**(12): 1848-1854.
- Basser, P. J. and C. Pierpaoli (1996). Microstructural and physiological features of tissues elucidated by quantitative-diffusion-tensor MRI. *J Magn Reson B* **111**(3): 209-219.
- Bloom, J. S. and G. W. Hynd (2005). The role of the corpus callosum in interhemispheric transfer of information: excitation or inhibition? *Neuropsychol Rev* **15**(2): 59-71.
- Bonekamp, D., L. M. Nagae, M. Degaonkar, M. Matson, W. M. Abdalla, P. B. Barker, S. Mori and A. Horska (2007). Diffusion tensor imaging in children and adolescents: reproducibility, hemispheric, and age-related differences. *Neuroimage* **34**(2): 733-742.
- Giedd, J. N., J. Blumenthal, N. O. Jeffries, J. C. Rajapakse, A. C. Vaituzis, H. Liu, Y. C. Berry, M. Tobin, J. Nelson and F. X. Castellanos (1999). Development of the human corpus callosum during childhood and adolescence: a longitudinal MRI study. *Prog Neuropsychopharmacol Biol Psychiatry* **23**(4): 571-588.
- Haselgrove, J. C. and J. R. Moore (1996). Correction for distortion of echo-planar images used to calculate the apparent diffusion coefficient. *Magn Reson Med* **36**(6): 960-964.
- Hooper, C. J., M. Luciana, H. M. Conklin and R. S. Yarger (2004). Adolescents' performance on the Iowa Gambling Task: implications for the development of decision making and ventromedial prefrontal cortex. *Dev Psychol* **40**(6): 1148-1158.
- Huttenlocher, P. R. (1990). Morphometric study of human cerebral cortex development. *Neuropsychologia* **28**(6): 517-527.
- Johansen-Berg, H., V. Della-Maggiore, T. E. Behrens, S. M. Smith and T. Paus (2007). Integrity of white matter in the corpus callosum correlates with bimanual co-ordination skills. *Neuroimage* **36 Suppl 2**: T16-21.
- Kaufman, J., B. Birmaher, D. Brent, U. Rao, C. Flynn, P. Moreci, D. Williamson and N. Ryan (1997). Schedule for Affective Disorders and Schizophrenia for School-Age Children-Present and Lifetime Version (K-SADS-PL): initial reliability and validity data. *J Am Acad Child Adolesc Psychiatry* **36**(7): 980-988.
- LaMantia, A. S. and P. Rakic (1990). Axon overproduction and elimination in the corpus callosum of the developing rhesus monkey. *J Neurosci* **10**(7): 2156-2175.
- Li, T. and M. D. Noseworthy (2002). Mapping the Development of White Matter Tracts with Diffusion Tensor Imaging. *Developmental Science* **5**(3): 293-300.
- Lippe, S., M. S. Roy, C. Perchet and M. Lassonde (2007). Electrophysiological markers of visuocortical development. *Cereb Cortex* **17**(1): 100-107.

- Marion, S. D., S. C. Kilian, T. L. Naramor and W. S. Brown (2003). Normal development of bimanual coordination: visuomotor and interhemispheric contributions. *Dev Neuropsychol* **23**(3): 399-421.
- Muller-Oehring, E. M., T. Schulte, C. Raassi, A. Pfefferbaum and E. V. Sullivan (2007). Local-global interference is modulated by age, sex and anterior corpus callosum size. *Brain Res* **1142**: 189-205.
- Oldfield, R. C. (1971). The assessment and analysis of handedness: the Edinburgh inventory. *Neuropsychologia* **9**(1): 97-113.
- Paus, T., A. Zijdenbos, K. Worsley, D. L. Collins, J. Blumenthal, J. N. Giedd, J. L. Rapoport and A. C. Evans (1999). Structural maturation of neural pathways in children and adolescents: In vivo study. *Science* **283**(5409): 1908-1911.
- Pelletier, J., M. Habib, O. Lyon-Caen, G. Salamon, M. Poncet and R. Khalil (1993). Functional and magnetic resonance imaging correlates of callosal involvement in multiple sclerosis. *Arch Neurol* **50**(10): 1077-1082.
- Pujol, J., P. Vendrell, C. Junque, J. L. Marti-Vilalta and A. Capdevila (1993). When does human brain development end? Evidence of corpus callosum growth up to adulthood. *Ann Neurol* **34**(1): 71-75.
- Roebuck, T. M., S. N. Mattson and E. P. Riley (2002). Interhemispheric transfer in children with heavy prenatal alcohol exposure. *Alcohol Clin Exp Res* **26**(12): 1863-1871.
- Schmahmann, J. D. and D. N. Pandya (2006). *Fiber pathways of the brain*. New York, Oxford University Press, Inc.
- Smith, S. M., M. Jenkinson, M. W. Woolrich, C. F. Beckmann, T. E. Behrens, H. Johansen-Berg, P. R. Bannister, M. De Luca, I. Drobnjak, D. E. Flitney, R. K. Niazy, J. Saunders, J. Vickers, Y. Zhang, N. De Stefano, J. M. Brady and P. M. Matthews (2004). Advances in functional and structural MR image analysis and implementation as FSL. *Neuroimage* **23 Suppl 1**: S208-219.
- Snook, L., C. Plewes and C. Beaulieu (2007). Voxel based versus region of interest analysis in diffusion tensor imaging of neurodevelopment. *Neuroimage* **34**(1): 243-252.
- SPSS for Windows, R. (2003). Chicago, SPSS Inc.
- Sullivan, E. V., E. Adalsteinsson, M. Hedehus, C. Ju, M. Moseley, K. O. Lim and A. Pfefferbaum (2001). Equivalent disruption of regional white matter microstructure in ageing healthy men and women. *Neuroreport* **12**(1): 99-104.
- Sullivan, E. V. and A. Pfefferbaum (2006). Diffusion tensor imaging and aging. *Neurosci Biobehav Rev* **30**(6): 749-761.
- Thompson, P. M., J. N. Giedd, R. P. Woods, D. MacDonald, A. C. Evans and A. W. Toga (2000). Growth patterns in the developing brain detected by using continuum mechanical tensor maps. *Nature* **404**(6774): 190-193.
- Wechsler, D. (1999). *Manual for the Wechsler Abbreviated Scale of Intelligence*. San Antonio, TX, The Psychological Corporation.
- Witelson, S. F. (1989). Hand and sex differences in the isthmus and genu of the human corpus callosum. A postmortem morphological study. *Brain* **112**(Pt 3): 799-835.
- Wozniak, J. R. and K. O. Lim (2006). Advances in white matter imaging: a review of in vivo magnetic resonance methodologies and their applicability to the study of development and aging. *Neurosci Biobehav Rev* **30**(6): 762-774.



CHAPTER

3

White matter integrity and cognitive performance in school-age children: A population-based neuroimaging study

Ryan Muetzel, Sabine Mous, Jan van der Ende,
Laura Blanken, Aad van der Lugt, Vincent Jaddoe,
Frank Verhulst, Henning Tiemeier, Tonya White

NeuroImage, 2015, 119: 119-28

ABSTRACT

Child and adolescent brain development are typically accompanied by marked improvements in a wide range of cognitive abilities. However, limited information is available surrounding the role of white matter in shaping cognitive abilities in children. The current study examined associations between white matter microstructure and cognitive performance in a large sample (n=778) of 6- to 10-year-old children. Results show white matter microstructure is related to non-verbal intelligence and to visuospatial ability, independent of age. Specificity was demonstrated, as white matter associations with visuospatial ability were independent of general intellectual ability. Associations between white matter integrity and cognition were similar in boys and girls. In summary, results demonstrate white matter structure-function associations are present in children, independent of age and broader cognitive abilities. The presence of such associations in the general population is informative for studies examining child psychopathology.

INTRODUCTION

Magnetic resonance imaging (MRI) studies demonstrate significant neurodevelopmental changes throughout childhood and adolescence, into young-adulthood. These neurodevelopmental changes occur concurrently with observed improvements in a wide range of cognitive abilities. White matter development, including myelination, continues throughout childhood and adolescence and is thought to play a key role in cognitive function. As distant brain regions become more efficiently interconnected, it is expected that the ability to utilize and manipulate information also becomes more efficient. The role of white matter in shaping cognitive abilities has been previously explored, however the literature in children, especially studies with large sample sizes, remains limited. Further, while such structure-function associations seem intuitive, current *in vivo* neurobiological measures of the brain do not always demonstrate a straightforward link with neuropsychological performance, especially in the absence of severe neurological or psychiatric symptoms.

White matter maturational effects have been studied *in vivo* for over a decade using morphological information (i.e., volume, density) and, more recently, using measures of microstructural integrity (Lenroot and Giedd, 2006; Schmithorst and Yuan, 2010). Diffusion tensor imaging (DTI) is a non-invasive technique that provides such microstructural information related to white matter status (Basser et al., 1994). White matter integrity is inferred from DTI based on its ability to measure patterns of water diffusion in the brain. The water diffusion profile in white matter is distinct from that of gray matter due to the myelin sheath, axonal arrangement and packing, and axonal diameter (Beaulieu, 2002). Common parameters describing white matter integrity from DTI include fractional anisotropy (FA) and mean diffusivity (MD). Fractional anisotropy, ranging from 0-to-1, describes the degree of anisotropic diffusion, with 0 being completely isotropic (equal in all directions) and 1 being completely anisotropic (diffusion along only one axis). Mean diffusivity simply describes the average diffusion in all directions (Basser and Pierpaoli, 1996). Various cytoarchitectural features contribute to the diffusion signal by creating boundaries that impede or facilitate free water diffusion (e.g., axonal packing and myelin), and it has been shown that FA and MD (in addition to other scalar metrics) can contribute unique information (Beaulieu, 2002).

Beginning with morphological information from structural imaging, and more recently with DTI, white matter development in children and adolescents has been examined using both cross-sectional and longitudinal designs (Barnea-Goraly et al., 2005; Giedd et al., 1999; Giorgio et al., 2008; Lebel et al., 2008; Schmithorst et al., 2002; Schmithorst and Yuan, 2010). The majority of literature in children demonstrates that with age, both white matter volume and microstructural integrity increase. The precise determinant of these maturational effects has yet to be fully delineated, however the primary hypothesis suggests a combination of

increases in myelination coupled with an optimized structural organization of axons (Paus, 2010). Interestingly, studies have demonstrated differential developmental trajectories in white matter between boys and girls (Erus et al., 2014; Simmonds et al., 2014), which may underlie some of the subtle cognitive differences (Maitland et al., 2000).

While studied to a lesser extent than white matter maturation, associations between white matter and cognitive performance have also been examined in children (Erus et al., 2014; Fryer et al., 2008; Johansen-Berg et al., 2007; Muetzel et al., 2008; Navas-Sanchez et al., 2014; Schmithorst et al., 2005). In an early study of roughly 50 children, 5-to-18 years old, Schmithorst et al. (2005) found positive associations between white matter microstructure (i.e., DTI metrics) and intelligence, irrespective of age and sex. A more recent study of 36 children and adolescents 11-to-15 years of age also showed a positive association between white matter microstructure and intelligence (Navas-Sanchez et al., 2014). These studies show IQ to be linked to white matter microstructure in multiple regions, including frontal, parietal and occipital lobes, and the corpus callosum. In general, available studies of white matter microstructure and cognitive ability demonstrate brain-behavior associations that suggest white matter integrity is linked to better cognitive performance.

The current study aims to describe associations between white matter microstructure and cognition across a wide range of neuropsychological domains in a large sample of 6-to-10 year-old children. We hypothesized age-independent associations between DTI measures and cognitive performance across all domains. Based on developmental literature, fractional anisotropy and axial diffusivity are hypothesized to associate positively with cognition, whereas mean diffusivity and radial diffusivity will associate negatively. Given substantial evidence for involvement of widespread brain regions in general intellectual ability (Jung and Haier, 2007), we hypothesize global associations across multiple white matter areas. For more specific cognitive functions, we also hypothesize involvement from multiple regions, but to a lesser extent than with general intelligence. As previous work has already demonstrated distinct patterns of white matter maturation in boys and girls, we also hypothesize differential structure-function associations in boys and girls, specifically in cognitive domains where differences in ability have been demonstrated (e.g., language and spatial ability).

METHODS

Participants

The current study is embedded within the Generation R Study, which is a large, population-based cohort investigating children's health from fetal life onwards in Rotterdam, the Netherlands (Jaddoe et al., 2012). A sub-sample of 1,070 children visited the research center for neuropsychological testing and MRI scanning. Further details of the selection and recruitment of subjects, the research protocol, and overall design of this MRI sub-study are described elsewhere (White et al., 2013). Of the 1,070 children who visited the research center for an MRI, 1,033 received a DTI scan. Of the 1,033 DTI scans, 255 (25%) were excluded due to excessive motion / artifact (described below), leaving 778 datasets for analysis. The Medical Ethics Committee of the Erasmus Medical Center approved all study procedures, and parents provided written informed consent.

Cognitive and Behavioral Assessments

Intelligence Assessment

General intellectual functioning was assessed during the age-6 assessment wave using an abbreviated version of the Snijders-Oomen Niet-verbale Intelligentie Test – Revisie (SON-R 2½-7) (Tellegen et al., 2005; Tiemeier et al., 2012). The SON-R 2½-7 is a measure of non-verbal intelligence for children between 2.5 and 7 years of age and was selected in order to minimize language-dependent confounds that may be present in a large, ethnically diverse sample such as the Generation R Study. An intelligence quotient (IQ) was estimated from the two SON-R performance subtests that were administered (*Mosaics* and *Categories*), which is highly correlated with estimates resulting from the complete version (Basten et al., 2014).

Neuropsychological Assessment

Neuropsychological functioning was assessed using the NEPSY-II-NL, a Dutch translation and adaptation of the NEPSY-II (Brooks et al., 2010). Due to time constraints, a selection of tests from the NEPSY-II-NL was chosen in order to examine five areas of cognitive ability: attention and executive functioning, language, memory and learning, sensorimotor functioning, and visuospatial processing (Mous et al., In press). In order to limit the number of statistical tests performed, and because the NEPSY-II-NL does not provide domain-specific summary scores, a data reduction technique was utilized to derive empirical scores. Initially, a confirmatory factor analysis was applied to create domain scores, however model fit indices were very low, which is potentially a reflection of the abbreviated neuropsychological test battery used in the current study. Thus, an overall performance score was derived by using a principal component analysis (PCA) on all raw (i.e., non-age-normed) summary scores from the NEPSY-II-NL and selecting only the first unrotated factor score. Next, for the Attention

& Executive Function, Language, Learning and Memory, and Visuospatial domains, a similar approach was utilized. NEPSY-II-NL test items belonging to a given domain were submitted to PCA, and again only the first unrotated factor score was selected as the summary score for that cognitive domain. Given the nature of the summary scores in the Sensorimotor domain, namely that the completion time and error scores together can reflect a particular strategy (e.g., fast with many errors vs. slow with few errors) making interpretations in isolation difficult, a different approach was employed. For this domain, a simple trade-off score was generated by computing the standardized product of the completion time and errors. Of note, as the overall domain was constructed using a standard PCA, certain test domains that are overrepresented in the test battery are similarly overrepresented in the overall PCA score. However, this is not the case with the other domain scores.

Assessment of Behavioral Problems

Behavioral problems in children were assessed using the Child Behavior Checklist (CBCL/1½-5) from the age-6 assessment wave (Tiemeier et al., 2012). All children were assessed with one instrument; the preschool CBCL was selected because many children were younger than six years of age at the time of the assessment, and the other versions are inappropriate for such young children. The CBCL is a 99-item parental report inventory that utilizes a Likert response format (“Not True”, “Somewhat True”, “Very True”) for a variety of behaviors. A simple sum of all items was used to create a total behavioral problems score, which was square root transformed to approximate a normal distribution (Achenbach and Rescorla, 2000).

MRI

MR-Image Acquisition

Prior to neuroimaging, all children underwent a 30-minute mock scanning session in order to acclimate them to the MR-environment (White et al., 2013). Magnetic resonance imaging data were acquired on a 3 Tesla GE MR-750 system (General Electric, Milwaukee, WI). A short, three-plane localizer sequence was initially run and used to position all subsequent scans. Diffusion tensor imaging data were acquired using a single-shot, echo-planar imaging sequence with the following parameters: TR = 11,000 ms, TE = 83 ms, flip angle = 90, matrix = 128 x 128, FOV = 256 mm x 256 mm, slice thickness = 2 mm, number of slices = 77, acquisition time = 7 min 40 sec. In total, 35 volumes with diffusion weighting ($b = 1000 \text{ s/mm}^2$) and 3 volumes without diffusion weighting ($b = 0 \text{ s/mm}^2$) were acquired.

MR-Image Preprocessing

Data were processed using the Functional MRI of the Brain's Software Library (FMRIB, FSL, Jenkinson et al., 2012) and the Camino Diffusion MRI Toolkit (Cook et al., 2006). Image processing tools were executed in Python (version 2.7) through the Neuroimaging in Python Pipelines and Interfaces package (Nipype, version 0.92) (Gorgolewski et al., 2011). Images were first adjusted for motion and eddy-current induced artifacts (Haselgrove and Moore, 1996) using the FSL “eddy_correct” tool (Jenkinson and Smith, 2001). The resulting transformation matrices were then used to rotate the gradient direction table, in order to account for the rotations applied to the image data (Jones and Cercignani, 2010; Leemans and Jones, 2009). Non-brain tissue was removed using the FSL Brain Extraction Tool (Smith, 2002). As limitations have been cited with respect to the ordinary least squares method (Veraart et al., 2013), the diffusion tensor was fit using the RESTORE method implemented in Camino (Chang et al., 2005), and common scalar maps (i.e., FA, MD, axial diffusivity (AD), radial diffusivity (RD)) were then computed.

Probabilistic Fiber Tractography

Fully automated probabilistic fiber tractography was performed using the FSL plugin, “AutoPtx” (de Groot et al., 2015). The method generates subject-specific, probabilistic representations of multiple white matter fiber bundles using FSL tools. Briefly, the diffusion data were first processed using the Bayesian Estimation of Diffusion Parameters Obtained using Sampling Techniques (BEDPOSTx), accounting for two fiber orientations at each voxel (Behrens et al., 2007; Behrens et al., 2003). Next, for each subject, the FA map was aligned to the FMRIB-58 FA template image with the FSL nonlinear registration tool (FNIRT). The inverse of this nonlinear warp field was computed, and applied to a series of predefined seed, target, exclusion, and termination masks provided by the AutoPtx plugin (<http://fsl.fmrib.ox.ac.uk/fsl/fslwiki/AutoPtx>). Probabilistic fiber tracking was then performed with the FSL Probtrackx module using these supplied tract-specific masks (i.e., seed, target, etc.) that were warped to the native diffusion image space of each subject (Behrens et al., 2007). The resulting path distributions were normalized to a scale from 0 to 1 using the total number of successful seed-to-target attempts, and were subsequently thresholded to remove low-probability voxels likely related to noise. For each tract, the number of samples used for probabilistic tracking, and the probability thresholds applied to the resulting distributions, were selected based on previously established values (CB: 0.01, CST: 0.005, FMa: 0.005, FMi: 0.01, ILF: 0.005, SLF: 0.001, UF: 0.01; de Groot et al., 2015). After the tracts were thresholded, weighted average DTI scalar measures were computed within each tract using the normalized path distributions as the weights. The tracts used in the current analyses are presented in Table 1 and illustrated in Figure 1.

Table 1. Confirmatory factor analysis of DTI measures in white matter tracts

Tract	Hemisphere	Standardized Factor Loading			
		FA	MD	AD	RD
Cingulum Bundle	Left	0.645	0.675	0.528	0.673
	Right	0.637	0.667	0.502	0.674
Corticospinal Tract	Left	0.346	0.586	0.232	0.536
	Right	0.388	0.592	0.281	0.557
Forceps Major	-	0.595	0.348	0.271	0.424
Forceps Minor	-	0.360	0.609	0.470	0.523
Inferior Longitudinal Fasciculus	Left	0.686	0.752	0.637	0.743
	Right	0.709	0.782	0.689	0.774
Superior Longitudinal Fasciculus	Left	0.685	0.800	0.785	0.738
	Right	0.745	0.776	0.780	0.760
Uncinate Fasciculus	Left	0.547	0.723	0.553	0.675
	Right	0.591	0.758	0.571	0.732
<u>Fit Measures</u>					
CFI		0.949	0.973	0.965	0.971
TLI		0.931	0.964	0.953	0.961
RMSEA		0.079	0.061	0.060	0.063
SRMR		0.045	0.030	0.046	0.031

Note: Factor loadings are for weighted mean DTI measures in each white matter tract. CFI = Comparative Fit Index, RMSEA = Root Mean Squared Error of Approximation, SRMR = Standardized Root Mean Square Residual, TLI = Tucker Lewis Index.

Image Quality Assurance

Raw image quality was assessed with both a visual inspection and with automated software. For the visual inspection, maps of the sum of squares error (SSE) of the tensor fit were inspected for structured signal that is consistent with motion and other artifacts in the diffusion-weighted images (e.g., attenuated slices in diffusion-weighted images), and datasets determined to be of poor quality were excluded ($n=109$, ~10%). In addition to this visual inspection, slice-wise signal intensity was examined for attenuation resulting from motion, cardiac pulsation and other artifacts using the automated DTIprep quality control tool (<http://www.nitrc.org/projects/dtiprep/>, see Supplemental Material for further details). An additional 146 (14%) datasets were excluded based on the DTIprep results, leaving 778 DTI datasets for analysis.

Probabilistic tractography data were inspected visually in two ways. First, the native space FA map to FMRIB-58 FA space registration was inspected, to ensure images were all properly aligned to the template (and thus seed / target / etc. masks were properly mapped to native space). Second, all tracts were visualized to ensure accurate path reconstruction.

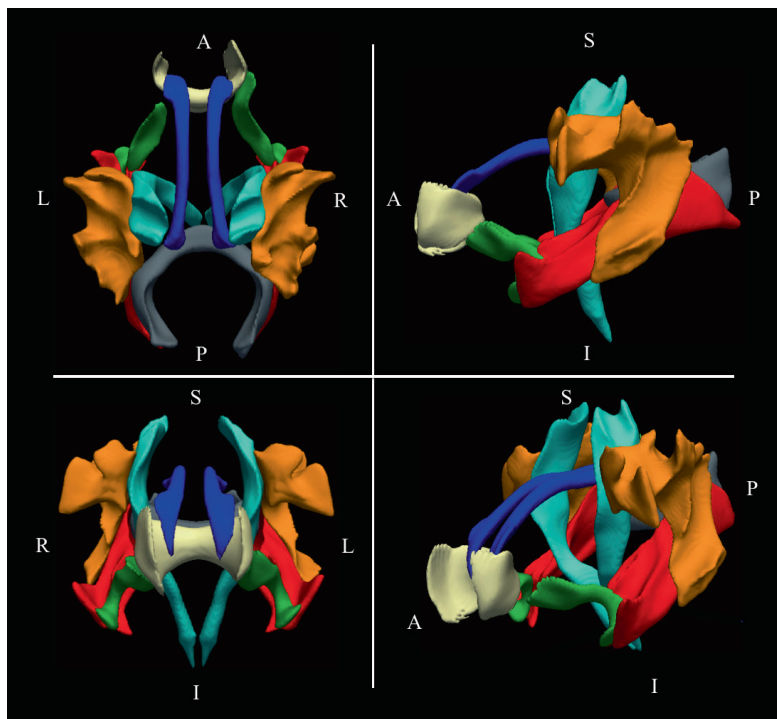


Figure 1.

The 12 tracts used in the analyses. Upper Left = Axial, Upper Right = Sagittal, Lower Left = Coronal, Lower Right = Oblique. Blue = Cingulum Bundle, Cyan = Corticospinal Tract, Green = Uncinate Fasciculus, Gray = Forceps Major, Orange = Superior Longitudinal Fasciculus, Red = Inferior Longitudinal Fasciculus, Tan = Forceps Minor.

Missing Data

Neuropsychological assessments were missing in 11 children (1.5%). Further, in some datasets, fiber tracts were not reconstructed. Specifically, data were missing in the left ($n = 31$, 4%) and the right ($n = 15$, 2%) cingulum bundle. This is likely the result of a relatively small fiber bundle coupled with the comparatively large spatial resolution of the DTI data. Lastly, from the age-6 assessment wave, data on behavioral problems were missing in 58 children (8%), and IQ was not available in 59 children (8%). A description of how missing data were handled is provided below.

Statistical Analysis

General Approach

Statistical analyses were performed using the R Statistical Software version 3.1.3 (R Core Team, 2014). Data were first inspected for normality and subsequently transformed to approximate a normal distribution when necessary (i.e., CBCL total problems score).

Structural equation modeling (SEM) was used to model associations between DTI scalar measures and cognitive domain scores (lavaan, Rosseel, 2012). Cognitive variables were entered into the model as the dependent variable and latent variables constructed from DTI measures were entered as the independent variable (described below). In order to mitigate confounding effects, models were also adjusted for covariates, namely age, sex, and the total behavioral problems score measured by the CBCL.

An illustration of the general modeling strategy is depicted in Figure 2. Models were estimated using a Maximum Likelihood (ML) procedure. Goodness of fit was judged based on the Comparative Fit Index (CFI), the Root Mean Square Error of Approximation (RMSEA), the Tucker Lewis Index, and the Standardized Root Mean Square Residual (SRMR). While it has also been shown that strict cutoff values of these fit indices are generally not recommended, a guide of a CFI > 0.95, a TLI > 0.95, an RMSEA < 0.06 and an SRMR < 0.09 indicate good model fit (Hu and Bentler, 1999). To address the issue of missing data, the full-information maximum likelihood estimator provided by the lavaan package was implemented. SEM analyses were run on FA, MD, AD and RD for each cognitive domain, and adjusted for multiple comparisons by first computing the effect number of tests ($M_{eff} = 7.43$, Galwey, 2009) and then using a Šidák correction to compute the new alpha ($\alpha = 0.0069$, Šidák, 1967)

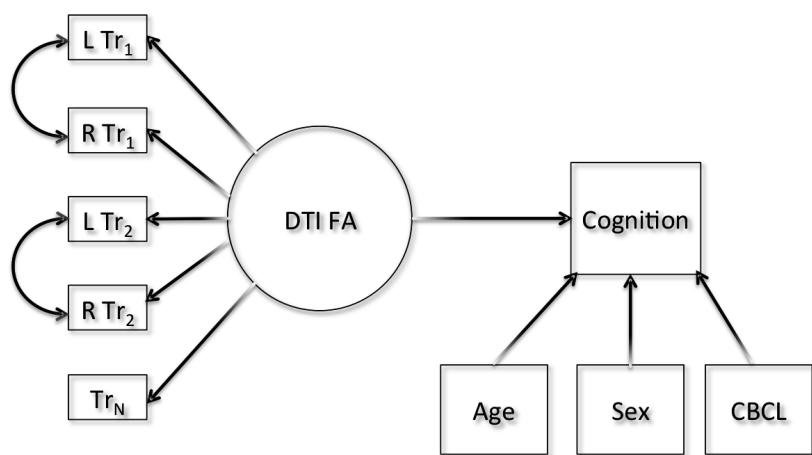


Figure 2. Outline of general structural equation modeling strategy.
 Note: Tr denotes the various tracts comprising the latent factor, and CBCL = Child Behavior Checklist total sum score.

Latent DTI Predictors and Confirmatory Factor Analyses

Within the SEM framework, latent variables were modeled from the DTI data and used in structural regression models to predict cognitive performance. While limited evidence to date suggests that associations between white matter microstructure and cognitive performance are restricted to focal brain regions or to a particular set of tracts, it is also possible that intelligence and certain aspects of cognition are global, and related to many tracts. We hypothesize such a scenario given that IQ is a general measure of cognitive ability, which likely requires orchestration of widespread brain regions. For the individual cognitive domains from the NEPSY, we hypothesize there to also be an association with global FA across multiple regions, however to a lesser extent than what will be observed with IQ given fewer regions will be involved in a given, specific cognitive domain. Within this construct, a hierarchical approach was used to examine associations between white matter microstructure and cognition. First, to assess whether global measures of white matter integrity predict cognitive performance, a number of tracts commonly reported in the literature were combined into a single latent factor (“global factor”). Large, commonly studied fiber tracts were selected for inclusion in the global factor based on previous reports (Navas-Sanchez et al., 2014; Schmithorst et al., 2005) and detailed descriptions of the anatomy and function of the tracts (Schmahmann et al., 2007) in order to encompass a broad range of cognitive abilities. Prior to SEM analyses, in order to ensure that the global DTI latent predictor was statistically valid, a confirmatory factor analysis (CFA) was run. Two separate models were tested; one where lavaan defaults were used and no constraints were placed on residual variances, and another where constraints on zero covariance between residual variances for corresponding left and right hemisphere DTI metrics were released (e.g., Left and Right Cingulum Bundle FA residual variances were allowed to covary). For the first scenario, where no constraints were placed on residual variances, model fit was relatively poor (CFI = 0.62, TLI = 0.54, RMSEA = 0.2, and SRMR = 0.1). As can be seen in Table 1, when residual variances between left and right hemisphere DTI metrics (for a given tract) were allowed to covary, model fit was within acceptable limits, suggesting the global factor can be used to model the association between white matter and cognition. The same modeling strategy for the global latent DTI factor used in the CFA analysis was then applied in all SEM analyses. For the second part of this hierarchical approach, to hone in on specificity of tracts, multiple linear regressions were run on the individual tracts when the global analysis yielded a significant association between global DTI metrics and cognitive performance. The multiple linear regressions were set up identical to the structural regressions used in SEM analyses, except individual tract metrics were used as opposed to latent DTI variables. Covariates with missing values in multiple linear regression analyses were handled using multiple imputation from the Amelia package in R (v1.7.3, Honaker et al., 2011). A total of 100 imputed data sets were utilized, and pooled estimates were extracted using the Zelig

package in R (<http://gking.harvard.edu/zelig>). Given the number of regressions run in these post-hoc tests, correction for multiple comparisons was employed by first computing the effective number of statistical tests (Galwey, 2009), and then employing a Šidák correction based on the effective number of independent tests, which yields a new alpha value required for statistical significance (Šidák, 1967).

Supporting Analyses

In order to ensure that children with behavioral problems were not responsible for driving associations, sensitivity analyses were run in a subgroup of children who scored below the clinical cutoff on all CBCL scales (Tick et al., 2007). Next, to demonstrate specificity in structure-function associations in NEPSY domain scores, non-verbal IQ was added in a separate step to the SEM model. In order to test for differential structure-function associations between boys and girls, the ‘multi group’ function in Lavaan was utilized by entering sex as the grouping factor. The model was first run allowing the FA structural regression coefficient to vary between boys and girls, and a second time where the FA structural regression coefficient was estimated for boys and girls together. The χ^2 difference between these models was computed, and the p-value for the difference was obtained from the standard χ^2 distribution. Lastly, the presence of residual age confounding was examined in two ways. First, using a strategy similar to what is outlined above for the sex-by-FA interaction effect, children were grouped into one of two age categories defined by the median age of the sample (below or above median age = 8.07 years). This median age grouping was entered into the multi-group feature of lavaan, and structure function associations in the below/above median age groups were compared using the same χ^2 difference test outlined above for sex. The second strategy to explore residual age confounding consisted of running SEM analyses in a subset of children where the range in age was restricted (between the ages of 8-and-9 years, $n = 295$), in order to minimize the impact of age on the structure-function associations.

RESULTS

Demographics

Children were on average 7.99 ± 1.02 years old, and boys ($n = 401$) and girls ($n = 377$) did not differ in age ($t(774) = 0.98$, $p=0.33$). Average non-verbal IQ in the sample was 102.5 ± 14.3 . Additional demographic and descriptive details are presented in Table 2, including information on the smaller, sensitivity analysis sample, which excludes children with behavioral problems ($n = 521$).

Table 2. Sample Descriptive Information

	Full Sample n = 778	Sensitivity Analyses n = 521
Age of MRI	7.99 ± 1.02	7.96 ± 1.02
Sex (F / M)(%)	377 (48)/ 401 (52)	255 (49) / 266 (51)
IQ	102.5 ± 14.3	103.6 ± 14.03
Ethnicity (%)		
Dutch	543 (70)	349 (76)
Western	56 (7)	37 (7)
Non-Western	179 (23)	90 (17)

Sensitivity analyses exclude subjects who score above the clinical cutoff for behavioral problems. IQ = non-verbal intelligence quotient.

IQ

Results from SEM analyses using a global DTI factors are presented in Table 3. A significant positive association was observed between IQ and FA (Standardized Estimate = 0.12, $p = 0.005$, Figure 3). Latent DTI measures of AD were also associated with IQ, however only marginally significant (standardized estimate = 0.10, $p = 0.015$), and none survived correction for multiple comparisons. In order to further determine if all or only some of the tracts contribute to these effects, a hierarchical approach using univariate regression analyses was used (Supplemental Table S1). Correction for multiple comparisons was based on 12 tracts, 4 DTI metrics and 2 cognitive domains (IQ and visuospatial ability, see below) for a total of 96 tests. Based on the correlation structure of the data, it was determined that 20.4 effective tests were run, resulting in a corrected alpha of 0.0025. After adjusting for multiple comparisons, only FA in the right UF remained significant ($\beta = 0.14$, $p = 0.0002$). However, FA in the bilateral SLF, right ILF, and right CST were marginally positively associated with IQ. AD in the bilateral UF and right CST were also marginally positively associated with IQ.

Table 3. Associations between global DTI measures and cognition

Outcome	DTI	Structural Regression Summary				Model Fit Measures			
		B	SE	95% CI	Standardized Est.	p	CFI	TLI	RMSEA
IQ	FA	0.498	0.179	0.147, 0.848	0.119	0.005	0.904	0.883	0.079
	MD	0.010	0.255	-0.489, 0.509	0.002	0.969	0.935	0.921	0.069
	AD	0.496	0.204	0.097, 0.895	0.101	0.015	0.933	0.918	0.060
Overall NEPSY	RD	-0.254	0.180	-0.607, 0.099	-0.059	0.158	0.925	0.908	0.074
	FA	0.012	0.009	-0.005, 0.029	0.047	0.175	0.911	0.891	0.078
	MD	-0.019	0.013	-0.045, 0.006	-0.051	0.132	0.938	0.924	0.069
Att. & EF	AD	-0.007	0.010	-0.026, 0.013	-0.022	0.512	0.938	0.924	0.060
	RD	-0.013	0.009	-0.031, 0.004	-0.051	0.139	0.928	0.912	0.074
	FA	0.005	0.010	-0.014, 0.023	0.019	0.612	0.908	0.887	0.078
Lang.	MD	-0.021	0.014	-0.048, 0.006	-0.057	0.132	0.937	0.923	0.069
	AD	-0.014	0.011	-0.035, 0.007	-0.049	0.193	0.937	0.924	0.059
	RD	-0.010	0.010	-0.029, 0.009	-0.039	0.315	0.926	0.910	0.074
Mem. & Learn.	FA	0.000	0.010	-0.020, 0.020	-0.001	0.972	0.909	0.889	0.078
	MD	-0.013	0.014	-0.041, 0.015	-0.033	0.355	0.937	0.923	0.069
	AD	-0.001	0.011	-0.023, 0.020	-0.004	0.904	0.937	0.923	0.060
Sensorimotor	RD	-0.011	0.010	-0.030, 0.009	-0.039	0.283	0.927	0.911	0.074
	FA	0.010	0.010	-0.009, 0.029	0.038	0.295	0.910	0.890	0.078
	MD	0.001	0.015	-0.028, 0.031	0.003	0.922	0.937	0.924	0.069
Vis. Spat	AD	-0.002	0.012	-0.025, 0.021	-0.006	0.860	0.937	0.923	0.060
	RD	0.002	0.010	-0.019, 0.022	0.006	0.872	0.927	0.912	0.074
	FA	0.009	0.009	-0.010, 0.027	0.033	0.350	0.912	0.892	0.078
Vis. Spat	MD	-0.001	0.014	-0.028, 0.026	-0.003	0.932	0.939	0.926	0.068
	AD	0.005	0.011	-0.016, 0.026	0.018	0.608	0.941	0.928	0.058
	RD	-0.005	0.010	-0.024, 0.014	-0.018	0.616	0.929	0.913	0.073
Vis. Spat	FA	0.030	0.010	0.010, 0.050	0.112	0.003	0.909	0.890	0.078
	MD	-0.013	0.015	-0.042, 0.017	-0.032	0.398	0.935	0.920	0.079
	AD	0.016	0.012	-0.007, 0.039	0.051	0.169	0.937	0.923	0.059
RD	RD	-0.021	0.010	-0.042, -0.001	-0.078	0.040	0.926	0.910	0.074

Structural regression models adjusted for age, sex and behavioral problems. Correction for multiple comparisons, corrected alpha = 0.0069. CFI = Comparative fit index, 95% CI = confidence interval of B, RMSEA = Root Mean Square Error of Approximation, Standardized Root Mean Square Residual, SE=standard error of B, Standardized Est. = Standardized regression estimate, TLI = Tucker Lewis Index. AD = Axial Diffusivity, FA = Fractional Anisotropy, MD = Mean Diffusivity, RD = Radial Diffusivity. Att. & EF = Attention & Executive Function, Mem. & Learn = Memory & Learning, Sens. = Sensory, Vis. = Visual.

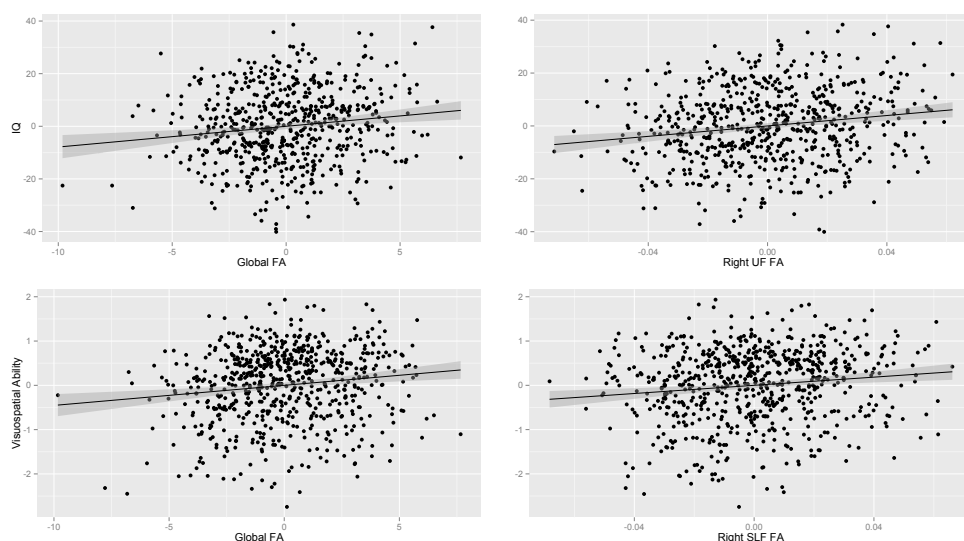


Figure 3.

Scatter plots showing the association between FA and cognitive data. The upper panel shows the association between IQ and global FA and the lower panel shows the association between visuospatial ability and global FA. Both plots are adjusted for age, sex and behavioral problems.

Neuropsychological Performance

Table 3 shows the analyses examining DTI associations with neuropsychological performance. Only the visuospatial domain was significantly associated with FA (Standardized Estimate = 0.13, $p = 0.001$, Figure 3). RD was associated with visuospatial ability (Standardized Estimate = -0.08, $p = 0.04$), however this association did not survive correction for multiple testing ($p < 0.0067$). In order to further investigate associations with visuospatial ability, tracts comprising the global DTI latent predictor were individually submitted to linear regression analysis, similar to what was done with IQ (Supplemental Table S2). After adjusting for multiple comparisons, no tracts were significantly associated with visuospatial ability. However, at a trend level, RD in the right SLF was negatively associated and FA in the left ILF was positively associated with the visuospatial domain. For informative purposes, the other NEPSY domains were also associated with the individual tract measures and are presented in Supplemental Table S3.

Sensitivity Analyses

In order to confirm that data from children with higher levels of problem behavior were not driving the observed associations in FA, SEM sensitivity analyses were run excluding these children who scored in the clinical range on any CBCL scale. Results in these 521 children remained consistent for both IQ (standardized estimate = 0.12, $p = 0.02$) and for the visuospatial domain (standardized estimate = 0.12, $p = 0.01$).

Supporting Analyses: effects of age, sex, and IQ

For illustrative purposes, the effect of age in the structure-function associations is presented in two ways. First, the association between age and the global FA latent factor is highly significant (Standardized Estimate = 0.31, $p < 1 \times 10^{-15}$). Second, to further visualize the effect of age, Supplemental Table S4 shows the structure-function associations when age is not entered in the models, and all neuropsychological domains show a significant association with FA. For all NEPSY domains, a considerable increase in standardized estimates, accompanied by a decrease in p-value, is observed, suggesting a highly confounded structure-function relationship when age is not accounted for. In addition to adjusting for age, to rule out the possibility of residual confounding of age, two additional analyses were run. First, the sample was split into two groups; younger and older children based on the median age (8.07 years). This group factor was used in SEM analyses of FA to test whether the structure-function associations were different between the younger and older groups of children, while still adjusting for age. Results yielded no significant effect for IQ ($p = 0.5$) or for visuospatial ability ($p = 0.7$), suggesting the structure-function associations are equivalent in younger and older children. The second and final test to determine whether residual confounding of age remained was to select a subset of children within a narrow age-range (8-to-9 years, $n = 295$) and re-run SEM analyses for FA in this subsample (again, still adjusting models for age). Results showed the effect estimates actually strengthened in this narrow age-range, both for IQ (standardized estimate = 0.22, $p = 0.001$) and for visuospatial ability (standardized estimate = 0.20, $p = 0.002$).

As previous research has shown differential developmental trajectories in white matter for boys and girls, it was of interest to determine whether the structure-function associations varied similarly. Results from testing for FA-by-sex interactions are presented in Table 4. For all cognitive domains the interaction effect was non-significant. Of note, even though the interaction effect was non-significant for the visuospatial domain ($p = 0.14$), the standardized structural regression coefficient for boys was more than twice as large compared to girls (0.16 and 0.06, respectively).

Table 4. Test of interaction effect of sex and FA on cognition

	χ^2	p
IQ	1.239	0.266
Overall NEPSY	1.357	0.244
Att. & EF	0.643	0.423
Lang.	1.480	0.224
Mem. & Learn.	0.031	0.859
Sensorimotor	1.241	0.265
Vis. Spatial	2.202	0.138

Note: Table shows χ^2 difference in models where multi-group SEM is used with and without constraining the regression coefficient for FA for boys and girls.

Lastly, in order to rule out that the associations with visuospatial ability were the result of general intellectual ability, child IQ was also entered into the SEM models. While the effect estimates are lower, the structure-function association remained significant (Standardized Estimate = 0.07, $p = 0.04$), suggesting some specificity in the association between white matter integrity and visuospatial ability.

DISCUSSION

The current study demonstrates the presence of associations between cognition and white matter integrity in a large sample of young children. Specifically, we observed associations between general intellectual functioning, assessed through non-verbal IQ, and white matter integrity. In addition, visuospatial ability was associated with white matter integrity independent of age, sex, and general intellectual functioning. Both IQ and visuospatial ability were positively associated with FA. In terms of general direction of association, these findings are largely consistent with previous work in developmental age-association studies examining white matter microstructure. The data show evidence for somewhat global effects across multiple white matter fiber bundles. Lastly, despite evidence of differential developmental effects for boys and girls in the literature, such effects were not observed in the present study.

Previous work in children has demonstrated associations between white matter microstructure and IQ (Navas-Sanchez et al., 2014; Schmithorst et al., 2005). Schmithorst et al. (2005) used a voxel-based approach to show positive associations between IQ and FA in multiple regions, particularly association bundles connecting frontal, parietal and occipital lobes. The same study also showed negative associations between IQ and MD, mostly in frontal white matter. Using voxel-based and region-of-interest methods, Navas-Sanchez et al. (2014) found associations between IQ and FA, primarily in the corpus callosum. In the present study, the association fibers included in these analyses, especially the SLF, overlap well with voxel-wise clusters observed in Schmithorst et al. (2005). Of importance, the models were adjusted for age (among other covariates), demonstrating the structure-function relationship is independent of the age-related developmental effects previously reported (Schmithorst and Yuan, 2010).

From the neuropsychological test battery administered in the current study, only the visuospatial domain was significantly associated with white matter integrity. Similar to what was observed for IQ, these associations were independent of age. Of importance, a considerable amount of variability in white matter microstructure is explained by age, even in this restricted age-range; thus, such a structure-function association that is independent

of age is of interest. Further, when the child's non-verbal IQ was added to the model, the association remained significant, suggesting specificity in the association between white matter microstructure and visuospatial ability. This is interesting given the measure of non-verbal IQ taps a similar construct as the visuospatial domain. Few studies have examined associations between white matter and visuospatial ability in typically developing children. Fryer et al. (2008) examined the corpus callosum in adolescents and found a relationship between white matter microstructure and visuospatial ability. Not surprisingly, a fair bit of work in this area has been conducted in children with autism (McGrath et al., 2013; Sahyoun et al., 2010). For instance, white matter microstructure in the SLF has been positively related to visuospatial ability in controls, but not in high-functioning children with autism (Sahyoun et al., 2010). In another study of young adults with autism, disruptions in the inferior fronto-occipital fasciculus were related to problems in visuospatial processing ability (McGrath et al., 2013).

While the visuospatial cognitive domain was associated with white matter, the other domains (Attention and Executive Function, Language, Learning and Memory, and Sensorimotor) were not. Previous work has shown associations between white matter integrity and these other cognitive abilities (Ge et al., 2013; Klarborg et al., 2013; Mabbott et al., 2009; Muetzel et al., 2008; Qiu et al., 2008), though considerable factors that could lead to this inconsistency are plausible. One possible explanation is that individual differences in brain development interfere with our ability to detect certain structure-function associations. As an example, consider that the heritability of white matter volume increases with age (Wallace et al., 2006), and that this is the result of a complex interplay between various genetic and environmental factors. The presence of age-related heritability may indicate some individual differences in the process of white matter maturation, even within a narrow age-range, leading to differences in timing and rate of development. Such a process can potentially explain the absence of structure-function associations in children, which then perhaps stabilize later in life. Along similar lines, other studies examining brain-behavior associations typically do so with a larger age-range, suggesting residual age-effects could be contributing to the observed structure-function associations. In the current study, all domains show significant associations with white matter when models are not adjusted for age (Supplemental Table S4).

Despite a growing literature of differential white matter effects between boys and girls, the current study was unable to statistically demonstrate such an interaction in associations between white matter integrity and cognition. Previous work has shown sex differences, both in brain development and in behavioral and cognitive associations (Hanggi et al., 2010; Schmithorst, 2009; Schmithorst et al., 2008; Simmonds et al., 2014; Wang et al., 2012).

One potential explanation for the lack of an interaction effect in the present study is that the effects are focal rather than global. In all analyses, the present study examined global domains of cognition, as well as global latent factors of white matter integrity. It is possible there are differential structure-function effects in boys and girls, however we do not observe them because the measures are too broad. A voxel-wise approach may be more sensitive in uncovering such differential sex effects. An alternative hypothesis is that such differential effects emerge at a different point in development, which our restricted age-range did not capture.

Even with the extensive application of DTI in the study of white matter status for more than a decade, limited information is available on precisely how the underlying neurobiology contributes to the MR-diffusion profile. However, some early studies do offer insight into this important question. For instance, it has been demonstrated that myelin is not a requisite of anisotropic diffusion (Beaulieu and Allen, 1994). While previous work has shown that axonal structure and packing are likely the main determinates of the diffusion profile observed by DTI, myelin does play a role in modulating diffusion anisotropy (Beaulieu, 2002; Gulani et al., 2001). Interestingly, perpendicular diffusion and trace diffusion are higher in the absence of myelin. Thus, in the context of the current study, one may postulate that associations between IQ and AD are potentially the result of axonal packing and structure, whereas the associations between visuospatial ability and RD are perhaps related to myelination. This is only one of many possibilities, given the complexities associated with disentangling the various cellular contributions to the diffusion signal.

One obvious strength of the current study is the large sample size. This allows us to adjust for multiple important variables (i.e., behavioral problems, child IQ, and maternal IQ) and to also conduct analyses in boys and girls separately, while maintaining a relatively high level of power. In addition to the large sample size, we focused our recruitment effort to children within a relatively restricted age range. This reduces potential confounding, and increases our ability to focus more on associations with cognition and less on age-related developmental effects. Further, the current study uses a probabilistic tractography approach, providing native-space information on white matter tracts, which is not sensitive to common problems associated with voxel-based analyses (e.g., misalignment). Another strength of the study is the use of SEM. In particular, one appealing feature of SEM is the ability to estimate latent variables from multiple predictors, which can then be used in standard regression models. This is an elegant approach to data reduction that should be explored further in tract-based analyses, where numerous tracts and scalar metrics are available for analysis. Not only does this limit the number of statistical tests and Type-I error, but also gives future work a guide for more focal hypotheses.

The current study is not without limitations. Importantly, the associations presented here are cross-sectional, and thus we cannot rule out reverse causality. While the Generation R Study is now conducting MRI scanning on all children during the 10-year assessment and will eventually have longitudinal data, we currently only have a single time-point. Another potential limitation is the separation in time between the assessment of non-verbal IQ and the MRI scan (on average 1.8 years apart). Even though non-verbal intelligence and white matter microstructure were assessed at separate visits nearly two years apart, a robust association between white matter and IQ was observed. Thus, the associations for IQ and white matter observed in this study are likely underestimates of the true association. Further, as the sample used in the present study is a sub-sample of the larger population-based study that oversampled children with specific behavioral problems, it is reasonable to question whether our estimates of cognition are representative of the general population. However, as can be seen in Table 2, average IQ in the present study was consistent with the normalized distribution (mean of 100, standard deviation of 15). Further, there is still potential for residual confounding in the present study. One possible source could be age-related. However, we attempted to mitigate these effects by using age as a covariate, and by demonstrating consistent results when restricting the age-range and when testing for differential effects in younger and older children. For the associations with IQ, previous work has shown relative stability of IQ estimates over time, suggesting a structure-function association between FA and IQ would not be confounded by age. Lastly, the current study utilizes an automated fiber tracking algorithm that was developed using data from adults. While this raises the potential for mis-registration of the seed and target masks, inspection of both the registration of the data to standard space and all reconstructed fiber pathways showed the algorithm works well even in children ages 6-to-10 years old. Further, to counteract any potential issues with anomalies in reconstructed tract volume related to such mis-registrations, average DTI metrics were weighted based on the probabilities from the probabilistic tractography.

CONCLUSIONS

The current study demonstrates that non-verbal intelligence and visuospatial ability are associated with white matter microstructure in children ages 6-to-10 years old. Such structure-function associations are useful in improving our understanding of brain maturation and cognitive development, and may even one day become a viable clinical utility to aid in diagnosis, prognosis and treatment of neurological and psychiatric disorders. The current study focuses on broad domains of cognitive function, and future work should explore the specific components that make up non-verbal IQ and visuospatial ability. Further, it will be

of interest to explore potential cognitive associations in resting-state functional MRI, and perhaps even multi-modal metrics utilizing both functional and structural connectivity (Sui et al., 2012).

REFERENCES

- Achenbach, T.M., Rescorla, L.A., 2000. Manual for ASEBA preschool forms & profiles. University of Vermont, Research Center for Children, Youth & Families, Burlington, VT.
- Barnea-Goraly, N., Menon, V., Eckert, M., Tamm, L., Bammmer, R., Karchemskiy, A., Dant, C.C., Reiss, A.L., 2005. White matter development during childhood and adolescence: a cross-sectional diffusion tensor imaging study. *Cereb Cortex* 15, 1848-1854.
- Basser, P.J., Mattiello, J., LeBihan, D., 1994. MR diffusion tensor spectroscopy and imaging. *Biophys J* 66, 259-267.
- Basser, P.J., Pierpaoli, C., 1996. Microstructural and physiological features of tissues elucidated by quantitative-diffusion-tensor MRI. *Journal of magnetic resonance. Series B* 111, 209-219.
- Basten, M., van der Ende, J., Tiemeier, H., Althoff, R.R., Rijlaarsdam, J., Jaddoe, V.W., Hofman, A., Hudziak, J.J., Verhulst, F.C., White, T., 2014. Nonverbal intelligence in young children with dysregulation: the Generation R Study. *European child & adolescent psychiatry* 23, 1061-1070.
- Beaulieu, C., 2002. The basis of anisotropic water diffusion in the nervous system - a technical review. *NMR Biomed* 15, 435-455.
- Beaulieu, C., Allen, P.S., 1994. Determinants of anisotropic water diffusion in nerves. *Magn Reson Med* 31, 394-400.
- Behrens, T.E., Berg, H.J., Jbabdi, S., Rushworth, M.F., Woolrich, M.W., 2007. Probabilistic diffusion tractography with multiple fibre orientations: What can we gain? *Neuroimage* 34, 144-155.
- Behrens, T.E., Woolrich, M.W., Jenkinson, M., Johansen-Berg, H., Nunes, R.G., Clare, S., Matthews, P.M., Brady, J.M., Smith, S.M., 2003. Characterization and propagation of uncertainty in diffusion-weighted MR imaging. *Magn Reson Med* 50, 1077-1088.
- Brooks, B.L., Sherman, E.M., Iverson, G.L., 2010. Healthy children get low scores too: prevalence of low scores on the NEPSY-II in preschoolers, children, and adolescents. *Arch Clin Neuropsychol* 25, 182-190.
- Chang, L.C., Jones, D.K., Pierpaoli, C., 2005. RESTORE: robust estimation of tensors by outlier rejection. *Magn Reson Med* 53, 1088-1095.
- Cook, P.A., Bai, Y., Nedjati-Gilani, S., Seunarine, K.K., Hall, M.G., Parker, G.J., Alexander, D.C., 2006. Camino: Open-Source Diffusion-MRI Reconstruction and Processing. 14th Scientific Meeting of the International Society for Magnetic Resonance in Medicine, Seattle, WA, USA, p. 2759.
- de Groot, M., Ikram, M.A., Akoudad, S., Krestin, G.P., Hofman, A., van der Lugt, A., Niessen, W.J., Vernooij, M.W., 2015. Tract-specific white matter degeneration in aging: The Rotterdam Study. *Alzheimers Dement* 11, 321-330.
- Erus, G., Battapady, H., Satterthwaite, T.D., Hakonarson, H., Gur, R.E., Davatzikos, C., Gur, R.C., 2014. Imaging Patterns of Brain Development and their Relationship to Cognition. *Cereb Cortex*.
- Fryer, S.L., Frank, L.R., Spadoni, A.D., Theilmann, R.J., Nagel, B.J., Schweinsburg, A.D., Tapert, S.F., 2008. Microstructural integrity of the corpus callosum linked with neuropsychological performance in adolescents. *Brain Cogn* 67, 225-233.
- Galwey, N.W., 2009. A new measure of the effective number of tests, a practical tool for comparing families of non-independent significance tests. *Genetic epidemiology* 33, 559-568.
- Ge, H., Yin, X., Xu, J., Tang, Y., Han, Y., Xu, W., Pang, Z., Meng, H., Liu, S., 2013. Fiber pathways of attention subnetworks revealed with tract-based spatial statistics (TBSS) and probabilistic tractography. *PLoS one* 8, e78831.
- Giedd, J.N., Blumenthal, J., Jeffries, N.O., Castellanos, F.X., Liu, H., Zijdenbos, A., Paus, T., Evans, A.C., Rapoport, J.L., 1999. Brain development during childhood and adolescence: a longitudinal MRI study. *Nature neuroscience* 2, 861-863.

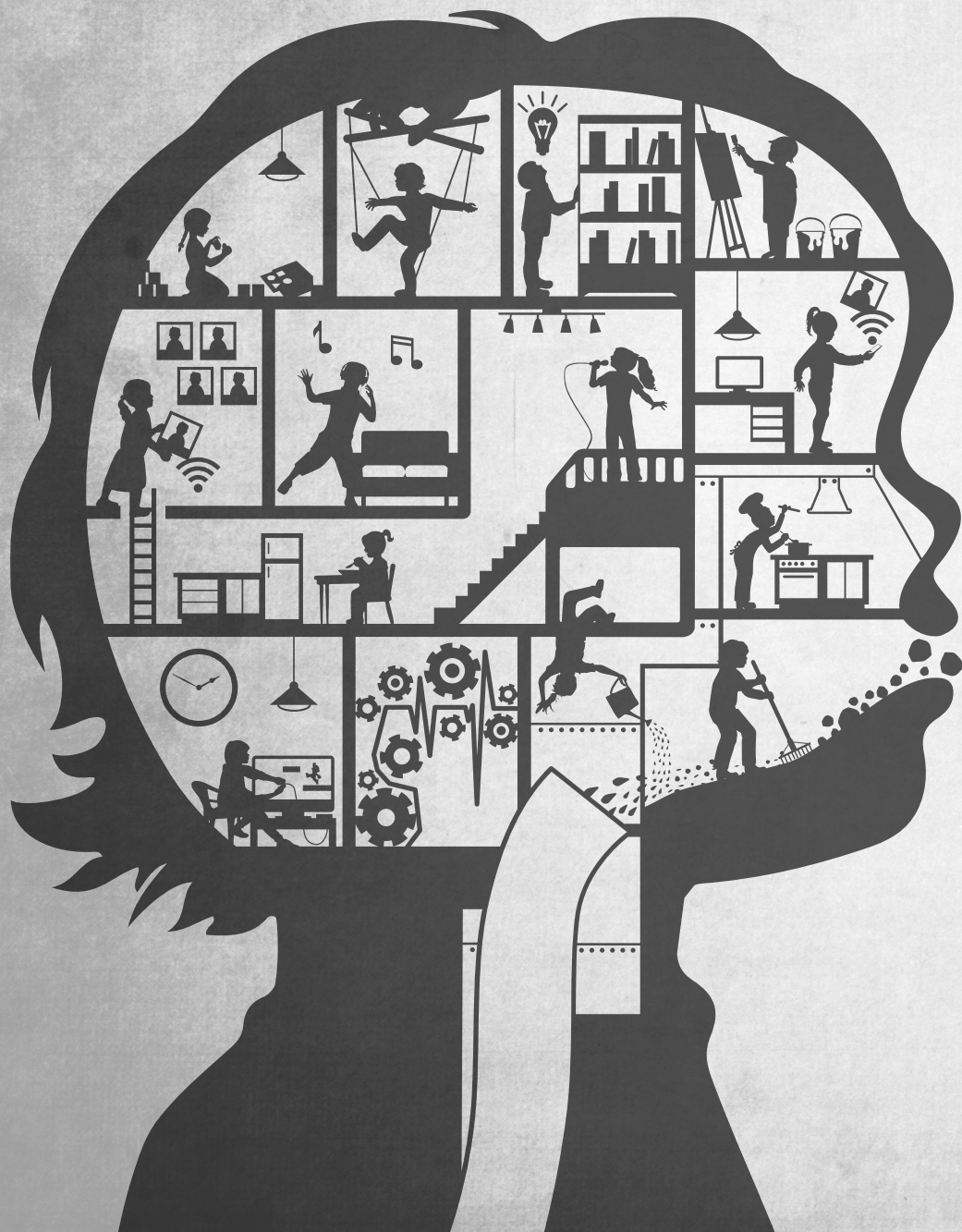
- Giorgio, A., Watkins, K.E., Douaud, G., James, A.C., James, S., De Stefano, N., Matthews, P.M., Smith, S.M., Johansen-Berg, H., 2008. Changes in white matter microstructure during adolescence. *Neuroimage* 39, 52-61.
- Gorgolewski, K., Burns, C.D., Madison, C., Clark, D., Halchenko, Y.O., Waskom, M.L., Ghosh, S.S., 2011. Nipype: a flexible, lightweight and extensible neuroimaging data processing framework in python. *Frontiers in neuroinformatics* 5, 13.
- Gulani, V., Webb, A.G., Duncan, I.D., Lauterbur, P.C., 2001. Apparent diffusion tensor measurements in myelin-deficient rat spinal cords. *Magn Reson Med* 45, 191-195.
- Hanggi, J., Buchmann, A., Mondadori, C.R., Henke, K., Jancke, L., Hock, C., 2010. Sexual dimorphism in the parietal substrate associated with visuospatial cognition independent of general intelligence. *J Cogn Neurosci* 22, 139-155.
- Haselgrove, J.C., Moore, J.R., 1996. Correction for distortion of echo-planar images used to calculate the apparent diffusion coefficient. *Magn Reson Med* 36, 960-964.
- Honaker, J., King, G., Blackwell, M., 2011. Amelia II: A program for missing data. *Journal of Statistical Software* 45, 1-47.
- Hu, L.T., Bentler, P.M., 1999. Cutoff Criteria for Fit Indexes in Covariance Structure Analysis: Conventional Criteria Versus New Alternatives. *Structural Equation Modeling-a Multidisciplinary Journal* 6, 1-55.
- Jaddoe, V.W., van Duijn, C.M., Franco, O.H., van der Heijden, A.J., van Iizendoorn, M.H., de Jongste, J.C., van der Lugt, A., Mackenbach, J.P., Moll, H.A., Raat, H., Rivadeneira, F., Steegers, E.A., Tiemeier, H., Uitterlinden, A.G., Verhulst, F.C., Hofman, A., 2012. The Generation R Study: design and cohort update 2012. *European journal of epidemiology* 27, 739-756.
- Jenkinson, M., Beckmann, C.F., Behrens, T.E., Woolrich, M.W., Smith, S.M., 2012. Fsl. *Neuroimage* 62, 782-790.
- Jenkinson, M., Smith, S., 2001. A global optimisation method for robust affine registration of brain images. *Med Image Anal* 5, 143-156.
- Johansen-Berg, H., Della-Maggiore, V., Behrens, T.E., Smith, S.M., Paus, T., 2007. Integrity of white matter in the corpus callosum correlates with bimanual co-ordination skills. *Neuroimage* 36 Suppl 2, T16-21.
- Jones, D.K., Cercignani, M., 2010. Twenty-five pitfalls in the analysis of diffusion MRI data. *NMR Biomed* 23, 803-820.
- Jung, R.E., Haier, R.J., 2007. The Parieto-Frontal Integration Theory (P-FIT) of intelligence: Converging neuroimaging evidence. *Behavioral and Brain Sciences* 30, 135-+.
- Klarborg, B., Skak Madsen, K., Vestergaard, M., Skimminge, A., Jernigan, T.L., Baare, W.F., 2013. Sustained attention is associated with right superior longitudinal fasciculus and superior parietal white matter microstructure in children. *Hum Brain Mapp* 34, 3216-3232.
- Lebel, C., Walker, L., Leemans, A., Phillips, L., Beaulieu, C., 2008. Microstructural maturation of the human brain from childhood to adulthood. *Neuroimage* 40, 1044-1055.
- Leemans, A., Jones, D.K., 2009. The B-matrix must be rotated when correcting for subject motion in DTI data. *Magn Reson Med* 61, 1336-1349.
- Lenroot, R.K., Giedd, J.N., 2006. Brain development in children and adolescents: insights from anatomical magnetic resonance imaging. *Neurosci Biobehav Rev* 30, 718-729.
- Mabbott, D.J., Rovet, J., Noseworthy, M.D., Smith, M.L., Rockel, C., 2009. The relations between white matter and declarative memory in older children and adolescents. *Brain Res* 1294, 80-90.
- Maitland, S.B., Intrieri, R.C., Schaie, W.K., Willis, S.L., 2000. Gender Differences and Changes in Cognitive Abilities Across the Adult Life Span. *Aging, Neuropsychology, and Cognition* 7, 32-53.
- McGrath, J., Johnson, K., O'Hanlon, E., Garavan, H., Gallagher, L., Leemans, A., 2013. White matter and visuospatial processing in autism: a constrained spherical deconvolution tractography study. *Autism Res* 6, 307-319.

- Mous, S.E., Schoemaker, N.K., Blanken, L.M.E., Thijssen, S., van der Ende, J., Polderman, T.J.C., Jaddoe, V., Hofman, A., Verhulst, F., Tiemeier, H., White, T., In press. The association of gender, age and intelligence with neuropsychological functioning in young typically developing children - The Generation R Study. *Applied neuropsychology: child*.
- Muetzel, R.L., Collins, P.F., Mueller, B.A., A, M.S., Lim, K.O., Luciana, M., 2008. The development of corpus callosum microstructure and associations with bimanual task performance in healthy adolescents. *Neuroimage* 39, 1918-1925.
- Navas-Sanchez, F.J., Aleman-Gomez, Y., Sanchez-Gonzalez, J., Guzman-De-Villoria, J.A., Franco, C., Robles, O., Arango, C., Desco, M., 2014. White matter microstructure correlates of mathematical giftedness and intelligence quotient. *Hum Brain Mapp* 35, 2619-2631.
- Paus, T., 2010. Growth of white matter in the adolescent brain: myelin or axon? *Brain Cogn* 72, 26-35.
- Qiu, D., Tan, L.H., Zhou, K., Khong, P.L., 2008. Diffusion tensor imaging of normal white matter maturation from late childhood to young adulthood: voxel-wise evaluation of mean diffusivity, fractional anisotropy, radial and axial diffusivities, and correlation with reading development. *Neuroimage* 41, 223-232.
- R Core Team, 2014. R: A Language and Environment for Statistical Computing. R foundation for Statistical Computing, Vienna, Austria.
- Rosseel, Y., 2012. lavaan: An R package for structural equation modeling. *Journal of Statistical Software* 48, 1-36.
- Sahyoun, C.P., Belliveau, J.W., Mody, M., 2010. White matter integrity and pictorial reasoning in high-functioning children with autism. *Brain Cogn* 73, 180-188.
- Schmahmann, J.D., Pandya, D.N., Wang, R., Dai, G., D'Arceuil, H.E., de Crespigny, A.J., Wedeen, V.J., 2007. Association fibre pathways of the brain: parallel observations from diffusion spectrum imaging and autoradiography. *Brain* 130, 630-653.
- Schmithorst, V.J., 2009. Developmental Sex Differences in the Relation of Neuroanatomical Connectivity to Intelligence. *Intelligence* 37, 164-173.
- Schmithorst, V.J., Holland, S.K., Dardzinski, B.J., 2008. Developmental differences in white matter architecture between boys and girls. *Hum Brain Mapp* 29, 696-710.
- Schmithorst, V.J., Wilke, M., Dardzinski, B.J., Holland, S.K., 2002. Correlation of white matter diffusivity and anisotropy with age during childhood and adolescence: a cross-sectional diffusion-tensor MR imaging study. *Radiology* 222, 212-218.
- Schmithorst, V.J., Wilke, M., Dardzinski, B.J., Holland, S.K., 2005. Cognitive functions correlate with white matter architecture in a normal pediatric population: a diffusion tensor MRI study. *Hum Brain Mapp* 26, 139-147.
- Schmithorst, V.J., Yuan, W., 2010. White matter development during adolescence as shown by diffusion MRI. *Brain Cogn* 72, 16-25.
- Šidák, Z., 1967. Rectangular confidence regions for the means of multivariate normal distributions. *Journal of the American Statistical Association* 62, 626-633.
- Simmonds, D.J., Hallquist, M.N., Asato, M., Luna, B., 2014. Developmental stages and sex differences of white matter and behavioral development through adolescence: a longitudinal diffusion tensor imaging (DTI) study. *Neuroimage* 92, 356-368.
- Smith, S.M., 2002. Fast robust automated brain extraction. *Hum Brain Mapp* 17, 143-155.
- Sui, J., Adali, T., Yu, Q., Chen, J., Calhoun, V.D., 2012. A review of multivariate methods for multimodal fusion of brain imaging data. *J Neurosci Methods* 204, 68-81.
- Tellegen, P.J., Winkel, M., Wijnberg-Williams, B., Laros, J.A., 2005. *Snijders-Oomen Niet-Verbale Intelligentietest: SON-R 2-1/2 -to-7*. Boom Testuitgevers, Amsterdam.

- Tick, N.T., van der Ende, J., Koot, H.M., Verhulst, F.C., 2007. 14-year changes in emotional and behavioral problems of very young Dutch children. *Journal of the American Academy of Child and Adolescent Psychiatry* 46, 1333-1340.
- Tiemeier, H., Velders, F.P., Szekely, E., Roza, S.J., Dieleman, G., Jaddoe, V.W., Uitterlinden, A.G., White, T.J., Bakermans-Kranenburg, M.J., Hofman, A., Van Ijzendoorn, M.H., Hudziak, J.J., Verhulst, F.C., 2012. The Generation R Study: A review of design, findings to date, and a study of the 5-HTTLPR by environmental interaction from fetal life onward. *Journal of the American Academy of Child and Adolescent Psychiatry* 51, 1119-1135 e1117.
- Veraart, J., Sijbers, J., Sunaert, S., Leemans, A., Jeurissen, B., 2013. Weighted linear least squares estimation of diffusion MRI parameters: strengths, limitations, and pitfalls. *Neuroimage* 81, 335-346.
- Wallace, G.L., Schmitt, J.E., Lenroot, R., Viding, E., Ordaz, S., Rosenthal, M.A., Molloy, E.A., Clasen, L.S., Kendler, K.S., Neale, M.C., Giedd, J.N., 2006. A pediatric twin study of brain morphometry. *Journal of Child Psychology and Psychiatry* 47, 987-993.
- Wang, Y., Adamson, C., Yuan, W., Altaye, M., Rajagopal, A., Byars, A.W., Holland, S.K., 2012. Sex differences in white matter development during adolescence: a DTI study. *Brain Res* 1478, 1-15.
- White, T., El Marroun, H., Nijs, I., Schmidt, M., van der Lugt, A., Wielopolski, P.A., Jaddoe, V.W., Hofman, A., Krestin, G.P., Tiemeier, H., Verhulst, F.C., 2013. Pediatric population-based neuroimaging and the Generation R Study: the intersection of developmental neuroscience and epidemiology. *European journal of epidemiology* 28, 99-111.

SUPPLEMENTAL MATERIAL

Supplemental and supporting information can be found Online via the NeuroImage website (doi: 10.1016/j.neuroimage.2015.06.014).



CHAPTER

4

White matter microstructure in children with autistic traits

Laura M.E. Blanken, Ryan L. Muetzel,
Vincent W.V. Jaddoe, Frank C. Verhulst, Aad van der Lugt,
Henning Tiemeier, Tonya White

Manuscript submitted for publication

ABSTRACT

Background: Autism spectrum disorder (ASD) is thought to arise from aberrant development of connections in the brain. Previous studies have identified differences in white matter integrity in children with ASD compared to controls, offering support to such hypotheses of disrupted connectivity. While ASD is thought to represent the severe end of a spectrum of traits, there are no studies evaluating white matter integrity in relation to autistic traits along a continuum in children from the general population.

Methods: In a sample of 604 children from the Generation R Study, a population-based cohort in Rotterdam, the Netherlands, we assessed the relation between a continuous measure of autistic traits, measured by the Social Responsiveness Scale and white matter integrity, using both probabilistic tractography and Tract-Based Spatial Statistics (TBSS).

Results: No widespread associations were observed between autistic traits and white matter integrity in these children. The tractography approach revealed a negative association between autistic traits and fractional anisotropy (FA) in the bilateral corticospinal tract but after adjusting for confounders the association disappeared. Using the TBSS approach, a small cluster in the left superior longitudinal fasciculus (SLF) was identified where FA showed a negative association with autistic traits. This association remained after adjustment for confounders and when excluding children with a confirmed diagnosis of ASD. Further, in this SLF cluster, a trend to lower FA was observed in 19 children with ASD, compared to 61 matched controls.

Conclusion: We found evidence for a localized association between autistic traits on a continuum and white matter integrity in school-aged children from the general population. Autistic symptoms were associated with lower FA in the left SLF, which has been consistently reported in clinical studies in children with ASD. Thus, lower FA in the SLF could indicate a continuum of the neurobiology along the spectrum of autistic symptoms. Since we only found a very localized association, some other white matter abnormalities that are commonly reported in DTI studies in children with ASD may not relate to continuously measured social problems in the general population and may be restricted to clinically affected children.

INTRODUCTION

Children with autism spectrum disorder (ASD) show impairment in reciprocal communication, as well as patterns of restrictive and repetitive behavior. Despite major research efforts, the neurobiology of ASD remains elusive. One prominent unifying theory conceptualizes ASD as a developmental disorder characterized by aberrant connectivity between different regions of the brain (Geschwind and Levitt 2007, Uddin et al. 2013). Notably, connectivity involving long-distance connections in the brain appears to be reduced, accompanied by greater localized connectivity (Belmonte et al. 2004). While efficient communication between spatially separated regions of the brain is facilitated by myelinated neuronal fibers, the role of white matter microstructure in ASD is not yet clear (Delmonte et al. 2013, Mueller et al. 2013, Nair et al. 2013).

The microstructural architecture of white matter tracts in the brain can be examined *in vivo* using diffusion tensor imaging (DTI), a non-invasive technique that provides a measure of white matter integrity by assessing properties of water diffusion. The most commonly studied DTI metrics are fractional anisotropy (FA) and mean diffusivity (MD). FA summarizes the directionality of water diffusion in different tissues as a scalar measure between 0 and 1, where higher values indicate more unidirectional diffusion, thought to reflect higher white matter microstructural integrity. MD represents the average diffusivity across all directions, where lower values are usually associated with higher integrity of white matter. Typical white matter development is characterized by gradual increases in FA and decreases in MD (Schmithorst and Yuan 2010). Psychopathology in general is typically, but not exclusively, associated with lower FA and higher MD in various brain regions. Biologically, this can reflect a wide range of developmental and pathophysiological processes, including differences in myelination, and degree of alignment and density of axons (Beaulieu 2002, Dennis and Thompson 2013).

A number of groups have applied this technique to the study of ASD and reported abnormal white matter integrity, both in adults and children (Ameis and Catani 2015). These differences in white matter microstructure have been localized to a number of tracts, including bundles connecting the limbic system to frontal regions and in interhemispheric fibers (Ameis and Catani 2015). However, considerable debate remains around the presence of such abnormalities, given the inconsistencies amongst different studies. Different studies are difficult to compare due to the heterogeneity in clinical characteristics and differences in methodologies applied to image processing and statistical analyses. Further, not all studies evaluate the same set of white matter regions. While most published reports show group differences in DTI metrics (Aoki et al. 2013, Ameis and Catani 2015), there are also studies showing little or no differences in white matter features between children with ASD and controls (Travers et al. 2012, Ameis and Catani 2015).

An important trend conceptualizes ASD as a spectrum of social communication problems that extend into the general population (Constantino 2011). Thus, it is plausible that the neurobiological underpinnings of ASD are not confined to the most severely affected individuals, but extend to those without a diagnosis. This notion is supported by evidence that white matter abnormalities in children with ASD extend to their unaffected siblings (Barnea-Goraly et al. 2010). Further, like other neurobiological features of ASD (Di Martino et al. 2009, Blanken et al. 2015), white matter integrity may also relate to levels of autistic traits in the general population. A number of studies have evaluated white matter microstructure in relation to symptom severity, mostly in samples restricted to patients with ASD. Cheon and colleagues reported higher SRS scores were related to lower FA in the right uncinate fasciculus and the right anterior thalamic radiation in a sample of 17 school-aged boys with ASD (Cheon et al. 2011). Poustka et al. reported widespread negative correlations of FA with ADOS and ADI-R symptom severity indices, and Noriuchi et al. found that lower FA in white matter near the left dorsolateral prefrontal cortex was related to higher SRS scores in a small group of children with ASD (Noriuchi et al. 2010, Poustka et al. 2012). In contrast, Jou et al. found no association between white matter and SRS scores (Jou et al. 2011). However, the majority of studies operate within a case-control design, with trait analyses restricted to symptom severity associations in children with clinical ASD (Vogan et al. 2016). Only a few studies have evaluated differences along a continuum of autistic traits, extending to non-clinically affected individuals (Iidaka et al. 2012, Jakab et al. 2013, Koolschijn et al. 2015). Two studies showed associations between autistic traits and white matter integrity in neurotypical adults (Iidaka, Miyakoshi et al. 2012, Jakab, Emri et al. 2013), while another study did not demonstrate such associations (Koolschijn, Geurts et al. 2015). Iidaka et al. reported that Autism Quotient scores were positively correlated with volume of a white matter tract connecting the amygdala and the superior temporal sulcus. Jakab et al. reported a negative association between SRS scores and fractional anisotropy in the bilateral temporal fusiform and parahippocampal gyri. There have been no studies to date evaluating the relationship between autistic traits along a continuum and white matter integrity in young children from the general population. Importantly, as neurobiological findings in ASD have been shown to be highly sensitive to development (Uddin, Supekar et al. 2013), the question remains whether white matter differences are present in young children with autistic traits. Previously, in this sample, we identified differences in gyrification in relation to autistic traits and it has been suggested that differences in gyrification may be driven by differences in the underlying structural connectivity (Van Essen 1997). Therefore, in this study, we examined the association between autistic traits and white matter microstructure in six-to-ten year-old children from the general population. To evaluate this and to facilitate comparisons with the current literature, we applied two commonly used methodologies to evaluate white matter characteristics: the voxel based approach Tract Based Spatial Statistics (TBSS) and probabilistic tractography of large, commonly studied white matter tracts.

We hypothesized that white matter microstructural abnormalities in children with autistic traits would mimic the more consistent findings in children with clinically diagnosed ASD. Thus, we expected subtle, but widespread, negative associations between autistic traits and FA, primarily in tracts that facilitate long-range connections: corpus callosum, the uncinate fasciculus (UF), and the superior longitudinal fasciculus (SLF) (Aoki, Abe et al. 2013). To assess whether associations between autistic traits and white matter were truly present on a continuum, we additionally evaluated whether they remained after excluding children with a confirmed diagnosis of ASD. In addition, any differences found along the continuum of traits were also evaluated in children with confirmed ASD, compared to a group of age, sex and IQ-matched controls.

METHODS

Participants

The current study is part of the Generation R Study, a population-based cohort of mothers and children in Rotterdam, the Netherlands (Jaddoe et al. 2012). When the children were approximately 6 to 8 years of age, a sub-sample of 1,070 children was recruited for MRI scanning (White et al. 2013). In this sub-sample, there were 36 children who did not receive a DTI scan and 256 children with insufficient quality DTI data, leaving 778 children with usable DTI data. After excluding children with missing information on autistic traits ($n=144$), the study sample included 634 children. For 30 children, one of the tracts (usually the cingulum bundle) could not be reconstructed in the tractography approach and we excluded them in both approaches, after which the final study sample consisted of 604 children. The Medical Ethics Committee of the Erasmus Medical Center approved all study procedures, and parents provided written informed consent after they had received a full description of the study.

Autistic traits

At approximately 6 years of age, the Social Responsiveness Scale (SRS) was administered to parents (90.4% mothers) of all participating children to obtain a quantitative measure of autistic traits (Constantino 2002). The Social Responsiveness Scale provides a valid quantitative measure of subclinical and clinical levels of autistic traits (Constantino 2002). Parents were asked to rate their child's social behavior during the past six months. We used the 18-item abbreviated version of the scale, which shows correlations ranging from 0.93 to 0.99 with the full scale in three different large studies (Blanken, Mous et al. 2015). Item scores were summed and weighed for the number of items completed. Higher total scores indicate more problems. Total scores were square-root transformed to approach normality.

ASD diagnosis

Identification of children with a diagnosis of ASD was a multi-step process. Children who scored in the top 15th percentile on the CBCL/1 ½-5 total score and those who scored in the upper 2% on the PDP subscale underwent a screening procedure for ASD using the Social Communication Questionnaire (SCQ), a 40-item parent-reported screening instrument for ASD (Berument et al. 1999). We contacted general practitioners of children who scored screen-positive on the SRS, SCQ or for whom the mother reported a diagnosis of ASD, in order to confirm this diagnosis based on the medical records. In the Netherlands, the general practitioner holds the central medical records, including information on treatment by (medical) specialists. Only children with a diagnosis of ASD documented in the medical records were considered ASD cases. In this study sample, we identified 19 children with a medical records-confirmed diagnosis of ASD. To create a control group, these children were subsequently matched 1:4 on age at the time of MRI, sex and non-verbal IQ. Sixty-one suitable matches were identified.

Image acquisition

Prior to MRI scanning, all children underwent a 30-minute mock scanning session in order to familiarize them with the MR-environment (White et al. 2013). Data were acquired on a 3 Tesla General Electric scanner (GE, MR750, Milwaukee, WI). Diffusion MRI data were collected with 3 $b=0$ volumes and 35 diffusion directions using an echo planar imaging sequence ($T_R = 11,000$ ms, $T_E = 83$ ms, Field of view = 256 mm x 256 mm, Acquisition Matrix = 128 x 128, slice thickness = 2 mm, number of slices = 77, $b = 1000$ s/mm²).

Data quality assurance

Data quality assurance was a multi-step process including both visual inspection and automated software. Details on this procedure have been reported elsewhere (Muetzel et al. 2015). Briefly, sum of square maps from the tensor fit were visually inspected for structured patterns / artifact. Further, raw image quality was also evaluated using an automated quality control tool (DTIprep, <http://www.nitrc.org/projects/dtiprep/>). Probabilistic tractography and TBSS registrations to standard space were inspected for accuracy, to ensure all data were properly aligned. Further, all probabilistic tracts were visualized to ensure accurate path reconstruction.

Image preprocessing

Image preprocessing was conducted using the Functional MRI of the Brain's Software Library (FMRIB, FSL, version 5.0.5, Jenkinson et al. 2012) and the Camino Diffusion Toolkit (Cook et al. 2006) via the Neuroimaging in Python Pipelines and Interfaces package (Nipype, version 0.92, Gorgolewski et al. 2011). Details of the image processing have been described

in detail elsewhere (Muetzel, Mous et al. 2015). Briefly, non-brain tissue was removed (Jenkinson, Beckmann et al. 2012) and diffusion images were corrected for eddy current-induced artifacts (Haselgrove and Moore 1996) and translations/rotations resulting from head motion (Jenkinson and Smith 2001). In order to account for rotations applied to the diffusion data, the resulting transformation matrices were used to rotate the diffusion gradient direction table (Jones and Cercignani 2010). The diffusion tensor was computed using the Camino toolkit's embedded RESTORE method (Chang et al. 2005), and common scalar metrics (e.g., FA, MD) were subsequently computed.

Probabilistic fiber tractography

Probabilistic fiber tractography was run on each subject's diffusion data using the fully automated, freely available FSL plugin, "AutoPtx" (de Groot et al. 2015). Briefly, the Bayesian Estimation of Diffusion Parameters Obtained using Sampling Techniques (BEDPOSTx) package from FSL was used to estimate the diffusion parameters at each voxel, accounting for two fiber orientations (Behrens et al. 2007). Next, a predefined set of seed and target masks, supplied by the AutoPtx software, were aligned to each subject's diffusion data using a nonlinear registration. The FSL probabilistic fiber tracking algorithm, Probtrackx, was then used to identify connectivity distributions for a number of large, commonly reported fiber bundles, based on the predefined seed and target marks. Connectivity distributions obtained in the fiber tracking process were normalized based on the number of successful seed-to-target attempts, with a threshold applied to remove voxels that were unlikely to be part of the true distribution. For each tract, average DTI scalar metrics (e.g., FA, MD), weighted by the connectivity distribution, were computed (Muetzel, Mous et al. 2015). Thus, voxels with a high probability of being part of the true white matter bundle have a higher contribution to the average DTI scalar value computed across the entire tract, compared to voxels with a lower probability. A depiction of the tracts examined in this study is provided in Supplementary Figure 1.

Tract based spatial statistics

Voxel-wise statistical analysis of the FA and MD scalar data was performed using Tract-Based Spatial Statistics (TBSS) (Smith et al. 2006), which is part of FSL (Smith et al. 2004). First, FA data were aligned into a common space (FMRIB58 FA map) using the nonlinear registration tool FNIRT (Andersson 2007, Andersson et al. 2007). The resulting non-linear warp fields for the FA maps were then applied to MD maps. Next, the mean FA image was created and thresholded to create a mean FA skeleton, which is the area representing the geometric center of all tracts common to the sample. A threshold of FA > 0.2 was applied to the skeleton to include only major fiber bundles. Each subject's aligned FA/MD data was then projected onto this skeleton and the resulting data were fed into voxel-wise cross-subject statistics (see below for details).

Covariates

Covariates were chosen *a priori* based on confounding effects in a previous study of gyrification and autistic traits in this sample (Blanken, Mous et al. 2015). Sex, age at MRI scanning and age at administration of the SRS were default covariates. Maternal education and history of smoking and alcohol during pregnancy were assessed by questionnaires. The child's ethnic background was defined based on the country of birth of both parents. Maternal education was defined by the highest completed education. Maternal smoking was assessed at enrollment and in mid- and late pregnancy.

Non-verbal intelligence of the child was assessed at approximately 6 years of age using two subtests of the Snijders-Oomen Niet-verbale intelligentie Test – Revisie (SON-R 2.5–7), a nonverbal intelligence test suited for children between 2.5–7 years of age (Tellegen et al. 2005). Child attention problems, which often occur with autistic traits (Grzadzinski et al. 2011), were assessed at age 6 using the CBCL/ 1.5-5 (Achenbach and Rescorla 2000).

Statistical analysis

Statistical analyses were conducted using the R Statistical Software version 3.1.3 (R Core Team, 2014), SPSS version 21 (IBM Corp., Armonk, NY, USA), and FSL's built-in tool "Randomise" (Winkler et al. 2014). For the tractography approach, the Lavaan package (Rosseel 2012) was used to compute global DTI measures using confirmatory factor analysis. The details of this approach have been described elsewhere (Muetzel, Mous et al. 2015). Briefly, separately for FA and MD, multiple tracts were summarized as a single latent factor, and the predicted factor scores for each subject were generated.

In TBSS, FSL's tool "Randomise" was used to perform voxel-wise analyses (Winkler, Ridgway et al. 2014). A total of 5000 permutations were run per analysis, and family-wise error corrected p-values were used to evaluate significant clusters ($p_{\text{FWE}} < 0.05$). Because the Randomise tool does not allow for multiple imputation of missing data for confounders, average FA and MD values were computed for each subject within significant clusters, and fully adjusted analyses were performed in SPSS. Multiple imputation of missing data for confounders, regression analyses, and matching of children with ASD were all performed in SPSS. For associations that remained after adjustment for a set of standard confounders, we additionally performed a sensitivity analysis adjusting for IQ and attention problems.

Additionally, we evaluated whether any associations with white matter microstructure remained after excluding children with a confirmed diagnosis of ASD. Lastly, any differences identified using the trait approach were also evaluated in the 19 children in our sample with clinically confirmed ASD, compared to a group of age, sex and IQ-matched controls. For this analysis, group status (ASD/control) was used as a predictor in linear regression models.

RESULTS

Sample characteristics

Sample characteristics are presented in Table 1.

Table 1. Participant characteristics (n=604)

Child characteristics		n	
Gender (% boy)		604	53.0
Ethnicity		604	
	Dutch		65.2
	Other Western		9.3
	Non-Western		25.5
Social Responsiveness Scale			
	Weighted total score	604	0.27 (0.29)
Age at Social Responsiveness Scale (years)		604	6.17 (0.44)
Age at MRI (years)		604	8.02 (1.03)
Non-verbal IQ		554	103.4 (14.1)
Maternal characteristics			
Education level (%)		591	
	High		57.3
	Medium		29.5
	Low		11.1
Alcohol in pregnancy (%)		563	
	Never		32.7
	Until pregnancy was known		14.9
	Continued occasionally		40.7
	Continued frequently		11.7
Smoking in pregnancy (%)		583	
	Never		77.4
	Until pregnancy was known		6.3
	Continued		16.3

Note. Values are mean and SD unless otherwise indicated.

Autistic traits and white matter integrity: global and specific tracts

To facilitate comparison with other studies, linear regression analyses were first performed using a minimally adjusted model with age at administration of the SRS, age at the time of scanning and sex as covariates (model 1). Subsequently, we additionally adjusted for ethnicity, maternal alcohol use and smoking during pregnancy, and maternal education. Autistic traits were not associated with global FA and MD (Table 2). To assess potential tract-specific differences that were obscured in the analyses of the global measures, we also examined FA and MD in individual tracts. In the bilateral corticospinal tract, we found a negative association with FA, where children with more autistic traits showed lower FA (Left: $\beta=-0.08$, $p=0.04$, and right: $\beta=0.09$, $p=0.03$, uncorrected for multiple comparisons). However, after adjustment for confounders, associations disappeared (Table 3).

Table 2. Autistic traits and global FA and MD

		B (95%CI)	Beta	p
Global FA	model 1	-0.35 (-1.11; 0.42)	-0.04	.38
	model 2	-0.06 (-0.85; 0.74)	-0.01	.89
Global MD	model 1	0.00 (-0.06; 0.06)	0.00	.99
	model 2	0.00 (-0.07; 0.06)	0.00	.93

Note: Global DTI metrics from confirmatory factor analysis of multiple white matter tracts. Model 1 was adjusted for sex, age at the time of scanning and age at the time of SRS. Model 2 was additionally adjusted for ethnicity, maternal alcohol use and smoking during pregnancy, and maternal education.

Tract-based spatial statistics

Autistic traits were significantly associated with FA in a small cluster in the left superior longitudinal fasciculus after controlling for multiple testing. In this cluster, children with more autistic traits showed lower FA (Figure 1 and Table 4, $\beta=-0.20$, $p<0.001$). When examining this association in the context of additional covariates (model 2), the association remained. In a sensitivity analysis, we also assessed the association after additionally adjusting for non-verbal IQ and attention problems and results remained the same. When evaluating the association between SRS-score and FA in this cluster after excluding children with confirmed ASD, it remained highly consistent ($\beta=-0.20$, $p<0.001$, model fully adjusted). Lastly, case-control analyses showed that there was a trend to lower FA in this cluster in the 19 children with confirmed ASD, compared to the 61 matched controls ($\beta=-0.20$, $p=0.07$). We did not identify any clusters where autistic traits were associated with MD.

Table 3. Autistic traits and tract-specific FA and MD

		FA			MD		
		B (95%CI)	Beta	p	B (95% CI)	Beta	p
SLF L	model 1	-0.46 (-1.32; 0.40)	-0.04	.29	-0.01 (-0.09; 0.07)	-0.01	.80
	model 2	-0.22 (-1.12; 0.68)	-0.02	.64	-0.01 (-0.09; 0.07)	-0.01	.85
SLF R	model 1	-0.09 (-0.75; 0.93)	0.01	.83	-0.02 (-0.09; 0.06)	-0.02	.69
	model 2	0.34 (-0.53; 1.22)	0.03	.44	-0.03 (-0.11; 0.05)	-0.03	.49
ILF L	model 1	-0.32 (-0.99; 0.36)	-0.04	.36	-0.01 (-0.10; 0.07)	-0.01	.76
	model 2	-0.14 (-0.85; 0.58)	-0.02	.71	-0.02 (-0.10; 0.07)	-0.01	.75
ILF R	model 1	-0.53 (-1.21; 0.15)	-0.06	.13	0.06 (-0.03; 0.14)	0.05	.18
	model 2	-0.41 (-1.13; 0.31)	-0.05	.26	0.07 (-0.01; 0.16)	0.07	.10
UF L	model 1	-0.21 (-1.10; 0.68)	-0.02	.64	-0.01 (-0.08; 0.06)	-0.01	.79
	model 2	-0.07 (-1.01; 0.87)	-0.01	.89	-0.01 (-0.09; 0.06)	-0.02	.71
UF R	model 1	-0.32 (-1.04; 0.40)	-0.04	.38	-0.02 (-0.08; 0.05)	-0.02	.64
	model 2	-0.16 (-0.92; 0.60)	-0.02	.68	-0.02 (-0.09; 0.05)	-0.02	.63
CST L	model 1	-0.83 (-1.61; -0.05)	-0.08	.04	-0.03 (-0.08; 0.03)	-0.03	.41
	model 2	-0.37 (-1.17; 0.44)	-0.04	.37	-0.05 (-0.11; 0.01)	-0.06	.13
CST R	model 1	-0.86 (-1.62; -0.10)	-0.09	.03	-0.04 (-0.10; 0.02)	-0.05	.22
	model 2	-0.43 (-1.21; 0.36)	-0.04	.29	-0.05 (-0.11; 0.01)	-0.06	.13
Cingulum L	model 1	0.41 (-0.97; 1.80)	0.02	.56	-0.02 (-0.11; 0.07)	-0.02	.69
	model 2	0.83 (-0.63; 2.28)	0.05	.26	-0.04 (-0.14; 0.05)	-0.04	.37
Cingulum R	model 1	0.91 (-0.42; 2.25)	0.05	.18	0.03 (-0.06; 0.11)	0.02	.59
	model 2	1.05 (-0.35; 2.45)	0.06	.14	0.01 (-0.08; 0.10)	0.01	.83
Forceps Major	model 1	-0.56 (-1.65; 0.52)	-0.04	.31	-0.02 (-0.21; 0.17)	-0.01	.83
	model 2	-0.42 (-1.56; 0.71)	-0.03	.46	-0.01 (-0.21; 0.20)	0.00	.96
Forceps Minor	model 1	-0.01 (-0.98; 0.96)	0.00	.98	0.06 (-0.06; 0.18)	0.04	.30
	model 2	0.16 (-0.86; 1.17)	0.01	.76	0.08 (-0.04; 0.20)	0.05	.20

Note: model 1 was adjusted for sex, age at the time of scanning and age at the time of SRS. Model 2 was additionally adjusted for ethnicity, maternal alcohol use and smoking during pregnancy and maternal education.

Table 4. TBSS: autistic traits and FA (n=604)

		B (95% CI)	Beta	p
Left Superior Longitudinal Fasciculus	model 1	-0.04 (-0.05; -0.02)	-0.20	<.001
	model 2	-0.04 (-0.06; -0.02)	-0.20	<.001

Note: model 1 was adjusted for sex, age at the time of scanning and age at the time of SRS. Model 2 was additionally adjusted for ethnicity, maternal alcohol use and smoking during pregnancy, and maternal education.

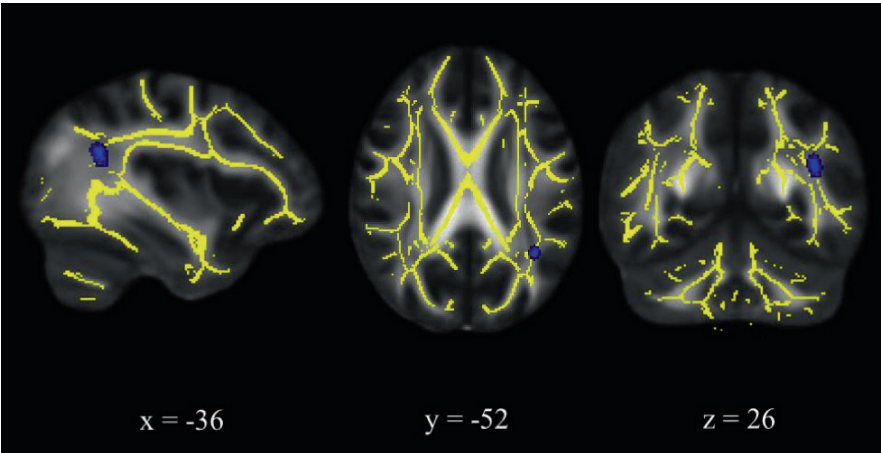


Figure 1. FA and autistic traits. The blue cluster in the left Superior Longitudinal Fasciculus represents a negative correlation between autistic traits and FA. Coordinates are in MNI space.

DISCUSSION

In a large sample of school-aged children we found that autistic traits were not associated with widespread differences in white matter integrity in the brain; this was consistent across two different methodologies. However, when using the TBSS approach, we identified a small cluster in the left superior longitudinal fasciculus where children with more autistic traits showed lower FA.

Our finding in the left superior longitudinal fasciculus was consistent with our hypothesis and represents one of the most replicated differences in ASD (Aoki, Abe et al. 2013). Consistent with our hypothesis that the white matter differences would show a continuum, the association remained after excluding children with a confirmed diagnosis of ASD. Further, there was a trend to a similar effect at the severe end of the spectrum, when comparing a small group of children with clinically confirmed ASD to matched controls. This supports the notion that brain features of ASD potentially extend into the general population. The superior longitudinal fasciculus is a long-range white matter tract that connects frontal

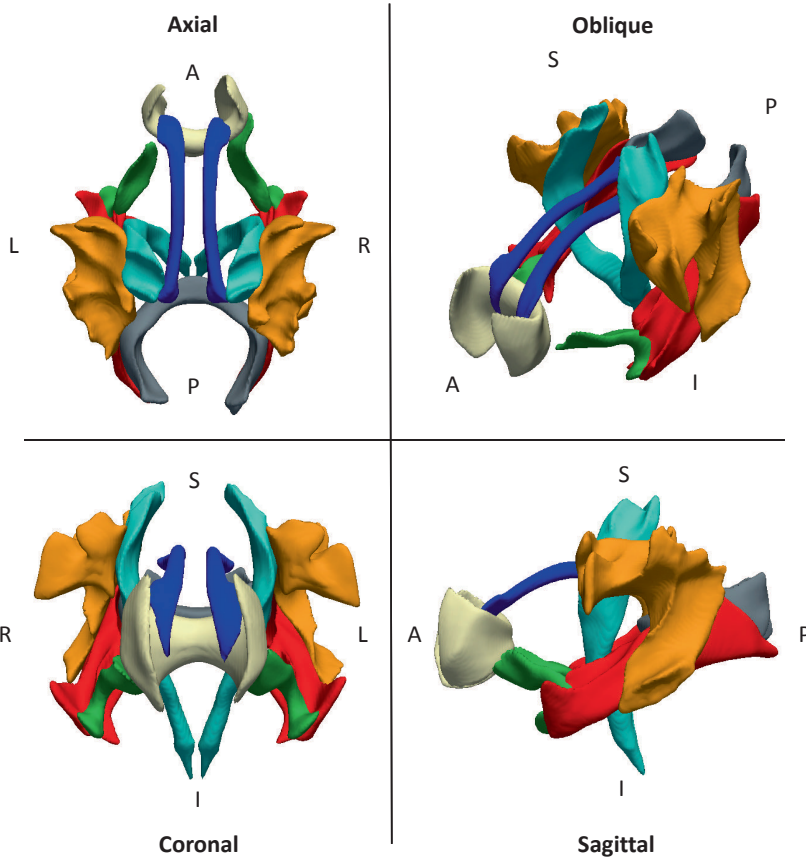
areas of the brain with dorsal areas. It is implicated in a number of cognitive functions, including language, fine-motor ability and attention (Zhang et al. 2010, Unger et al. 2015). Lower microstructural white matter integrity in a long-range tract is consistent with the conceptualization of ASD as a “developmental disconnection syndrome” (Geschwind and Levitt 2007). Further, in the minimally adjusted tractography models, we observed an association between autistic traits and lower FA in the CST, although this association was not corrected for multiple testing. This finding is in line with other studies that have also reported lower FA in the CST in children or adolescents with ASD (Ben Bashat et al. 2007, Brito et al. 2009). In addition, a recent study by Carper et al. found higher mean diffusivity of the corticospinal tract in adolescents with ASD (Carper et al. 2015). Importantly, we did not find the same region in the TBSS approach and the effects we observed in the CST disappeared after adjusting for confounders.

While we observed a localized association in the left superior longitudinal fasciculus, our results do not support our original hypothesis of global differences in white matter microstructure. More specifically, despite the large sample size of our study, we did not find associations in all three hypothesized regions. There are several potential reasons for this. First, it is possible that some white matter differences that are commonly reported in ASD may represent more severe alterations that are restricted to more severely affected patient groups and do not, like some other neurobiological features, extend to the general population. Symptoms of children in the general population may be too mild to reveal associations in such regions. The scarcity of findings in the general population is in line with a study of Koolschijn and colleagues, who did not find any differences in white matter integrity related to the continuum of autistic traits in a large sample of neurotypical adults (Koolschijn, Geurts et al. 2015). However, in contrast to this study, we did find that cortical morphology in our sample were related to autistic traits, lending support to a continuum with autistic symptoms in at least some neurobiological features (Blanken, Mous et al. 2015). Of note, the previous studies showing differences in white matter in relation to autistic traits investigated older participants (Iidaka, Miyakoshi et al. 2012, Jakob, Emri et al. 2013). Therefore, it is possible that some white matter differences occur as a consequence of long-term manifestation of autistic traits. White matter development is a dynamic process that continues into adulthood (Lebel et al. 2008) and some abnormalities in ASD have been shown to be specific to certain periods of development. For instance, a longitudinal study showed that children with ASD exhibited increased FA in infancy, followed by decreased FA at age 2 (Wolff et al. 2012). Second, heterogeneity of white matter involvement may play a role. The literature of DTI studies in children with ASD is not very consistent. While there are many reports of abnormalities in various white matter tracts in subjects with ASD, there are also studies reporting no differences in those same tracts (Ameis and Catani 2015). Further, additional studies with negative results may not have been published (Joober et al. 2012).

Methodological differences, as well as sample characteristics, such as age, IQ or sex of the participants contribute to, but likely do not explain, discrepant results between studies. Heterogeneity is a central feature of ASD, and it likely does not only affect its symptomology and cognitive aspects, but also its etiology (Kendler 2013). While this issue is still poorly understood, there are likely many different etiologic pathways that lead to ASD, affecting the brain at many different levels (Happé et al. 2006, Kendler 2013). At this point, there are over 100 genes associated with ASD (Betancur 2011). In some cases, the specific genetic pathway causing ASD may determine the nature and localization of white matter involvement. For instance, a study comparing white matter in children with Klinefelter syndrome to children with idiopathic ASD found differences in the localization of white matter impairments despite the fact that both groups exhibited autism-like symptoms (Goddard et al. 2015). This heterogeneity might complicate the identification of group differences related to ASD or autistic traits. In addition, social impairment as measured by the SRS is only one potential endophenotype of ASD and not all features of the neurobiology may relate to this dimension of ASD.

To our knowledge, this is the first study in school-aged children that focused on white matter integrity and autistic traits along a continuum. Strengths of this study include the population-based design and the large sample size, as well as the implementation of two different methods of assessing white matter integrity. One of the factors likely contributing to the lack of consistency in DTI findings in children with ASD is that different studies typically utilize different methods. Here, we applied two commonly used approaches to assess white matter integrity, which allow us to detect global, as well as more subtle, localized differences in white matter structural integrity. There are also limitations to our study. While there was a time lag between administration of the SRS and the neuroimaging session, we do not expect that this caused our lack of findings, as we expect relative stability of this trait in this age range and we also adjusted for this statistically. Further, since this study was cross-sectional, we could not evaluate longitudinal trajectories of white matter development.

In conclusion, we found a localized association between autistic traits and white matter integrity in school-aged children drawn from the general population. In a small region in the left superior longitudinal fasciculus, we found evidence of a continuum in white matter integrity related to autistic traits. However, most of the white matter abnormalities commonly reported in children with ASD were not observed in this sample. This suggests that these differences may not form a continuum related to autistic traits in the population and may be restricted to more severely affected children.



Supplementary Figure 1.

Tracts are group average representations in standard coordinate space. Blue indicates the cingulum bundle, gray the forceps major, tan the forceps minor, red the inferior longitudinal fasciculus, orange the superior longitudinal fasciculus, and green the uncinate fasciculus. R = Right, L = Left, A = Anterior, P = Posterior, I = Inferior, S = Superior.

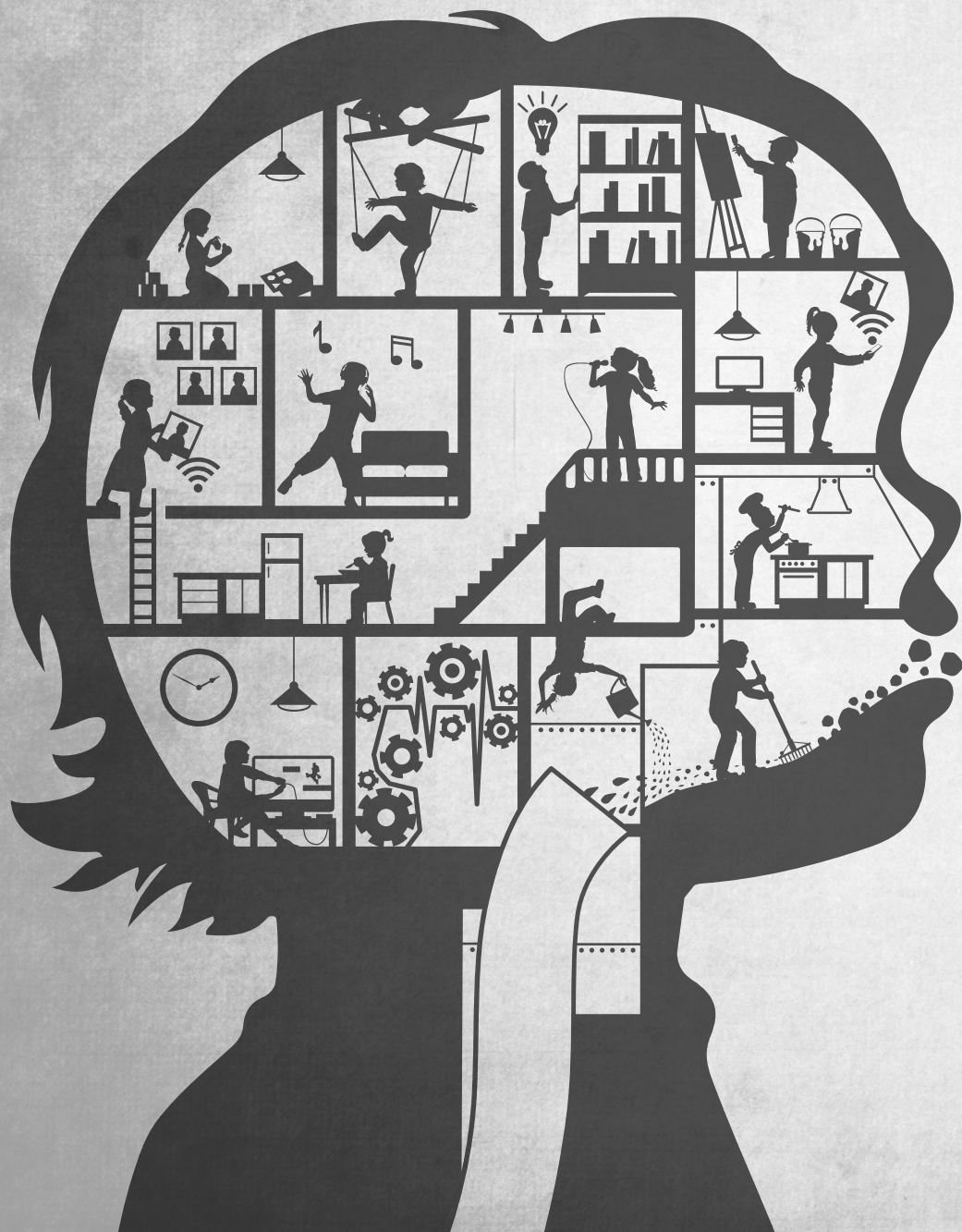
REFERENCES

- Achenbach, T. M. and L. A. Rescorla (2000). Manual for the ASEBA Preschool Forms & Profiles. Burlington, VT., University of Vermont, Research Center for Children, Youth and Families.
- Ameis, S. H. and M. Catani (2015). Altered white matter connectivity as a neural substrate for social impairment in Autism Spectrum Disorder. *Cortex* **62**: 158-181.
- Andersson, J. L. R. (2007). Non-linear optimisation.
- Andersson, L. R., M. Jenkinson and S. Smith (2007). Non-linear registration, aka Spatial normalisation
- Aoki, Y., O. Abe, Y. Nippashi and H. Yamasue (2013). Comparison of white matter integrity between autism spectrum disorder subjects and typically developing individuals: a meta-analysis of diffusion tensor imaging tractography studies. *Molecular Autism* **4**.
- Barnea-Goraly, N., L. J. Lotspeich and A. L. Reiss (2010). Similar white matter aberrations in children with autism and their unaffected siblings: a diffusion tensor imaging study using tract-based spatial statistics. *Arch Gen Psychiatry* **67**(10): 1052-1060.
- Beaulieu, C. (2002). The basis of anisotropic water diffusion in the nervous system - a technical review. *NMR Biomed* **15**(7-8): 435-455.
- Behrens, T. E., H. J. Berg, S. Jbabdi, M. F. Rushworth and M. W. Woolrich (2007). Probabilistic diffusion tractography with multiple fibre orientations: What can we gain? *Neuroimage* **34**(1): 144-155.
- Belmonte, M. K., G. Allen, A. Beckel-Mitchener, L. M. Boulanger, R. A. Carper and S. J. Webb (2004). Autism and abnormal development of brain connectivity. *J Neurosci* **24**(42): 9228-9231.
- Ben Bashat, D., V. Kronfeld-Duenias, D. A. Zachor, P. M. Ekstein, T. Hendler, R. Tarrasch, A. Even, Y. Levy and L. Ben Sira (2007). Accelerated maturation of white matter in young children with autism: a high b value DWI study. *Neuroimage* **37**(1): 40-47.
- Berument, S. K., M. Rutter, C. Lord, A. Pickles and A. Bailey (1999). Autism screening questionnaire: diagnostic validity. *British Journal of Psychiatry* **175**: 444-451.
- Betancur, C. (2011). Etiological heterogeneity in autism spectrum disorders: more than 100 genetic and genomic disorders and still counting. *Brain Res* **1380**: 42-77.
- Blanken, L. M. E., S. E. Mous, A. Ghassabian, R. L. Muetzel, N. K. Schoemaker, H. El Marroun, A. van der Lugt, V. W. V. Jaddoe, A. Hofman, F. C. Verhulst, H. Tiemeier and T. White (2015). Cortical Morphology in 6-to 10-Year Old Children With Autistic Traits: A Population-Based Neuroimaging Study. *American Journal of Psychiatry* **172**(5): 479-486.
- Brito, A. R., M. M. Vasconcelos, R. C. Domingues, L. C. Hygino da Cruz, Jr., S. Rodrigues Lde, E. L. Gasparetto and C. A. Calcada (2009). Diffusion tensor imaging findings in school-aged autistic children. *J Neuroimaging* **19**(4): 337-343.
- Carper, R. A., S. Solders, J. M. Treiber, I. Fishman and R. A. Muller (2015). Corticospinal tract anatomy and functional connectivity of primary motor cortex in autism. *J Am Acad Child Adolesc Psychiatry* **54**(10): 859-867.
- Chang, L. C., D. K. Jones and C. Pierpaoli (2005). RESTORE: robust estimation of tensors by outlier rejection. *Magn Reson Med* **53**(5): 1088-1095.
- Cheon, K. A., Y. S. Kim, S. H. Oh, S. Y. Park, H. W. Yoon, J. Herrington, A. Nair, Y. J. Koh, D. P. Jang, Y. B. Kim, B. L. Leventhal, Z. H. Cho, F. X. Castellanos and R. T. Schultz (2011). Involvement of the anterior thalamic radiation in boys with high functioning autism spectrum disorders: a Diffusion Tensor Imaging study. *Brain Res* **1417**: 77-86.
- Constantino, J. N. (2002). Social Responsiveness Scale (SRS), Manual. Los Angeles, Western Psychological Services.
- Constantino, J. N. (2011). The quantitative nature of autistic social impairment. *Pediatr Res* **69**(5 Pt 2): 55R-62R.

- Cook, P. A., Y. Bai, S. Nedjati-Gilani, K. K. Seunarine, M. G. Hall, G. J. Parker and D. C. Alexander (2006). Camino: Open-Source Diffusion-MRI Reconstruction and Processing. 14th Scientific Meeting of the International Society for Magnetic Resonance in Medicine. Seattle, WA, USA: 2759.
- de Groot, M., M. A. Ikram, S. Akoudad, G. P. Krestin, A. Hofman, A. van der Lugt, W. J. Niessen and M. W. Vernooij (2015). Tract-specific white matter degeneration in aging: The Rotterdam Study. *Alzheimers Dement* **11**(3): 321-330.
- Delmonte, S., L. Gallagher, E. O'Hanlon, J. McGrath and J. H. Balsters (2013). Functional and structural connectivity of frontostriatal circuitry in Autism Spectrum Disorder. *Front Hum Neurosci* **7**: 430.
- Dennis, E. L. and P. M. Thompson (2013). Typical and atypical brain development: a review of neuroimaging studies. *Dialogues Clin Neurosci* **15**(3): 359-384.
- Di Martino, A., Z. Shehzad, C. Kelly, A. K. Roy, D. G. Gee, L. Q. Uddin, K. Gotimer, D. F. Klein, F. X. Castellanos and M. P. Milham (2009). Relationship between cingulo-insular functional connectivity and autistic traits in neurotypical adults. *Am J Psychiatry* **166**(8): 891-899.
- Geschwind, D. H. and P. Levitt (2007). Autism spectrum disorders: developmental disconnection syndromes. *Curr Opin Neurobiol* **17**(1): 103-111.
- Goddard, M. N., S. van Rijn, S. A. Rombouts and H. Swaab (2015). White matter microstructure in a genetically defined group at increased risk of autism symptoms, and a comparison with idiopathic autism: an exploratory study. *Brain Imaging Behav*.
- Gorgolewski, K., C. D. Burns, C. Madison, D. Clark, Y. O. Halchenko, M. L. Waskom and S. S. Ghosh (2011). Nipype: a flexible, lightweight and extensible neuroimaging data processing framework in python. *Front Neuroinform* **5**: 13.
- Grzadzinski, R., A. Di Martino, E. Brady, M. A. Mairena, M. O'Neale, E. Petkova, C. Lord and F. X. Castellanos (2011). Examining autistic traits in children with ADHD: does the autism spectrum extend to ADHD? *Journal of Autism and Developmental Disorders* **41**(9): 1178-1191.
- Happé, F., A. Ronald and R. Plomin (2006). Time to give up on a single explanation for autism. *Nat Neurosci* **9**(10): 1218-1220.
- Haselgrove, J. C. and J. R. Moore (1996). Correction for distortion of echo-planar images used to calculate the apparent diffusion coefficient. *Magn Reson Med* **36**(6): 960-964.
- Iidaka, T., M. Miyakoshi, T. Harada and T. Nakai (2012). White matter connectivity between superior temporal sulcus and amygdala is associated with autistic trait in healthy humans. *Neurosci Lett* **510**(2): 154-158.
- Jaddoe, V. W., C. M. van Duijn, O. H. Franco, A. J. van der Heijden, M. H. van Iizendoorn, J. C. de Jongste, A. van der Lugt, J. P. Mackenbach, H. A. Moll, H. Raat, F. Rivadeneira, E. A. Steegers, H. Tiemeier, A. G. Uitterlinden, F. C. Verhulst and A. Hofman (2012). The Generation R Study: design and cohort update 2012. *European journal of epidemiology* **27**(9): 739-756.
- Jakab, A., M. Emri, T. Spisak, A. Szeman-Nagy, M. Beres, S. A. Kis, P. Molnar and E. Berenyi (2013). Autistic traits in neurotypical adults: correlates of graph theoretical functional network topology and white matter anisotropy patterns. *PLoS One* **8**(4): e60982.
- Jenkinson, M., C. F. Beckmann, T. E. Behrens, M. W. Woolrich and S. M. Smith (2012). Fsl. *Neuroimage* **62**(2): 782-790.
- Jenkinson, M. and S. Smith (2001). A global optimisation method for robust affine registration of brain images. *Med Image Anal* **5**(2): 143-156.
- Jones, D. K. and M. Cercignani (2010). Twenty-five pitfalls in the analysis of diffusion MRI data. *NMR Biomed* **23**(7): 803-820.
- Joober, R., N. Schmitz, L. Annable and P. Boksa (2012). Publication bias: what are the challenges and can they be overcome? *J Psychiatry Neurosci* **37**(3): 149-152.
- Jou, R. J., N. Mateljevic, M. D. Kaiser, D. R. Sugrue, F. R. Volkmar and K. A. Pelphrey (2011). Structural neural phenotype of autism: preliminary evidence from a diffusion tensor imaging study using tract-based spatial statistics. *AJNR Am J Neuroradiol* **32**(9): 1607-1613.

- Kendler, K. S. (2013). What psychiatric genetics has taught us about the nature of psychiatric illness and what is left to learn. *Mol Psychiatry* **18**(10): 1058-1066.
- Koolschijn, P. C., H. M. Geurts, A. R. van der Leij and H. S. Scholte (2015). Are Autistic Traits in the General Population Related to Global and Regional Brain Differences? *J Autism Dev Disord* **45**(9): 2779-2791.
- Lebel, C., L. Walker, A. Leemans, L. Phillips and C. Beaulieu (2008). Microstructural maturation of the human brain from childhood to adulthood. *Neuroimage* **40**(3): 1044-1055.
- Mueller, S., D. Keeser, A. C. Samson, V. Kirsch, J. Blautzik, M. Grothe, O. Erat, M. Hegenloh, U. Coates, M. F. Reiser, K. Hennig-Fast and T. Meindl (2013). Convergent Findings of Altered Functional and Structural Brain Connectivity in Individuals with High Functioning Autism: A Multimodal MRI Study. *PLoS One* **8**(6): e67329.
- Muetzel, R. L., S. E. Mous, J. van der Ende, L. M. Blanken, A. van der Lugt, V. W. Jaddoe, F. C. Verhulst, H. Tiemeier and T. White (2015). White matter integrity and cognitive performance in school-age children: A population-based neuroimaging study. *Neuroimage* **119**: 119-128.
- Nair, A., J. M. Treiber, D. K. Shukla, P. Shih and R. A. Muller (2013). Impaired thalamocortical connectivity in autism spectrum disorder: a study of functional and anatomical connectivity. *Brain* **136**(Pt 6): 1942-1955.
- Noriuchi, M., Y. Kikuchi, T. Yoshiura, R. Kira, H. Shigeto, T. Hara, S. Tobimatsu and Y. Kamio (2010). Altered white matter fractional anisotropy and social impairment in children with autism spectrum disorder. *Brain Res* **1362**: 141-149.
- Poustka, L., C. Jennen-Steinmetz, R. Henze, K. Vomstein, J. Haffner and B. Sieltjes (2012). Fronto-temporal disconnectivity and symptom severity in children with autism spectrum disorder. *World J Biol Psychiatry* **13**(4): 269-280.
- Rosseel, Y. (2012). lavaan: An R Package for Structural Equation Modeling *Journal of Statistical Software* **48**(2): 1-36.
- Schmithorst, V. J. and W. Yuan (2010). White matter development during adolescence as shown by diffusion MRI. *Brain Cogn* **72**(1): 16-25.
- Smith, S. M., M. Jenkinson, H. Johansen-Berg, D. Rueckert, T. E. Nichols, C. E. Mackay, K. E. Watkins, O. Ciccarelli, M. Z. Cader, P. M. Matthews and T. E. Behrens (2006). Tract-based spatial statistics: voxelwise analysis of multi-subject diffusion data. *Neuroimage* **31**(4): 1487-1505.
- Smith, S. M., M. Jenkinson, M. W. Woolrich, C. F. Beckmann, T. E. Behrens, H. Johansen-Berg, P. R. Bannister, M. De Luca, I. Drobniak, D. E. Flitney, R. K. Niazy, J. Saunders, J. Vickers, Y. Zhang, N. De Stefano, J. M. Brady and P. M. Matthews (2004). Advances in functional and structural MR image analysis and implementation as FSL. *Neuroimage* **23 Suppl 1**: S208-219.
- Tellegen, P., B. Wijnberg-Williams and J. Laros (2005). *Snijders-Oomen Niet-Verbale Intelligentietest: SON-R 2.5 - 7/*. Amsterdam, Boom Testuitgevers.
- Travers, B. G., N. Adluru, C. Ennis, P. M. Tromp do, D. Destiche, S. Doran, E. D. Bigler, N. Lange, J. E. Lainhart and A. L. Alexander (2012). Diffusion tensor imaging in autism spectrum disorder: a review. *Autism Res* **5**(5): 289-313.
- Uddin, L. Q., K. Supekar and V. Menon (2013). Reconceptualizing functional brain connectivity in autism from a developmental perspective. *Front Hum Neurosci* **7**: 458.
- Urger, S. E., M. D. De Bellis, S. R. Hooper, D. P. Woolley, S. D. Chen and J. Provenza (2015). The superior longitudinal fasciculus in typically developing children and adolescents: diffusion tensor imaging and neuropsychological correlates. *J Child Neurol* **30**(1): 9-20.
- Van Essen, D. C. (1997). A tension-based theory of morphogenesis and compact wiring in the central nervous system. *Nature* **385**(6614): 313-318.
- Vogan, V. M., B. R. Morgan, R. C. Leung, E. Anagnostou, K. Doyle-Thomas and M. J. Taylor (2016). Widespread White Matter Differences in Children and Adolescents with Autism Spectrum Disorder. *J Autism Dev Disord* **46**(6): 2138-2147.

- White, T., H. El Marroun, I. Nijs, M. Schmidt, A. van der Lugt, P. A. Wielopolski, V. W. Jaddoe, A. Hofman, G. P. Krestin, H. Tiemeier and F. C. Verhulst (2013). Pediatric population-based neuroimaging and the Generation R Study: the intersection of developmental neuroscience and epidemiology. *European journal of epidemiology* **28**(1): 99-111.
- White, T., H. El Marroun, I. Nijs, M. Schmidt, A. van der Lugt, P. A. Wielopolski, V. W. Jaddoe, A. Hofman, G. P. Krestin, H. Tiemeier and F. C. Verhulst (2013). Pediatric population-based neuroimaging and the Generation R Study: the intersection of developmental neuroscience and epidemiology. *European Journal of Epidemiology* **28**(1): 99-111.
- Winkler, A. M., G. R. Ridgway, M. A. Webster, S. M. Smith and T. E. Nichols (2014). Permutation inference for the general linear model. *Neuroimage* **92**: 381-397.
- Wolff, J. J., H. Gu, G. Gerig, J. T. Ellison, M. Styner, S. Gouttard, K. N. Botteron, S. R. Dager, G. Dawson, A. M. Estes, A. C. Evans, H. C. Hazlett, P. Kostopoulos, R. C. McKinstry, S. J. Paterson, R. T. Schultz, L. Zwaigenbaum, J. Piven and I. Network (2012). Differences in white matter fiber tract development present from 6 to 24 months in infants with autism. *Am J Psychiatry* **169**(6): 589-600.
- Zhang, Y., C. Wang, X. Zhao, H. Chen, Z. Han and Y. Wang (2010). Diffusion tensor imaging depicting damage to the arcuate fasciculus in patients with conduction aphasia: a study of the Wernicke-Geschwind model. *Neurol Res* **32**(7): 775-778.



CHAPTER

5

Childhood psychiatric symptoms and white matter development: A longitudinal population-based neuroimaging study

Ryan L. Muetzel, Laura M.E. Blanken, Jan van der Ende,
Hanan El Marroun, PhD, Aad van der Lugt, Vincent Jaddoe,
Frank C. Verhulst, Henning Tiemeier, Tonya White

Manuscript submitted for publication

ABSTRACT

Objective: Psychiatric symptomatology during childhood is a known predictor of persistent mental illness later in life. While neuroimaging methodologies are routinely applied cross-sectionally to the study of child and adolescent psychopathology, the corresponding consequences to the underlying neurodevelopmental trajectories remain unclear. The current study examines the relationship of childhood psychiatric problems with longitudinal white matter development using a prospective cohort.

Methods: A population-based sample of 715 children participated in the study. Psychiatric symptoms were measured when children were on average 6 years old, and longitudinal diffusion tensor imaging data were collected at two time-points when children were, on average, 8 and 10 years of age, respectively. Psychiatric symptom ratings were used to predict changes in white matter microstructural integrity using linear mixed-effects models.

Results: Internalizing symptoms were related to changes in white matter microstructural development. Children with higher levels of internalizing symptoms at a young age showed slower white matter microstructural maturation relative to children with lower levels of internalizing symptoms. Sub-analyses revealed that affective, but not anxiety, symptoms predicted reduced microstructural development. The cingulum bundle and the superior longitudinal fasciculus may be of particular importance in this association. Externalizing problems were not related to white matter development.

Conclusions: Children presenting with internalizing problems at an early age show differential white matter development. This work expands upon existing literature by demonstrating that affective problems along a continuum in the general population are related to altered trajectories of white matter microstructural development.

INTRODUCTION

Considerable evidence suggests that children who experience psychiatric problems at a young age are at an increased risk for impaired functioning and continued psychopathology later in life (Pine et al. 1999, Hofstra et al. 2002). Neuroimaging has been an increasingly utilized tool in psychiatric research, offering a unique window into the underlying neurobiological substrates of pediatric brain development and mental illness (Pine et al. 2008, Mana et al. 2010, Hulvershorn et al. 2011, Giedd et al. 2015). Given the influence of maturational processes on morphological brain features (Lenroot and Giedd 2006) and white matter microstructure (Schmithorst and Yuan 2010), the importance of examining emerging psychopathology in the context of typical brain development has been highlighted (Di Martino et al. 2014). However, limited information exists on the exact interplay between psychiatric problems and neurodevelopmental trajectories of white matter microstructure.

Diffusion tensor imaging (DTI) is a sophisticated structural imaging method used to probe aspects of white matter microstructure by measuring the magnitude and direction of water diffusion in tissue (Basser et al. 1994). DTI is particularly suited for studying white matter, given the distinct diffusion profile arising from the inter- and intracellular barriers inherent to densely packed bundles of myelinated axons (Beaulieu 2002). Previous cross-sectional work has demonstrated the utility of DTI in uncovering neurobiological features of different psychiatric disorders in children. Specifically, evidence exists for altered frontolimbic circuitry in internalizing disorders (LeWinn et al. 2014), and frontostriatal components in externalizing disorders (van Ewijk et al. 2012). While longitudinal studies of typical development have already demonstrated mostly linear increases in white matter microstructure from childhood into young adulthood (Giorgio et al. 2009), extensions to investigating similar neurodevelopmental trajectories in child psychiatric conditions are rare.

The majority of studies examining white matter microstructure in child psychopathology have done so using clinical samples within a traditional dichotomous framework (i.e., comparing cases with controls). Similar to many other medical conditions such as heart disease or diabetes, psychiatric symptoms likely exist on a continuum in the general population, with individuals displaying a range in severity of symptoms for a given psychiatric construct. Recent efforts in the field have favored the estimation of psychopathology from a dimensional perspective, specifically in the context of physiological measures ranging from genomics to indices of brain connectivity (Garvey et al. 2016). While some studies conceptualize psychopathology along a continuum in relation to DTI (Regier 2007), this is typically done within a clinical sample (e.g., symptom severity) and not within the general population. Dimensional analyses in large, population-based studies have demonstrated that symptoms covary with neurobiological features, lending further support for this framework (Mous et al. 2014, Blanken et al. 2015). To date, only one study has examined a

specific aspect of child psychiatric symptoms along a continuum in relation to longitudinal white matter development (Albaugh et al. 2016).

The present study examined the association of psychiatric problems with longitudinal white matter development in a large sample of children from the general population. A dimensional approach was applied in the quantification of internalizing and externalizing problems, which are broad, top-level constructs for most psychiatric disorders in young children. Given previous clinical studies showing white matter deficits in patients, and longitudinal work showing increases in white matter microstructure over time during typical development, we hypothesized the presence of psychiatric problems along a continuum at an early age would be accompanied by a decreased level of white matter maturation. Specifically, we hypothesized that internalizing problems would be related to the development of frontolimbic circuitry, and that externalizing problems would be related to development of frontal and motor circuitry.

METHODS

Participants

The current study is part of the Generation R Study, a population-based cohort study of maternal and child health from fetal life onwards, in Rotterdam, the Netherlands (Jaddoe et al. 2012). Alongside the behavioral assessment wave (Figure 1, Tiemeier et al. 2012), a sub-sample of 1,070 children were recruited for MRI scanning (from now on referred to as Time-1, White et al. 2013). As of March 2015, as part of the ongoing age-10 assessment wave (from now on referred to as Time-2), 383 children who had a scan at Time-1 also visited our research-dedicated imaging facility for MRI scanning at Time-2. Figure 1 outlines the timeline of the various data collection efforts, and the flow chart depicted in Supplemental Figure S1 illustrates the exclusion of MRI data for both time points. The final sample consisted of 715 usable DTI datasets at Time-1 and 297 usable DTI datasets at Time 2. The Medical Ethics Committee of the Erasmus Medical Center approved all study procedures, and all parents provided written informed consent.

Child psychopathology assessment

Child psychopathology was assessed using the Child Behavior Checklist (CBCL/1½-5) when the children were on average 6 years old (Tiemeier, Velders et al. 2012). The CBCL/1½-5 is a widely-used 100-item inventory that provides parental report information on a wide array of behavioral problems in young children (Achenbach and Rescorla 2000). The CBCL/1½-5 has demonstrated good reliability and validity (Achenbach and Rescorla 2000), and multiple scales have been shown to be highly generalizable throughout the world

(Ivanova et al. 2010). The instrument provides two broadband scales (internalizing and externalizing), as well as syndrome scales and the DSM-oriented scales. The DSM-oriented scales were developed to view the rated problems in the context of a formal diagnostic system (Achenbach and Rescorla 2000), and have been shown to correspond to actual clinical diagnoses (van Lang et al. 2005). For this reason, the affective problems and anxiety problems scales (which correspond to DSM internalizing disorders), and the attention deficit/hyperactivity problems and oppositional defiant problems scales (which correspond to DSM externalizing disorders) were chosen for the present study. The items utilize a three-point scale (“Not True”, “Somewhat or Sometimes True”, “Very or Often True”), and were filled in by the primary caregiver, which was most often the biological mother (92%). Some example affective problem scale items include, “Looks unhappy without good reason” and “Unhappy, sad, or depressed”, and example anxiety problem items consist of, “Worries” and “Nervous, high-strung, or tense”. The two broadband scales (externalizing and internalizing) and the four DSM-oriented subscales were considered for analyses (see statistical analysis below). Raw scores were mathematically transformed using a square-root function.

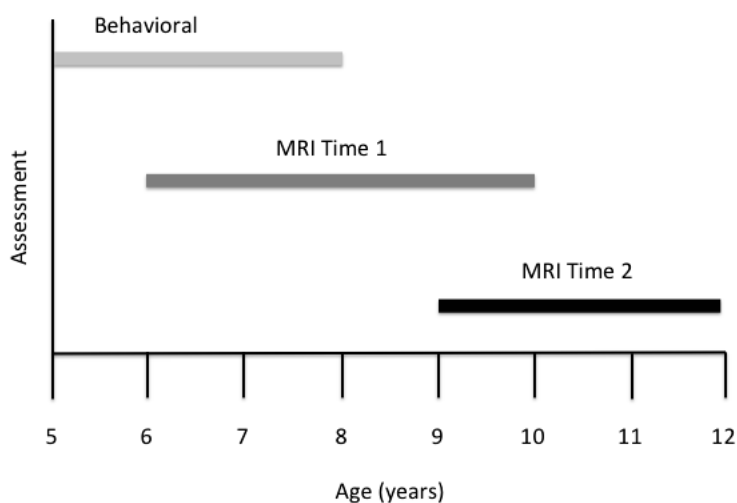


Figure 1.
Timeline of the study data collection points
Figure indicates the age ranges of study participants during each type of assessment

Image acquisition

Prior to scanning, all children underwent a 30-minute mock scanning session in order to acclimate them to the MR-environment (White, El Marroun et al. 2013). Data were acquired on two, 3 Tesla General Electric scanners (GE, MR750 (Time-1) MR750W (Time-2),

Milwaukee, WI). Both systems utilized an 8-channel receive-only head coil. Diffusion MRI data were collected at Time-1 with 3 $b=0$ volumes and 35 diffusion directions using an echo planar imaging sequence ($T_R = 11,000$ ms, $T_E = 83$ ms, Field of view = 256 mm x 256 mm, Acquisition Matrix = 128 x 128, slice thickness = 2 mm, number of slices = 77, $b = 1000$ s/mm²). For Time-2, a similar 35-direction echo planar imaging sequence was utilized ($T_R = 12,500$ ms, $T_E = 72$ ms, Field of view = 240 mm x 240 mm, Acquisition Matrix = 120 x 120, slice thickness = 2 mm, number of slices = 65, Asset Acceleration Factor = 2, $b=1000$ s/mm²).

Image preprocessing

Image preprocessing was conducted using the Functional MRI of the Brain's Software Library (FSL, version 5.0.5, Jenkinson et al. 2012) and the Camino Diffusion Toolkit (Cook et al. 2006). Diffusion images were first corrected for eddy current-induced artifacts and translations/rotations resulting from head motion, and non-brain tissue was removed. In order to account for rotations applied to the diffusion data, the resulting transformation matrices were used to rotate the diffusion gradient direction table. The diffusion tensor was fit at each voxel, and common scalar metrics (e.g., FA, MD) were subsequently computed. Additional details on pre- and post-processing of DTI data are available in the Supplemental Data section.

Fiber tractography

Probabilistic fiber tractography was run on each subject's diffusion data using the fully automated FSL plugin, "AutoPtx" (see Supplemental Material, de Groot et al. 2015). Connectivity distributions were estimated for 12 large fiber bundles, including the cingulum bundle, corticospinal tract, forceps major, forceps minor, inferior longitudinal fasciculus, superior longitudinal fasciculus, and uncinate fasciculus (Supplemental Table S1). Using these connectivity distributions, average FA and MD values were then computed for each fiber bundle.

Image quality assurance

Raw and processed diffusion image quality was assessed using a combination of automated and manual methods, which are described in detail in the Supplemental Material. The flow chart in Supplemental Figure S1 outlines the number of datasets excluded.

Statistical Analysis

Statistical analyses were conducted using the R Statistical Software version 3.1.3 (R Core Team 2014). Confirmatory factor analysis was used to compute global DTI measures (i.e., across multiple brain regions) using the Lavaan package (Rosseel 2012). The details of this approach have been described extensively elsewhere (Muetzel et al. 2015). For each DTI

scalar metric, the tracts depicted in Figure 2 (and listed in Supplemental Table S1) were summarized as a single latent factor, and the predicted factor scores for each subject were generated. Factor scores were computed separately for Time-1 and for Time-2, given the two waves were acquired on different MR-scanners, and were normally distributed. Linear mixed-effects models were fit using the LME4 package (Bates et al. 2015) to assess the association between psychiatric symptom scores and longitudinal changes in white matter microstructure. Linear mixed-effects models have numerous appealing features, including modeling of random effects, flexibility in uneven durations between time-points and handling of missing time-points. Equation 1 in the Supplemental Material outlines the general modeling strategy used. Primary analyses were run using all available MRI data at Time-1 ($n=715$) and Time-2 ($n=297$). To ensure missing data at follow-up was not contributing to (biasing) observed effects, supplemental analyses were also run using only complete data at Time-1 and Time-2 ($n=297$).

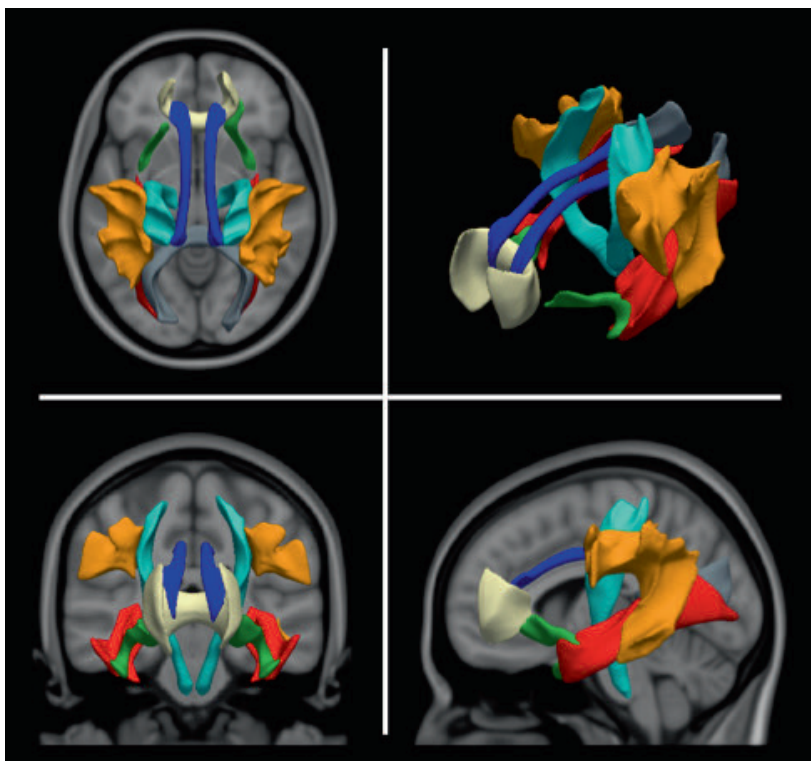


Figure 2.

Depiction of the tracts used in the global DTI metric

Note: Tracts are group average representations in standard coordinate space. Blue indicates the cingulum bundle, gray the forceps major, tan the forceps minor, red the inferior longitudinal fasciculus, orange the superior longitudinal fasciculus, and green the uncinate fasciculus.

In order to evaluate the specificity of the effects, a hierarchical approach was imposed. First, we tested whether broadband CBCL measures were associated with changes in global DTI metrics. If an association was observed with one of the CBCL broadband measures ($p < 0.05$), follow-up associations between the corresponding DSM-oriented scales (see above) and DTI metrics were then tested. This approach was utilized in order to determine whether broadly defined or specific psychiatric symptoms were related to white matter development. Second, along similar lines, in order to determine whether the effects on white matter microstructure were global (i.e., wide-spread in the brain) or focal (i.e., limited to a particular set of tracts), CBCL scores showing an association with global DTI metrics were associated with changes in DTI metrics within individual tracts. When examining individual tracts rather than the global factor, each tract was z-transformed within the time-point to control for any confounding effects of MR-scanner. Further, given the number of statistical tests examined with individual tracts, a false discovery rate (FDR) correction was applied to control for Type-I error (Benjamini and Hochberg 1995).

Non-response Analysis

A non-response analysis was conducted to compare characteristics of children with and without a Time-2 assessment. A two-sample t-test showed a difference in age at Time-1 between children with ($M = 7.7$ years) and without ($M = 8.2$ years) a Time-2 assessment ($t(713) = 5.9, p < 0.05$). Chi-squared tests did not show a difference in distribution of sex ($\chi(1, 715) = 0.4, p = 0.53$) or ethnicity ($\chi(2, 715) = 1.3, p = 0.51$). The internalizing problems scores ($t(713) = 1.3, p = 0.21$) and externalizing problems scores ($t(713) = 1.9, p = 0.06$) did not differ between children with and without a Time-2 MRI.

RESULTS

Sample Characteristics

Table 1 presents information on the characteristics of the sample. Children were approximately 8 years of age at the Time-1 MRI, and 10 years of age at the Time-2 MRI. Boys and girls were equally represented in the sample, and the average non-verbal IQ was slightly higher than the population mean.

Table 1. Sample characteristics

	Time 1	Time 2
N	715	297
Age	8.0 ± 1.03	10.2 ± 0.60
Sex (F/M, %)	48/52	49/51
non-Verbal IQ	103 ± 14	105 ± 14
Ethnicity (%)		
Dutch	71	73
Non-Western	21	20
Other Western	8	7

Longitudinal white matter development

Similar to other reports in the literature (Giorgio, Watkins et al. 2009), robust age-related changes in white matter were observed. Global FA increased over time (Estimate = 0.21, SE = 0.04, $p < 10^{-6}$) and global MD decreased over time (Estimate = -0.02, SE = 0.003, $p < 10^{-9}$). Effect estimates for age-related changes in FA and MD were similar across individual tracts.

Longitudinal white matter development and associations with psychiatric symptoms

Internalizing scores were negatively related to global changes in FA (Figure 3 and Table 2). Children with high levels of internalizing problems showed slower white matter development, relative to children with lower levels of problems (Estimate = -0.059, $p = 0.049$). Internalizing problems were not associated with changes in global MD (Table 2). When only complete data were analyzed (both Time-1 and Time-2 MRI, $n = 297$), results remained highly consistent for the effect observed between internalizing scores and changes in FA (Estimate = -0.061, $p = 0.055$). Externalizing problems were not associated with changes in global FA or MD (Table 2).

Table 2. Association between psychiatric symptoms and changes in white matter microstructure using linear mixed-effects models

Analysis Step	Predictor	DTI	Est	SE	t	χ^2	p
Primary	Externalizing	FA	-0.042	0.028	-1.521	2.313	0.128
		MD	0.000	0.002	-0.062	0.004	0.950
	Internalizing	FA	-0.059	0.030	-1.967	3.871	0.049
		MD	0.002	0.002	1.050	1.102	0.294
Secondary	Affective	FA	-0.154	0.048	-3.245	10.529	0.001
		MD	0.006	0.004	1.600	2.560	0.110
	Anxiety	FA	-0.052	0.043	-1.219	1.486	0.223
		MD	0.001	0.003	0.343	0.118	0.731

Note: Models adjusted for fixed effects, age at MRI assessment, sex, and ethnicity, and random effects of subject. CBCL scores are square root transformed, and model estimates represent the association between psychiatric problems and change in DTI metric. Analysis step refers to the hierarchical approach taken.

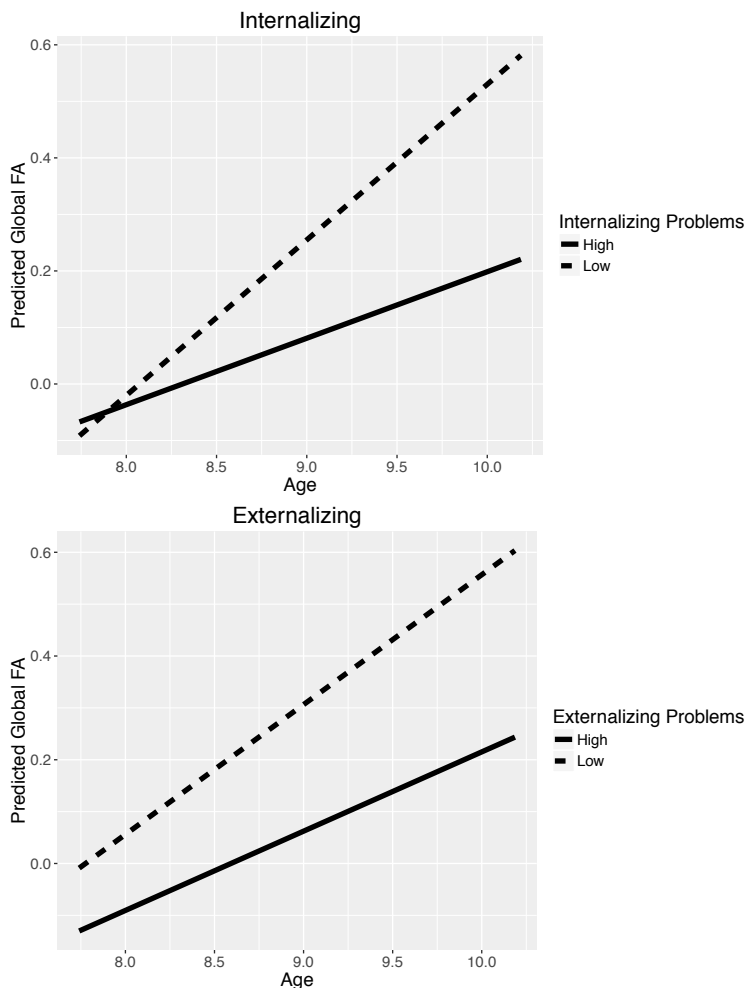


Figure 3.

Association between high and low levels of psychopathology and white matter development
Figure represents predicted model estimates derived from linear mixed effects models. The top panel shows broadband internalizing problems and the bottom panel shows broadband externalizing problems. Separate lines for 1 standard deviation above the mean problem score ("high") and 1 standard deviation below the mean problem score ("low"), with the Y-axis representing the predicted global FA value based on model estimates.

Specificity: affective and anxiety problems

Given that internalizing scores were related to changes in FA from Time-1 to Time-2, the two DSM-oriented internalizing scales, anxiety problems and affective problems, were also examined for associations with global FA and MD (Table 2). Affective problem scores were negatively associated with changes in global FA (Estimate = -0.15, $p = 0.001$). Children

with higher levels of affective symptoms showed slower white matter development. Anxiety problem scores were not associated with changes in FA. Changes in MD were not associated with affective or anxiety problem scores. Similar to what is described above, when only complete data were used (i.e., no missing data at follow-up, $N = 297$), the association of affective problem scores with changes in global FA remained highly consistent (Estimate = -0.16 , $p = 0.002$).

Individual tract analyses

In order to examine to what extent effects reported above were global (i.e., throughout the brain) or regional (i.e., limited to a subset of tracts), linear mixed effects analyses were run on the individual tracts (Supplemental Table S2). Broadband internalizing problem scores were associated with changes in FA in the right superior longitudinal fasciculus (Estimate = -0.06 , $p_{FDR} < 0.0001$). Internalizing problem scores were also related to slower changes in FA over time in the right cingulum bundle (Estimate = -0.021 , $p_{FDR} = 0.09$) and the left superior longitudinal fasciculus (Estimate = -0.03 , $p_{FDR} = 0.09$), though at a trend level after adjusting for multiple comparisons.

The DSM-oriented affective scale was associated with slower change in FA in the right cingulum bundle (Estimate = -0.06 , $p_{FDR} = 0.02$), inferior longitudinal fasciculus (Estimate = -0.06 , $p_{FDR} = 0.02$), and superior longitudinal fasciculus (Estimate = -0.011 , $p_{FDR} < 0.00001$). While not significant after adjustment for multiple comparisons, affective problems were related to slower changes in FA in the left cingulum bundle (Estimate = -0.05 , $p_{FDR} < 0.08$).

DISCUSSION

The present study demonstrates a link between psychiatric symptoms and white matter microstructural development in a large sample of children from the general population. Even in the general population, where psychiatric problems are typically milder than in clinical samples, problems were related to an altered trajectory of white matter development. Internalizing problems, specifically affective symptoms, were related to a reduced rate of white matter maturation while externalizing problems were not.

The present study is the largest to date that demonstrates a link between psychiatric problems on a continuum and altered white matter microstructural development, using over 1000 brain scans. In a recent study, a measure of both affective and anxiety symptoms combined was related to slower white matter microstructural development across a number of tracts in a smaller sample of children and adolescents (Albaugh, Ducharme et al. 2016). These data are consistent with the current study, although we demonstrate that a metric of affective problems (not combined with anxiety) is related to slower white matter maturation.

Given this association with affective problems, we primarily rely on available literature of DTI in patients with clinical depression to aid in the interpretation of findings. The present study showed both specific and global measures of white matter matured slower in children with internalizing problems. When examined on the tract level, children with higher levels of affective problems displayed altered white matter microstructural development in the cingulum bundle, inferior longitudinal fasciculus, and superior longitudinal fasciculus. Cross-sectional DTI studies of pediatric unipolar depression have shown lower FA in interhemispheric fibers, the cingulum, and the uncinate (LeWinn, Connolly et al. 2014). Studies in adults are more abundant, demonstrating lower FA in the superior longitudinal fasciculus (Murphy and Frodl 2011) and the uncinate (Bracht et al. 2015). However, not all reports are consistent, with some showing that higher FA is associated with depression. For example, higher FA was observed in the corticospinal tract in adults with major depression (Sacchet et al. 2014). Subclinical internalizing symptoms have also previously been linked to abnormal cortical neurodevelopment in children, particularly in areas of the ventromedial prefrontal cortex (Ducharme et al. 2014) that are innervated by the uncinate and to a lesser extent the superior longitudinal fasciculus (Schmahmann et al. 2007).

Given its functional significance, a large amount of work in depression and anxiety has focused on the amygdala and its white matter innervations such as the cingulum and the uncinate (Hulvershorn, Cullen et al. 2011). The amygdala is thought to be responsible for various aspects of emotion, and such aberrant white matter innervations that typically support higher-level emotional regulation could help to explain certain internalizing symptomatology. We found that FA in the cingulum bundle and inferior longitudinal fasciculus showed reduced maturation in children with higher levels of affective problems. These observations are consistent with the majority of available reports of depression in children, and potentially fit with theories of underlying amygdala dysfunction. Further, the direction of effects observed in all tracts and at the global level is consistent with the majority of reports in DTI that show lower FA and higher MD to be related to abnormal development or disease status.

Another intriguing observation from the present study was that the broad externalizing symptoms were not related to a differential developmental trajectory of white matter maturation. However, as can be seen in Figure 3, there is a visual suggestion of a ‘level’ rather than ‘slope’ difference in development. When evaluating broadband externalizing symptoms cross-sectionally, there is a marginal association with global FA at Time-2 ($p = 0.08$), but not at Time-1. It is possible that white matter microstructural deficits appear earlier in life in externalizing disorders compared with an apparent slowing of development in internalizing disorders. It is also possible that broadband externalizing symptoms along a continuum do not associate with global white matter maturation uniformly, especially given the heterogeneity in findings in, for instance, the ADHD literature (van Ewijk, Heslenfeld et al. 2012).

One of the main strengths of the current study is the large sample size and longitudinal design, with nearly 300 repeated DTI scans and over 1000 total scans included in analyses. With repeated measures, it is possible to not only look at cross-sectional associations between independent and dependent variables, but also examine changes in brain structure over time in relation to psychiatric symptoms. Further, the sample studied was part of a large cohort study, which is drawn from the general population. This has implications regarding the generalizability of findings in a broader context. Lastly, we characterized psychiatric symptoms along a continuum rather than utilizing a case-control design with clinical diagnoses. Dimensional approaches offer increased statistical power compared with dichotomous classifications, and also provide better generalizability compared with clinical samples. This approach is also consistent with current initiatives to improve our understanding of mental illness above and beyond traditional diagnostic constructs (e.g., the National Institute of Mental Health's Research Domain Criteria, Garvey, Avenevoli et al. 2016). However, important limitations warrant mention. First, the present study only examined a subset of white matter fiber bundles in the brain. It is possible there is Type-II error in the study related to either a white matter tract that was not included in the analyses or white matter deficits related to psychiatric disease that do not conform to the data-driven, anatomical boundaries determined by our tracking algorithm (i.e., a deficit is 'averaged out'). Second, imaging data were acquired on two separate MRI systems, possibly causing problems with the longitudinal interpretation of results. However, acquisitions were made as similar as possible (e.g., gradient table, head coil, etc.) and a number of steps were introduced to mitigate such problems, including within-scanner normalization of DTI metrics (e.g., confirmatory factor analysis and Z-score standardization), which should remove any effect of scanner. Further, we used linear mixed-effects analyses in the present study to test the association between psychiatric problems and change in DTI metrics, which is on the relative, rather than absolute, scale. Lastly, the assessment of psychiatric problems was conducted nearly two years prior to the first imaging assessment. However, adding age of psychiatric problem assessment to models did not change the results. Further, it is arguably relevant that a simple behavioral inventory at an early age can predict the trajectory of white matter development some years later.

In conclusion, this study demonstrates affective problems are related to altered white matter maturation in a large sample of children from the general population. Tracking the emergence of psychopathology in children, both in terms of symptomatology and neurobiology, may help guide not only diagnosticians, but also improve the selection and timing of treatments (Singh et al. 2015, Wolfers et al. 2015).

REFERENCES

- Achenbach, T. M. and L. A. Rescorla (2000). Manual for ASEBA preschool forms & profiles. Burlington, VT, University of Vermont, Research Center for Children, Youth & Families.
- Albaugh, M. D., S. Ducharme, S. Karama, R. Watts, J. D. Lewis, C. Orr, T. V. Nguyen, R. C. McKinstry, K. N. Botteron, A. C. Evans, J. J. Hudziak and G. Brain Development Cooperative (2016). Anxious/depressed symptoms are related to microstructural maturation of white matter in typically developing youths. *Dev Psychopathol*: 1-8.
- Basser, P. J., J. Mattiello and D. LeBihan (1994). MR diffusion tensor spectroscopy and imaging. *Biophys J* **66**(1): 259-267.
- Bates, D., M. Maechler, B. Bolker and S. Walker (2015). lme4: Linear mixed-effects models using Eigen and S4. <https://CRAN.R-project.org/package=lme4>.
- Beaulieu, C. (2002). The basis of anisotropic water diffusion in the nervous system - a technical review. *NMR Biomed* **15**(7-8): 435-455.
- Benjamini, Y. and Y. Hochberg (1995). Controlling the false discovery rate: a practical and powerful approach to multiple testing. *Journal of the Royal Statistical Society* **57**(1): 289-300.
- Blanken, L. M., S. E. Mous, A. Ghassabian, R. L. Muetzel, N. K. Schoemaker, H. El Marroun, A. van der Lugt, V. W. Jaddoe, A. Hofman, F. C. Verhulst, H. Tiemeier and T. White (2015). Cortical morphology in 6- to 10-year old children with autistic traits: a population-based neuroimaging study. *Am J Psychiatry* **172**(5): 479-486.
- Bracht, T., D. Linden and P. Keedwell (2015). A review of white matter microstructure alterations of pathways of the reward circuit in depression. *J Affect Disord* **187**: 45-53.
- Cook, P. A., Y. Bai, S. Nedjati-Gilani, K. K. Seunarine, M. G. Hall, G. J. Parker and D. C. Alexander (2006). Camino: Open-Source Diffusion-MRI Reconstruction and Processing. 14th Scientific Meeting of the International Society for Magnetic Resonance in Medicine. Seattle, WA, USA: 2759.
- de Groot, M., M. A. Ikram, S. Akoudad, G. P. Krestin, A. Hofman, A. van der Lugt, W. J. Niessen and M. W. Vernooij (2015). Tract-specific white matter degeneration in aging: The Rotterdam Study. *Alzheimers Dement* **11**(3): 321-330.
- Di Martino, A., D. A. Fair, C. Kelly, T. D. Satterthwaite, F. X. Castellanos, M. E. Thomason, R. C. Craddock, B. Luna, B. L. Leventhal, X. N. Zuo and M. P. Milham (2014). Unraveling the miswired connectome: a developmental perspective. *Neuron* **83**(6): 1335-1353.
- Ducharme, S., M. D. Albaugh, J. J. Hudziak, K. N. Botteron, T. V. Nguyen, C. Truong, A. C. Evans, S. Karama and G. Brain Development Cooperative (2014). Anxious/depressed symptoms are linked to right ventromedial prefrontal cortical thickness maturation in healthy children and young adults. *Cereb Cortex* **24**(11): 2941-2950.
- Garvey, M., S. Avenevoli and K. Anderson (2016). The National Institute of Mental Health Research Domain Criteria and Clinical Research in Child and Adolescent Psychiatry. *J Am Acad Child Adolesc Psychiatry* **55**(2): 93-98.
- Giedd, J. N., A. Raznahan, A. Alexander-Bloch, E. Schmitt, N. Gogtay and J. L. Rapoport (2015). Child psychiatry branch of the National Institute of Mental Health longitudinal structural magnetic resonance imaging study of human brain development. *Neuropsychopharmacology* **40**(1): 43-49.
- Giorgio, A., K. E. Watkins, M. Chadwick, S. James, L. Winmill, G. Douaud, N. De Stefano, P. M. Matthews, S. M. Smith, H. Johansen-Berg and A. C. James (2009). Longitudinal changes in grey and white matter during adolescence. *Neuroimage*.
- Hofstra, M. B., J. van der Ende and F. C. Verhulst (2002). Child and adolescent problems predict DSM-IV disorders in adulthood: a 14-year follow-up of a Dutch epidemiological sample. *J Am Acad Child Adolesc Psychiatry* **41**(2): 182-189.

- Hulvershorn, L. A., K. Cullen and A. Anand (2011). Toward dysfunctional connectivity: a review of neuroimaging findings in pediatric major depressive disorder. *Brain Imaging Behav* **5**(4): 307-328.
- Ivanova, M. Y., T. M. Achenbach, L. A. Rescorla, V. S. Harder, R. P. Ang, N. Bilenberg, G. Bjarnadottir, C. Capron, S. S. De Pauw, P. Dias, A. Dobrean, M. Doepfner, M. Duyme, V. Eapen, N. Erol, E. M. Esmaeili, L. Ezpeleta, A. Frigerio, M. M. Goncalves, H. S. Gudmundsson, S. F. Jeng, P. Jetishi, R. Jusiene, Y. A. Kim, S. Kristensen, F. Lecannelier, P. W. Leung, J. Liu, R. Montirosso, K. J. Oh, J. Plueck, R. Pomalima, M. Shahini, J. R. Silva, Z. Simsek, A. Sourander, J. Valverde, K. G. Van Leeuwen, B. S. Woo, Y. T. Wu, S. R. Zubrick and F. C. Verhulst (2010). Preschool psychopathology reported by parents in 23 societies: testing the seven-syndrome model of the child behavior checklist for ages 1.5-5. *J Am Acad Child Adolesc Psychiatry* **49**(12): 1215-1224.
- Jaddoe, V. W., C. M. van Duijn, O. H. Franco, A. J. van der Heijden, M. H. van Iizendoorn, J. C. de Jongste, A. van der Lugt, J. P. Mackenbach, H. A. Moll, H. Raat, F. Rivadeneira, E. A. Steegers, H. Tiemeier, A. G. Uitterlinden, F. C. Verhulst and A. Hofman (2012). The Generation R Study: design and cohort update 2012. *European journal of epidemiology* **27**(9): 739-756.
- Jenkinson, M., C. F. Beckmann, T. E. Behrens, M. W. Woolrich and S. M. Smith (2012). *Fsl*. *Neuroimage* **62**(2): 782-790.
- Lenroot, R. K. and J. N. Giedd (2006). Brain development in children and adolescents: insights from anatomical magnetic resonance imaging. *Neurosci Biobehav Rev* **30**(6): 718-729.
- LeWinn, K. Z., C. G. Connolly, J. Wu, M. Drahos, F. Hoeft, T. C. Ho, A. N. Simmons and T. T. Yang (2014). White matter correlates of adolescent depression: structural evidence for frontolimbic disconnectivity. *J Am Acad Child Adolesc Psychiatry* **53**(8): 899-909, 909 e891-897.
- Mana, S., M. L. Paillere Martinot and J. L. Martinot (2010). Brain imaging findings in children and adolescents with mental disorders: a cross-sectional review. *Eur Psychiatry* **25**(6): 345-354.
- Mous, S. E., R. L. Muetzel, H. El Marroun, T. J. C. Polderman, V. W. Jaddoe, A. Hofman, F. Verhulst, H. Tiemeier, D. Posthuma and T. White (2014). Cortical Thickness and Inattention/Hyperactivity Symptoms in Young Children: a population-based study. *Psychological Medicine* **in press**.
- Muetzel, R. L., S. E. Mous, J. van der Ende, L. M. Blanken, A. van der Lugt, V. W. Jaddoe, F. C. Verhulst, H. Tiemeier and T. White (2015). White matter integrity and cognitive performance in school-age children: A population-based neuroimaging study. *Neuroimage* **119**: 119-128.
- Murphy, M. L. and T. Frodl (2011). Meta-analysis of diffusion tensor imaging studies shows altered fractional anisotropy occurring in distinct brain areas in association with depression. *Biol Mood Anxiety Disord* **1**(1): 3.
- Pine, D. S., E. Cohen, P. Cohen and J. Brook (1999). Adolescent depressive symptoms as predictors of adult depression: moodiness or mood disorder? *Am J Psychiatry* **156**(1): 133-135.
- Pine, D. S., A. E. Guyer and E. Leibenluft (2008). Functional magnetic resonance imaging and pediatric anxiety. *J Am Acad Child Adolesc Psychiatry* **47**(11): 1217-1221.
- R Core Team (2014). *R: A Language and Environment for Statistical Computing*. Vienna, Austria, R foundation for Statistical Computing.
- Regier, D. A. (2007). Dimensional approaches to psychiatric classification: refining the research agenda for DSM-V: an introduction. *Int J Methods Psychiatr Res* **16 Suppl 1**: S1-5.
- Rosseel, Y. (2012). *lavaan*: An R package for structural equation modeling. *Journal of Statistical Software* **48**(2): 1-36.
- Sacchet, M. D., G. Prasad, L. C. Foland-Ross, S. H. Joshi, J. P. Hamilton, P. M. Thompson and I. H. Gotlib (2014). Structural abnormality of the corticospinal tract in major depressive disorder. *Biol Mood Anxiety Disord* **4**: 8.
- Schmahmann, J. D., D. N. Pandya, R. Wang, G. Dai, H. E. D'Arceuil, A. J. de Crespigny and V. J. Wedeen (2007). Association fibre pathways of the brain: parallel observations from diffusion spectrum imaging and autoradiography. *Brain* **130**(Pt 3): 630-653.

- Schmithorst, V. J. and W. Yuan (2010). White matter development during adolescence as shown by diffusion MRI. *Brain Cogn* **72**(1): 16-25.
- Singh, M. K., A. S. Garrett and K. D. Chang (2015). Using neuroimaging to evaluate and guide pharmacological and psychotherapeutic treatments for mood disorders in children. *CNS Spectr* **20**(4): 359-368.
- Tiemeier, H., F. P. Velders, E. Szekely, S. J. Roza, G. Dieleman, V. W. Jaddoe, A. G. Uitterlinden, T. J. White, M. J. Bakermans-Kranenburg, A. Hofman, M. H. Van Ijzendoorn, J. J. Hudziak and F. C. Verhulst (2012). The Generation R Study: A review of design, findings to date, and a study of the 5-HTTLPR by environmental interaction from fetal life onward. *Journal of the American Academy of Child and Adolescent Psychiatry* **51**(11): 1119-1135 e1117.
- van Ewijk, H., D. J. Heslenfeld, M. P. Zwiers, J. K. Buitelaar and J. Oosterlaan (2012). Diffusion tensor imaging in attention deficit/hyperactivity disorder: a systematic review and meta-analysis. *Neurosci Biobehav Rev* **36**(4): 1093-1106.
- van Lang, N. D., R. F. Ferdinand, A. J. Oldehinkel, J. Ormel and F. C. Verhulst (2005). Concurrent validity of the DSM-IV scales Affective Problems and Anxiety Problems of the Youth Self-Report. *Behav Res Ther* **43**(11): 1485-1494.
- White, T., H. El Marroun, I. Nijs, M. Schmidt, A. van der Lugt, P. A. Wielopolski, V. W. Jaddoe, A. Hofman, G. P. Krestin, H. Tiemeier and F. C. Verhulst (2013). Pediatric population-based neuroimaging and the Generation R Study: the intersection of developmental neuroscience and epidemiology. *European journal of epidemiology* **28**(1): 99-111.
- Wolfers, T., J. K. Buitelaar, C. F. Beckmann, B. Franke and A. F. Marquand (2015). From estimating activation locality to predicting disorder: A review of pattern recognition for neuroimaging-based psychiatric diagnostics. *Neurosci Biobehav Rev* **57**: 328-349.

SUPPLEMENTAL MATERIAL

METHODS

Image preprocessing

Image preprocessing was conducted using the Functional MRI of the Brain's Software Library (FSL, version 5.0.5, Jenkinson et al. 2012) and the Camino Diffusion Toolkit (Cook et al. 2006) via the Neuroimaging in Python Pipelines and Interfaces package (Nipype, version 0.92, Gorgolewski et al. 2011). Details of the image processing have been described in detail elsewhere (Muetzel et al. 2015). Briefly, diffusion images were first corrected for eddy current-induced artifacts and translations/rotations resulting from head motion, and non-brain tissue was removed (Jenkinson and Smith 2001). In order to account for rotations applied to the diffusion data, the resulting transformation matrices were used to rotate the diffusion gradient direction table. The diffusion tensor was fit using the RESTORE method (Chang et al. 2005), and common scalar metrics (e.g., FA, MD) were subsequently computed.

Fiber tractography

Probabilistic fiber tractography was run on each subject's diffusion data using the fully automated, freely available FSL plugin, "AutoPtx" (de Groot et al. 2015). Briefly, the Bayesian Estimation of Diffusion Parameters Obtained using Sampling Techniques (BESTPOSTx) package from FSL was first used to estimate the diffusion parameters at each voxel, accounting for two fiber orientations (Behrens et al. 2007). Next, a predefined set of seed and target masks, supplied by the AutoPtx software, were aligned to each subject's diffusion data in native space using a nonlinear registration. The FSL probabilistic fiber tracking algorithm, Probtrackx, was then used to identify connectivity distributions for a number of large, commonly reported fiber bundles, based on the predefined seed and target marks (Supplemental Table S1). Connectivity distributions obtained from the fiber tracking process were then normalized based on the number of successful seed-to-target attempts, and then thresholded to remove voxels that were unlikely to be part of the true distribution. For each tract, average DTI scalar metrics (e.g., FA, MD), weighted by the connectivity distribution, were computed (Muetzel, Mous et al. 2015). Thus, compared to voxels with a lower probability, voxels with a high probability of being part of the true white matter bundle have a higher contribution to the average DTI scalar value computed across the entire tract.

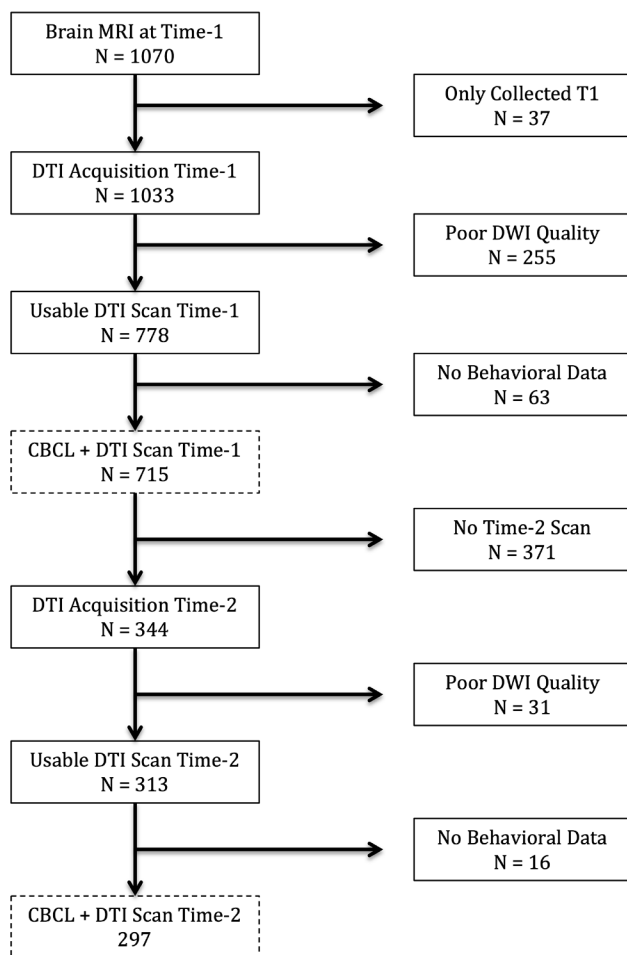
Supplemental Table S1. Tracts used in analyses and factor loadings for global latent factor

Tract	Hemisphere	FA	MD
Cingulum Bundle	Left	0.645	0.675
	Right	0.637	0.667
Corticospinal Tract	Left	0.346	0.586
	Right	0.388	0.592
Forceps Major	-	0.595	0.348
Forceps Minor	-	0.360	0.609
Inferior Longitudinal Fasciculus	Left	0.686	0.752
	Right	0.709	0.782
Superior Longitudinal Fasciculus	Left	0.685	0.800
	Right	0.745	0.776
Uncinate Fasciculus	Left	0.547	0.723
	Right	0.591	0.758
<u>Fit Measures</u>			
CFI		0.949	0.973
TLI		0.931	0.964
RMSEA		0.079	0.061
SRMR		0.045	0.030

Note: Factor loadings are based on Time-1 DTI data. Factor loadings for Time-2 were highly similar.

Image quality assurance

Diffusion image quality was assessed using two methods. First, the DTIPrep tool (<https://www.nitrc.org/projects/dtiprep/>) was used to automatically examine the data for slicewise variation, characteristic of artifact, in each diffusion-weighted volume. Second, the sum-of-squares error (SSE) maps from the diffusion tensor calculations were examined for structured signal that was indicative of artifact. Each SSE map was rated from 0-to-3 (0: “None”, 1: “Mild”, 2: “Moderate”, 3: “Severe”). Any cases not excluded by the automated DTIPrep tool but still had a “Severe” score from the SSE rating were also excluded from analyses. Processed tractography data were also examined for problems in two ways. First, the registration of the DTI data to standard space was inspected for accuracy. Second, each tract was examined for grossly misclassified voxels in the connectivity distribution. The flow chart in Supplemental Figure S1 outlines the number of datasets excluded for each of the above outlined quality assurance measures.



Supplemental Figure S1.

Flow chart indicating data inclusion/exclusion

Note: Boxes with dotted lines indicate the sample used in the current study. CBCL = Child behavior checklist.

Statistical Analysis

Equation 1.

$$DTI_{ij} \sim Age_{ij} + Sex_i + Ethnicity_i + CBCL_i + Age_{ij} \times CBCL_i + (1 | Subject)$$

Where the i subscript denotes the subject, the j subscript denotes the time-point, Age is the age at MRI, CBCL is the square-root transformed problem score measured by the CBCL (i.e., broadband or DSM scale), and DTI is the global DTI factor (i.e., for FA or MD). Fixed

effects in this model are age, sex, ethnicity, CBCL and the CBCL-by-age interaction, and the subject identifier is used to model random effects (i.e., intercepts for each subject). Models were estimated with a Maximum-Likelihood Estimator (ML), and the Wald χ^2 from a step-wise ANOVA method (“car” package, Fox and Weisberg 2011) was used to evaluate different models and the contribution of each model term above-and-beyond the other terms.

Supplemental Table S2. Individual Tract Analyses

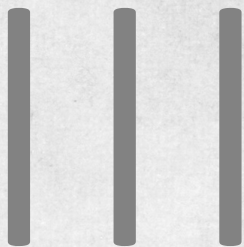
Predictor	Tract	Hemisphere	Est	SE	t	χ^2	p	p_{FDR}
Internalizing	CB	L	-0.021	0.013	-1.582	2.501	0.114	0.228
		R	-0.029	0.013	-2.269	5.148	0.023	0.093
	CST	L	0.002	0.014	0.173	0.030	0.863	0.863
		R	0.009	0.014	0.597	0.357	0.550	0.804
	FMa	-	-0.006	0.012	-0.520	0.271	0.603	0.804
	FMi	-	-0.011	0.015	-0.710	0.505	0.477	0.804
	ILF	L	-0.020	0.012	-1.619	2.620	0.106	0.228
		R	-0.025	0.014	-1.795	3.223	0.073	0.218
	SLF	L	-0.030	0.013	-2.345	5.500	0.019	0.093
		R	-0.060	0.013	-4.565	20.837	<1x10 ⁻⁴	<1x10 ⁻⁴
Affective	UF	L	0.004	0.013	0.311	0.097	0.756	0.852
		R	-0.004	0.014	-0.278	0.077	0.781	0.852
	CB	L	-0.046	0.021	-2.218	4.920	0.027	0.080
		R	-0.059	0.020	-2.924	8.553	0.003	0.020
	CST	L	0.018	0.022	0.800	0.641	0.424	0.462
		R	0.031	0.023	1.342	1.801	0.180	0.239
	FMa	-	-0.012	0.020	-0.622	0.387	0.534	0.534
	FMi	-	-0.035	0.025	-1.430	2.045	0.153	0.229
	ILF	L	-0.031	0.020	-1.565	2.450	0.118	0.201
		R	-0.062	0.022	-2.809	7.890	0.005	0.020
	SLF	L	-0.039	0.021	-1.878	3.526	0.060	0.145
		R	-0.106	0.021	-5.016	25.162	<1x10 ⁻⁵	<1x10 ⁻⁵
	UF	L	-0.018	0.021	-0.860	0.740	0.390	0.462
		R	-0.036	0.022	-1.629	2.653	0.103	0.201

Note: Linear mixed effects models demonstrating the association between psychiatric problems and individual tract FA values. CB = cingulum bundle, CST = cortical spinal tract, FMa = forceps major, FMi = forceps minor, ILF = inferior longitudinal fasciculus, SLF = superior longitudinal fasciculus, UF = uncinate fasciculus. p_{FDR} indicates a false discovery rate correction was applied to p-values.

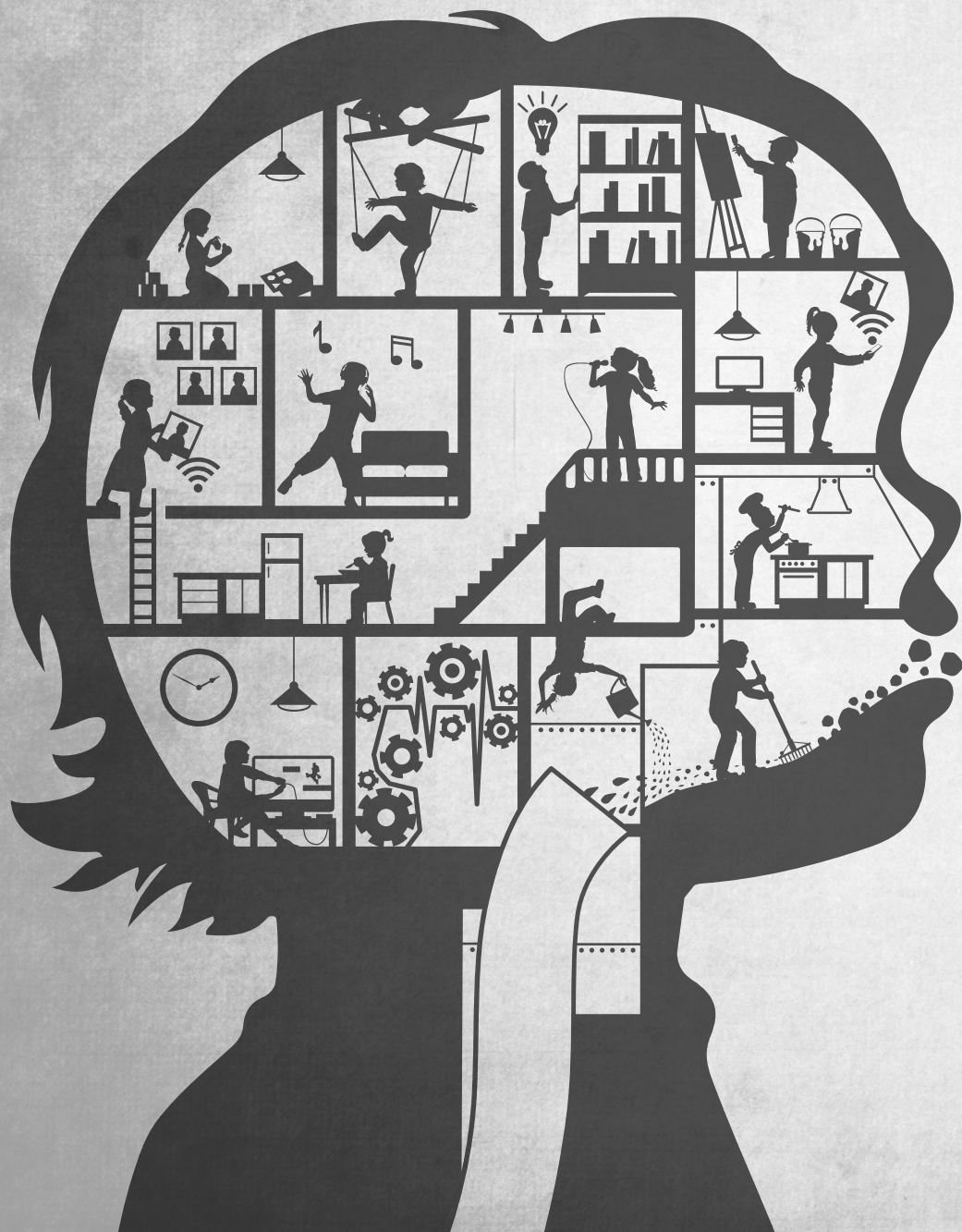
REFERENCES

- Behrens, T. E., H. J. Berg, S. Jbabdi, M. F. Rushworth and M. W. Woolrich (2007). Probabilistic diffusion tractography with multiple fibre orientations: What can we gain? *Neuroimage* **34**(1): 144-155.
- Chang, L. C., D. K. Jones and C. Pierpaoli (2005). RESTORE: robust estimation of tensors by outlier rejection. *Magn Reson Med* **53**(5): 1088-1095.
- Cook, P. A., Y. Bai, S. Nedjati-Gilani, K. K. Seunarine, M. G. Hall, G. J. Parker and D. C. Alexander (2006). Camino: Open-Source Diffusion-MRI Reconstruction and Processing. 14th Scientific Meeting of the International Society for Magnetic Resonance in Medicine. Seattle, WA, USA: 2759.
- de Groot, M., M. A. Ikram, S. Akoudad, G. P. Krestin, A. Hofman, A. van der Lugt, W. J. Niessen and M. W. Vernooij (2015). Tract-specific white matter degeneration in aging: The Rotterdam Study. *Alzheimers Dement* **11**(3): 321-330.
- Fox, J. and S. Weisberg (2011). *An R Companion to Applied Regression*. Thousand Oaks, CA, Sage.
- Gorgolewski, K., C. D. Burns, C. Madison, D. Clark, Y. O. Halchenko, M. L. Waskom and S. S. Ghosh (2011). Nipype: a flexible, lightweight and extensible neuroimaging data processing framework in python. *Front Neuroinform* **5**: 13.
- Jenkinson, M., C. F. Beckmann, T. E. Behrens, M. W. Woolrich and S. M. Smith (2012). Fsl. *Neuroimage* **62**(2): 782-790.
- Jenkinson, M. and S. Smith (2001). A global optimisation method for robust affine registration of brain images. *Med Image Anal* **5**(2): 143-156.
- Muetzel, R. L., S. E. Mous, J. van der Ende, L. M. Blanken, A. van der Lugt, V. W. Jaddoe, F. C. Verhulst, H. Tiemeier and T. White (2015). White matter integrity and cognitive performance in school-age children: A population-based neuroimaging study. *Neuroimage* **119**: 119-128.

PART



Intrinsic Functional Connectivity During Childhood



CHAPTER

6

Resting-state networks in 6-to-10 year-old children

Ryan L. Muetzel, Laura M. E. Blanken, Sandra Thijssen,
Aad van der Lugt, Vincent W.V. Jaddoe, Frank C. Verhulst,
Henning Tiemeier, Tonya White

Human Brain Mapping (in press)

ABSTRACT

Resting-state functional magnetic resonance imaging provides a non-invasive approach to the study of intrinsic functional brain networks. When applied to the study of brain development, most studies consist of relatively small samples that are not always representative of the general population. Descriptions of these networks in the general population offer important insight for clinical studies examining, for instance, psychopathology or neurological conditions. Thus our goal was to characterize resting-state networks in a large sample of children using independent component analysis (ICA). We further aimed to describe the robustness of these networks by examining which networks occur frequently after repeated ICA. Resting-state networks were obtained from a sample of 536 6-to-10 year-old children. Distributions of networks were built from repeated subsampling and group ICA analyses, and meta-ICA was used to construct a representative set of components. Within- and between-network properties were tested for age-related developmental associations using spatio-temporal regression. After repeated ICA, many networks were present over 95% of the time suggesting the components are highly reproducible. Some networks were less robust, and were observed less than 70% of the time. Age-related associations were also observed in a selection of networks, including the default-mode network, offering further evidence of development in these networks at an early age. ICA-derived resting-state networks appear to be robust, although some networks should be further scrutinized if subjected to group-level statistical analyses, such as spatiotemporal regression. The final set of ICA-derived networks and an age-appropriate T_1 -weighted template are made available to the neuroimaging community.

INTRODUCTION

Resting-state functional magnetic resonance imaging (RS-fMRI) relies on a phenomenon referred to as intrinsic brain activity, or brain activity that is not induced by an external stimulus. In the context of RS-fMRI, functional connectivity is explored when temporal fluctuations in blood oxygen level-dependent maps are used to identify brain regions with high temporal correlation. Quantifying functional connectivity can be achieved through various analysis strategies, such as seed-based analyses, graph theoretical models, and independent component analyses (ICA) (Cole et al. 2010). The ICA of RS-fMRI data aims to reduce complex data into statistically distinct components (Calhoun et al. 2001, Beckmann et al. 2005). These distinct components can be classified to describe either brain RS-fMRI networks (RSNs, e.g., the default mode network) or noise signals (e.g., motion, flow artifact, non-neuronal physiological noise). However, heterogeneity exists in the literature in terms of the selection (subset) of components reported; for instance, one study of children reports the executive control network (Jolles et al. 2011) while another does not (de Bie et al. 2012). Further, reports of RSNs from ICA are limited in young children and are typically based on relatively small sample sizes.

Studying RSNs in healthy children contributes significantly to the literature, both in terms of describing normal brain development and in comparisons with neurological and psychiatric problems. To date, three studies have used a pure ICA approach to examine RSNs in young, typically developing children (Littow et al. 2010, Jolles, van Buchem et al. 2011, de Bie, Boersma et al. 2012). In a study of 5-to-8 year-old children (n=18), de Bie et al. (2012) labeled fourteen components as RSNs, based on the anatomical locations of the spatial maps, and the power spectra of the accompanying time series. Jolles et al. (2010) examined a sample of 11-to-13 year-olds (n=19) and a group of young adults (n=29) using RS-fMRI. Thirteen components were labeled as functionally relevant and were further evaluated for age-related differences in RSNs. Finally, Littow et al. (2010) examined a large sample (n=168) of healthy adolescents and adults, categorized into three groups: adolescents, young adults and older adults. The authors identified 21 RSNs, some of which showed differences across the age-groupings, both in terms of spatial extent of the components and the power spectra. In addition to the above literature in children and adolescents, certain resting-state components, including the default mode network, have also been identified very early in development (Gao et al. 2009).

In both the adult and pediatric literature, two specific aspects of ICA analysis deserve mention. First, many common ICA algorithms available for use with RS-fMRI data operate under certain assumptions to increase efficiency, given the computational resources necessary to accommodate the magnitude of information in typical fMRI datasets. This has been shown to lead to variability in the resulting components (Himberg et al. 2004,

Franco et al. 2013). Along similar lines, other unexpected factors that are algorithm-dependent can influence components resulting from ICA, such as subject order (Zhang et al. 2010). Secondly, in many studies utilizing group ICA, only the components of interest are commonly reported, meaning components of non-interest or noise are often neglected. Thus, there is variability in the literature in terms of the components that are examined, which may be related to methodological aspects of ICA analysis, or simply because of subjectivity in which components are reported. Further, it is possible that some of these ‘noise’ components, such as those related to susceptibility artifact or to blood flow artifact, will be highly consistent across studies, while others (e.g., thermal or scanner-specific) will not. The presence or absence of certain components may also be impacted by the level of “cleaning” or “denoising” applied to the data, for instance censoring corrupt volumes (Power et al. 2012) or ICA-based artifact removal (Griffanti et al. 2014). This is of particular importance when studying children, given their tendency to have higher levels of motion compared to adults (Satterthwaite et al. 2012).

Within this context, it was the goal of this study to characterize ICA-derived resting-state networks in school-age children. We utilized a large sample of 6-to-10 year-old children to develop an age-appropriate, standardized set of RSNs using a subsampling approach to account for some of the sources of variability. We hypothesized some networks (for instance those reported frequently in the literature) would be robust across multiple ICA analyses, whereas others would be observed less frequently. We also examine developmental aspects in a subset of components by using within- and between-network age-associations. The present study expands upon the current literature in multiple ways. First, the only other resting-state studies in children utilizing ICA are based on relatively small samples. Second, RS-fMRI studies utilizing ICA typically report only a subset of the components identified, making more global comparisons across studies difficult. Lastly, the current study reports on the frequency different components are identified by ICA, offering future work a framework for deciding what level of caution to be used when interpreting results from certain low-frequency components. Components robust against repeated subsampling can be regarded as valid in previous studies and confidently analyzed in future efforts. Components shown to be more variable should be interpreted carefully, as they could be the result of a number of factors, including age-related effects, individual differences or even artifacts or methodological issues.

MATERIALS AND METHODS

Participants

The current study is embedded in the Generation R Study, which is a large, population-based birth cohort in Rotterdam, the Netherlands (Jaddoe et al. 2012). One thousand seventy children, ages 6-to-10 years, were scanned between September 2009 and July 2013 as part of a sub-study within the Generation R Study (White et al. 2013). General exclusion criteria for the current study include severe motor or sensory disorders (deafness or blindness), neurological disorders, moderate to severe head injuries with loss of consciousness, claustrophobia, and contraindications to MRI. Informed consent was obtained from parents, and all procedures were approved by the Medical Ethics Committee of the Erasmus Medical Center.

Of the 1,070 children with an MR-scanning session, 964 completed a RS-fMRI scan. Of the children with a RS-fMRI scan, 652 were characterized as not having behavioral problems (see Section 2.2 below for assessment of child behavioral problems). Of those 652 data sets, 88 showed excessive motion (described in section 2.4.4), and an additional 28 datasets had problems with pre-processing (e.g., poor registration to common space) rendering them unfit for post-processing. Thus, 536 children (mean age 7.9 years, 49% female) were included in the final sample for data analysis (Table 1).

Table 1. Sample Characteristics

	N = 536
Child Characteristics	
<i>General</i>	
Age at MRI (years)	7.96 ± 0.98
Sex (M/F, %)	51.5 / 48.5
Non-Verbal IQ	103.8 ± 14.0
Handedness (Right/Left, %)	89.9 / 10.1
<i>Ethnicity</i>	
Dutch (%)	75.9
Non-Western (%)	16.6
Other Western (%)	7.5
<i>fMRI Motion Parameters</i>	
Avg. RMS Relative (mm)	0.13 ± 0.11
Maternal Characteristics	
<i>Educational level (%)</i>	
Primary	5.0
Secondary	40.3
Higher	54.6

Note: Data presented are mean ± standard deviation, unless otherwise noted.

Behavioral assessment

Behavioral problems in children were assessed through maternal report using the Child Behavioral Checklist (CBCL/1½-5) (Achenbach and Rescorla 2000) as part of the age 6 assessment wave (Tiemeier et al. 2012). The CBCL is a 99-item inventory that uses a Likert response format (e.g., “Not True”, “Somewhat True”, “Very True”). Seven syndrome scales, five DSM-oriented scales, and three broadband scales are commonly derived summary measures from the CBCL (Achenbach and Ruffle 2000, Tick et al. 2007). In order to obtain a set of networks that are not influenced by potentially aberrant networks that may be present in children with behavioral problems, participants who scored higher than the clinical cutoff on any syndrome scale, DSM-oriented scale, broadband scale, or total problems score were excluded from analyses. Cutoff scores used in this study were based on norms from the Dutch population (Tick, van der Ende et al. 2007). As mentioned above, of the 964 children with an RS-fMRI scan, 312 children with CBCL scores above the clinical cutoff were excluded.

MR data acquisition

Magnetic resonance imaging data were acquired on a 3 Tesla scanner (Discovery 750, General Electric, Milwaukee, WI) using a standard 8-channel, receive-only head coil. A three-plane localizer was run first and used to position all subsequent scans. Structural T_1 -weighted images were acquired using a fast spoiled gradient-recalled echo (FSPGR) sequence (TR = 10.3 ms, TE = 4.2 ms, TI = 350 ms, NEX = 1, flip angle = 16°, matrix = 256 x 256, field of view (FOV) = 230.4 mm, slice thickness = 0.9mm). Echo planar imaging was used for the RS-fMRI session with the following parameters: TR = 2000 ms, TE = 30 ms, flip angle = 85°, matrix = 64 x 64, FOV = 230 mm x 230 mm, slice thickness = 4 mm. In order to determine the number of TRs necessary for functional connectivity analyses, early acquisitions acquired 250 TRs (acquisition time = 8min 20sec). After it was determined fewer TRs were required for these analyses, the number of TRs was reduced to 160 (acquisition time = 5min 20, see section 2.4.1 for additional details) (Langeslag et al. 2012, White et al. 2014). Children were instructed to stay awake, keep their eyes closed, and not to think about anything in particular during the RS-fMRI scan. Further details on the entire scanning protocol can be found elsewhere (White, El Marroun et al. 2013).

MR data processing

MR data pre-processing

Data were first converted from DICOM to Nifti format using the “dcm2nii” tool from the MRICRO library (<http://www.mccauslandcenter.sc.edu/mricro/mricron/dcm2nii.html>). Prior to analysis, in cases where 250 RS-fMRI volumes were acquired (see section 2.3), the scans were trimmed to 160 volumes by omitting volumes at the end of the acquisition to

ensure full compatibility with the other, 160 volume datasets. Data were pre-processed using the Functional MRI of the Brain (FMRIB) Software Library (v5.0.5, FSL, <http://fsl.fmrib.ox.ac.uk/fsl/fslwiki>) (Jenkinson et al. 2012). FSL's FMRI Expert Analysis Tool (FEAT) was used for preprocessing the RS-FMRI data, which consisted of exclusion of the first four volumes, motion correction, high-pass temporal filtering ($\sigma = 50$ s), brain extraction, pre-whitening, and spatial filtering (FWHM = 8 mm). Registration of the RS-FMRI data to an age-appropriate, standard space, T_1 -weighted template (see Section 2.4.3 for details) was achieved using a two-step process. First, the RS-FMRI data were registered to the T_1 -weighted anatomical image with the FSL-Linear Registration Tool (FLIRT), using 6 degrees of freedom (DOF) and the boundary based registration (BBR) cost function. In the second stage, the T_1 -weighted image was registered to the age-appropriate, standard space T_1 -weighted template image using FLIRT with 12 DOF. The two resulting transformation matrices were concatenated and applied to the preprocessed RS-FMRI data.

Subject-level ICA-based artifact removal

In addition to standard FMRI pre-processing, each data set was cleaned to remove potential biases resulting from subject motion, cardiac / respiratory physiology, and scanner noise using the FMRIB ICA-based Xnoiseifier (FIX v1.06, Griffanti, Salimi-Khorshidi et al. 2014, Salimi-Khorshidi et al. 2014). With the aid of a training set, FIX automatically classifies subject-level ICA components as “signal” or “noise”, and subsequently “denoises” the RS-FMRI data by regressing out time series classified as noise. A thorough and sophisticated cleaning procedure, such as FIX, is especially relevant in the context of pediatric RS-FMRI, given recent reports on the impact of motion on functional connectivity (Power, Barnes et al. 2012, Satterthwaite, Wolf et al. 2012). All RS-FMRI datasets underwent a single-session ICA using the Multivariate Exploratory Linear Optimized Decomposition into Independent Components (MELODIC, v5.0.5) tool from FSL, followed by the artifact removal with FIX, including the removal of motion confounds (Griffanti, Salimi-Khorshidi et al. 2014). The FIX classifier was trained using manually labeled, subject-level ICA data from a random sample of 50 subjects with usable data. Briefly, the subject-level ICA data from these 50 subjects was loaded into the Melview viewer (<http://fsl.fmrib.ox.ac.uk/fsl/fslwiki/Melview>), and both the spatial and temporal (power spectrum and time series) characteristics were used to classify components as either “signal” or “noise”. The performance of the training set was then measured using a leave-one-out cross validation, where a single subject is excluded from the training set, which is subsequently used to classify that (left out) subject's data. We found the training set to perform well, with a mean true-positive rate (correctly labeled “signal” components) of 93.4% and a true negative rate (correctly labeled “noise” components) of 85.8%.

Study-specific, age-appropriate template for registration

Given the age of the sample, it was important to use an age-appropriate template for registration of the functional data to standard space. One hundred thirty T_1 -weighted images from children without behavioral problems, also rated as having excellent quality, were used to construct the structural template for registration. An iterative approach using both linear and nonlinear algorithms was used (Sanchez et al. 2012), and is represented graphically in the supplemental data section (Supplemental Figure 1). Briefly, T_1 -weighted images from each of the 130 subjects were first aligned to the MNI-152 1mm brain using a linear, 6 degree of freedom approach (FLIRT). All registered images were then averaged and used as the template brain for the subsequent step, which was a nonlinear registration (FNIRT). Once again, the result from the nonlinear registration was averaged and used as the template for the subsequent iteration. This routine continued for a total of five nonlinear iterations, where it has been shown the template image stabilizes considerably (Sanchez, Richards et al. 2012). The result of the fifth and final nonlinear registration was averaged, resampled to 2 mm isotropic resolution, and then used as the standard-space template for all RS-fMRI datasets. The average age and IQ, and the distribution of sex and handedness of the subjects used in creating the template was similar to that of the larger sample used in RS-fMRI analyses (age = 7.86 ± 0.99 , IQ = 105 ± 14.0 , sex = 50.4% Female, 49.6% Male, handedness = 90.2% Right, 9.8% Left).

Data quality

Data quality was assessed in two steps. First, as the subject-level ICA de-noising of the data is not sufficient in datasets severely corrupted by motion, a mean root-mean-squared relative motion greater than 0.5 mm was used as a cutoff to exclude data of poor quality ($n=88$). Second, all standard space registrations were examined using the middle functional volume from the time-series, and poorly registered datasets were excluded ($n=28$). Registrations were checked by merging the middle, 3D functional volume from each participant into a single 4D nifti file, and scrolling through the images, inspecting for gross translational or rotational shifts from the standard-space template (> 1 voxel shift).

Independent component analyses

Two ICA approaches were utilized. For the first approach, a repeated subsampling was used to generate distributions of the functional connectivity components and identify which were robust across multiple ICA runs. In total, 500 resamples were completed. For a given resample, 50 datasets were randomly selected from the pool of 536 datasets, and run through the multi-session temporal concatenation method from the MELODIC tool from FSL (v5.0.5) to generate spatial component maps. Dimensionality was set to 25 components, as a large number of previous studies used a similar value and our tests with these data showed robust networks that correspond with existing reports in the literature (Smith et al.

2009, Jolles, van Buchem et al. 2011, de Bie, Boersma et al. 2012). The decision to use 50 cases per resample was guided by current, typical sample sizes in RS-fMRI studies. For the second approach, the components resulting from the 500 resamples (25 components x 500 subsamples = 12,500 components) were summarized using a meta-ICA (Biswal et al. 2010), with the dimensionality set to 25 to match that of the individual group ICA runs. Components resulting from the meta-ICA were further summarized anatomically by determining overlap with the Harvard-Oxford anatomical atlases available in FSL after being registered to the MNI152 brain using a linear transform (Desikan et al. 2006).

Within- and between-network associations

In order to explore age-related associations with various ICA-derived networks, the “Dual Regression”, or spatiotemporal regression, approach from FSL was utilized to generate subject-specific time courses and spatial maps for each component (Filippini et al. 2009). In the first step of the Dual Regression, the spatial components resulting from the above-described meta ICA were regressed on each subject’s denoised RS-fMRI data to create subject-specific time courses for each component. Next, these time courses were regressed on the RS-fMRI data to create subject-specific spatial maps for each component.

To study within-network associations and limit the number of tests performed, four networks of interest were selected (right and left parietofrontal networks, default mode network, and executive control network) and whole-brain, voxel-wise statistics were employed on the dual regression maps using the FSL tool “Randomise” (Winkler et al. 2014). The General Linear Model was used, with age entered as the predictor of interest and sex, ethnicity (dummy-coded with Dutch as the reference), and total CBCL behavioral problems entered as covariates. For each contrast, 10,000 permutations were run, and the threshold-free cluster enhancement option was utilized (Smith and Nichols 2009). To account for the number of voxel-wise statistical tests run, p-values were adjusted for Family-wise error (FWE). Further, given that four networks were examined, a simple Bonferroni correction was applied to FWE-corrected p-value maps to indicate significance (where $p_{corrected} < 0.05$ from this point on is based on Bonferroni correction due to the four networks, positive and negative age contrasts, yielding 8 tests and $p < 0.00625$ applied to FWE corrected maps).

Between-network associations were studied with the Matlab-based (vR2011B, Mathworks Inc., Natick, MA) “FSLnets” plugin (<http://fsl.fmrib.ox.ac.uk/fsl/fslwiki/FSLNets>). A 13x13 correlation matrix of non-noise networks was built by correlating subject-specific time courses from the dual regression analysis for each component of interest, after regressing away components labeled as noise. Correlation coefficients were then transformed to z-values, and were subsequently used in statistical analyses with the randomise tool. As above in within-network analyses, randomise was used to associate age with each cell in the lower half of the correlation matrix, with sex, ethnicity and total CBCL behavioral problems entered as covariates. Using data from 10,000 permutations, correction for multiple testing was again attained with Family-wise error correction.

RESULTS

Meta ICA

The spatial components from the 500 subsamples were summarized using a meta-ICA and the results are depicted in Figures 1-3. Numerous components previously described in adults were observed, including the default-mode, lateralized frontoparietal, parietal, sensorimotor, visual networks (Damoiseaux et al. 2006, Smith, Fox et al. 2009). In addition to true RSNs, networks likely resulting from noise (physiological, scanner, image processing, etc) are also depicted. Table 2 outlines basic anatomical information about the components and also includes the ratio of summed power above/below 0.1Hz, averaged across the 500 subsamples, for each component. This power ratio has been indicated in previous work as a useful metric in classifying components as true RSNs and noise. Intrinsic functional connectivity is thought to be most represented in the 0.01-0.10 Hz range, and noise resulting from various sources is represented at higher frequencies. For instance, components 6 and 7, both in the brainstem, have a high-to-low power ratio 2-to-3 times that of true RSNs, such as the default-mode and frontoparietal networks, indicating the majority of the represented frequencies are above the 0.10 Hz level.

Distribution of components from subsampling

Certain RS-fMRI ICA networks appear in the literature frequently, while others are less frequently reported. In addition to defining ICA networks in young children, we aimed to also describe the frequency of which these components appear after repeated subsampling of the data. Each of 12,500 components resulting from the 500 subsamples was classified as one of the 25 meta-ICA components, or as a unique component not represented in the 25 meta-ICA components. To classify the components, set theory was used to label components based on spatial overlap (White, Muetzel et al. 2014). In total, 35 components were identified; 25 meta-ICA components (Figures 1-3), plus an additional 10 components (Supplemental Figure 2) that were not in the meta-ICA set. Components represented in figures are numbered and ordered according to the times present (%) in resamples, which is depicted in histogram format in Figure 4. As can be seen, components 1-to-10 were present in 96% or more of the ICA resamples, components 11-to-14 were present in 91% or more of the ICA resamples, and components 15-to-22 were present in 77% or more of the ICA resamples. These included components frequently reported in the literature, including the cerebellar, default-mode, executive control, frontoparietal, parietal, sensorimotor, and visual networks. However, other components were present in substantially fewer ICA resamples. Component 24, a visual area component, was only present in roughly 50% of the resamples. Further, component 30 (Supplemental Figure 2), a parietal component previously reported in the literature, was only present in 21% of the ICA resamples. Interestingly, in addition to components often considered true RSNs (e.g., the DMN), components with a

spatial distribution and power spectrum likely attributable to noise are still present in 98% of the subsamples. For example, this is the case in two brainstem components (components 6 and 7) that are potentially related to physiological noise. However, some of these ‘noise’ components occurred less frequently, including a frontal component indicative of motion (component 26) and a component related to white matter signal (component 31, see Supplemental Figure 2). Given features of the histogram presented in Figure 4, it is possible to classify components as robust or variable based on ‘drop offs’ in the frequencies depicted in the histogram. For instance, components 1 through 9 could be considered highly robust, and components 10 through 22 could be considered robust. However, given the relatively steep decrease in observed frequency at component 23, components 23 through 35 could be considered more variable.

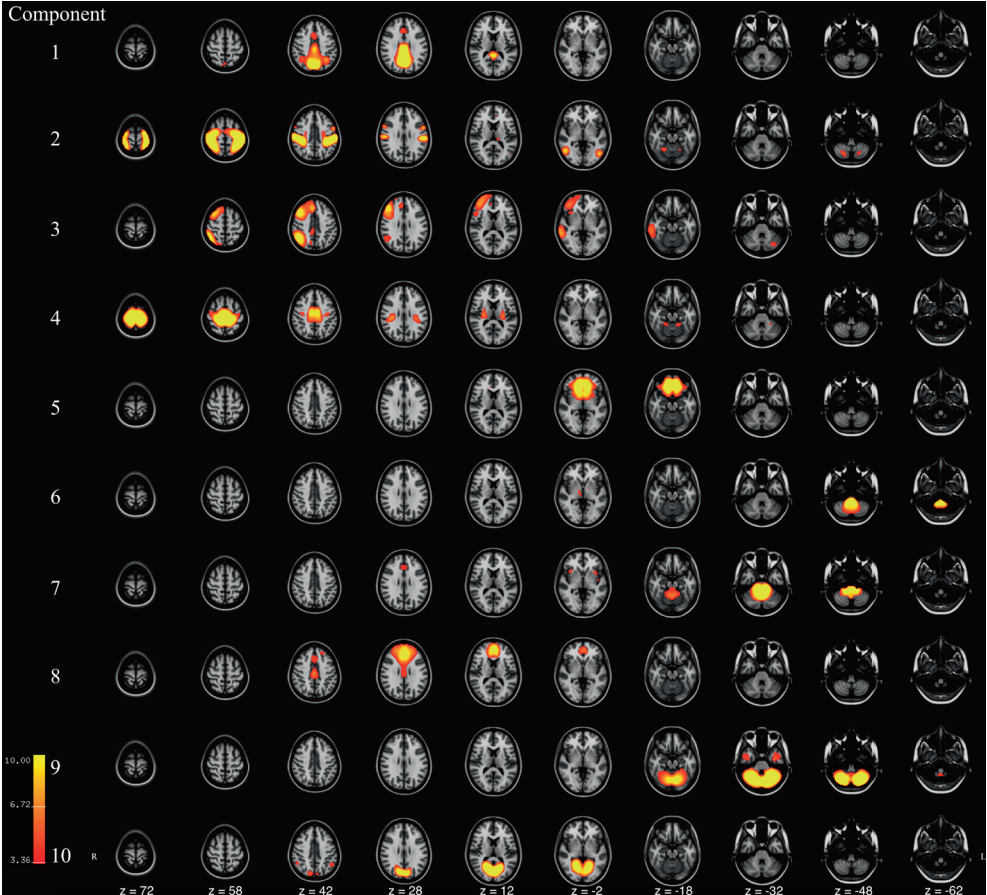


Figure 1. Axial slices of components 1-to-10 resulting from meta ICA of 500 repeated ICA samples. Components are thresholded at $z = 3.09$ ($p < 0.001$). Component Labels: 1=Default Mode Network I, 2=Sensor, 3=Right Frontoparietal, 4=Sensorimotor, 5=Inferior Frontal, 6=Lower Brainstem, 7=Brainstem, 8=Middle Frontal, 9=Cerebellar, 10=Anterior Visual.

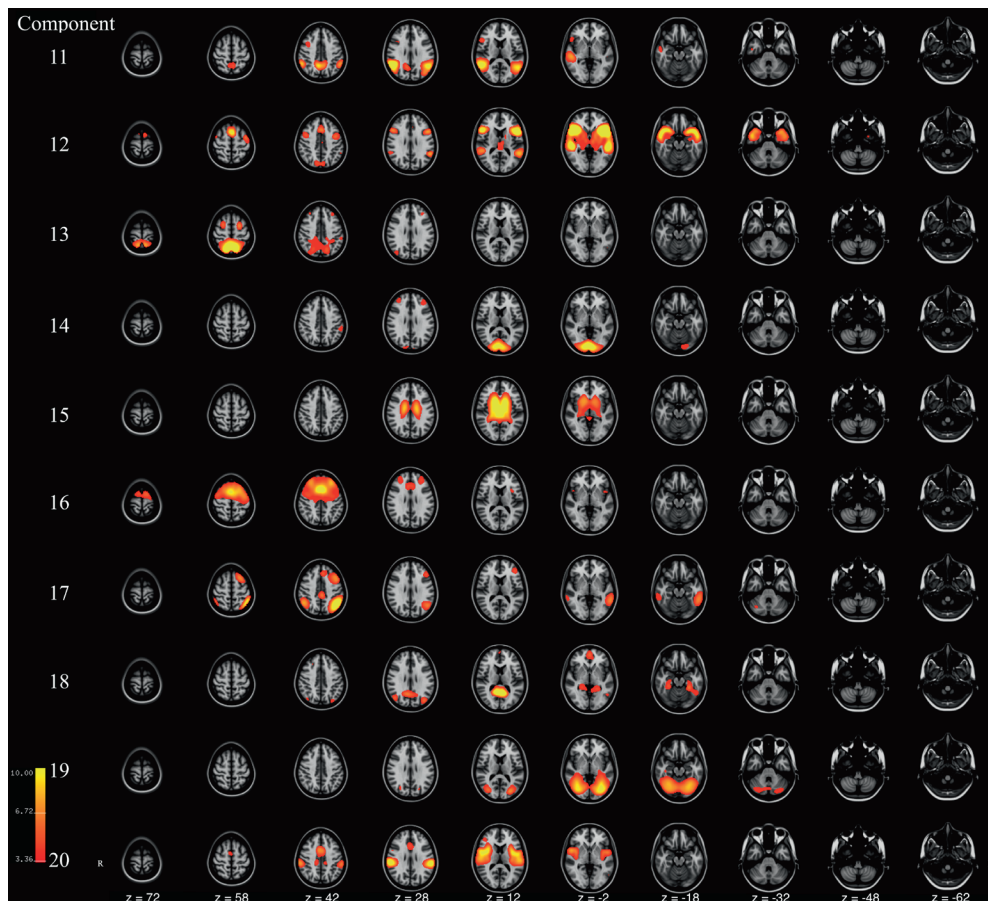


Figure 2.

Axial slices of components 11-to-20 resulting from meta ICA of 500 repeated ICA samples. Components are thresholded at $z = 3.09$ ($p < 0.001$). Component Labels: 11=Precuneus, 12 = Lateral Frontal, 13=Parietal, 14=Visual, 15=Ventricular, 16=Executive Control, 17=Left Frontoparietal, 18=Default Mode Network II, 19=Cerebellar-Occipital, 20=Insular.

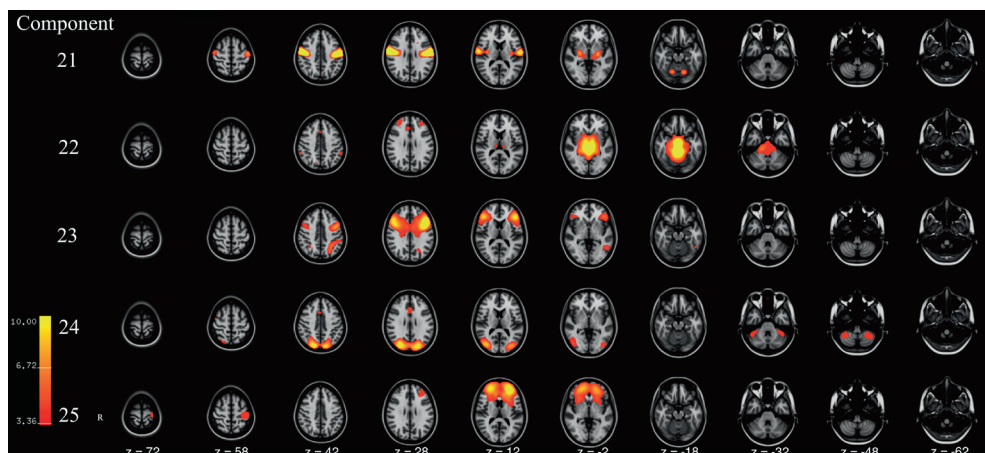


Figure 3. Axial slices of components 21-25 resulting from meta ICA of 500 repeated ICA samples. Components are thresholded at $z = 3.09$ ($p < 0.001$). Component Labels: 21=Motor, 22=Upper Brainstem, 23=Frontal-temporal-Parietal, 24=Lateral Visual, 25=Lateral Middle Frontal.

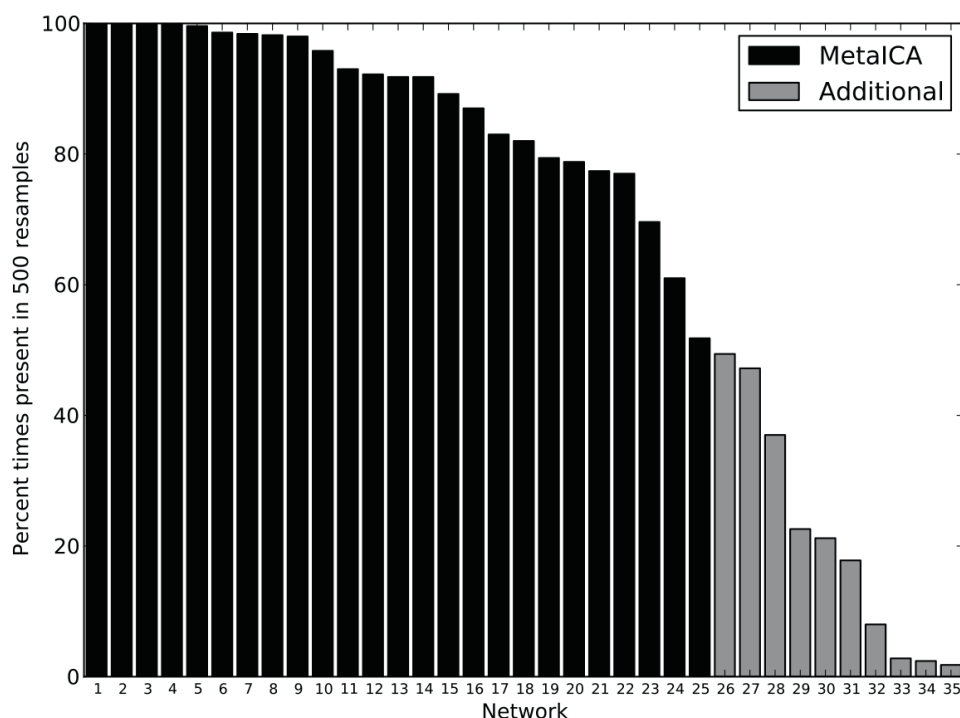


Figure 4. Frequencies (presence) of components observed after repeated ICA subsampling. Components observed in only the meta-ICA (black), and those found in repeated subsamples but not represented in the meta-ICA (gray) are shown.

Table 2. Descriptive information of meta-ICA derived components

Component	Functional Label	Anatomical Labels	0.1Hz Power Ratio
1	DMN-I	Precuneus, Cingulate-PD, Lat. Occipital-SD, Cingulate-AD, Cuneus, Paracingulate, Sup. Parietal, Angular	0.33 ± 0.04
2	Sensory	Postcentral, Precuneus, Sup. Parietal, Supramarginal-AD, Lat. Occipital-ID, Lat. Occipital-SD, Sup. Frontal, Supramarginal-PD, Juxtapositional, Mid. Frontal, Mid. Temporal	0.46 ± 0.08
3	R. Frontoparietal	Frontal Pole, Mid. Frontal, Lat. Occipital-SD, Sup. Frontal, Angular, Mid. Temporal-PD, Sup. Parietal, Supramarginal-PD, Paracingulate, Precentral, Mid. Temporal, Pars Opercularis, Inf. Temporal, Cingulate-PD, Sup. Temporal-PD	0.38 ± 0.05
4	Sensorimotor	Precentral, Postcentral, Juxtapositional, Cingulate-PD, Sup. Parietal, Precuneus, Sup. Frontal, Parietal Operculum, Cingulate-AD	0.54 ± 0.10
5	Inf. Frontal	Frontal Pole, Orbital Frontal, Subcallosal, Med. Frontal, Paracingulate, Cingulate-AD, L. Putamen, R. Putamen, R. Caudate, L. Caudate	0.71 ± 0.10
6	Lower Brainstem	Brainstem, R. Thalamus	0.90 ± 0.10
7	Brainstem	Brainstem, Insular, Cingulate-AD	0.90 ± 0.08
8	Mid. Frontal	Frontal Pole, Paracingulate, Cingulate-AD, Cingulate-PD, Sup. Frontal, Mid. Frontal	0.66 ± 0.18
9	Cerebellar	Temporal-Occipital Fusiform, Occipital Fusiform, Lingual, Temporal Fusiform-PD, Inf. Temporal-AD	0.91 ± 0.11
10	Ant. Visual	Lingual, Precuneus, Intracalcarine, Cuneus, Occipital Fusiform, Lat. Occipital-SD, Angular, Temporal-Occipital Fusiform, Supracalcarine, Cingulate-PD, Occipital Pole	0.56 ± 0.09
11	Precuneus	Precuneus, Angular, Lat. Occipital-SD, Supramarginal-PD, Mid. Temporal, Sup. Temporal-PD, Lat. Occipital-ID, Mid. Temporal-PD, Pars Opercularis, Mid. Frontal, Supramarginal-AD	0.47 ± 0.09
12	Lat. Frontal	Temporal Pole, Orbital Frontal, Insular, Precentral, Sup. Temporal-PD, Pars Opercularis, Mid. Temporal-PD, Mid. Frontal, Sup. Frontal, L. Thalamus, Pars Triangularis, Supramarginal-PD, Paracingulate, Planum Polare, L. Putamen, R. Thalamus, Frontal Operculum, Mid. Temporal-AD, Mid. Temporal, Angular, R. Putamen, Sup. Temporal-AD, Temporal Fusiform-AD, Juxtapositional, Central Opercular	0.46 ± 0.07
13	Parietal	Lat. Occipital-SD, Precuneus, Sup. Parietal, Postcentral, Sup. Frontal, Mid. Frontal, Frontal Pole	0.45 ± 0.07
14	Visual	Occipital Pole, Lingual Gyrus, Intracalcarine, Occipital Fusiform, Lat. Occipital-ID, Frontal Pole, Supramarginal-AD, Mid. Frontal, Cuneus, Supracalcarine, Lat. Occipital-SD	0.63 ± 0.10
15	Ventricular	R. Thalamus, L. Thalamus, L. Lat. Ventricle, R. Lat. Ventricle, R. Putamen, L. Putamen, R. Caudate, L. Caudate, L. Pallidum, R. Pallidum, Insular	0.64 ± 0.11

16	Executive Control	Sup. Frontal, Mid. Frontal, Precentral, Frontal Pole, Juxtapositional, Paracingulate, Cingulate-AD	0.64 ± 0.14
17	L. Frontoparietal	Lat. Occipital-SD, Mid. Frontal, Angular, Mid. Temporal-PD, Sup. Frontal, Supramarginal-PD, Inf. Temporal, Mid. Temporal, Sup. Parietal, Cingulate-PD, Inf. Temporal-PD, Supramarginal-AD, Frontal Pole, Paracingulate	0.39 ± 0.06
18	DMN-II	Precuneus, Lat. Occipital-SD, Cingulate-PD, Lingual, Paracingulate, Temporal-Occipital Fusiform, Frontal Pole, Inf. Temporal, Temporal Fusiform-PD, R. Hippocampus, L. Hippocampus, Parahippocampal-PD, Intracalcarine	0.33 ± 0.06
19	Cerebellum-Occ.	Lat. Occipita-ID, Lingual, Occipital Fusiform, Temporal-Occipital Fusiform, Inf. Temporal, Lat. Occipital-SD, Mid. Temporal	0.83 ± 0.14
20	Insular	Central Opercular Supramarginal-AD, Insular, Parietal Operculum, Cingulate-AD, Planum Temporale, Precentral, Supramarginal-PD, Postcentral, Heschl's, Juxtapositional, Frontal Operculum, Paracingulate, Planum Polare, Sup. Temporal-PD, R. Putamen, L. Putamen, Pars Opercularis.	0.48 ± 0.07
21	Motor	Precentral, Postcentral, Cent. Opercular, L. Thalamus, R. Putamen, L. Putamen, R. Thalamus, Insular	0.46 ± 0.06
22	Upper Brainstem	Brainstem, L. Thalamus, R. Thalamus, Parahippocampal-PD, Lingual, R. Hippocampus, L. Hippocampus, Frontal Pole, Paracingulate, Parahippocampal-AD, R. Pallidum, L. Pallidum, R. Putamen, Temporal Fusiform-PD	0.88 ± 0.11
23	Frontal-Temporal-Parietal	Mid. Frontal, Frontal Pole, Precentral, Pars Opercularis, Pars Triangularis, Lat. Occipital-SD, Sup. Parietal, Orbital Frontal, Frontal Operculum, Inf. Temporal, Cingulate-AD	0.40 ± 0.08
24	Lateral Visual	Lat. Occipital-SD, Lat. Occipital-ID, Cuneous, Occipital Pole, Precuneus, Cingulate-AD	0.59 ± 0.10
25	Lat. Mid. Frontal	Frontal Pole, Paracingulate, Cingulate-AD, Poscentral, Insular, Precentral, Frontal Operculum, L. Caudate, L. Putamen, R. Caudate	0.81 ± 0.17

Note: Component numbers correspond to those used in other figures. Anatomical labels are ordered according to their overlap with the component, in descending order. Abbreviations: AD = anterior division, Inf = inferior, ID = inferior division, Lat = lateral, L = left, Mid = middle, PD = posterior division, Sup = Superior, SD = superior division, R = right

The spatial variability in components across resamples was explored using a voxel-wise 1-sample t-test on all matched components ($p_{\text{FWE}} < 0.05$). Supplemental Figure 3 illustrates these maps in the 25 meta-ICA components. As can be seen, there is high overlap in the center of most nodes of the components across the 500 ICA runs (see corresponding meta-ICA components in Figures 1-3). Interestingly, lower overlap across the 500 ICA runs is apparent in certain nodes of components that split into separate/distinct components with higher dimensionality (e.g., the frontal node of the DMN).

Within-network associations with age

Results from voxel-wise statistics on subject-specific component maps from dual regression are presented in Figure 5. For the DMN, a negative association with age was observed in the precuneus/posterior cingulate node. Similarly, for the executive control network, a negative correlation was observed in the frontal and anterior cingulate aspects of the network. In the right front-parietal network, a positive association with age is observed in the left hemisphere, mainly in the insula and temporal lobe. No significant associations were observed between age and the left frontoparietal network after adjusting for confounders and multiple testing.

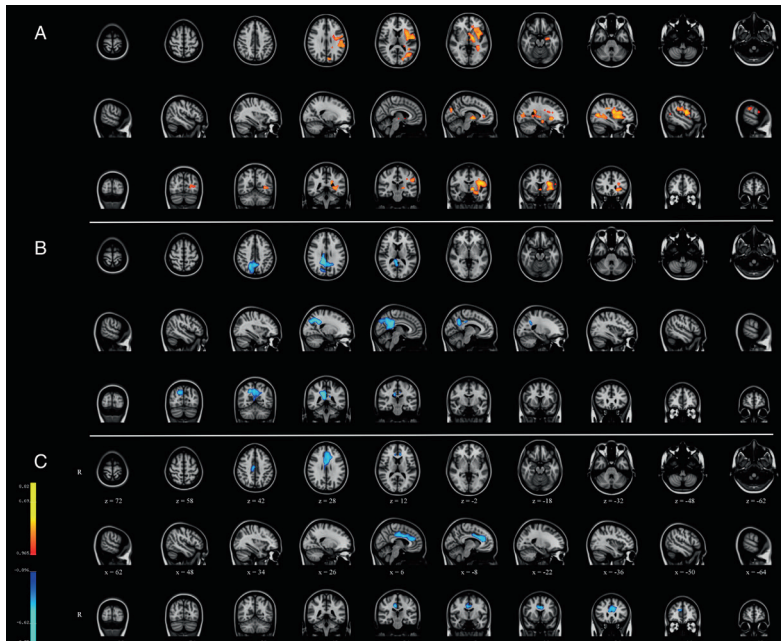


Figure 5. Within-network associations with age using spatiotemporal regression. Clusters are t-values indicating significant association at $p_{\text{corrected}} < 0.05$, with red indicating a positive association with age and blue indicating a negative association with age. a.) meta-ICA component 3 / right frontoparietal, b.) meta-ICA component 1 / default mode network, and c.) meta-ICA component 16 / executive control network.

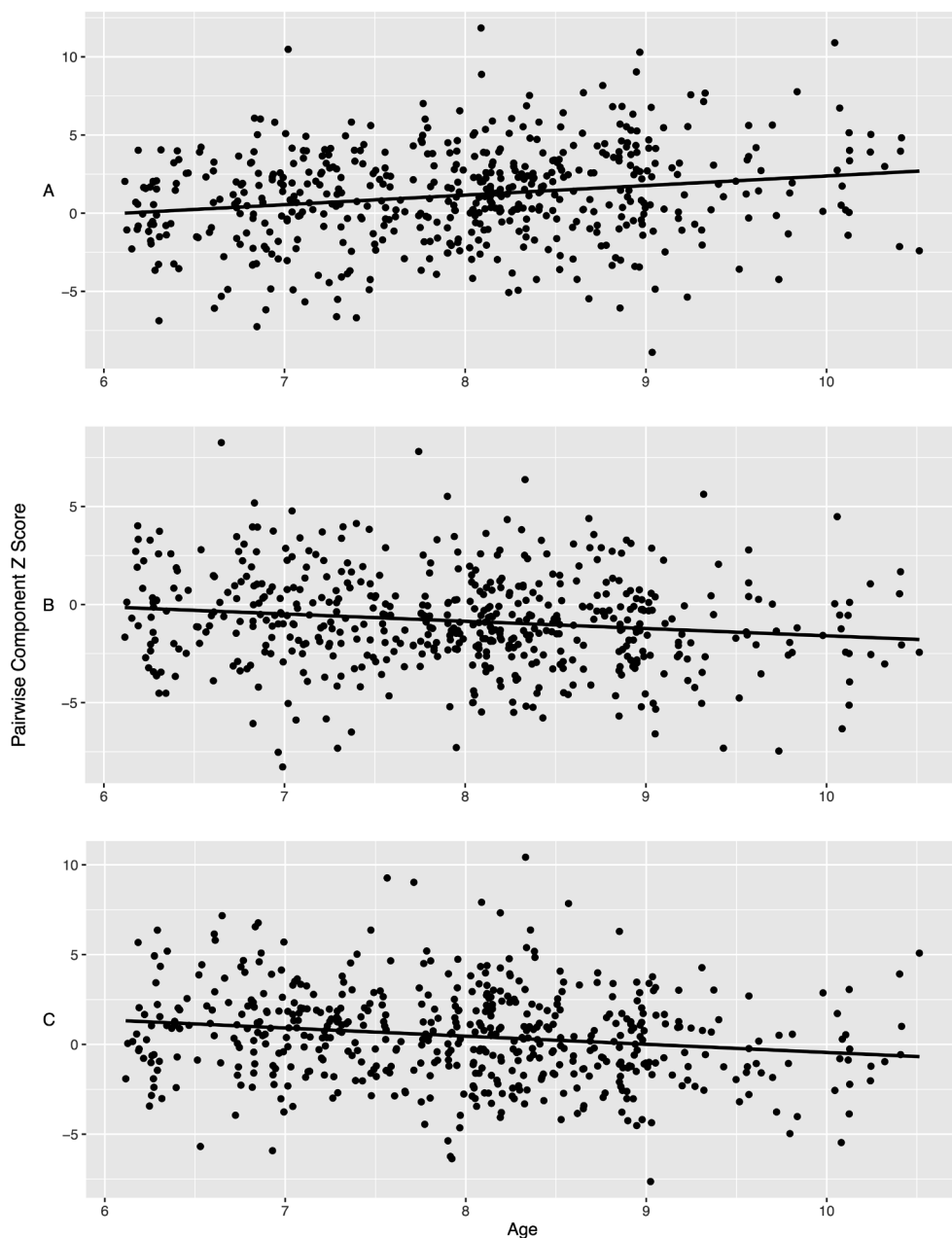


Figure 6.

Between-network associations with age. The x-axis reflects age in years and the y-axis is the pairwise correlations between time courses of two components, transformed to the Z distribution. A = Components 11 and 12, B = Components 3 and 13, and C = Components 2 and 3.

Between-network associations with age

Regression analyses of between-network connectivity revealed that the correlation between Component 11 (Precuneus) and Component 12 (Lateral Frontal) was positively associated with age ($\beta = 0.20$, $p_{\text{FWE}} = 0.0004$). Thus, the correlation between these networks was stronger (becoming more positive) in older children (Figure 6). Further, the correlation between Component 3 (Right Frontoparietal) and Component 13 (Parietal) was negatively associated with age ($\beta = -0.17$, $p_{\text{FWE}} = 0.0056$). In older children, the correlation between these networks is lower (becoming more negative, Figure 6). Lastly, the correlation between Component 2 (Sensory) and Component 3 (Right Frontoparietal) was negatively associated with age ($\beta = -0.15$, $p_{\text{FWE}} = 0.027$).

DISCUSSION

The present study examines resting-state fMRI networks in a large sample of 6-to-10 year-old children using independent component analyses. A subsampling approach was used to generate a representative set of components, and to identify robustness of components across repeated ICA runs. The subsampling revealed that many components commonly reported in the literature show a high level of stability across repeated sampling. Further, many of the components that are typically identified in studies of adults were also found in the current sample of young children. Interestingly, networks believed to be the result of noise and/or artifact were also observed at frequencies similar to true RSNs after iterative ICA subsampling. Lastly, even within a very narrow age-range, the study demonstrated age-related associations with various networks, suggesting continued refinement of networks is occurring during childhood.

The subsampling procedure used in the current study highlights important characteristics of RS-fMRI ICA analyses, namely that many components are quite robust. This is true for both what is considered RSNs and for ‘noise’ signals. Previous studies have already discussed issues surrounding ICA, for example variability related to subject order or ICA reliability (Himberg, Hyvarinen et al. 2004, Zhang, Zuo et al. 2010, Franco, Mannell et al. 2013). In the present study we expand upon this showing that many components typically characterized in the literature as RSNs were observed frequently across the repeated ICA runs (e.g., the DMN, sensory, motor, and frontoparietal networks). While these results do not give a clear indication of the precise reliability of the spatial extent of the various components, they do demonstrate that many components from ICA can be repeatedly extracted from RS-fMRI data in young children, despite variability in the sample and algorithm-dependent variability in ICAs. The data also show that components suggestive of noise in RS-fMRI data (e.g., resulting from hardware, physiological, image analysis, etc.) can be reliably detected

in children using ICA. For example, components 6 and 7 (both part of the brainstem) were present in over 98% of the repeated ICA analyses.

However, given that certain components were not observed as frequently as others (i.e., roughly 55% of the time or less), it is prudent to critically evaluate these components in future studies (for instance, components 29 and 30). This may be especially important in ICA-derived components considered to be RSNs and subjected to further analysis using the myriad of methods available (e.g., spatiotemporal regression, backwards-reconstruction, seed-based, etc. Calhoun et al. 2008, Filippini, MacIntosh et al. 2009, Tian et al. 2013), to ensure they are not simply artifacts of the data or image analysis algorithm. It is however interesting to consider the possibility that some of these less frequently occurring components are not artifact or algorithm-dependent, but rather arise from other sources. For instance, the variability could reflect individual differences in RS-fMRI networks in typically developing children (Michael et al. 2014). If such individual differences exist and can be observed, those components could offer further insight into brain development, various neurological or psychiatric disorders, or in the fields of social or behavioral neuroscience. Conversely, while the age-range in the current study is comparatively narrow compared to many studies of brain development, it is possible that the observed variability in components is simply age-related. For instance, networks not present in all resamples could be subject to neurodevelopment processes that later stabilize in adulthood. Thus, generalizations to other age-ranges should be made carefully and similar analyses should be explored in adolescents and young adults, or preferably, networks should be tracked using longitudinal designs.

While not traditionally done in the existing literature, the current study also presents components that are typically labeled as ‘noise’ or ‘other’ and discarded from analyses. Many components that are likely attributable to noise actually were very robust in repeated sampling. This suggests that many noise signals are present in different subject groups and that ICA can reliably detect them. This information also hopefully gives other groups a point of reference when examining group ICA components, and also may help future work in deciding which of these components are generalizable across studies, and which are not (i.e., those that are MR-scanner dependent, sequence dependent, etc.). It is unclear how useful this information will be across studies, as some of the noise components were highly variable, and could be related to the scanner hardware, thermal noise, or even the performance of the ICA-based artifact removal. However, while beyond the scope of the current study, the repeated subsampling results with and without the subject-level ICA denoising step were run and produced group meta-ICA results similar to those reported in the current study (Supplemental Figure 4). This is particularly interesting given the increased attention surrounding pediatric imaging with respect to motion confounds. However, while the cleanup procedure may only marginally influence the results of group ICA, it has been

previously shown to influence other important aspects of analyses, such as spatiotemporal regression, and thus should not be considered unnecessary (Mowinckel et al. 2012, Satterthwaite, Wolf et al. 2012).

Age-related associations within the DMN revealed the central, posterior cingulate / precuneus node of the default mode network to be negatively correlated with age, after adjusting for sex, behavioral problems and ethnicity. This observation was previously only reported in adults, where a highly similar spatial pattern of aging rather than developmental effects was observed in individuals 21-to-81 years of age using spatiotemporal regression (Mowinckel, Espeseth et al. 2012). We also observed a positive association between age and the contralateral hemisphere of the right frontoparietal network, suggesting a potential increase in interhemispheric communication with age. Lastly, between network analyses revealed that certain networks (i.e., the precuneus and lateral frontal) become more strongly connected with increasing age, whereas other networks become less strongly connected with age (e.g., the right frontoparietal and sensory). These results taken together are particularly intriguing, given they demonstrate evidence for maturation of functional connectivity in a very narrow age-range.

Another aspect worthy of discussion is the study sample. In the extant literature, it is relatively clear, and occasionally noted, that the labels “typically developing” or “normal” are at times somewhat misleading. Studies of normative brain development often times experience selection bias, including children with higher than average IQ and social economic status. Further, diversity in ethnic background tends to be limited, and the prevalence of behavioral problems in these samples is likely lower than what would be observed in a true random sampling of the population. A similar scenario has been considered in the context of case-control studies (Schwartz and Susser 2011). In the current study, the children were sampled from a population-based cohort. Importantly, severe behavioral problems were an exclusion criteria, and thus the sample is not truly representative at the population level. However, other aspects of the study sample, including non-verbal IQ show close correspondence with the population average (current study mean = 103, population average = 100). Further, ethnicity in the current sample was fairly representative of the catchment area, with roughly 17% of the sample was of non-Western decent. These factors, when taken together, suggest the current sample is less representative of a “hyper-normal” group and more representative of the overall population compared many studies of typical brain development.

In addition to describing RSNs in children, another goal of the present study was to facilitate replication and generalizability in RS-fMRI data analyses. Thus, the final set of meta-ICA spatial maps have been made available under a non-commercial license to the neuroimaging community via the Neuroimaging Informatics Tools and Clearinghouse (NITRC) website (<http://www.nitrc.org/projects/genr/>). Interested researchers are able

to utilize the components to aid in their research efforts, for example in comparison against those identified in their own studies, for use in spatial-temporal regression (dual regression), or as an “atlas” for reference with other RS-FMRI ICA studies, task-based FMRI studies and structural neuroimaging studies. Further, the age-appropriate T_1 -weighted brain described in section 2.4.3 is also available for those interested in a pediatric structural brain for registration.

While the current study has many strengths, some limitations are present and deserve attention. First, the current study presents independent component analyses of resting-state data in children, imposing a dimensionality of 25. While it is highly unlikely 25 components represent the true set of RSNs in the brain, this number was chosen because it fits well with the existing literature and generates a similar set of components to what has been presented previously in both child, adolescent and adult studies. With increasing spatial and temporal resolution of acquired RS-FMRI data, using higher dimensionalities becomes more feasible, even though it has been observed that increasing the dimensionality may actually simply split components into sub-networks (Smith, Fox et al. 2009). There is also interesting evidence from large studies suggesting the brain is organized into a relatively low number of networks (Yeo et al. 2011). While noise components are reported in the current study, and it is likely that some of them will be generalizable (i.e., replicate) across studies/research groups, some of these noise components will not be generalizable. For example, certain components could be related to a particular MR-scanner profile, which may or may not even replicate within a given model/manufacture of scanner (Friedman et al. 2008). However, some of these components (e.g., those related to respiratory and cardiac physiology) will most likely be applicable across site, and it will be interesting to see how they compare to components other groups observe. Lastly, while the current study did investigate the frequency components were observed after repeated subsampling, it was beyond the scope of the study to examine the spatial variability of the components in detail. Future studies may wish to examine this, perhaps in the context of higher and lower dimensionality.

The current study presents evidence that many RSNs in young children are quite robust, occurring frequently under repeated ICAs, while other RSNs are less frequently observed and require additional scrutiny when involving between-group comparisons. Further, these components demonstrate age-related associations, suggesting they are sensitive to subtle developmental changes. The final meta-ICA group components and pediatric T_1 -weighted structural template are made available to the neuroimaging community for research purposes.

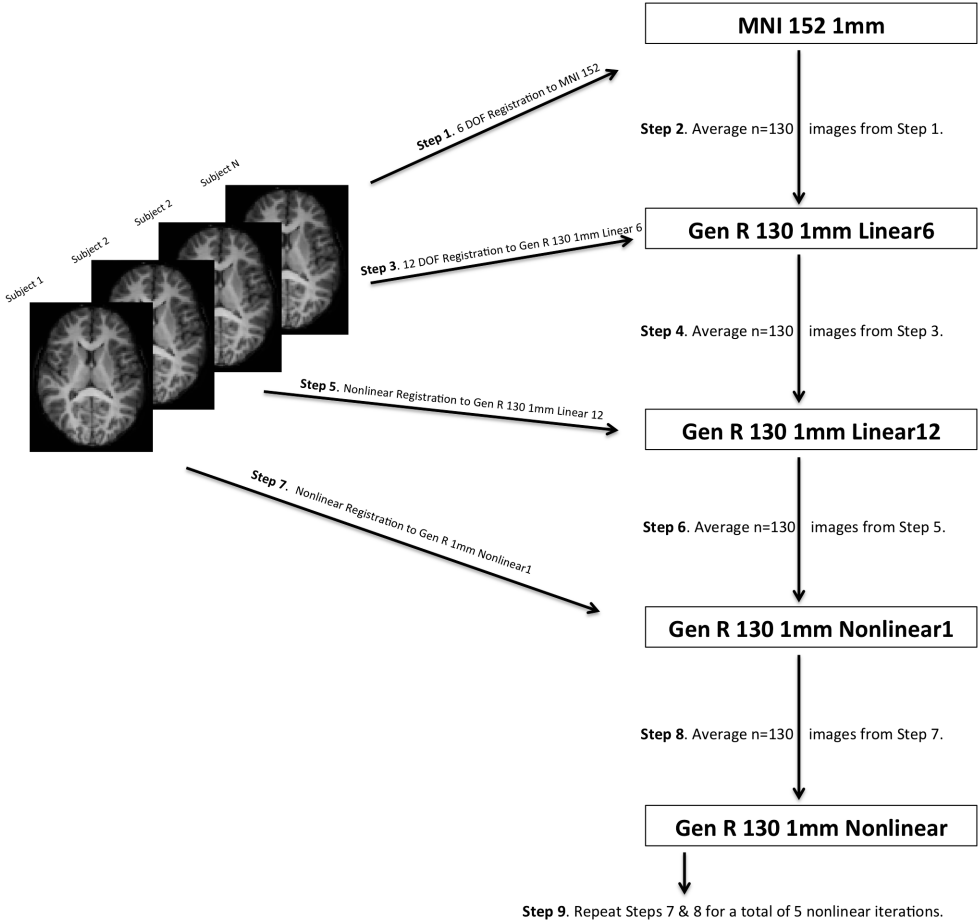
REFERENCES

- Achenbach, T. M. and L. A. Rescorla (2000). Manual for ASEBA preschool forms & profiles. Burlington, VT, University of Vermont, Research Center for Children, Youth & Families.
- Achenbach, T. M. and T. M. Ruffle (2000). The Child Behavior Checklist and related forms for assessing behavioral/emotional problems and competencies. *Pediatrics in review / American Academy of Pediatrics* **21**(8): 265-271.
- Beckmann, C. F., M. DeLuca, J. T. Devlin and S. M. Smith (2005). Investigations into resting-state connectivity using independent component analysis. *Philosophical transactions of the Royal Society of London. Series B, Biological sciences* **360**(1457): 1001-1013.
- Biswal, B. B., M. Mennes, X. N. Zuo, S. Gohel, C. Kelly, S. M. Smith, C. F. Beckmann, J. S. Adelstein, R. L. Buckner, S. Colcombe, A. M. Dogonowski, M. Ernst, D. Fair, M. Hampson, M. J. Hoptman, J. S. Hyde, V. J. Kiviniemi, R. Kotter, S. J. Li, C. P. Lin, M. J. Lowe, C. Mackay, D. J. Madden, K. H. Madsen, D. S. Margulies, H. S. Mayberg, K. McMahon, C. S. Monk, S. H. Mostofsky, B. J. Nagel, J. J. Pekar, S. J. Peltier, S. E. Petersen, V. Riedl, S. A. Rombouts, B. Rypma, B. L. Schlaggar, S. Schmidt, R. D. Seidler, G. J. Siegle, C. Sorg, G. J. Teng, J. Veijola, A. Villringer, M. Walter, L. Wang, X. C. Weng, S. Whitfield-Gabrieli, P. Williamson, C. Windischberger, Y. F. Zang, H. Y. Zhang, F. X. Castellanos and M. P. Milham (2010). Toward discovery science of human brain function. *Proc Natl Acad Sci U S A* **107**(10): 4734-4739.
- Calhoun, V. D., T. Adali, G. D. Pearlson and J. J. Pekar (2001). A method for making group inferences from functional MRI data using independent component analysis. *Human brain mapping* **14**(3): 140-151.
- Calhoun, V. D., P. K. Maciejewski, G. D. Pearlson and K. A. Kiehl (2008). Temporal lobe and “default” hemodynamic brain modes discriminate between schizophrenia and bipolar disorder. *Hum Brain Mapp* **29**(11): 1265-1275.
- Cole, D. M., S. M. Smith and C. F. Beckmann (2010). Advances and pitfalls in the analysis and interpretation of resting-state FMRI data. *Frontiers in systems neuroscience* **4**: 8.
- Damoiseaux, J. S., S. A. Rombouts, F. Barkhof, P. Scheltens, C. J. Stam, S. M. Smith and C. F. Beckmann (2006). Consistent resting-state networks across healthy subjects. *Proceedings of the National Academy of Sciences of the United States of America* **103**(37): 13848-13853.
- de Bie, H. M., M. Boersma, S. Adriaanse, D. J. Veltman, A. M. Wink, S. D. Roosendaal, F. Barkhof, C. J. Stam, K. J. Oostrom, H. A. Delemarre-van de Waal and E. J. Sanz-Arigita (2012). Resting-state networks in awake five- to eight-year old children. *Human brain mapping* **33**(5): 1189-1201.
- Desikan, R. S., F. Segonne, B. Fischl, B. T. Quinn, B. C. Dickerson, D. Blacker, R. L. Buckner, A. M. Dale, R. P. Maguire, B. T. Hyman, M. S. Albert and R. J. Killiany (2006). An automated labeling system for subdividing the human cerebral cortex on MRI scans into gyral based regions of interest. *Neuroimage* **31**(3): 968-980.
- Filippini, N., B. J. MacIntosh, M. G. Hough, G. M. Goodwin, G. B. Frisoni, S. M. Smith, P. M. Matthews, C. F. Beckmann and C. E. Mackay (2009). Distinct patterns of brain activity in young carriers of the APOE-epsilon4 allele. *Proceedings of the National Academy of Sciences of the United States of America* **106**(17): 7209-7214.
- Franco, A. R., M. V. Mannell, V. D. Calhoun and A. R. Mayer (2013). Impact of analysis methods on the reproducibility and reliability of resting-state networks. *Brain connectivity* **3**(4): 363-374.
- Friedman, L., H. Stern, G. G. Brown, D. H. Mathalon, J. Turner, G. H. Glover, R. L. Gollub, J. Lauriello, K. O. Lim, T. Cannon, D. N. Greve, H. J. Bockholt, A. Belger, B. Mueller, M. J. Doty, J. He, W. Wells, P. Smyth, S. Pieper, S. Kim, M. Kubicki, M. Vangel and S. G. Potkin (2008). Test-retest and between-site reliability in a multicenter fMRI study. *Hum Brain Mapp* **29**(8): 958-972.
- Gao, W., H. Zhu, K. S. Giovanello, J. K. Smith, D. Shen, J. H. Gilmore and W. Lin (2009). Evidence on the emergence of the brain's default network from 2-week-old to 2-year-old healthy pediatric subjects. *Proc Natl Acad Sci U S A* **106**(16): 6790-6795.

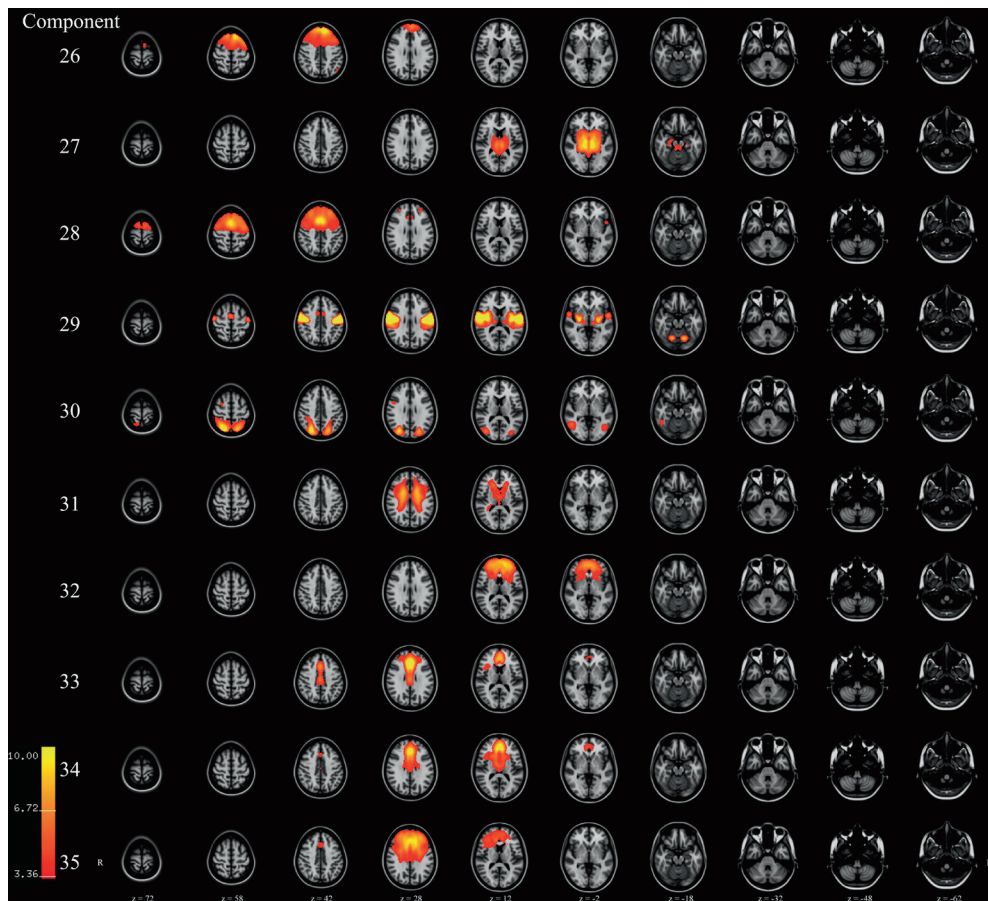
- Griffanti, L., G. Salimi-Khorshidi, C. F. Beckmann, E. J. Auerbach, G. Douaud, C. E. Sexton, E. Zsoldos, K. P. Ebmeier, N. Filippini, C. E. Mackay, S. Moeller, J. Xu, E. Yacoub, G. Baselli, K. Ugurbil, K. L. Miller and S. M. Smith (2014). ICA-based artefact removal and accelerated fMRI acquisition for improved resting state network imaging. *Neuroimage* **95**: 232-247.
- Himberg, J., A. Hyvarinen and F. Esposito (2004). Validating the independent components of neuroimaging time series via clustering and visualization. *Neuroimage* **22**(3): 1214-1222.
- Jaddoe, V. W., C. M. van Duijn, O. H. Franco, A. J. van der Heijden, M. H. van Iizendoorn, J. C. de Jongste, A. van der Lugt, J. P. Mackenbach, H. A. Moll, H. Raat, F. Rivadeneira, E. A. Steegers, H. Tiemeier, A. G. Uitterlinden, F. C. Verhulst and A. Hofman (2012). The Generation R Study: design and cohort update 2012. *European journal of epidemiology* **27**(9): 739-756.
- Jenkinson, M., C. F. Beckmann, T. E. Behrens, M. W. Woolrich and S. M. Smith (2012). Fsl. *Neuroimage* **62**(2): 782-790.
- Jolles, D. D., M. A. van Buchem, E. A. Crone and S. A. Rombouts (2011). A comprehensive study of whole-brain functional connectivity in children and young adults. *Cerebral cortex* **21**(2): 385-391.
- Langeslag, S. J., M. Schmidt, A. Ghassabian, V. W. Jaddoe, A. Hofman, A. van der Lugt, F. C. Verhulst, H. Tiemeier and T. J. White (2012). Functional connectivity between parietal and frontal brain regions and intelligence in young children: The Generation R study. *Human brain mapping*.
- Littow, H., A. A. Elseoud, M. Haapea, M. Isohanni, I. Moilanen, K. Mankinen, J. Nikkinen, J. Rahko, H. Rantala, J. Remes, T. Starck, O. Tervonen, J. Veijola, C. Beckmann and V. J. Kiviniemi (2010). Age-Related Differences in Functional Nodes of the Brain Cortex - A High Model Order Group ICA Study. *Front Syst Neurosci* **4**.
- Michael, A. M., M. Anderson, R. L. Miller, T. Adali and V. D. Calhoun (2014). Preserving subject variability in group fMRI analysis: performance evaluation of GICA vs. IVA. *Front Syst Neurosci* **8**: 106.
- Mowinckel, A. M., T. Espeseth and L. T. Westlye (2012). Network-specific effects of age and in-scanner subject motion: a resting-state fMRI study of 238 healthy adults. *Neuroimage* **63**(3): 1364-1373.
- Power, J. D., K. A. Barnes, A. Z. Snyder, B. L. Schlaggar and S. E. Petersen (2012). Spurious but systematic correlations in functional connectivity MRI networks arise from subject motion. *Neuroimage* **59**(3): 2142-2154.
- Salimi-Khorshidi, G., G. Douaud, C. F. Beckmann, M. F. Glasser, L. Griffanti and S. M. Smith (2014). Automatic denoising of functional MRI data: Combining independent component analysis and hierarchical fusion of classifiers. *Neuroimage*.
- Sanchez, C. E., J. E. Richards and C. R. Almlil (2012). Age-specific MRI templates for pediatric neuroimaging. *Developmental neuropsychology* **37**(5): 379-399.
- Satterthwaite, T. D., D. H. Wolf, J. Loughhead, K. Ruparel, M. A. Elliott, H. Hakonarson, R. C. Gur and R. E. Gur (2012). Impact of in-scanner head motion on multiple measures of functional connectivity: relevance for studies of neurodevelopment in youth. *Neuroimage* **60**(1): 623-632.
- Schwartz, S. and E. Susser (2011). The use of well controls: an unhealthy practice in psychiatric research. *Psychological Medicine* **41**(6): 1127-1131.
- Smith, S. M., P. T. Fox, K. L. Miller, D. C. Glahn, P. M. Fox, C. E. Mackay, N. Filippini, K. E. Watkins, R. Toro, A. R. Laird and C. F. Beckmann (2009). Correspondence of the brain's functional architecture during activation and rest. *Proceedings of the National Academy of Sciences of the United States of America* **106**(31): 13040-13045.
- Smith, S. M. and T. E. Nichols (2009). Threshold-free cluster enhancement: addressing problems of smoothing, threshold dependence and localisation in cluster inference. *Neuroimage* **44**(1): 83-98.
- Tian, L., Y. Kong, J. Ren, G. Varoquaux, Y. Zang and S. M. Smith (2013). Spatial vs. Temporal Features in ICA of Resting-State fMRI - A Quantitative and Qualitative Investigation in the Context of Response Inhibition. *PLoS One* **8**(6): e66572.

- Tick, N. T., J. van der Ende, H. M. Koot and F. C. Verhulst (2007). 14-year changes in emotional and behavioral problems of very young Dutch children. *Journal of the American Academy of Child and Adolescent Psychiatry* **46**(10): 1333-1340.
- Tiemeier, H., F. P. Velders, E. Szekely, S. J. Roza, G. Dieleman, V. W. Jaddoe, A. G. Uitterlinden, T. J. White, M. J. Bakermans-Kranenburg, A. Hofman, M. H. Van Ijzendoorn, J. J. Hudziak and F. C. Verhulst (2012). The Generation R Study: A review of design, findings to date, and a study of the 5-HTTLPR by environmental interaction from fetal life onward. *Journal of the American Academy of Child and Adolescent Psychiatry* **51**(11): 1119-1135 e1117.
- White, T., H. El Marroun, I. Nijs, M. Schmidt, A. van der Lugt, P. A. Wielopolski, V. W. Jaddoe, A. Hofman, G. P. Krestin, H. Tiemeier and F. C. Verhulst (2013). Pediatric population-based neuroimaging and the Generation R Study: the intersection of developmental neuroscience and epidemiology. *European journal of epidemiology* **28**(1): 99-111.
- White, T., R. Muetzel, M. Schmidt, S. J. Langeslag, V. Jaddoe, A. Hofman, V. D. Calhoun, F. C. Verhulst and H. Tiemeier (2014). Time of Acquisition and Network Stability in Pediatric Resting-State Functional MRI. *Brain Connect*.
- Winkler, A. M., G. R. Ridgway, M. A. Webster, S. M. Smith and T. E. Nichols (2014). Permutation inference for the general linear model. *Neuroimage* **92**: 381-397.
- Yeo, B. T., F. M. Krienen, J. Sepulcre, M. R. Sabuncu, D. Lashkari, M. Hollinshead, J. L. Roffman, J. W. Smoller, L. Zollei, J. R. Polimeni, B. Fischl, H. Liu and R. L. Buckner (2011). The organization of the human cerebral cortex estimated by intrinsic functional connectivity. *J Neurophysiol* **106**(3): 1125-1165.
- Zhang, H., X. N. Zuo, S. Y. Ma, Y. F. Zang, M. P. Milham and C. Z. Zhu (2010). Subject order-independent group ICA (SOI-GICA) for functional MRI data analysis. *Neuroimage* **51**(4): 1414-1424.

SUPPLEMENTAL MATERIAL

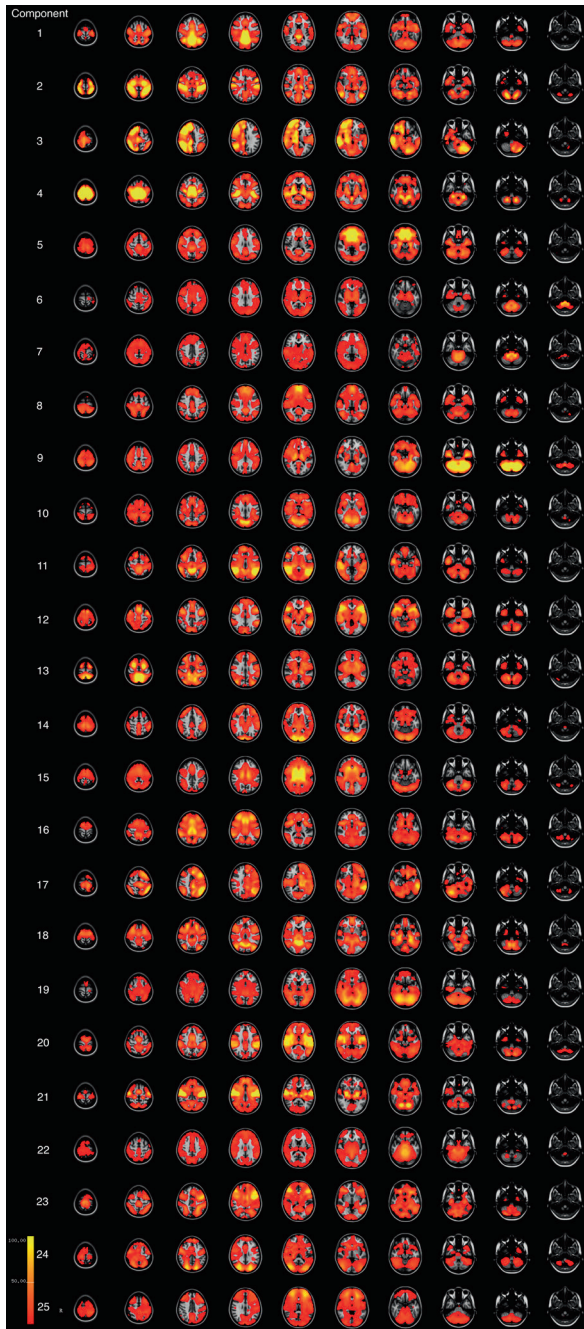


Supplemental Figure 1.
Depiction of process used to create age-appropriate structural brain template.



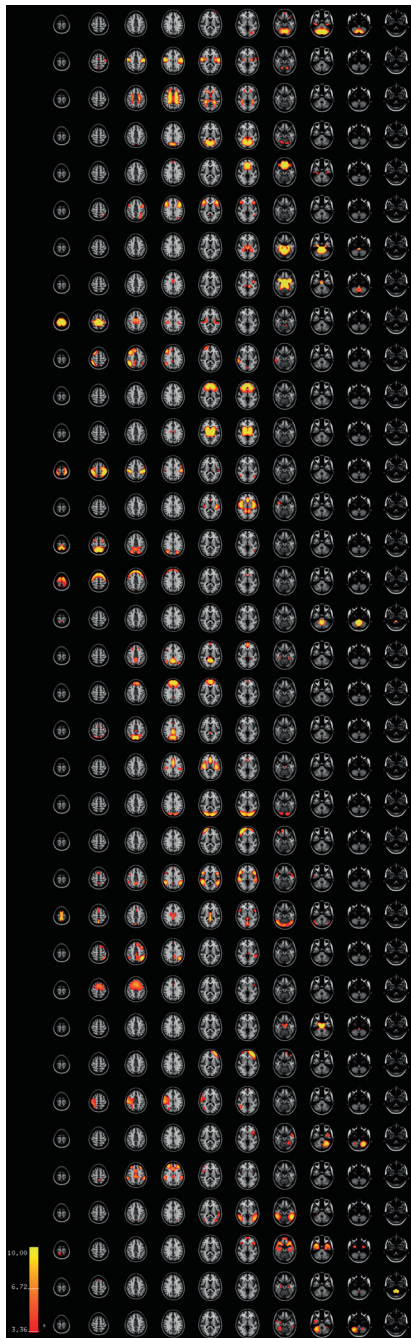
Supplemental Figure 2.

Components from subsampling approach not represented in the meta-ICA. Components are averaged z-maps of all matched resamples, thresholded at $z = 3.09$ ($p < 0.001$).



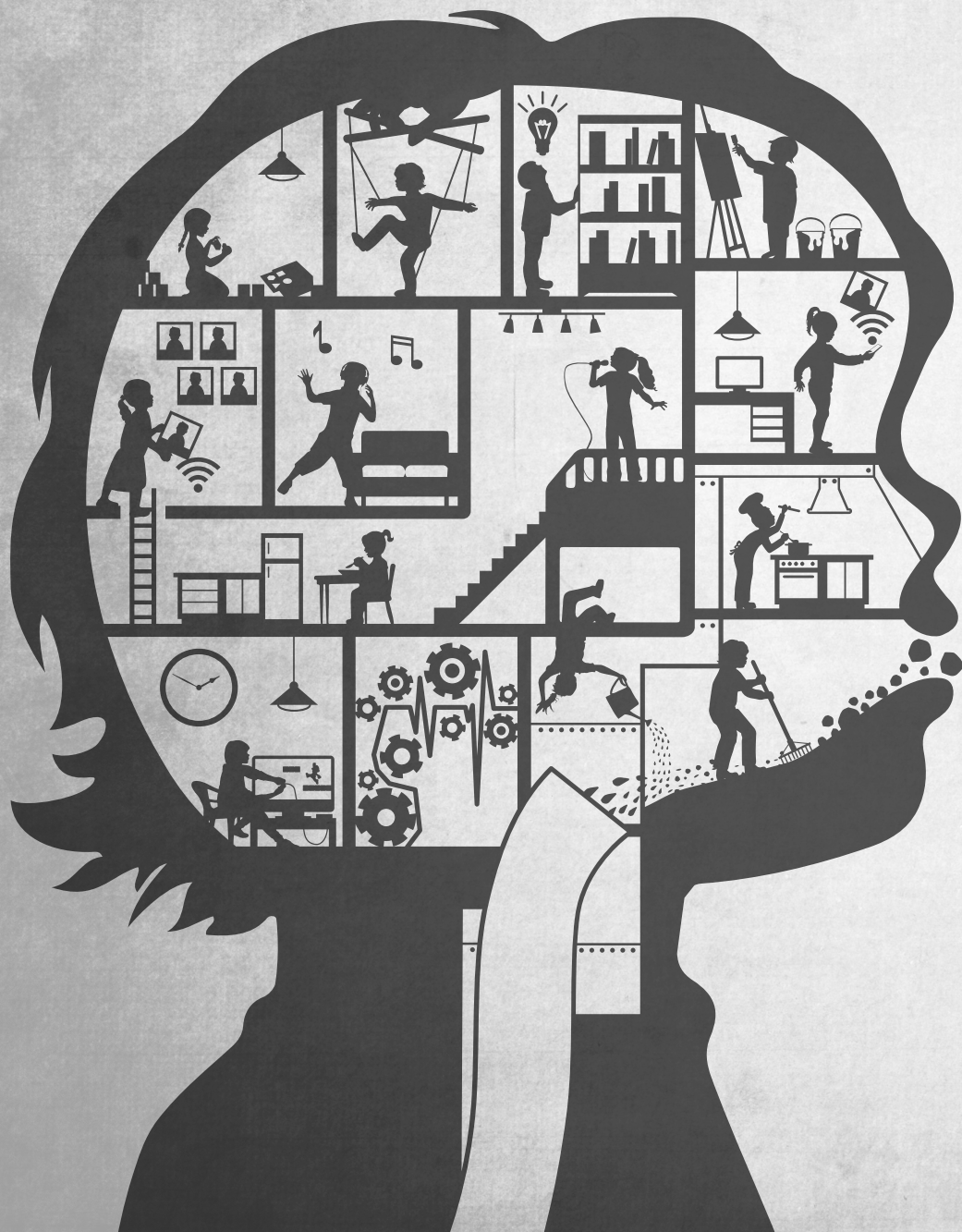
Supplemental Figure 3.

Depiction of spatial variability in meta-ICA components 1-to-25. For each component, 10,000 permutations were run on all matched resamples to compute the mean component of the resamples. Images are T-maps thresholded at $p_{FWE} < 0.05$.



Supplemental Figure 4.

Axial slices of components resulting from meta-ICA when no ICA-based artifact removal is applied at the subject-level prior to group ICA. Analyses are done with 1000 subsamples with group ICA. Components are thresholded at $z = 3.09$ ($p < 0.001$).



CHAPTER

7

From Chronnectivity To Chronnectopathy: Connectivity Dynamics of Typical Development And Autistic Traits

Ryan L. Muetzel*, Laura M. E. Blanken*, Barnaly Rashid*,
Robyn Miller, Eswar Damaraju, Mohammad R. Arbabshirani,
Erik B. Erhardt, Frank C. Verhulst, Aad van der Lugt, Vincent W. V.
Jaddoe, Henning Tiemeier, Tonya White, Vince Calhoun

** authors contributed equally to this work*

Manuscript submitted for publication

ABSTRACT

Autism spectrum disorder is often studied with little context of typical brain development. In addition, most functional connectivity studies operate under the assumption that connectivity remains static over multiple minutes. We hypothesized that relaxing this stationarity assumption would reveal novel features of both autism and typical brain development. We employed a 'chronnectomic' (recurring, time-varying patterns of connectivity) approach to evaluate transient states of connectivity using resting-state functional MRI in a sample of 774 6-to-10 year-old children. Whole-brain dynamic connectivity was evaluated using a sliding window technique, and revealed four transient states. Inter-domain connectivity increased with age in modularized dynamic states, illustrating an important pattern of connectivity associated with the developing brain. Furthermore, we demonstrate that higher levels of autistic traits were associated with more time spent in a globally disconnected state. These results provide a road map to the chronnectomic organization of the brain and also suggest that children with autistic traits exhibit delayed characteristics of functional brain maturation.

INTRODUCTION

A number of developmental disorders, including autism spectrum disorder (ASD), have demonstrated abnormal functional hypoconnectivity and hyperconnectivity within the connectome (Uddin et al. 2013). Atypical development of neural interactions has been considered as a major basis in theoretical models of neuropsychiatric disorders (Geschwind and Levitt 2007). Evidence suggests that short-range or intra-domain connectivity is more dominant during infancy (Fransson et al. 2007, Gao et al. 2011) and decreases with age during childhood and adolescence, while long-range or inter-domain connectivity becomes more dominant in early adulthood (Fair et al. 2009, Dosenbach et al. 2010). To our knowledge, no study has provided a baseline to understand how the brain's dynamic functional connectivity (i.e. chonnectivity) matures with age during childhood, and compared this baseline with the dysfunctional chonnectopathy of emerging mental illness. Likewise, the majority of existing models have made the assumption that the brain's functional connectivity is static over a period of multiple minutes. This has been shown to be a major limitation as important dynamic patterns of connectivity could be overlooked (Calhoun et al. 2014). In the context of this paper, the term chonnectome (and therefore chonnectivity) refers to dynamics in the functional network connectivity among multiple brain regions. Also, in this paper, the term connectome refers to the functional network connectivity at a macro-scale, with the assumption that the functional connectivity over this period of time is relatively static. In this work, we address both of these limitations by performing a chonnectomic analysis of typical development and autistic traits.

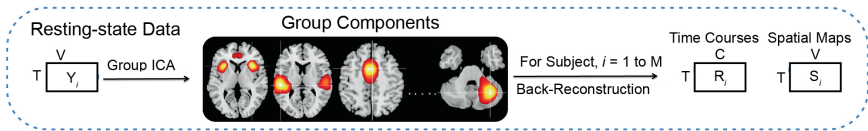
Over the past decade, various *in vivo* techniques, including functional magnetic resonance imaging (fMRI), have been increasingly used to study neuronal connectivity in the developing brain, particularly during rest (rs-fMRI). A wide array of methods has been used to categorize the brain into functionally interconnected parcels, or intrinsic connectivity networks (ICNs), such as the default-mode network. Importantly, the majority of existing rs-fMRI analysis strategies operate under the assumption that connectivity remains stationary or static throughout the entire measurement period (static functional network connectivity (sFNC)), potentially obscuring transient patterns of connectivity at different time instances. Recent advances in analysis methods have relaxed this stationarity assumption to yield indices of dynamic functional network connectivity (dFNC) that offer unique chonnectomic information (Hutchison et al. 2013, Allen et al. 2014) and are sensitive to neurobiological features of normal brain development (Hutchison and Morton 2015) and psychopathology (Rashid et al. 2014).

Despite the presence of an extensive and expanding literature, the neurobiological etiology of severe mental disorders such as autism spectrum disorder remains elusive. ASD has traditionally been conceptualized categorically, but is increasingly recognized as the severe end of a continuum of traits that extend into the general population (Constantino and Todd 2003). Imaging studies using a phenotype of quantitative social impairment can complement case-control studies to better understand the neurobiology of ASD. Irrespective of classification approach, one of the prominent hypotheses on the origins of ASD is an aberrant development of neuronal connections throughout the brain (i.e., ‘developmental disconnection syndrome’, Geschwind and Levitt 2007).

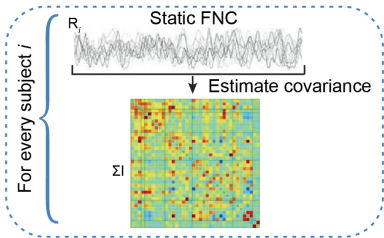
Within this context, we utilized resting-state fMRI scans from a large, population-based cohort study of children (Jaddoe et al. 2012, White et al. 2013) to search for both underlying maturational properties of dFNC that characterize age- and sex-specific connectivity dynamics, and an underlying neurobiological substrate of autistic traits in the general population. We hypothesized the presence of distinct dynamic connectivity states in children that are similar to those already reported in adults, given many static networks are already present at a young age (Gao, Gilmore et al. 2011). Further we expect age-related correlates of dynamic connectivity to resemble adult-like patterns, where increasing age is associated with states previously reported in adults. Lastly, as previous work has shown aberrant connectivity dynamics in psychopathology, we hypothesize to see an association between aberrant dynamic connectivity and features of autism. As traits of ASD have been shown to form a continuum in the general population, we hypothesized that such connectivity features would also be present along a continuum. Results showed that multiple brain domains (comprised of sets of ICNs) that are widely recognized in studies of adults (e.g., sub-cortical, default-mode and sensorimotor) are also identified in this large group of young children. Results also reveal that the dynamic properties of connectivity vary with both age and sex. Specifically, we found increased inter-domain connectivity with age in the more mature, “adult-like” dFNC states, in which older children also spent more time compared to the younger children. Interestingly, children with autistic traits spent more time in a globally disconnected state, which resembled the connectivity dynamics observed in younger children. These results show a link between the typical and atypical development trajectories as captured by dynamic FNC, where individuals with higher levels of autistic traits show a potentially delayed transition to spending time in the globally modularized or more heavily connected states. Taken together, the present study provides a conceptual framework to support further investigations of typical and atypical brain development in the general population using novel neuroimaging methodology and clinical insight.

RESULTS

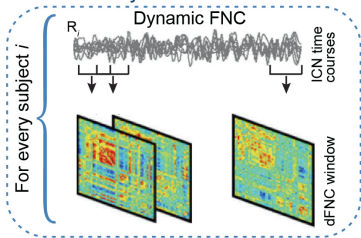
A. Identification of Intrinsic Connectivity Networks (ICNs)



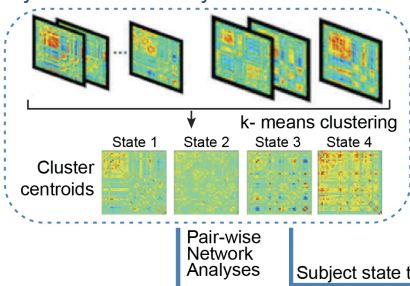
B. Estimation of Static FNC



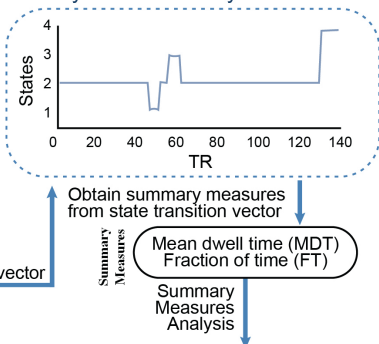
C. Estimation of dynamic FNC



D. Dynamic connectivity states



E. Summary measures of dynamic states



F. Highlights of key findings

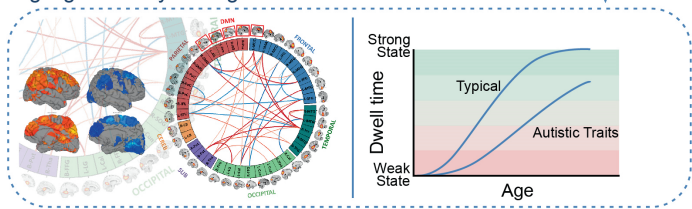


Figure 1. Graphical depiction of the analysis method and key findings. **(A)** The static and dynamic functional network connectivity (FNC) approach begin with group independent component analysis (ICA) to decompose resting-state fMRI data into intrinsic connectivity networks (ICNs). The group ICA approach provides a measure of the component time courses (TC) and spatial maps for each subject using the back-reconstruction technique. **(B)** Static FNC between components is estimated as the covariance of the time courses. **(C)** Dynamic FNC is estimated as the covariance from windowed portions of the time courses. **(D)** K-means clustering is used to identify discrete dynamic connectivity states. **(E)** Results obtained from k-means clustering are used to determine which state a given subject is occupying at a given time, and summary measures of dynamic states, such as, mean dwell time (MDT) and fraction of time (FT) spent in each state over the duration of the measurement period are computed. **(F)** Highlights of the key findings for pairwise network analyses and summary measures analyses in association with age, sex and autistic traits.

Characterizing static and dynamic functional network connectivity during development

Our first goal was to characterize the connectivity in typical development through age associations in a large sample of 774 school-age children. To do this we first evaluated the properties of both static and dynamic FNC (**Figure 1(A-D)**) of the developing brain using 38 ICNs (extracted from a 100 component, group independent component analysis (Calhoun et al. 2001)) grouped into brain domains according to their anatomical and functional properties (**Figure 2**). The static FNC of the developing brain showed similar patterns as previous large-scale analyses of adults (Allen, Damaraju et al. 2014, Damaraju et al. 2014) for both intra- and inter-domain connectivity. The default mode network was strongly connected within itself, and less connected to other brain networks (**Figure S1**). The dynamic connectivity analysis (**Figure 3**) identified two modularized states (State-1: globally modularized, i.e. modularized FNCs were present globally in intra- and inter-domain connectivity, and State-3: default-mode modularized, i.e. strong intra-domain positive connectivity and inter-domain negative connectivity in DMN). In addition, one globally disconnected state was identified (State-2: globally loosely connected intra- and inter-domain connectivity captured, a state not previously observed in adults) and one globally hyperconnected state (State-4: high positive connectivity found globally). Previous dynamic connectivity studies with adult subjects reported occurrence of three out of these four dynamic states (Allen, Damaraju et al. 2014).

Development of dynamic FNC states

Next, we evaluated the relationship of age and sex with the discrete dynamic FNC states to evaluate the trajectory of the states from a less to a more mature representation of FNC patterns (**Figure 4**). The age-related associations were mostly localized in (but not limited to) State-1, the globally modularized dynamic state. In particular, positive age-related associations among frontal-temporal components, and both positive and negative age-related associations among frontal-parietal and temporal-parietal components were observed in State-1. Also, the sex-related associations were mostly localized in (but not limited to) State-3, a state characterized by a modularized DMN. This particular dynamic state showed greater connectivity among frontal-temporal and frontal-occipital components in girls, and greater connectivity between a parietal component (right angular gyrus (also a DMN component)) and a temporal component (right middle temporal gyrus) in boys. In other FNC states, the age- and sex-specific changes were mostly localized to the DMN. Specifically, the left middle cingulate cortex (MCC) DMN component showed increased inter-domain connectivity with age in all FNC states, and increased intra-domain connectivity with age in State-4. Lastly, the left MCC showed an increase in inter-domain connectivity for girls in all FNC states, and an increase in intra-domain connectivity for boys in State-3.

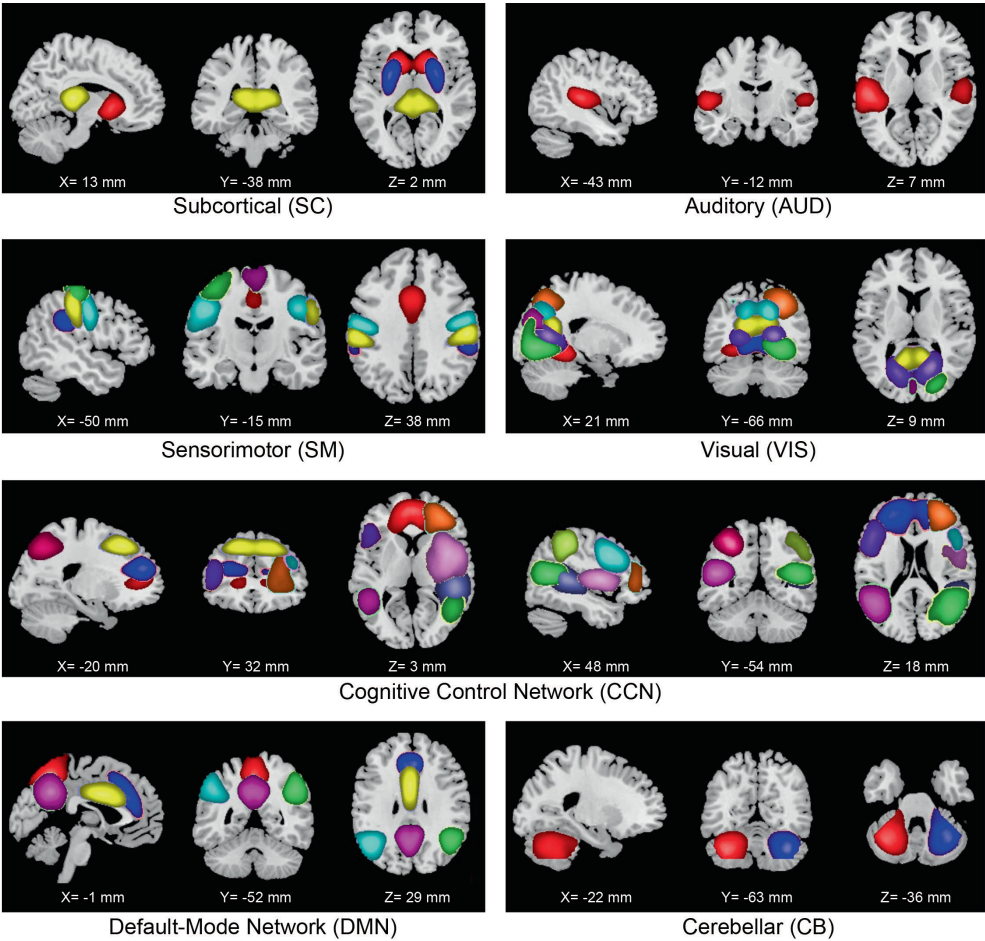


Figure 2. Non-artifactual intrinsic connectivity networks (ICNs). Composite maps of the 38 identified intrinsic connectivity networks (ICNs) used in static and dynamic functional network connectivity (FNC) analyses. The ICNs are divided into seven subcategories and arranged based on their anatomical and functional properties. Within each functional network, each color in the composite maps corresponds to a different ICN. Component labels and peak coordinates are provided in **Table S2**.

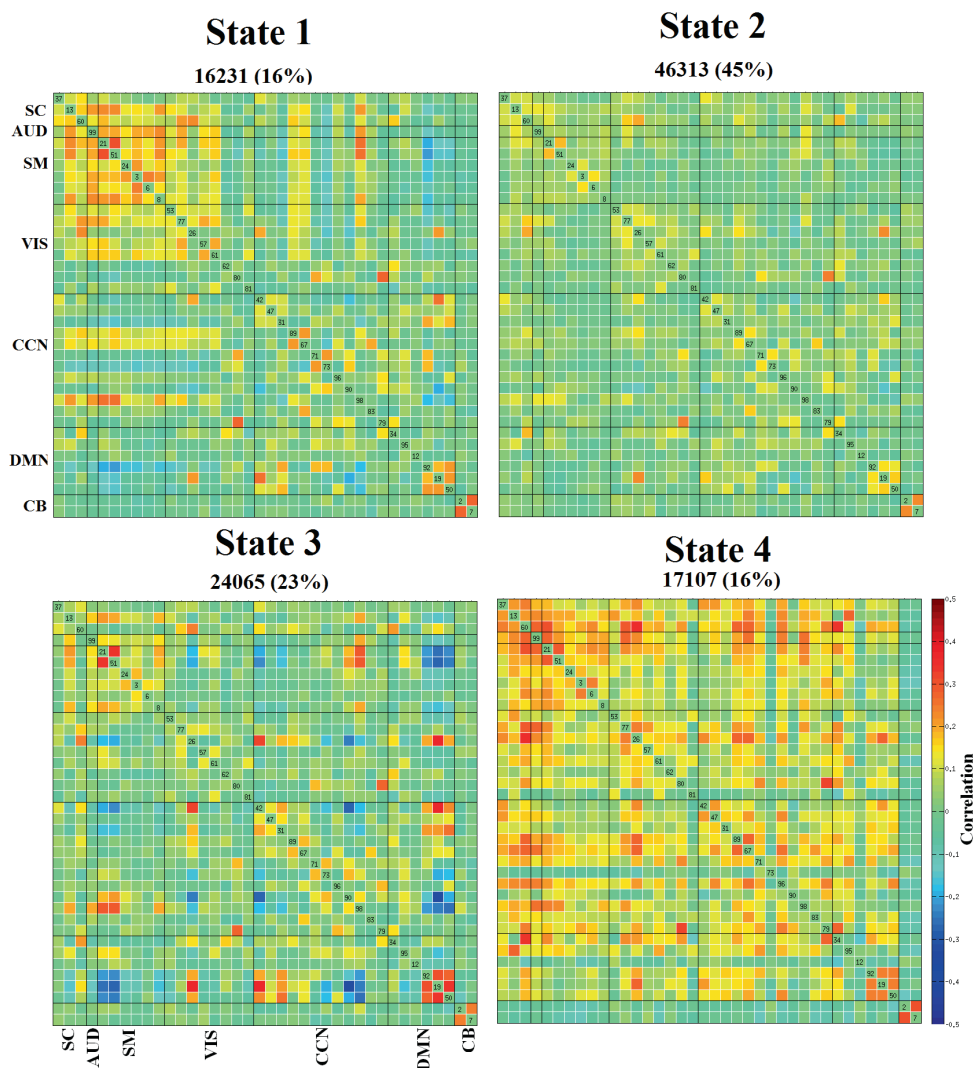


Figure 3. Dynamic functional network connectivity (FNC) states. The four dynamic states represented in connectivity matrices are symmetrically grouped by functional networks, and colors represent the average strength and direction of the pairwise correlation between two components, with red-yellow indicating a position correlation, and blue indicating a negative correlation. Here, SC: subcortical, AUD: auditory, SM: sensorimotor, VIS: visual, CCN: cognitive control network, DMN: default-mode network, and CB: cerebellar network. Labels for the dynamic states include, state-1: globally modularized, state-2: globally disconnected, state-3: DMN modularized, and state-4: globally hyperconnected.

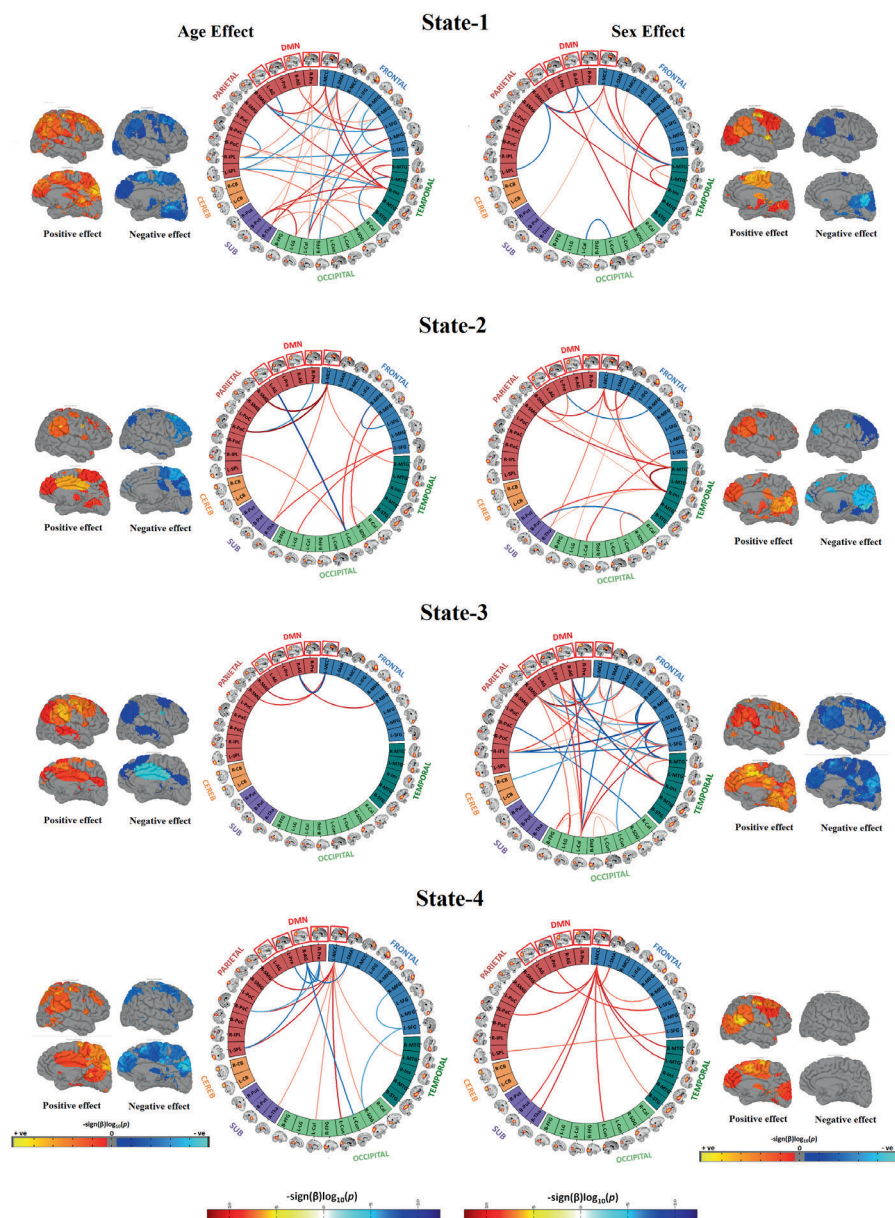


Figure 4. Connectogram and rendering maps showing age and sex associations across the dynamic connectivity states. Connectograms are sorted by major brain lobes. Rendering maps are divided into average positive and negative effects. For age analyses, red lines indicate positive association between a particular pairwise connection and age, whereas blue lines indicate a negative age association. For analyses of sex, red lines indicate where female subjects showed stronger connectivity than male subjects, and blue lines indicate where male subjects showed stronger connectivity compared to female subjects. All the results presented in the connectograms survived the false discovery rate (FDR) multiple comparison correction threshold of $p_{FDR} = 0.05$.

Age- and sex-related associations with time spent in dynamic states

Next, we explored how dynamic connectivity properties such as mean dwell time (MDT) and fraction of time spent in dynamic states (FT) change as functions of age and sex (**Figure 5**). Here, for each of the dynamic FNC states, we computed the MDT (how long an individual spends in a given state on average) and FT (total time spent in a given state). The equations for MDT and FT are given in the online method section. We found that older children showed higher MDT and FT in the globally modularized dFNC state, or State-1. Conversely, younger subjects showed higher MDT and FT in the globally disconnected state, or State-2. We also investigated the sex-related differences in MDT and FT in the dynamic states. We found that in the disconnected state (State-2), boys showed higher FT, whereas in DMN-modularized state (State-3), girls showed higher MDT and FT. The other two dynamic states, the globally modularized state (State-1) and the globally hyperconnected state (State-4) showed trend-level sex effects, where boys showed higher MDT and FT compared to girls in States-1 and -4.

Characterization of dynamic connectopathy (chronnectopathy) in autistic traits and children with ASD

In addition to characterizing static and dynamic FNCs in typical development, we also studied the chronnectopathy, or disruption of the typical dynamic connectivity patterns, in children with autistic traits. We assessed autistic traits using the Social Responsiveness Scale (SRS) (Constantino et al. 2003) in a subset of children (n=560). For static connectivity, one component pair (the left supplementary motor area, i.e. SMA, and the right supramarginal gyrus, i.e. SmG), showed an association with autistic traits. Specifically, children with more autistic traits showed weaker static FNC. Interestingly, for dFNC State-3, children with more autistic traits showed higher connectivity in three component pairs (right insula and left superior frontal gyrus, right SmG and left precuneus i.e. preC, and right insula and left preC) and lower connectivity in two component pairs (right-insula and right SmG, and left SMA and right SmG). Next, we assessed how MDT and FT vary with respect to autistic trait scores (**Figure 6**). In the globally disconnected state (State-2), autistic traits showed a positive association with MDT. In the DMN-modularized state (State-3), autistic traits were negatively associated with MDT. Thus, children with high levels of autistic traits spent more time in the globally disconnected state (State-2) and children with lower levels spent more time in the DMN-modularized state (State-3). Results remained highly consistent when models were additionally adjusted for non-verbal IQ. A similar pattern of effects was observed at the severe end of the spectrum, when 22 children with clinical ASD were compared to 88 age, sex and IQ matched controls (**Figure S6**). Further, in order to assess whether the above-mentioned associations are a core feature of the trait-continuum or if effects were driven by the most severely affected children, sensitivity analyses were run. In these sensitivity

analyses, children with clinical ASD or an autistic traits score above the screening threshold were excluded, and results remained consistent (Figure S7).

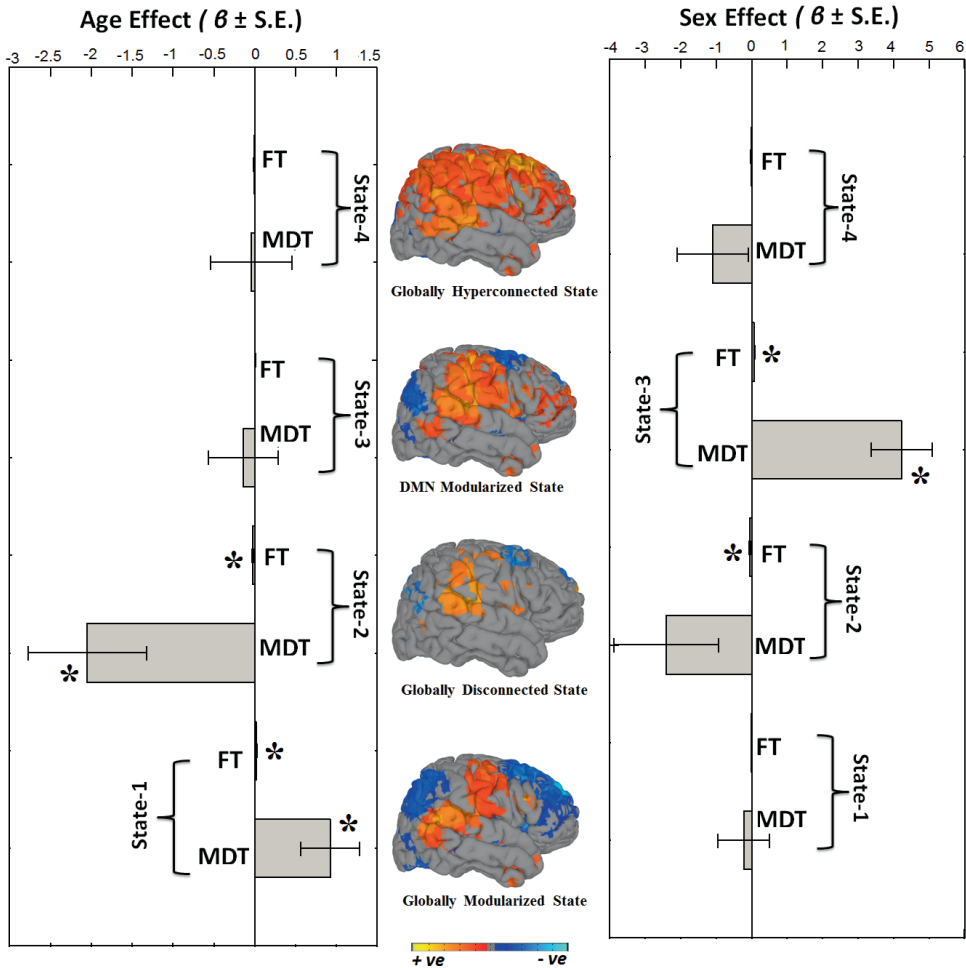


Figure 5. Summary metrics and age- and sex- effects. Summary metrics from the four dynamic connectivity states in relation to age and sex. Mean dwell time (MDT) represents how long an individual spends in a given state on average, and fraction of time (FT) is the summed total time spent in a given state over the course of the measurement period. For age associations, positive beta coefficient (β) indicates older children spend more time in that particular state whereas negative beta coefficient (β) indicates younger children spend more time in a particular state. For sex analyses, positive beta coefficient (β) indicates girls spend more time in the state relative to boys, and negative beta coefficient (β) indicates that boys spend more time in the state relative to girls. Bar graphs indicate the unstandardized beta coefficients (β) with standard error (S.E.) from regression models, and asterisks (*) indicate the results survived the false discovery rate (FDR) multiple comparison correction threshold of $p_{FDR} = 0.05$. The rendering brain maps are showing modularized positive (red) and negative (blue) connectivity for the corresponding dynamic states.

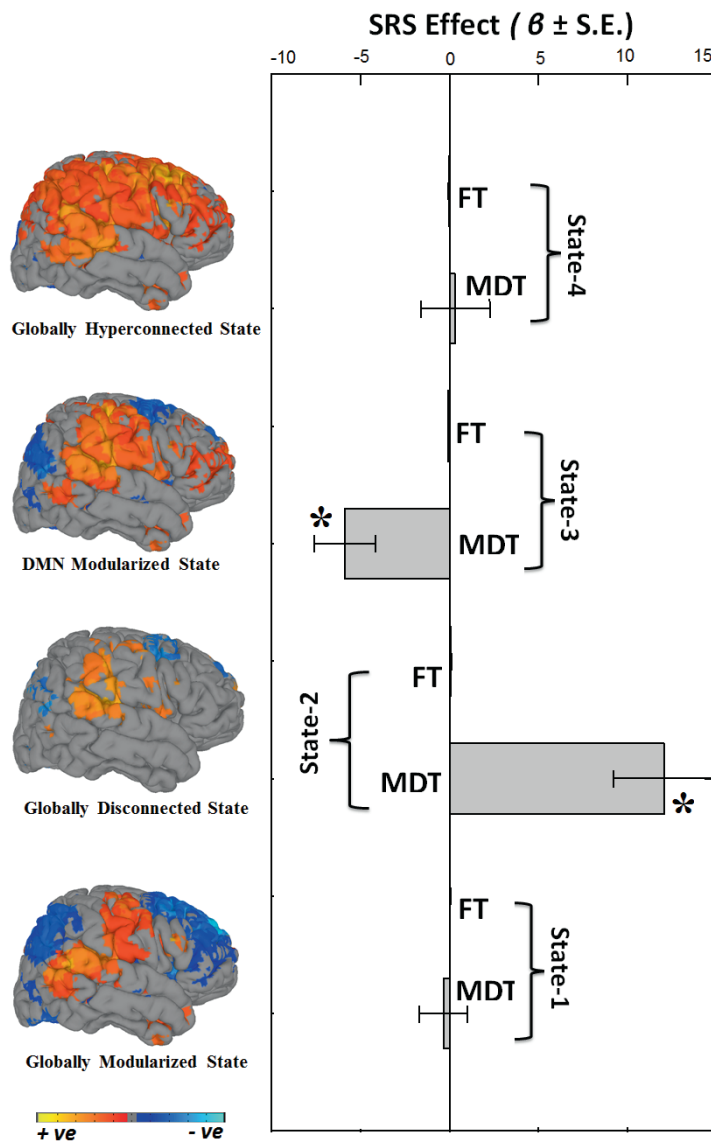


Figure 6. Summary metrics and autistic trait effects. Summary metrics from the four dynamic connectivity states in relation to autistic traits. Mean dwell time (MDT) represents how long an individual spends in a given state on average, and fraction of time (FT) is the summed total time spent in a given state over the course of the measurement period. Positive beta coefficient (β) indicates that higher levels of autistic traits are associated with more time spent in a particular state; whereas negative beta coefficient (β) indicate lower levels of autistic traits are associated with more time spent in a particular state. Bar graphs indicate the unstandardized beta coefficients (β) with standard error (S.E.) from regression models, and Asterisks (*) indicate the results survived the false discovery rate (FDR) multiple comparison correction threshold of $p_{\text{FDR}} = 0.05$. The rendering brain maps are showing modularized positive (red) and negative (blue) connectivity for the corresponding dynamic states.

DISCUSSION

Here we apply a novel approach to the study of brain connectivity, both in typical and atypical child development. Complementing the existing static functional connectivity literature, we show age-related associations with discrete dynamic states that illustrate higher order maturational effects on the chronnectome. We also provide additional support for a disconnection construct in children with autistic traits using dynamic functional connectivity. In the context of often subjective and qualitative interpretations of static network matrices, we demonstrate the utility and potential clinical relevance of quantitative metrics that summarize large amounts of complex chronnectomic information.

The development of whole-brain dynamic connectivity in young children

In a large group of young children with a narrow age-range, we demonstrate that older children spend more time in states typically observed in healthy adults. Age-related associations with static connectivity were consistent with previous reports, including decreased segregation and increased integration of control networks (Fair et al. 2007). This validation of the existing static connectivity literature is nicely complemented with new information where assumptions of network stationarity are relaxed, and quantitative summary metrics, such as mean dwell time, are examined (Hutchison and Morton 2015). Interestingly, evidence for sexual dimorphism in FNC was also observed with girls spending more time in the modularized default-mode state and boys spending more time in the globally disconnected state. While no age-by-sex interaction was observed, given the narrow age range, this could complement existing evidence showing neuromaturational processes begin earlier in girls (Lenroot and Giedd 2006, Simmonds et al. 2014).

Functional connectivity and autistic traits

Novel neuroimaging findings in combination with a characteristic early onset have brought momentum to ASD being conceptualized as a developmental disconnection syndrome (Geschwind and Levitt 2007). Previous studies of static FNC in ASD have revealed mixed patterns of increased and decreased connectivity strength (Uddin, Supekar et al. 2013). Similarly, within the discrete dynamic FNC states, we found local patterns of increased as well as reduced connection strength. We found decreased connectivity between the right supramarginal gyrus and the right insula, which is consistent with findings of lower insula activation in subjects with ASD in a large number of task-based neuroimaging studies, covering a range of social processing tasks (Di Martino et al. 2009). However, we also found *hyperconnectivity* between the right insula, with the precuneus and the left superior frontal gyrus. Hyperconnectivity of the salience network, in which the insula is a key region, is particularly well replicated in the context of childhood ASD (Uddin et al. 2013).

Our findings in children in a similar age range suggest that the hyperconnectivity of the insula may also extend beyond regions of the salience network. Further, divergent findings of hypo- and hyperconnectivity in this region across studies, which have been previously attributed to developmental differences between samples (Uddin, Supekar et al. 2013), may in fact be present at the same developmental stage, but across different dynamic states and thus only apparent when using dynamic connectivity approaches.

Here, for the first time, we demonstrate that children with higher levels of autistic traits spend more time in a globally disconnected state during rest, whereas children with lower levels of autistic traits spend more time in a globally modularized state that resembles an adult-like pattern of connectivity. Interestingly, in schizophrenia, another disorder frequently classified as a disconnection syndrome, patients also spend more time in weakly connected dynamic states compared to healthy controls (Damaraju, Allen et al. 2014, Rashid, Damaraju et al. 2014). This also potentially fits with previous work in adults showing that, at the individual level, those with ASD may have distinct, noisy patterns of connectivity that may even mask ‘typical’ patterns of connectivity (Hasson et al. 2009). Higher levels of autistic traits were also associated with less time spent in a default-mode modularized state; a state where nodes from the well-documented default-mode network were prominent. Despite heterogeneity in much of the functional connectivity literature, there is a growing body of evidence that the default mode network is more weakly connected in individuals with ASD (Stigler et al. 2011, Jung et al. 2014). Interestingly, task-based data examining the effect of a cognitive load on the DMN has previously suggested the DMN does not ‘deactivate’ during a task in ASD (Kennedy et al. 2006). However, in the context of our findings, it is possible that rather failing to deactivate, the DMN actually fails to ‘activate’ in individuals with ASD; an interpretation that could be made from task-rest contrasts of BOLD activation. We also demonstrated that, in the absence of clinically relevant cases, autistic symptoms in the general pediatric population are related to dynamic aspects of network connectivity. This is further evidence that aspects of the neurobiology of autistic traits, similar to the symptomatology, indeed lie on a continuum (Constantino and Todd 2003, Di Martino et al. 2009, Blanken et al. 2015). In addition to the dimensional trait approach, children with confirmed ASD were compared to a group of age- and sex-matched controls, revealing similar patterns of increased dwell time within the globally disconnected state. Thus, we show that these dynamic functional connectivity features of autistic traits are also present in the most severely affected children. We propose to label this continuum of dynamic connectivity features “chronnectopathy”. However, it should be noted that, similar to the behavioral phenotype, only the severe end is “clinical” and certainly not all tendencies to this pattern should be considered as such. Interestingly, the increased mean dwell time in a less connected state observed in children with autistic traits and ASD which mimics the patterns in younger, typically developing children, is potentially indicative of a delayed or halted trajectory (Di Martino et al. 2014)

ADDITIONAL CONSIDERATIONS

Strengths of this study include the large, population-based sample of children in a narrow age range, enabling us to show subtle age effects during a crucial, pre-adolescent period of development. Further, the age-range included in the current study is particularly under-studied in the context of ASD (Uddin, Supekar et al. 2013). Another major strength is the use of a dynamic approach to resting state connectivity combined with an efficient and interpretable presentation of a wealth of data. While there is some consistency in the expansive static connectivity literature in ASD, it is unfortunately plagued by heterogeneity in clinical characteristics of the subjects, image acquisition, analysis strategy, and ultimately the core findings (Uddin, Supekar et al. 2013, Hernandez et al. 2015). The quantitative summary measures presented here could potentially aid in simplifying interpretations of complex network information, which historically are often subjectively evaluated. For instance, specific and isolated features of large (e.g., 80x80) connectivity matrices are often summarized when undoubtedly more complex patterns are present. While the present study also assigned labels to the four dynamic states, most of the interpretation comes from the quantitative MDT metric. This method may be especially suitable to study ASD, as disruptions of connectivity patterns in subjects with autism are thought to be highly idiosyncratic (Hahamy et al. 2015) and this method may be more suitable to pick up group differences in the context of such individual differences. The subjects were all scanned on the same MRI scanner, which reduces vendor- and hardware-dependent differences. Finally, the study of ASD is approached dimensionally as well as from a traditional case-control perspective, revealing dynamic connectivity features of ASD that lie along a continuum in the general population. While many studies of ASD include only boys, our sample was sex-balanced and also presented in the context of typical brain development. However, some limitations deserve mention. While increased scan duration is likely to reveal the complexity of dynamic connectivity states and their temporal aspects more accurately, our rs-fMRI scan was limited to just over 5 minutes to ensure high quality data, given the scale of the study and to minimize the burden on our young participants (White et al. 2014). Further, our study was cross-sectional and all participants were of school-age, so the interpretation of our results can not be extended to other stages of development. Longitudinal studies are warranted to reveal trajectories of dynamic connectivity in typical and atypical development.

In conclusion, our approach suggests that a hallmark of childhood is not limited to the under-development of the frontal lobe, but also about the efficient utilization of vast interconnections; in essence, younger children are less frequently tapping into the resources that they have. Also, children with higher levels of autistic traits are even less likely to efficiently use such connections and may have less capacity in this regard. This study revealed novel aspects of psychopathology and future studies should evaluate the utility

of this methodology in, for example, the classification, evaluation and treatment response prediction of conditions like ASD.

METHODS

Participants

The current study is embedded in the Generation R Study, which is a large, population-based birth cohort in Rotterdam, the Netherlands (Jaddoe, van Duijn et al. 2012). One thousand seventy children, ages 6-to-10 years, were scanned between September 2009 and July 2013 as part of a sub-study within the Generation R Study (White, El Marroun et al. 2013). General exclusion criteria for the current study include severe motor or sensory disorders (deafness or blindness), neurological disorders, moderate to severe head injuries with loss of consciousness, claustrophobia, and contraindications to MRI. Raw fMRI data from 964 subjects were available for our study, and after excluding children with bad data (e.g., motion, for details see below) 774 datasets were available for statistical analysis. Informed consent was obtained from the parents, and all procedures were approved by the Medical Ethics Committee of the Erasmus Medical Center.

Autistic Traits and Autism Spectrum Disorder

The Social Responsiveness Scale was administered when children were roughly age 6 years (range: 4.89–8.90 years) to measure autistic traits based on parental observation during the last six months (Constantino 2002). The Social Responsiveness Scale provides a valid quantitative measure of subclinical and clinical autistic traits, where higher scores indicate more symptoms related to ASD (Constantino 2002). We utilized the total score derived from the abbreviated, 18-item short-form of the scale, which shows correlations ranging from 0.93 to 0.99 with the full scale in three different large studies (Blanken, Mous et al. 2015). Cutoffs were based on recommendations for screening in population-based settings (consistent with weighted scores of 1.078 for boys and 1.000 for girls) (Constantino 2002).

At approximately age 7 years, children who scored in the top 15th percentile on the Child Behavior Checklist-1.5–5 total score and those who scored in the top 2nd percentile on the Pervasive Developmental Problems sub-scale underwent a screening procedure for ASD using the Social Communication Questionnaire (SCQ), a 40-item parent-reported screening instrument to assess characteristic autistic behavior. Social Communication Questionnaire scores ≥ 15 are considered positive for screening (Berument et al. 1999). We approached the general practitioners of children who scored screen-positive on the SRS, SCQ or for whom the mother reported a diagnosis of ASD in order to confirm this diagnosis with medical

records. In the Netherlands, the general practitioner holds the central medical records, including information on treatment by (medical) specialists. In this sample, 22 children with usable MRI data also had a confirmed diagnosis of ASD.

MRI Data Acquisition

Magnetic resonance imaging data were acquired on a 3 Tesla scanner (Discovery 750, General Electric, Milwaukee, WI) using a standard 8-channel, receive-only head coil. A three-plane localizer was run first and used to position all subsequent scans. Structural T1-weighted images were acquired using a fast spoiled gradient-recalled echo (FSPGR) sequence (TR = 10.3 ms, TE = 4.2 ms, TI = 350 ms, NEX = 1, flip angle = 16°, matrix = 256 x 256, field of view (FOV) = 230.4 mm, slice thickness = 0.9mm). Echo planar imaging was used for the rs-fMRI session with the following parameters: TR = 2000 ms, TE = 30 ms, flip angle = 85°, matrix = 64 x 64, FOV = 230 mm x 230 mm, slice thickness = 4 mm. In order to determine the number of TRs necessary for functional connectivity analyses, early acquisitions acquired 250 TRs (acquisition time = 8min 20sec). After it was determined fewer TRs were required for these analyses, the number of TRs was reduced to 160 (acquisition time = 5min 20sec) (White, Muetzel et al. 2014). Children were instructed to stay awake and keep their eyes closed during the rs-fMRI scan. Further details on the entire scanning protocol can be found elsewhere (White, El Marroun et al. 2013).

Image Preprocessing

Data preprocessing was performed using a combination of toolboxes (AFNI, <http://afni.nimh.nih.gov>, SPM: <http://www.fil.ion.ucl.ac.uk/spm>, GIFT, <http://mialab.mrn.org/software/gift>), and custom scripts were written in Matlab. We performed rigid body motion correction using the INRIAlign (Freire and Mangin 2001) toolbox in SPM to correct for subject head motion followed by slice-timing correction to account for timing differences in slice acquisition. Then the fMRI data were despiked using AFNI's 3dDespike algorithm to mitigate the impact of outliers. The fMRI data were subsequently warped to a Montreal Neurological Institute (MNI) template (<http://www.mni.mcgill.ca>) and resampled to 3 mm³ isotropic voxels. Then we smoothed the data with a Gaussian kernel to 5 mm full width at half maximum (FWHM). Each voxel time course was variance normalized prior to performing group independent component analysis as this has shown to better decompose subcortical sources in addition to cortical networks. In order to limit the impact of severe head motion, we excluded subjects' data with a maximum translation of > 5 mm and/or with signal-to-noise fluctuation ratio (SFNR) <200 from our analyses, resulting in a final dataset with 774 subjects.

Group Independent Component Analysis (ICA)

After preprocessing the data, functional data were analyzed using spatial group independent component analysis (GICA) framework as implemented in the GIFT software (Calhoun, Adali et al. 2001, Calhoun and Adali 2012). Spatial ICA decomposes the subject data into linear mixtures of spatially independent components that exhibit a unique time course profile. A subject-specific data reduction step was first used to reduce 160 time point data into 100 directions of maximal variability using principal component analysis. Then subject-reduced data were concatenated across time and a group data PCA step reduced this matrix further into 100 components along directions of maximal group variability. One hundred independent components were obtained from the group PCA reduced matrix using the infomax algorithm (Bell and Sejnowski 1995). To ensure stability of estimation, we repeated the ICA algorithm 20 times in ICASSO (<http://www.cis.hut.fi/projects/ica/icasso>), and aggregated spatial maps were estimated as the modes of component clusters (Himberg et al. 2004). Subject specific spatial maps (SMs) and time courses (TCs) were obtained using the spatiotemporal regression back reconstruction approach (Calhoun et al. 2001, Erhardt et al. 2011) implemented in GIFT software.

Post-ICA processing

Subject specific SMs and TCs underwent post-processing as described in our earlier work (Allen, Damaraju et al. 2014). Briefly, we obtained one sample t-test maps for each SM across all subjects and thresholded these maps to obtain regions of peak activation clusters for that component; we also computed mean power spectra of the corresponding TCs. We identified a set of components as intrinsic connectivity networks (ICNs) if their peak activation clusters fell on gray matter and showed less overlap with known vascular, susceptibility, ventricular, and edge regions corresponding to head motion. We also ensured that the mean power spectra of the selected ICN time courses showed higher low frequency spectral power. This selection procedure resulted in 38 ICNs out of the 100 independent components obtained.

The subject specific TCs corresponding to the ICNs selected were detrended, orthogonalized with respect to estimated subject motion parameters, and then despiked. The despiking procedure involved detecting spikes as determined by AFNI's 3dDespike algorithm and replacing spikes by values obtained from third order spline fit to neighboring clean portions of the data. The despiking process reduces the impact/ bias of outliers on subsequent FNC measures (see Supplemental Fig. 1 in (Allen, Damaraju et al. 2014)). Lastly, subject-level rs-fMRI data were denoised using automated artifact removal (Tohka et al. 2008, Rodriguez et al. 2010). Thus, signals attributed noise/artifact, including those related to motion, were removed from the data.

Static Functional Network Connectivity (sFNC)

We computed functional network connectivity (FNC), defined as pairwise correlation between ICN time courses, as a measure of average connectivity among different ICNs during the scan duration. In this work, the FNC computed using the whole ICN time courses is referred to as stationary or static FNC (sFNC). Since correlation among brain networks is primarily shown to be driven by low frequency fluctuations in BOLD fMRI data (Cordes et al. 2001), we band pass filtered the processed ICN time courses between [0.01–0.15] Hz using 5th order Butterworth filter prior to computing FNC between ICNs. The mean sFNC matrix was computed over subjects. The mean sFNC matrix was initially organized into modular partitions using the Louvain algorithm of the brain connectivity toolbox (<https://sites.google.com/site/bctnet>). The modular partitions obtained from the algorithm were slightly rearranged to match the order of sFNC matrix rows to our recent work (Allen, Damaraju et al. 2014). After this reordering, the rows of sFNC matrix were partitioned into sub-cortical (SC), auditory (AUD), visual (VIS), sensorimotor (SM), a broad set of regions involved in cognitive control (CCN) and attention, default-mode network (DMN) regions, and cerebellar (CB) components as shown in Figure S1.

Dynamic Functional Network Connectivity (dFNC)

As recent studies both in animals and humans have highlighted the nonstationary nature of functional connectivity in BOLD fMRI data (Chang and Glover 2010, Hutchison et al. 2013), we sought to determine whether the observed sFNC differences were primarily driven by certain connectivity configurations (Hutchison, Womelsdorf et al. 2013). Following our recent work (Allen, Damaraju et al. 2014), dynamic FNC (dFNC) between two ICA time courses was computed using a sliding window approach with a window size of 22 TR (44 s) in steps of 1 TR (Figure 1). As in our earlier work, the window constituted a rectangular window of 22 time points convolved with Gaussian of sigma 3 TRs to obtain tapering along the edges. Since estimation of covariance using time series of shorter length can be noisy, we estimated covariance from regularized inverse covariance matrix (ICOV) (Varoquaux et al. 2010, Smith et al. 2011) using the graphical LASSO framework (Friedman et al. 2008). We imposed an additional L1 norm constraint on the inverse covariance matrix to enforce sparsity. The regularization parameter was optimized for each subject by evaluating the log-likelihood of unseen data of the subject in a cross-validation framework. After computing dFNC values for each subject, these covariance values were Fisher-Z transformed.

Clustering and Dynamic States Detection

Based on our observation that patterns of dFNC connectivity reoccur within subjects across time and also across subjects, we used a k-means algorithm to cluster these dynamic FNC windows, partitioning the data into a set of separate clusters so as to maximize the

correlation within a cluster to the cluster centroid. Instead of clustering all of the dFNC windows across all subjects, initial clustering was performed on a subset of windows from each subject, called subject exemplars hereafter, corresponding to windows of maximal variability in correlation across component pairs. To obtain the exemplars, we first computed variance of dynamic connectivity across all pairs at each window. We then selected windows corresponding to local maxima in this variance time course. The optimal number of centroid states was estimated using the elbow criterion, defined as the ratio of within cluster to between cluster distances. A k of 4 was obtained using this method in a search window of k from 2 to 9. The correlation distance metric was chosen as it is more sensitive to the connectivity pattern irrespective of magnitude (although choosing other distance functions such as cityblock, cosine and L1-norm did not make any difference in observed results). These sets of initial group centroids were used as a starting point to cluster all of the dFNC windows from all subjects.

Also, summary measures such as mean dwell time (MDT) and fraction of time (FT) were computed from the state transition vector. Using the following equations (i) and (ii), we computed MDT and FT for each subject:

$$MDT^{state(k)} = \text{mean}(TR_{end} - TR_{start}) \dots\dots\dots (i)$$

where,

$$TR_{start} = \text{count}(\text{difference}(\text{state_vector}_{\text{subject}(i)}, \text{state_number}) == 1)$$

$$TR_{end} = \text{count}(\text{difference}(\text{state_vector}_{\text{subject}(i)}, \text{state_number}) == -1)$$

and,

$$FT^{state(k)} = \frac{\text{sum}(\text{state_vector}_{\text{subject}(i)} == 1)}{\text{Total number of TR}} \dots\dots\dots (ii)$$

Statistical Analyses

Statistical analyses were carried out in Matlab (version R2011b) using the statistics toolbox and linear model class. Multiple linear regression was used to examine associations with connectivity metrics. Two separate models were used to investigate associations with sFNC, dFNC and summary metrics from dFNC such as MDT and FT: first model where age, sex and age-sex interaction were entered as independent (predictor) variables and main effects for each were examined, and a second model where autistic traits (SRS) was entered as the independent variable and age, sex and age-sex interaction were added as covariates. All of the results reported correspond to a false discovery rate multiple comparison correction threshold $q < 0.05$.

The following models were used for investigating associations with sFNC. We also checked the effects of interaction between age-sex and SRS-sex (in **Model-1**: $\beta_{age_i} * sex_i$; in **Model-2**: $\beta_{SRS_i} * sex_i$).

$$\text{Model-1}_{\text{sFNC}}: \text{sFNC}_i \sim \beta_0 + \beta_1 \text{age}_i + \beta_2 \text{sex}_i + \epsilon_i$$

$$\text{Model-2}_{\text{sFNC}}: \text{sFNC}_i \sim \beta_0 + \beta_1 \text{SRS}_i + \beta_2 \text{age}_i + \beta_3 \text{sex}_i + \epsilon_i$$

For dFNC analyses, we computed a subject median (computed element-wise) for each partition from the subject windows that were assigned to that partition as a representative pattern of connectivity of the subject for that state. To investigate if the observed effects of age, sex and SRS on sFNC are primarily driven by certain dynamic FNC states, we used these subject medians for each state, as well as the summary matrices for each state, and evaluated the associations using two separate models as mentioned above.

The following models were used for investigating associations with dFNC. We also checked the effects of interaction between age-sex and SRS-sex (in **Model-3**: $\beta_1 \text{age}_i * \text{sex}_i$; in **Model-4**: $\beta_1 \text{SRS}_i * \text{sex}_i$).

$$\text{Model-3}_{\text{dFNC}}: \text{dFNC}_i^{\text{state}(k)} \sim \beta_0 + \beta_1 \text{age}_i + \beta_2 \text{sex}_i + \epsilon_i$$

$$\text{Model-4}_{\text{dFNC}}: \text{dFNC}_i^{\text{state}(k)} \sim \beta_0 + \beta_1 \text{SRS}_i + \beta_2 \text{age}_i + \beta_3 \text{sex}_i + \epsilon_i$$

The following models were used for investigating associations with summary matrices of dFNC (MDT and FT). We also checked the effects of interaction between age-sex and SRS-sex (in **Model-5** and **Model-7**: $\beta_1 \text{age}_i * \text{sex}_i$; in **Model-6** and **Model-8**: $\beta_1 \text{SRS}_i * \text{sex}_i$).

$$\text{Model-5}_{\text{MDT}}: \text{MDT}_i \sim \beta_0 + \beta_1 \text{age}_i + \beta_2 \text{sex}_i + \epsilon_i$$

$$\text{Model-6}_{\text{MDT}}: \text{MDT}_i \sim \beta_0 + \beta_1 \text{SRS}_i + \beta_2 \text{age}_i + \beta_3 \text{sex}_i + \epsilon_i$$

$$\text{Model-7}_{\text{FT}}: \text{FT}_i \sim \beta_0 + \beta_1 \text{age}_i + \beta_2 \text{sex}_i + \epsilon_i$$

$$\text{Model-8}_{\text{FT}}: \text{FT}_i \sim \beta_0 + \beta_1 \text{SRS}_i + \beta_2 \text{age}_i + \beta_3 \text{sex}_i + \epsilon_i$$

Pair-wise associations from the above mentioned models are depicted in connectivity matrices and in connectograms (Langen et al. 2015).

Several sensitivity analyses were run in order to ensure results were not influenced various confounding factors, and are reported in the Supplemental Data section. First, to ensure behavioral problems did not influence age- and sex-related associations, analyses were run where children with high levels of behavioral problems were excluded. Similarly, to test whether continuous associations between autistic traits and connectivity were truly along a continuum and not driven by extreme cases, analyses were run after excluding children scoring highest on the SRS.

REFERENCES

- Allen, E. A., E. Damaraju, S. M. Plis, E. B. Erhardt, T. Eichele and V. D. Calhoun (2014). Tracking whole-brain connectivity dynamics in the resting state. *Cereb Cortex* **24**(3): 663-676.
- Bell, A. J. and T. J. Sejnowski (1995). An information-maximization approach to blind separation and blind deconvolution. *Neural Comput* **7**(6): 1129-1159.
- Berument, S. K., M. Rutter, C. Lord, A. Pickles and A. Bailey (1999). Autism screening questionnaire: diagnostic validity. *British Journal of Psychiatry* **175**: 444-451.
- Blanken, L. M. E., S. E. Mous, A. Ghassabian, R. L. Muetzel, N. K. Schoemaker, H. El Marroun, A. van der Lugt, V. W. V. Jaddoe, A. Hofman, F. C. Verhulst, H. Tiemeier and T. White (2015). Cortical Morphology in 6-to 10-Year Old Children With Autistic Traits: A Population-Based Neuroimaging Study. *American Journal of Psychiatry* **172**(5): 479-486.
- Calhoun, V. D. and T. Adali (2012). Multisubject independent component analysis of fMRI: a decade of intrinsic networks, default mode, and neurodiagnostic discovery. *IEEE Rev Biomed Eng* **5**: 60-73.
- Calhoun, V. D., T. Adali, G. Pearlson and J. J. Pekar (2001). Group ICA of functional MRI data: separability, stationarity, and inference. *Proc. Int. Conf. on ICA and BSS San Diego, CA*.
- Calhoun, V. D., T. Adali, G. D. Pearlson and J. J. Pekar (2001). A method for making group inferences from functional MRI data using independent component analysis. *Hum Brain Mapp* **14**(3): 140-151.
- Calhoun, V. D., R. Miller, G. Pearlson and T. Adali (2014). The chronnectome: time-varying connectivity networks as the next frontier in fMRI data discovery. *Neuron* **84**(2): 262-274.
- Chang, C. and G. H. Glover (2010). Time-frequency dynamics of resting-state brain connectivity measured with fMRI. *Neuroimage* **50**(1): 81-98.
- Constantino, J. (2002). Social Responsiveness Scale (SRS), Manual. Los Angeles, Western Psychological services.
- Constantino, J. N., S. A. Davis, R. D. Todd, M. K. Schindler, M. M. Gross, S. L. Brophy, L. M. Metzger, C. S. Shoushtari, R. Splinter and W. Reich (2003). Validation of a brief quantitative measure of autistic traits: Comparison of the social responsiveness scale with the autism diagnostic interview-revised. *Journal of Autism and Developmental Disorders* **33**(4): 427-433.
- Constantino, J. N. and R. D. Todd (2003). Autistic traits in the general population: a twin study. *Arch Gen Psychiatry* **60**(5): 524-530.
- Cordes, D., V. M. Haughton, K. Arfanakis, J. D. Carew, P. A. Turski, C. H. Moritz, M. A. Quigley and M. E. Meyerand (2001). Frequencies contributing to functional connectivity in the cerebral cortex in "resting-state" data. *AJNR Am J Neuroradiol* **22**(7): 1326-1333.
- Damaraju, E., E. A. Allen, A. Belger, J. M. Ford, S. McEwen, D. H. Mathalon, B. A. Mueller, G. D. Pearlson, S. G. Potkin, A. Preda, J. A. Turner, J. G. Vaidya, T. G. van Erp and V. D. Calhoun (2014). Dynamic functional connectivity analysis reveals transient states of dysconnectivity in schizophrenia. *Neuroimage-Clinical* **5**: 298-308.
- Di Martino, A., D. A. Fair, C. Kelly, T. D. Satterthwaite, F. X. Castellanos, M. E. Thomason, R. C. Craddock, B. Luna, B. L. Leventhal, X. N. Zuo and M. P. Milham (2014). Unraveling the miswired connectome: a developmental perspective. *Neuron* **83**(6): 1335-1353.
- Di Martino, A., K. Ross, L. Q. Uddin, A. B. Sklar, F. X. Castellanos and M. P. Milham (2009). Functional brain correlates of social and nonsocial processes in autism spectrum disorders: an activation likelihood estimation meta-analysis. *Biol Psychiatry* **65**(1): 63-74.
- Di Martino, A., Z. Shehzad, C. Kelly, A. K. Roy, D. G. Gee, L. Q. Uddin, K. Gotimer, D. F. Klein, F. X. Castellanos and M. P. Milham (2009). Relationship between cingulo-insular functional connectivity and autistic traits in neurotypical adults. *Am J Psychiatry* **166**(8): 891-899.

- Dosenbach, N. U. F., B. Nardos, A. L. Cohen, D. A. Fair, J. D. Power, J. A. Church, S. M. Nelson, G. S. Wig, A. C. Vogel, C. N. Lessov-Schlaggar, K. A. Barnes, J. W. Dubis, E. Feczko, R. S. Coalson, J. R. Pruett, D. M. Barch, S. E. Petersen and B. L. Schlaggar (2010). Prediction of Individual Brain Maturity Using fMRI. *Science* **329**(5997): 1358-1361.
- Erhardt, E. B., S. Rachakonda, E. J. Bedrick, E. A. Allen, T. Adali and V. D. Calhoun (2011). Comparison of multi-subject ICA methods for analysis of fMRI data. *Hum Brain Mapp* **32**(12): 2075-2095.
- Fair, D. A., A. L. Cohen, J. D. Power, N. U. F. Dosenbach, J. A. Church, F. M. Miezin, B. L. Schlaggar and S. E. Petersen (2009). Functional Brain Networks Develop from a “Local to Distributed” Organization. *Plos Computational Biology* **5**(5).
- Fair, D. A., N. U. Dosenbach, J. A. Church, A. L. Cohen, S. Brahmbhatt, F. M. Miezin, D. M. Barch, M. E. Raichle, S. E. Petersen and B. L. Schlaggar (2007). Development of distinct control networks through segregation and integration. *Proc Natl Acad Sci U S A* **104**(33): 13507-13512.
- Fransson, P., B. Skiold, S. Horsch, A. Nordell, M. Blennow, H. Lagercrantz and U. Aden (2007). Resting-state networks in the infant brain. *Proceedings of the National Academy of Sciences of the United States of America* **104**(39): 15531-15536.
- Freire, L. and J. F. Mangin (2001). Motion correction algorithms may create spurious brain activations in the absence of subject motion. *Neuroimage* **14**(3): 709-722.
- Friedman, J., T. Hastie and R. Tibshirani (2008). Sparse inverse covariance estimation with the graphical lasso. *Biostatistics* **9**(3): 432-441.
- Gao, W., J. H. Gilmore, K. S. Giovanello, J. K. Smith, D. Shen, H. Zhu and W. Lin (2011). Temporal and spatial evolution of brain network topology during the first two years of life. *PLoS One* **6**(9): e25278.
- Geschwind, D. H. and P. Levitt (2007). Autism spectrum disorders: developmental disconnection syndromes. *Current Opinion in Neurobiology* **17**(1): 103-111.
- Hahamy, A., M. Behrmann and R. Malach (2015). The idiosyncratic brain: distortion of spontaneous connectivity patterns in autism spectrum disorder. *Nat Neurosci* **18**(2): 302-309.
- Hasson, U., G. Avidan, H. Gelbard, I. Vallines, M. Harel, N. Minshew and M. Behrmann (2009). Shared and idiosyncratic cortical activation patterns in autism revealed under continuous real-life viewing conditions. *Autism Res* **2**(4): 220-231.
- Hernandez, L. M., J. D. Rudie, S. A. Green, S. Bookheimer and M. Dapretto (2015). Neural signatures of autism spectrum disorders: insights into brain network dynamics. *Neuropsychopharmacology* **40**(1): 171-189.
- Himberg, J., A. Hyvarinen and F. Esposito (2004). Validating the independent components of neuroimaging time series via clustering and visualization. *Neuroimage* **22**(3): 1214-1222.
- Hutchison, R. M. and J. B. Morton (2015). Tracking the Brain’s Functional Coupling Dynamics over Development. *J Neurosci* **35**(17): 6849-6859.
- Hutchison, R. M., T. Womelsdorf, E. A. Allen, P. A. Bandettini, V. D. Calhoun, M. Corbetta, S. Penna, J. H. Duyn, G. H. Glover, J. Gonzalez-Castillo, D. A. Handwerker, S. Keilholz, V. Kiviniemi, D. A. Leopold, F. Pasquale, O. Sporns, M. Walter and C. Chang (2013). Dynamic functional connectivity: Promise, issues, and interpretations. *Neuroimage* **80**: 360-378.
- Hutchison, R. M., T. Womelsdorf, J. S. Gati, S. Everling and R. S. Menon (2013). Resting-state networks show dynamic functional connectivity in awake humans and anesthetized macaques. *Human Brain Mapping* **34**(9): 2154-2177.
- Jaddoe, V. W. V., C. M. van Duijn, O. H. Franco, A. J. van der Heijden, M. H. van Ilzendoorn, J. C. de Jongste, A. van der Lugt, J. P. Mackenbach, H. A. Moll, H. Raat, F. Rivadeneira, E. A. P. Steegers, H. Tiemeier, A. G. Uitterlinden, F. C. Verhulst and A. Hofman (2012). The Generation R Study: design and cohort update 2012. *European Journal of Epidemiology* **27**(9): 739-756.

- Jung, M., H. Kosaka, D. N. Saito, M. Ishitobi, T. Morita, K. Inohara, M. Asano, S. Arai, T. Munosue, A. Tomoda, Y. Wada, N. Sadato, H. Okazawa and T. Iidaka (2014). Default mode network in young male adults with autism spectrum disorder: relationship with autism spectrum traits. *Mol Autism* **5**: 35.
- Kennedy, D. P., E. Redcay and E. Courchesne (2006). Failing to deactivate: resting functional abnormalities in autism. *Proc Natl Acad Sci U S A* **103**(21): 8275-8280.
- Langen, C. D., T. White, M. A. Ikram, M. W. Vernooij and W. J. Niessen (2015). Integrated Analysis and Visualization of Group Differences in Structural and Functional Brain Connectivity: Applications in Typical Ageing and Schizophrenia. *PLoS One* **10**(9): e0137484.
- Lenroot, R. K. and J. N. Giedd (2006). Brain development in children and adolescents: insights from anatomical magnetic resonance imaging. *Neurosci Biobehav Rev* **30**(6): 718-729.
- Rashid, B., E. Damaraju, G. D. Pearlson and V. D. Calhoun (2014). Dynamic connectivity states estimated from resting fMRI Identify differences among Schizophrenia, bipolar disorder, and healthy control subjects. *Front Hum Neurosci* **8**: 897.
- Rodriguez, P., T. Adali, H. Li, N. Correa and V. D. Calhoun (2010). Phase correction and denoising for ICA of complex FMRI data. *IEEE International Conference on Acoustics, Speech and Signal Processing*. Dallas, TX.
- Simmonds, D. J., M. N. Hallquist, M. Asato and B. Luna (2014). Developmental stages and sex differences of white matter and behavioral development through adolescence: a longitudinal diffusion tensor imaging (DTI) study. *Neuroimage* **92**: 356-368.
- Smith, S. M., K. L. Miller, G. Salimi-Khorshidi, M. Webster, C. F. Beckmann, T. E. Nichols, J. D. Ramsey and M. W. Woolrich (2011). Network modelling methods for FMRI. *Neuroimage* **54**(2): 875-891.
- Stigler, K. A., B. C. McDonald, A. Anand, A. J. Saykin and C. J. McDougle (2011). Structural and functional magnetic resonance imaging of autism spectrum disorders. *Brain Res* **1380**: 146-161.
- Tohka, J., K. Foerde, A. R. Aron, S. M. Tom, A. W. Toga and R. A. Poldrack (2008). Automatic independent component labeling for artifact removal in fMRI. *Neuroimage* **39**(3): 1227-1245.
- Uddin, L. Q., K. Supekar, C. J. Lynch, A. Khouzam, J. Phillips, C. Feinstein, S. Ryali and V. Menon (2013). Salience Network-Based Classification and Prediction of Symptom Severity in Children With Autism. *Jama Psychiatry* **70**(8): 869-879.
- Uddin, L. Q., K. Supekar and V. Menon (2013). Reconceptualizing functional brain connectivity in autism from a developmental perspective. *Frontiers in Human Neuroscience* **7**.
- Varoquaux, G., F. Baronnet, A. Kleinschmidt, P. Fillard and B. Thirion (2010). Detection of brain functional-connectivity difference in post-stroke patients using group-level covariance modeling. *Med Image Comput Comput Assist Interv* **13**(Pt 1): 200-208.
- White, T., H. El Marroun, I. Nijs, M. Schmidt, A. van der Lugt, P. A. Wielopolski, V. W. V. Jaddoe, A. Hofman, G. P. Krestin, H. Tiemeier and F. C. Verhulst (2013). Pediatric population-based neuroimaging and the Generation R Study: the intersection of developmental neuroscience and epidemiology. *European Journal of Epidemiology* **28**(1): 99-111.
- White, T., R. Muetzel, M. Schmidt, S. J. Langeslag, V. Jaddoe, A. Hofman, V. D. Calhoun, F. C. Verhulst and H. Tiemeier (2014). Time of acquisition and network stability in pediatric resting-state functional magnetic resonance imaging. *Brain Connect* **4**(6): 417-427.

7

7

7



7

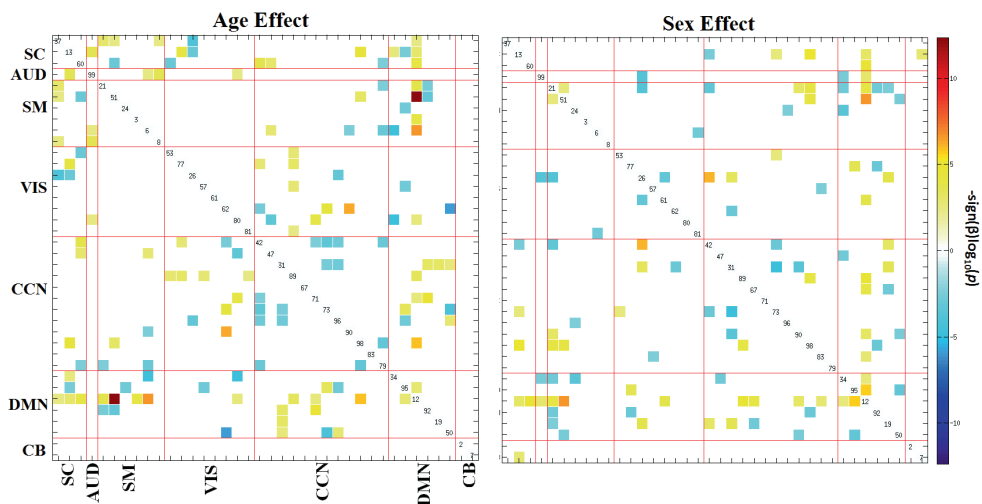


Figure S2. Age- and sex-related associations in static FNC.

For age analyses, red indicates positive association between that particular pairwise connection and age, whereas blue indicates a negative age association. For analyses of sex, red indicates where female subjects showed stronger connectivity than male subjects, and blue indicate where male subjects showed stronger connectivity compared to female subjects. All the results presented here survived the false discovery rate (FDR) multiple comparison correction threshold of $pFDR = 0.05$.

2. Validation framework for connectivity measures

2.1 Reproducibility of clusters

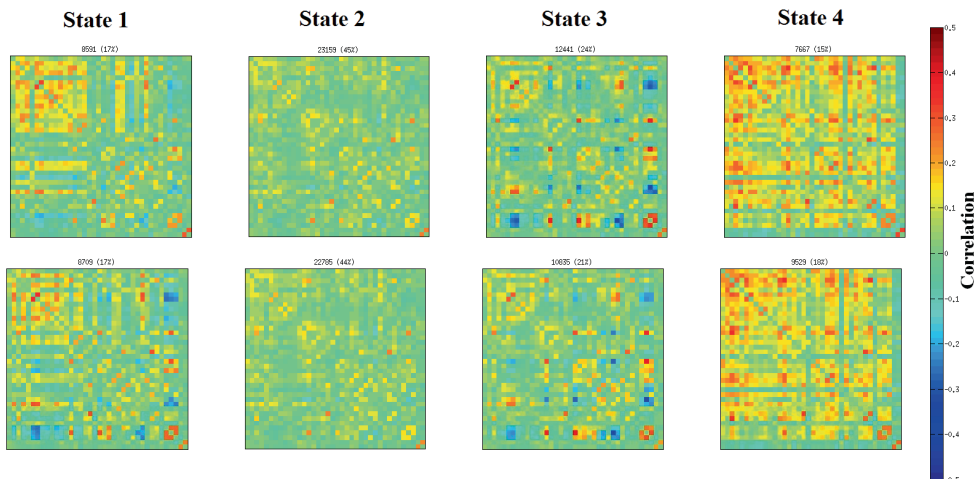


Figure S3.

Reproducibility of clusters was established via non-overlapping split-half samples of subjects. For half-split cross-validation, the subjects were split into two groups with equal number of subjects, and the k-means algorithm was applied with 500 repetitions to the subject exemplars in that group (~1500 instances). The total number and percentage of occurrences is listed above each centroid.

3. Sensitivity analyses of dynamic connectivity findings

3.1 Sensitivity analysis based on behavioral problems

In order to ensure that the results were not driven by subjects with higher levels of behavioral problems as measured by child behavior check list (CBCL) scores, sensitivity analyses were run. To perform the sensitivity analysis, we excluded all the subjects showing any child behavioral problem using CBCL scores from the original dataset (after exclusion, number of subjects=531). We then computed the age- and sex-specific effects on dynamic FNC (Figure S4) and summary measures of the dynamic FNC such as MDT and FT (Figure S5). These results also produced the same direction of effects for each of these connectivity measures, as found with the whole dataset.

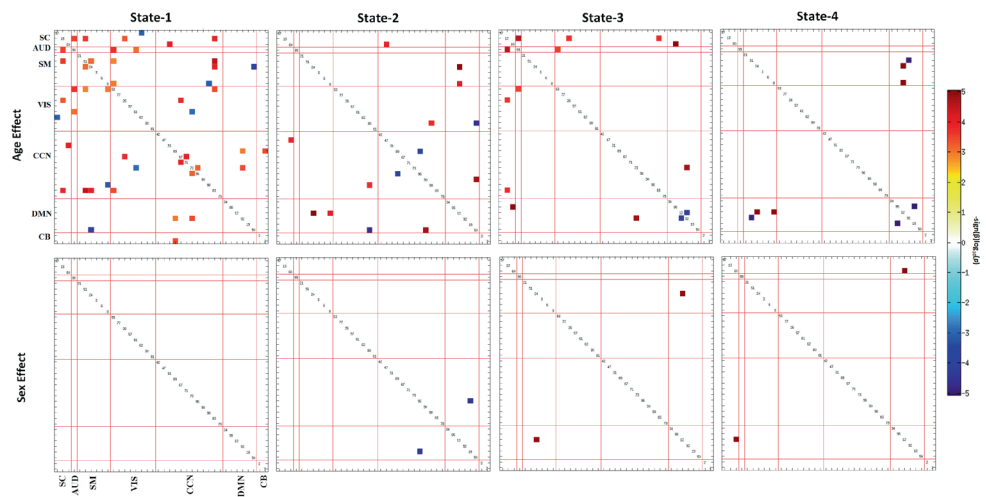


Figure S4. Results from age- and sex-related associations across dynamic connectivity states after excluding subjects with higher levels of behavioral problems. For age analyses, red indicates positive association between that particular pairwise connection and age, whereas blue indicates a negative age association. For analyses of sex, red indicates where female subjects showed stronger connectivity than male subjects, and blue indicate where male subjects showed stronger connectivity compared to female subjects. All the results presented here survived the false discovery rate (FDR) multiple comparison correction threshold of $pFDR = 0.05$.

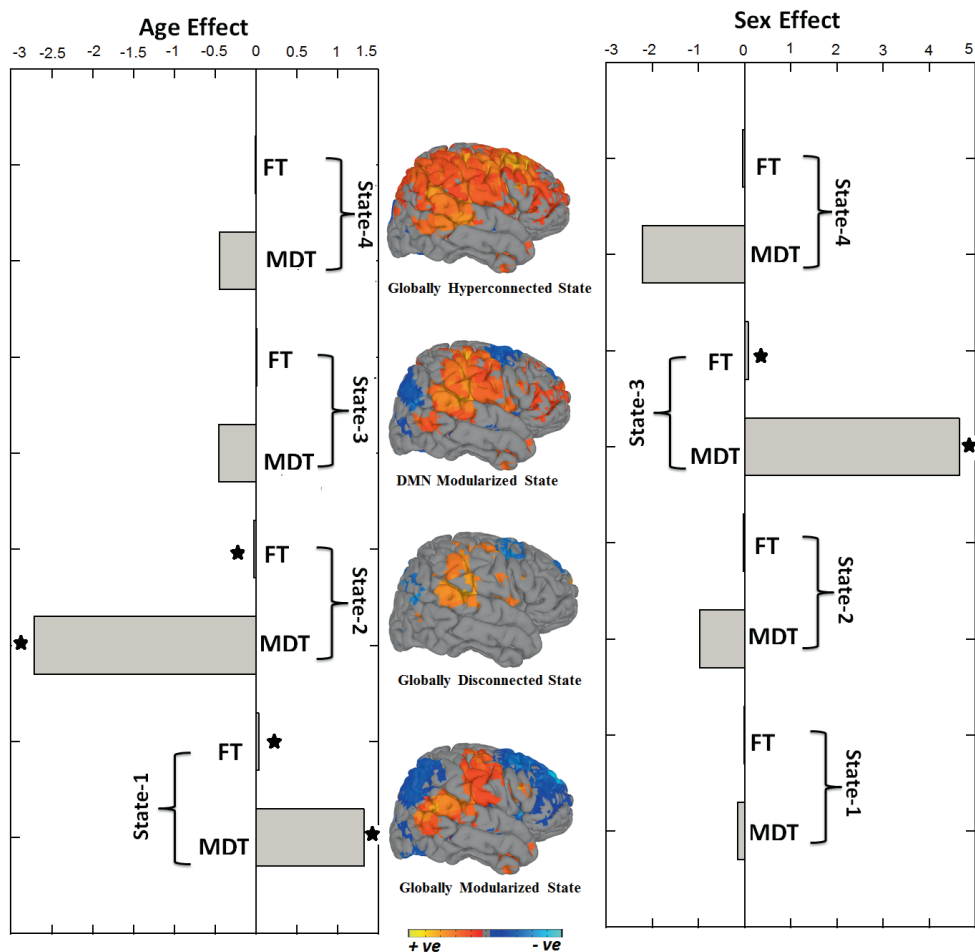


Figure S5.

Summary metrics from the four dynamic connectivity states in relation to age and sex after excluding subjects with higher levels of behavioral problems. For age associations, positive beta coefficient (β) indicates older children spend more time in that particular state whereas negative beta coefficient (β) indicates younger children spend more time in a particular state. For sex analyses, positive beta coefficient (β) indicates girls spend more time in the state relative to boys, and negative beta coefficient (β) indicates that boys spend more time in the state relative to girls. Bar graphs indicate the unstandardized beta coefficients (β) with standard error (S.E.) from regression models, and Asterisks (*) indicate the results survived the false discovery rate (FDR) multiple comparison correction threshold of $pFDR = 0.05$. The rendering brain maps are showing modularized positive (red) and negative (blue) connectivity for the corresponding dynamic states.

3.2 Case-control study for autism

We also designed a case-control study for subjects with autism spectrum disorder (ASD) and autistic traits, where we had age, sex and IQ matched 88 healthy subjects and 22 subjects

with autistic traits and ASD. We assessed the difference in dynamic FNC states between healthy control (HC) and autistic traits and ASD groups (Figure S6). Note that, these results are showing group differences between HC and ASD in state-1 and state-4, two of the dynamic states that did not capture any SRS effects (effects of autistic trait) in terms of mean dwell time (MDT) and fraction of time (FT) for the original analyses with 774 subjects.

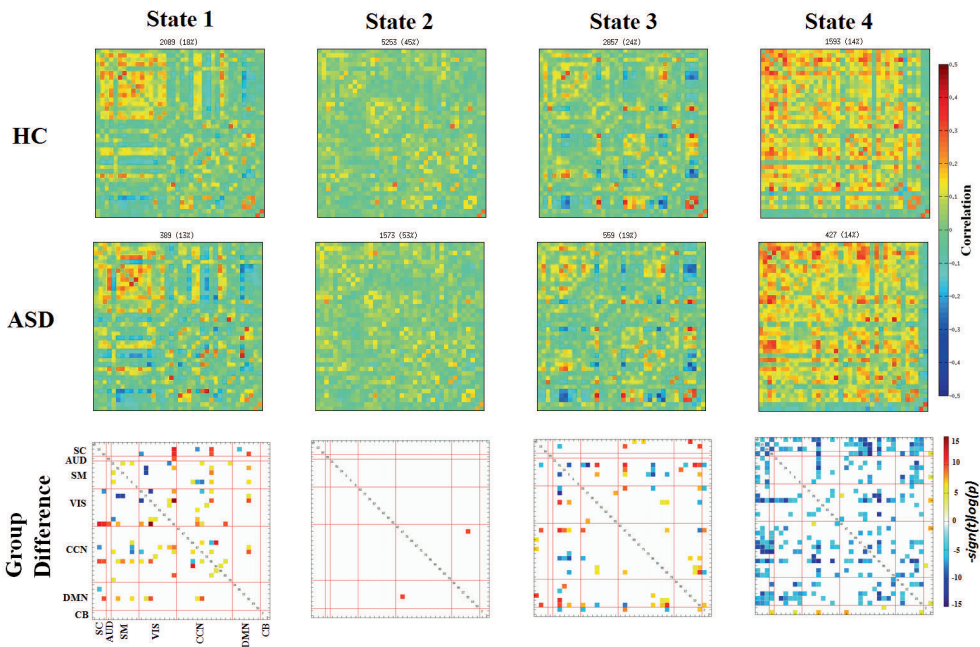


Figure S6. The medians of cluster centroids by state for HC (top) and ASD (middle) along with the count of subjects that had at least one window in each state are shown. The bottom row shows the FDR-corrected (indicate $p < 0.05$) results of two-sample t-test performed across subject median dFNC maps by state.

3.3 Sensitivity analysis based on autistic trait and autism

We also performed a sensitivity analysis to evaluate the effects of SRS scores on summary measures of the dynamic states (MDT and FT). We removed the subjects who are diagnosed with ASD, as well as the subjects with SRS scores above the screening cutoff. Using this subset of the subjects (after exclusion, number of subjects=528), we performed the analyses for SRS score effects on MDT and FT (Figure S7). The SRS sensitivity analysis did not reveal any FDR-corrected effect of autistic traits. However, the direction of the effects remained the same as the original analysis (with 774 subjects).

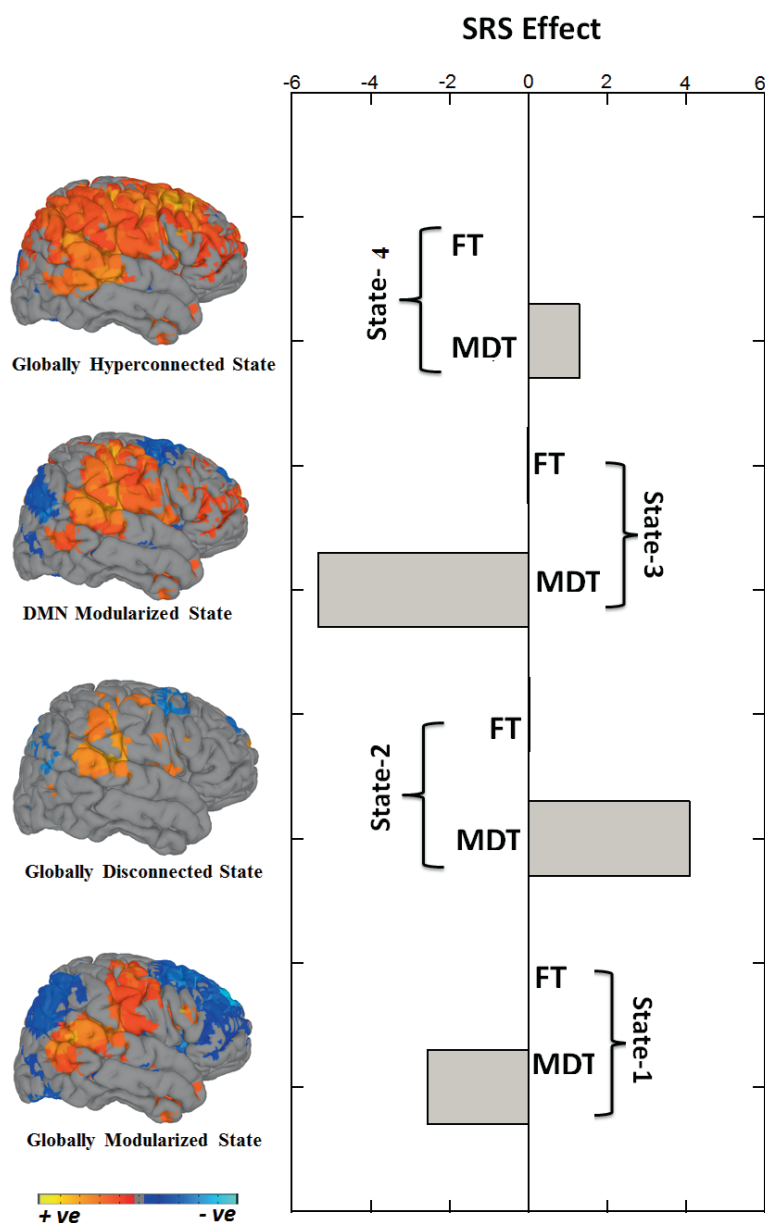


Figure S7: Summary metrics and autistic trait effects. Summary metrics from the 4 dynamic connectivity states in relation to autistic traits after removing subjects with autistic traits and ASD. Positive beta coefficient (β) indicates that higher levels of autistic traits are associated with more time spent in a particular state, whereas negative beta coefficient (β) indicate lower levels of autistic traits are associated with more time spent in a particular state. Bar graphs indicate the unstandardized beta coefficients (β) from regression models. The rendering brain maps are showing modularized positive (red) and negative (blue) connectivity for the corresponding dynamic states.

3.4 IQ – adjusted analyses

As ASD is often accompanied by deficits in cognition, it was important to also rule-out that any observed associations between autistic traits and dynamic connectivity were not simply a reflection of general intellectual ability. Analyses associating autistic traits with dynamic connectivity remained largely unchanged after adjusting for non-verbal IQ. Specifically, for whole-matrix associations in the four dynamic states, the general pattern of association remained. For the summary measure MDT, regression coefficients did not change more than 5%, suggesting the association is not confounded by IQ.

Table S1. Participant characteristics

Child characteristics (n=774)	
Age at MRI	7.99±1.01
Gender (% boy)	52.1
Ethnicity (%)	
Dutch	71.8
Other Western	6.5
Non-Western	21.7
Social Responsiveness Scale weighted total score	0.27±0.31
Age (years) at Social Responsiveness Scale assessment	6.2±0.46
non-verbal IQ	102.0±14.5

Table S2. ICN Descriptive Information

ICN regions	Peak (mm) X Y Z
SUB-CORTICAL (SC)	
IC: 37	
Right Putamen	[18 13 -6]
IC: 13	
Left Putamen	[-27 0 3]
Right Putamen	[27 3 3]
IC: 60	
Right Thalamus	[12 -30 9]
AUDITORY (AUD)	
IC:99	
Left Superior Temporal Gyrus	[-51 -27 9]
Right Superior Temporal Gyrus	[60 -18 9]
VISUAL (VIS)	
IC:21	
Left SMA	[-3 6 48]
IC: 51	
Right SupraMarginal Gyrus	[54 -33 27]
IC: 24	
Right SupraMarginal Gyrus	[-58 -24 41]
IC: 3	
Left Precentral Gyrus	[-36 -24 57]
IC: 6	
Right Paracentral Lobule	[6 -30 66]
IC: 8	
Right Postcentral Gyrus	[54 -9 33]
Left Postcentral Gyrus	[-51 -12 33]
SENSORIMOTOR (SM)	
IC: 53	
Right Fusiform Gyrus	[27 -45 -12]
Left Fusiform Gyrus	[-24 -48 -9]
IC: 77	
Left Lingual Gyrus	[-9 -57 0]
IC: 26	
Left Calcarine Gyrus	[-12 -60 18]
IC: 57	
Right Fusiform Gyrus	[30 -78 -6]
IC: 61	
Left Cuneus	[3 -84 24]
IC: 62	
Left Cuneus	[12 -72 36]
IC: 80	
Right Superior Occipital Gyrus	[30 -66 45]
IC: 81	
Right Superior Occipital Gyrus	

COGNITIVE CONTROL (CCN)

IC: 42	
Left Superior Medial Gyrus	[-6 55 9]
IC: 47	
Left Middle Frontal Gyrus	[-24 48 25]
IC: 31	
Left Superior Frontal Gyrus	[-18 22 53]
IC: 89	
Right Middle Temporal Gyrus	[45 -60 12]
IC: 67	
Left Middle Temporal Gyrus	[-48 -57 12]
IC: 71	
Right Middle Frontal Gyrus	[42 7 40]
IC: 73	
Right Middle Frontal Gyrus	[33 45 12]
IC: 96	
Left Inferior Frontal Gyrus	[-48 15 27]
IC: 90	
Right Inferior Parietal Lobule	[48 -39 48]
IC: 98	
Right Insula Lobe	[45 3 6]
IC: 83	
Right Middle Temporal Gyrus	[51 -39 6]
IC: 79	
Left Superior Parietal Lobule	[-30 -54 48]

DEFAULT-MODE (DMN)

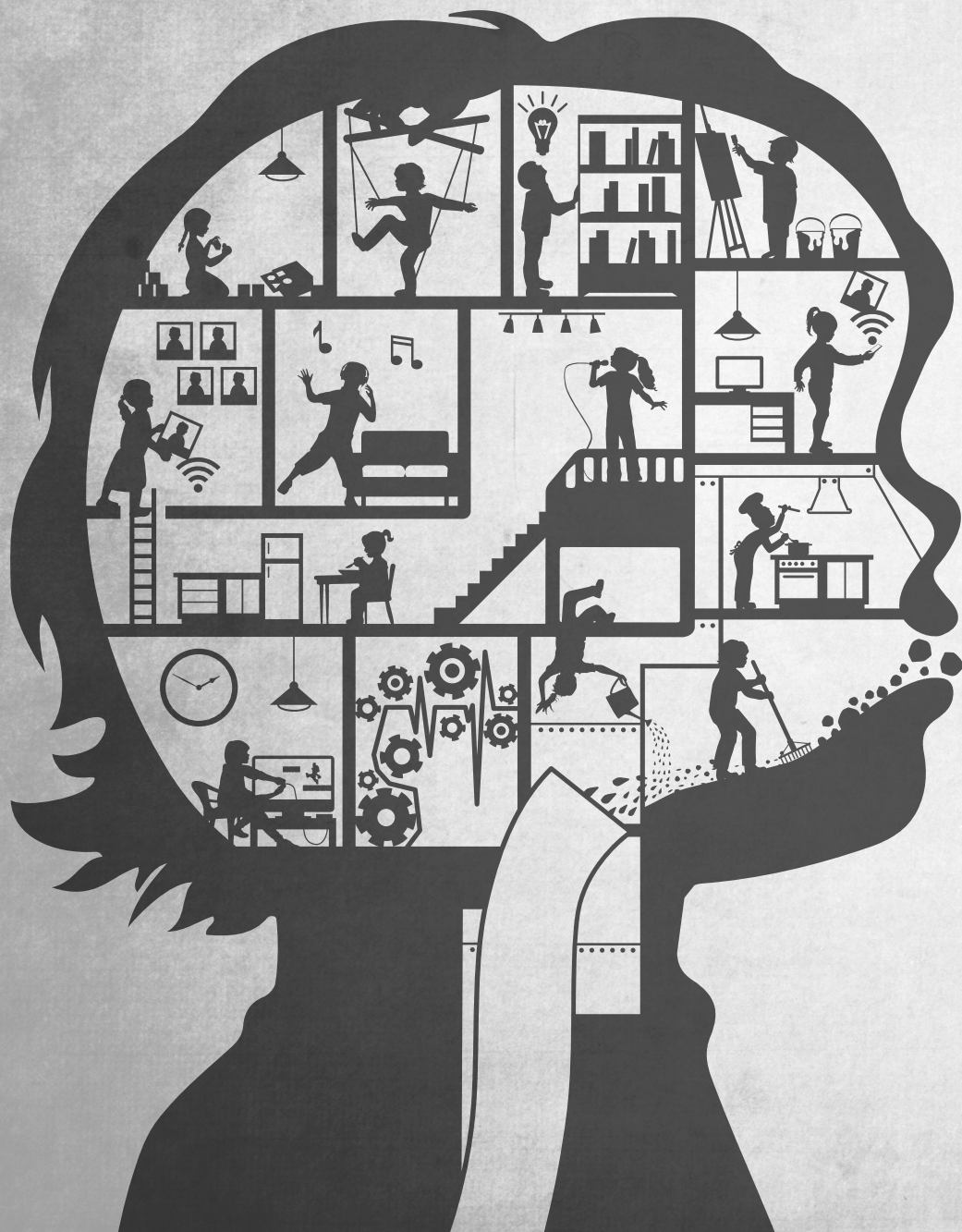
IC: 34	
Right Precuneus	[3 -65 55]
IC: 95	
Right Middle Cingulate Cortex	[6 30 30]
IC: 12	
Left Middle Cingulate Cortex	[0 0 33]
IC: 92	
Right Angular Gyrus	[48 -57 39]
IC: 19	
Left Precuneus	[0 -57 33]
IC: 50	
Left Angular Gyrus	[-45 -60 36]

CEREBELLAR (CB)

IC: 2	
Left Cerebellum	[-33 -66 -42]
IC: 7	
Right Cerebellum	[36 -63 -39]

PART

IV



CHAPTER

8

General Discussion

DISCUSSION

This thesis examined neurobiological features of brain development and psychopathology in large cohorts of children. Diffusion tensor imaging was used to probe white matter microstructure, and resting-state functional MRI was used to explore intrinsic brain activity. This chapter offers a general discussion of the results presented in previous chapters, insights into relevant methodological considerations, and proposes future directions for the field.

MAIN FINDINGS

Structure-function associations with white matter

An intuitive application of structural neuroimaging methods, such as diffusion tensor imaging (DTI), is to examine whether measures of white matter are related to neuropsychological functioning. Chapter 2 of this thesis investigates this question in a large sample of children, adolescents and young adults recruited from the community. In precisely measured metrics of white matter microstructure in the corpus callosum, we observed age-associations suggestive of developmental effects, particularly in the splenium. Further, age-independent associations between white matter integrity and bimanual motor performance on a finger-tapping task were observed. This work largely mirrored findings from morphological studies and confirmed previous DTI reports that the corpus callosum follows an anterior-to-posterior gradient of development. This is particularly intriguing, given the cortex follows a much different spatial pattern of development, flowing largely posterior-to-anterior (or, areas of sensorimotor to higher-level cognitive functions, Lenroot and Giedd 2006). In Chapter 3 of this thesis, we expand upon these findings by examining white matter microstructure with a wide-array of neuropsychological functions using fully-automated probabilistic tractography in a large, population-based sample. We found that global measures of white matter microstructure were related to general intellectual functioning (i.e., non-verbal intelligence quotient, IQ) and to visuospatial ability. Inspection of individual white matter fiber bundles revealed some tracts, such as the superior longitudinal fasciculus, might be particularly important in these associations. While residual confounding for age is certainly possible, analyses presented in Chapter 3 expand upon data presented in Chapter 2 by showing robust structure-function associations in a stratified sample and a highly restricted age-range (i.e., 8-to-9 years of age). The implications of age-independent structure-function associations for the study of the brain are promising. Demonstrating a link between features of brain structure and fine motor ability or neuropsychological function in healthy individuals establishes an important baseline for comparison with atypical brain development (e.g., in psychiatric conditions).

While structure-function associations seem intuitive, it is worth mention that the literature on typical development is not overly saturated with such studies. Our work in Chapter 3 illustrates that not all domains of neuropsychological functioning were associated with white matter microstructure. However, structure-function associations are relatively common in clinical samples where more severe cognitive deficits are related to deficits in white matter integrity, potentially suggesting additional variability in such populations (i.e., more range in cognitive ability and in white matter microstructure) is helpful in revealing structure-function associations (Alexander et al. 2007, Lebel et al. 2010, Wozniak et al. 2011, Magioncalda et al. 2016). An interesting extension to this work will be examining whether or not subtypes of psychopathology are associated with certain structure-function associations, or to probe whether various aspects of structural connectivity are related to functional connectivity (Wozniak, Mueller et al. 2011).

White matter and psychiatric symptoms

Once an appropriate baseline is established in typical development, it is feasible to probe white matter structural connectivity for features that are related to psychopathology (Di Martino et al. 2014). One aim of such work is to identify useful biomarkers in children with psychopathology that can eventually be further evaluated in elucidating etiology, or aid in the process of classification, estimation of prognosis, and/or prediction of treatment response. Chapter 4 of this thesis explores associations between autistic traits and structural connectivity. Analyses of probabilistic fiber tractography did not reveal an association with traits, though whole-brain voxel-based analyses suggested the superior longitudinal fasciculus is related to autism spectrum disorder (ASD). The latter is consistent with other case-control studies of clinical populations (Aoki et al. 2013). The superior longitudinal fasciculus interconnects multiple brain regions, and has been suggested to play a role in various aspects of language (Schmahmann et al. 2007). Deficits in this area are particularly interesting given widely reported language difficulties in ASD. However, while the vast literature of ASD routinely demonstrates differences in structural connectivity, there is substantial heterogeneity in results, both spatially and in direction of effect (Ameis and Catani 2015). Whether or not a distinct source of this heterogeneity in results exists is difficult to assess, though there are a number of potential factors that may contribute to it. For instance, as the presentation and symptomatology of ASD is quite complex, with children displaying varying levels and combinations of traits, it is possible certain aspects underlying the neurobiology are not shared amongst all individuals with a diagnosis. This would suggest that other, more specific image analysis tools could be useful in probing white matter microstructure in ASD (White et al. 2009). Alternatively, while there is overlap amongst studies in the types of image acquisition and analysis methodologies employed, there are still considerable differences reported in the literature. For instance, the use of region-of-interest versus whole-brain, voxel-wise analyses.

Early presentation of behavioral and psychiatric problems in children has been linked to poorer outcomes, including higher rates of psychopathology, later in life (Pine et al. 1999, Hofstra et al. 2002). Studies examining the neurobiological consequences of early-presenting psychiatric symptoms are sparse. Further, compared to cross-sectional studies, longitudinal designs examining structural connectivity in psychopathology have been less frequently utilized. Chapter 5 of this thesis examines psychiatric symptoms in young children in relation to the development of structural connectivity measured by DTI. Using linear mixed-effects models, we demonstrate that higher levels of internalizing problems are related to reduced white matter microstructural development. Higher levels of affective problems in particular were associated with smaller increases in fractional anisotropy from 6 to 10 years of age. While the data presented in Chapter 5 are from a large, population-based observational study, parallels can be made with existing cross-sectional literature utilizing clinical samples. In general, studies of clinical depression in children and adults show lower FA in a number of brain regions in patients with unipolar depression (Cullen et al. 2010, Murphy and Frodl 2011, LeWinn et al. 2014). Importantly, while reverse causality cannot be ruled out even with the longitudinal data presented in Chapter 5, it is worth noting that most biological hypotheses surrounding psychiatric conditions assume an underlying neuronal substrate as a causal factor. As this study examines psychiatric problems measured prior to neuroimaging, it is important for future work to assess structural connectivity at earlier ages along with contemporaneous behavioral assessments in order to reveal the precise temporal sequence of emerging neurobiological and behavioral features. Along similar lines, given only a weak association between psychiatric problems and connectivity was observed at an early age (i.e., within Time-1), it is likely that more sensitive imaging analysis approaches will be required to detect a subtle underlying neurobiological substrate prior to the presentation of symptoms.

Taken all together, this work not only demonstrates reduced white matter maturation in young children with high levels of psychiatric problems, but also shows that psychiatric and behavioral symptoms measured on a continuum are relevant in the study of brain development. The majority of studies utilizing neuroimaging to examine psychopathology do so within a dichotomous framework, where patients are compared with individuals without a psychiatric or neurological diagnosis ('controls'). However, for a number of years, psychological and psychiatric traits have been considered within a dimensional framework, where different traits lie on a continuum not only in patients, but also in the general population (Achenbach 1991, Constantino and Todd 2003, Hudziak et al. 2007). A more formal push towards using such dimensional approaches in the context of biological and physiological measures, such as neuroimaging and genetics, has also recently been introduced (Insel et al. 2010). Studying the structural neuroimaging features of psychopathology along a continuum

has already successfully uncovered new, unique information in the neurobiology of mental illness (Ducharme et al. 2014, Blanken et al. 2015), and promises to offer many new insights when coupled to large, longitudinal cohorts such as the Generation R Study.

Functional connectivity: brain development and psychopathology

Complimenting metrics of structural connectivity measured by DTI, resting-state functional connectivity is used to assess the correlation structure of temporal fluctuations resulting from intrinsic brain activity. A number of image analysis approaches have been developed to study functional connectivity, including data driven approaches such as spatial independent component analyses (ICA, Calhoun et al. 2001, Beckmann et al. 2009). Chapter 6 of this thesis applies ICA to a large set of resting-state MRI data with two goals: first characterize the variability in resulting ICA components through repeated subsampling of the data, and second characterize age-related associations within and between the resulting networks. We demonstrated that while some networks are present at low frequency across repeated subsampling, the majority of commonly reported ICA-based networks are robust and remain in the majority of resamples. A spatial meta-ICA of the resulting resamples revealed a number of networks commonly reported in adults were also present in children, such as the default-mode network, frontoparietal networks, and executive control network (Smith et al. 2009). Though these networks appear during childhood, age-related associations in the default-mode network and the executive control network suggest they are actively undergoing developmental refinements. This work provides two important contributions to the functional connectivity literature. First, it shows that despite a number of factors that have shown to influence ICA-based networks (Himberg et al. 2004, Zhang et al. 2010, Franco et al. 2013), many networks appear to be robust and can safely be interpreted for developmental and pathological effects. Second, we have demonstrated that a number of networks are likely still developing through childhood, which should be considered carefully in the context of psychopathology (Di Martino, Fair et al. 2014). However, several networks were less robust than others. This could simply be an artifact of the ICA analysis method (Zhang, Zuo et al. 2010, Franco, Mannell et al. 2013), or the variability could be of interest. For example, some networks may be transient, appearing during early childhood and disappearing later in life. Alternatively, such variability could be rooted in individual differences in functional connectivity. While this type of analysis would require a relatively large sample, the resulting information could be incredibly informative in the study of personality and behavior, and should be followed up with more sophisticated analysis techniques (e.g., machine learning).

One potentially limiting assumption made by most functional connectivity studies is that the temporal fluctuations are stationary throughout the measurement period (i.e., the level of connectivity amongst different brain regions remains constant). Recent advances in image processing have allowed this stationarity assumption to be relaxed such that connectivity dynamics can be examined (Allen et al. 2014). In Chapter 7, dynamic functional connectivity is studied in relation to typical development and autistic traits. By applying a sliding-window approach to each dataset, the resulting connectivity matrices are summarized with a clustering algorithm. We found that four dynamic states summarize the connectivity for this large sample of 6-to-10 year-old children. Specifically, there was a mean (static-like) state, a default-mode modularized state, a hyperconnected state, and a hypoconnected state. Age was positively associated with time spent in both the default-mode modularized state and the static-like state, and was negatively correlated with the hypoconnected state. In contrast, autistic traits were associated with more time spent in the hypoconnected state. Thus, younger children and children with higher levels of autistic traits spent more time in the hypoconnected state. This study demonstrates the utility of a novel image analysis method in the study of typical and atypical development. The method relaxes traditional assumptions of functional connectivity, potentially modeling intrinsic connectivity more accurately. Similar to the DTI literature in ASD, the functional connectivity literature is highly heterogeneous, with studies showing increased and decreased connectivity in various brain regions (Uddin et al. 2013). While it is possible that heterogeneity in the disorder is accompanied by a similarly diverse pattern of functional connectivity deficits, there are other potential explanations. For example, autism studies using task-based functional MRI data rather than pure resting-state fMRI are embedded in the functional connectivity literature (Jones et al. 2010), which has shown to produce comparable, yet different results. Alternatively, whole-brain functional connectivity analyses typically involve the interpretation of large, complex connectivity matrices that describe the degree of over- or under-connectivity in ASD. Complex depictions of connectivity are at times interpreted subjectively rather than quantitatively (e.g., increased/decreased segregation/integration), which could also lead to variability in the literature. Analyses utilizing dynamic functional connectivity also rely on rough interpretation of complex connectivity matrices, though more quantitative metrics can be applied to aid in the interpretation. For instance, metrics such as mean dwell time and number of transitions across states provide novel and data-driven information about functional connectivity that is relevant in psychopathology (Damaraju et al. 2014).

METHODOLOGICAL CONSIDERATIONS

Repeated measurements in neuroimaging

Repeated measurements provide information that is not only useful in making causal inferences, but also offer unique insight into the complex developmental processes and trajectories of neuronal growth. For instance, seminal work in the field has demonstrated differential inverted U-shaped trajectories of cortical maturation in psychopathology (Shaw et al. 2007). Given these distinct trajectories of morphological development with and without psychopathology, the use of cross-sectional data alone could lead to misleading and even inaccurate interpretation of results (i.e., increasing vs. decreasing side of the inverted-U trajectory). However, despite their considerable (and growing) application to the study of the brain, *in vivo* neuroimaging efforts have overwhelmingly been cross-sectional in nature. The reluctant adoption of longitudinal designs almost certainly stems from both the complexity of the methodology and the significant cost associated with repeated assessments. The process of collecting longitudinal data is laborious irrespective of the type of data being collected, but is particularly challenging in the field of MR-imaging. For instance, MR-scanner hardware and software have been shown to significantly influence the measurements obtained (Jovicich et al. 2006, Segall et al. 2009, Wonderlick et al. 2009, Glover et al. 2012, Chen et al. 2014). Without sufficient methods to address the systematic biases introduced by such vendor, hardware and software changes, imaging centers have begun to collect longitudinal data at a single, stable location (Ikram et al. 2015). Interestingly, even in situations where such extraneous variables are held constant, seemingly trivial aspects of the acquisition protocol can also negatively influence the nature of the data collected (e.g., head positioning in the coil, van der Kouwe et al. 2005). Another aspect that fortunately has received considerable attention in the accommodation of repeated MR-assessments is image processing. Most notably is the development of sophisticated registration routines that minimize bias in the degree of inter-subject linear or nonlinear fitting applied to an individual time-point (Smith et al. 2002, Reuter and Fischl 2011, Reuter et al. 2012). Lastly, the majority of whole-brain voxel-wise analysis packages offer general linear model-based options for statistical inference (Golland and Fischl 2003, Winkler et al. 2014). However, the field of repeated measures statistics has an immense array of options for the analysis of longitudinal data, including linear mixed-effects models (Bates et al. 2015) and nuanced structural equation models (McArdle 2009). For example, structural equation models, including latent change score models, may be of interest when time-points are evenly spaced and data reduction/latent variable techniques are of interest, or if particular mediation analyses are of interest. While some of these have been implemented in neuroimaging software packages (Bernal-Rusiel et al. 2013), there is still ample room for their implementation into fast and efficient voxel-wise tools that still offer other benefits,

such as the spatially-aware adjustments for multiple comparisons that are available for GLM-based packages (Worsley et al. 1996, Smith and Nichols 2009). Finally, practical and logistical factors contribute to the paucity of longitudinal neuroimaging studies. Scanning large numbers of subjects at multiple points in time places an additional burden on research staff involved with recruitment, data collection, and data management. Further, while costs for MR-scanning decline over time, the acquisition of complex neuroimaging data is accompanied by a considerable financial commitment.

Replication in neuroimaging

Replication in scientific research is a crucial step in assessing the robustness of results. While some lines of work in pediatric MR-imaging have been generally successful in replicating key findings, such as white matter microstructural development (Schmithorst and Yuan 2010), this is not the case for the field as a whole where reliability and reproducibility have been questioned (Bennett and Miller 2010). A number of factors likely contribute to this problem, including issues surrounding correction for multiple comparisons, heterogeneity in image acquisition, differences in image analysis, and also limitations in statistical power.

Multiple testing

Neuroimaging researchers often face unique challenges in accurately controlling for Type-I error; a situation where the null hypothesis is erroneously rejected. The generally accepted, yet somewhat arbitrarily defined, rate of 5% is based on assumptions of individual or independent statistical tests. Depending on the method employed, neuroimaging analyses execute hundreds of thousands of statistical tests simultaneously. This situation, similar to genome-wide association studies, strays from standard assumptions of statistical inference and requires more sophisticated strategies for ensuring the Type-I error rate is accurately estimated (and controlled). Failure to properly account for multiple testing, which has been suggested to be a relevant problem in the field (Bennett et al. 2009), undoubtedly leads to underestimates of the true Type-I error rate. This potential increase in Type-I error likely hinders attempts of replication in neuroimaging, as false positive effects will not be robust across studies. In genomics research, a simple Bonferroni correction that takes into account covariance in the data has become the method of choice (Dudbridge and Gusnanto 2008, Pe'er et al. 2008). The landscape in neuroimaging is less clear, and while there is no 'gold standard', numerous methods have been developed to adjust for multiple testing and concurrently account for the spatial characteristics of the data (Worsley, Marrett et al. 1996, Hayasaka and Nichols 2003, Winkler, Ridgway et al. 2014). Even with such tools, it is apparent that not all researchers properly implement adjustments for multiple testing, both at the voxel-level and at the predictor/outcome level. At minimum, researchers should report what (if any) correction was applied, so that the scientific community is able to properly

evaluate results. However, more optimally researchers should always adjust analyses for multiple comparisons. For voxel-/vertex-wise analyses, it is particularly important to utilize one of the prominent methods, such as family-wise error correction or false discovery rate. For region-of-interest studies, it is also important to realize when multiple comparisons are being conducted, and the extent of the issue (i.e., independence of the tests conducted). For a relatively small number of tests (e.g., <50), false discovery rate (Benjamini and Hochberg 1995) appears to closely approximate other more recent methods taking into account the covariance of the variables tested (Galwey 2009).

Acquisition and analysis

Variability of MR-data acquisition and analysis method also contributes to our ability to reproduce key findings. Unfortunately, MRI data are susceptible to a number of parameters that can dramatically influence different properties of the images, including the signal-to-noise ratio (SNR). As described above in the context of longitudinal designs, differences in acquisition hardware (e.g., vendor, field strength, receive coil, etc.) have been shown to influence characteristics of the data (Hoenig et al. 2005, Jovicich, Czanner et al. 2006, Friedman et al. 2008, Gallichan et al. 2010). Similar to the issue of MRI hardware, image acquisition parameters can also have a significant impact on the resulting data. For instance, in addition to being proportional to B_0 field strength, SNR is also proportional to voxel size (Edelstein et al. 1986). While increasing spatial resolution often seems desirable, it comes at the cost of reduced SNR and should be carefully considered in the context of the research question. Surprisingly, the choice of image analysis methodology (and individual parameters) can also have a considerable effect on results. For instance, choice of spatial normalization algorithm (Klein et al. 2009), spatial normalization template (Sanchez et al. 2012), spatial smoothing kernel size (White et al. 2001), rotation of the DTI b-gradient table (Leemans and Jones 2009), choice of DTI fitting method (Jones and Cercignani 2010), linear detrending of functional MRI (Strother et al. 2004), and data quality exclusion standards (Poline et al. 2006) have all been shown to influence results. It has even been shown that conducting image processing across different operating systems can have non-negligible effects on output (Gronenschild et al. 2012). Thus, it is apparent that each of these factors in isolation can impact the results of a study. However, the more realistic picture is that combinations of these influences are present and may impact the results considerably, further limiting our ability to replicate certain findings. First and foremost, neuroimaging researchers, but also journal reviewers and editors, should be aware of these issues and should take the proper precautions to ensure that not only are methodologies properly reported, but also that the most appropriate analysis pipelines available are being used for a particular dataset (Nichols et al. 2016). Further, researchers using ‘out of the box’ image processing algorithms should consult software developers to ensure their acquisition sequences are optimized for particular processing pipelines.

Sample size / statistical power

Another potentially limiting factor in the replication of neuroimaging studies is sample size. Small sample sizes (especially when coupled with small effect sizes) limit the probability that a statistically significant test represents a true effect (Button et al. 2013). Given the financial cost of scanning and non-trivial logistics required to successfully conduct a study, neuroimaging samples are often relatively small. This is especially true in clinical samples, where studies often contain less than 50 subjects (White et al. 2008, Uddin, Supekar et al. 2013). Alongside the other potential contributors for the lack of replication in the field, small sample sizes and consequently low power undoubtedly play a role. While different approaches have been proposed to mitigate the issue, such as meta-analyses (Peters et al. 2012), consortia (Biswal et al. 2010, Di Martino et al. 2014), and multi-center studies (Glover, Mueller et al. 2012), the non-trivial hurdles discussed in the previous section demonstrate the optimal strategy is to collect (very) large datasets on a single, stable scanner.

Generalizability in pediatric neuroimaging

Another topic worthy of discussion is generalizability of findings. Reported effects may be valid, but not necessarily applicable to the larger (or general) population. In order to initially demonstrate effects, extreme groups are at times considered (i.e., severely affected patients and ‘hypernormal’ controls) (Schwartz and Susser 2011). While these studies are able to demonstrate valid differences between patients and controls, the results may not apply to less severely affected patients or controls that better represent the general population given the nature of the sample. Greene et al. (2016) offer an alternative example of studying high functioning children with autism spectrum disorder. The authors describe that practical reasons enable such a comparisons to be more successful (e.g. due to less movement artifact and more compliance), but warn results may not generalize to more severely affected children with autism (Greene, Black et al. 2016). Selecting the optimal sampling and inclusion/exclusion criteria for control subjects remains a difficult question open for debate, and is likely linked to the research question. For instance, studying rare disorders may necessitate the use of extreme groups to achieve sufficient effect sizes. However, in more common forms of psychopathology, it is important to carefully consider that the control group is properly ‘matched’ in case control studies. Given comorbidities in many forms of psychopathology, heterogeneity in disorder presentation across individuals, as well as varying levels of accompanying neuropsychological sequelae, this is not a trivial task. At minimum cases and controls should be enrolled contemporaneously to avoid biases in data acquisition, and multiple features of the cases should be considered when selecting controls (e.g., socioeconomic status, comorbid behavior problems, cognitive ability, etc.) to ensure no biases are present. A similar issue is also apparent in studies of typical brain development, where there is a tendency of individuals of, for example, higher socioeconomic

status to participate in studies. One consequence of this selection bias is an average sample IQ that is 1 or more standard deviations above the population average (Giedd et al. 1996, Gogtay et al. 2004, Barnea-Goraly et al. 2005, de Bie et al. 2012). Large population-based studies ameliorate this issue by including a more randomness in the sampling scheme. While psychopathology is most often studied with case-control designs, which can be embedded within large cohort studies, an alternative approach is to quantify symptoms and problems along a continuum. Dimensional approaches are not a new concept (Hathaway and McKinley 1943, Achenbach and Ruffle 2000), though as mentioned above, recent initiatives in the field have pushed for more work in this area (Insel, Cuthbert et al. 2010). The application of such a model in large cohort studies favors generalizability, as the symptoms and problems are rated along a continuum in the general population.

CLINICAL IMPLICATIONS

The extent to which clinical implications can be drawn from observational neuroimaging work is limited. The studies presented in this thesis primarily examined typical brain development and psychiatric symptoms in a non-clinical, population-based sample. However, there are some aspects worthy of discussion here. First, in clinical samples, a crucial initial step in understanding the neuroimaging features of psychopathology is a solid understanding of the brain in the absence of psychopathology (Di Martino, Fair et al. 2014). This thesis attempts to lay a context of typical development for other clinical studies in aspects of white matter development, structure-function associations, static functional connectivity, and dynamic functional connectivity. Such information is useful to avoid developmental confounding factors when examining psychopathology. Second, this thesis offers additional support for dimensional approaches to psychopathology, showing that symptoms and traits measured along a continuum are related to structural and functional brain features. Continued work within the dimensional framework, especially in clinical settings, will be an important step in improving our understanding of child psychopathology. Lastly, examining the neurobiological correlates of behavioral and psychiatric symptoms on a continuum in a large population-based sample could help to facilitate new, hypothesis-driven research in smaller, clinical samples where correction for multiple testing is a recurring issue. For example, regions-of-interest (ROIs) or clusters from voxel-wise analyses that are identified in large neuroimaging cohorts can be adopted in *a priori* analyses in smaller samples; a feature of the considerable advantage in statistical power that coincides with continuous analyses in large, population-based cohorts.

FUTURE DIRECTIONS

Over the past three decades, substantial advances have been observed in the field of neuroimaging. The amount of data that can be collected in a reasonable (clinical) amount of time has grown exponentially thanks to developments in both hardware and software (Moeller et al. 2010). Image analysis methodologies have also progressed significantly, from hand tracings of MR-images on paper (Allen et al. 1991) to the utilization of fully automated algorithms in the extraction of precise, quantitative features of the brain (Muetzel et al. 2009). However, in the field of child psychiatry, we have witnessed slow progress in identifying clinically useful neuroimaging biomarkers of psychopathology. It has become evident that the underlying neurobiology of many neuropsychiatric conditions is not readily and reliably detectable using conventional neuroimaging methods. There are a number of ways we could see improvement in this area. First, as described above, much of the work in the field is cross-sectional. Gaining a better understanding of the longitudinal trajectories of brain development, both in the presence and absence of psychopathology, will potentially uncover novel biomarkers of psychopathology. Second, most neuroimaging studies examine a single modality at a time, for instance morphological MRI, DTI, or resting-state MRI. Because the underlying neurobiology of psychopathology is likely highly complex, the integration of multimodal neuroimaging techniques is essential (Sui et al. 2012, Arbabshirani et al. 2016). Lastly, more work is needed in utilizing neuroimaging and neurocognitive data in predicting outcomes and treatment response (Dunlop and Mayberg 2014, Schnack and Kahn 2016), as has been accomplished in other areas of psychiatric research (Huibers et al. 2015).

REFERENCES

- Achenbach, T. M. (1991). Manual for the revised child behavior checklist. Burlington, VT, University of Vermont Department of Psychiatry.
- Achenbach, T. M. and T. M. Ruffle (2000). The Child Behavior Checklist and related forms for assessing behavioral/emotional problems and competencies. *Pediatrics in review / American Academy of Pediatrics* **21**(8): 265-271.
- Alexander, A. L., J. E. Lee, M. Lazar, R. Boudos, M. B. DuBray, T. R. Oakes, J. N. Miller, J. Lu, E. K. Jeong, W. M. McMahon, E. D. Bigler and J. E. Lainhart (2007). Diffusion tensor imaging of the corpus callosum in Autism. *Neuroimage* **34**(1): 61-73.
- Allen, E. A., E. Damaraju, S. M. Plis, E. B. Erhardt, T. Eichele and V. D. Calhoun (2014). Tracking whole-brain connectivity dynamics in the resting state. *Cereb Cortex* **24**(3): 663-676.
- Allen, L. S., M. F. Richey, Y. M. Chai and R. A. Gorski (1991). Sex differences in the corpus callosum of the living human being. *J Neurosci* **11**(4): 933-942.
- Ameis, S. H. and M. Catani (2015). Altered white matter connectivity as a neural substrate for social impairment in Autism Spectrum Disorder. *Cortex* **62**: 158-181.
- Aoki, Y., O. Abe, Y. Nippashi and H. Yamasue (2013). Comparison of white matter integrity between autism spectrum disorder subjects and typically developing individuals: a meta-analysis of diffusion tensor imaging tractography studies. *Mol Autism* **4**(1): 25.
- Arbabshirani, M. R., S. Plis, J. Sui and V. D. Calhoun (2016). Single subject prediction of brain disorders in neuroimaging: Promises and pitfalls. *Neuroimage*.
- Barnea-Goraly, N., V. Menon, M. Eckert, L. Tamm, R. Bammer, A. Karchemskiy, C. C. Dant and A. L. Reiss (2005). White matter development during childhood and adolescence: a cross-sectional diffusion tensor imaging study. *Cereb Cortex* **15**(12): 1848-1854.
- Bates, D., M. Maechler, B. Bolker and S. Walker (2015). lme4: Linear mixed-effects models using Eigen and S4. <https://CRAN.R-project.org/package=lme4>.
- Beckmann, C. F., C. E. Mackay, N. Filippini and S. M. Smith (2009). Group comparison of resting-state fMRI data using multi-subject ICA and dual regression. Organization for Human Brain Mapping. San Francisco, CA.
- Benjamini, Y. and Y. Hochberg (1995). Controlling the false discovery rate: a practical and powerful approach to multiple testing. *Journal of the Royal Statistical Society* **57**(1): 289-300.
- Bennett, C. M. and M. B. Miller (2010). How reliable are the results from functional magnetic resonance imaging? *Ann N Y Acad Sci* **1191**: 133-155.
- Bennett, C. M., G. L. Wolford and M. B. Miller (2009). The principled control of false positives in neuroimaging. *Soc Cogn Affect Neurosci* **4**(4): 417-422.
- Bernal-Rusiel, J. L., D. N. Greve, M. Reuter, B. Fischl, M. R. Sabuncu and I. Alzheimer's Disease Neuroimaging (2013). Statistical analysis of longitudinal neuroimage data with Linear Mixed Effects models. *Neuroimage* **66**: 249-260.
- Biswal, B. B., M. Mennes, X. N. Zuo, S. Gohel, C. Kelly, S. M. Smith, C. F. Beckmann, J. S. Adelstein, R. L. Buckner, S. Colcombe, A. M. Dogonowski, M. Ernst, D. Fair, M. Hampson, M. J. Hoptman, J. S. Hyde, V. J. Kiviniemi, R. Kotter, S. J. Li, C. P. Lin, M. J. Lowe, C. Mackay, D. J. Madden, K. H. Madsen, D. S. Margulies, H. S. Mayberg, K. McMahon, C. S. Monk, S. H. Mostofsky, B. J. Nagel, J. J. Pekar, S. J. Peltier, S. E. Petersen, V. Riedl, S. A. Rombouts, B. Rypma, B. L. Schlaggar, S. Schmidt, R. D. Seidler, G. J. Siegle, C. Sorg, G. J. Teng, J. Veijola, A. Villringer, M. Walter, L. Wang, X. C. Weng, S. Whitfield-Gabrieli, P. Williamson, C. Windischberger, Y. F. Zang, H. Y. Zhang, F. X. Castellanos and M. P. Milham (2010). Toward discovery science of human brain function. *Proc Natl Acad Sci U S A* **107**(10): 4734-4739.

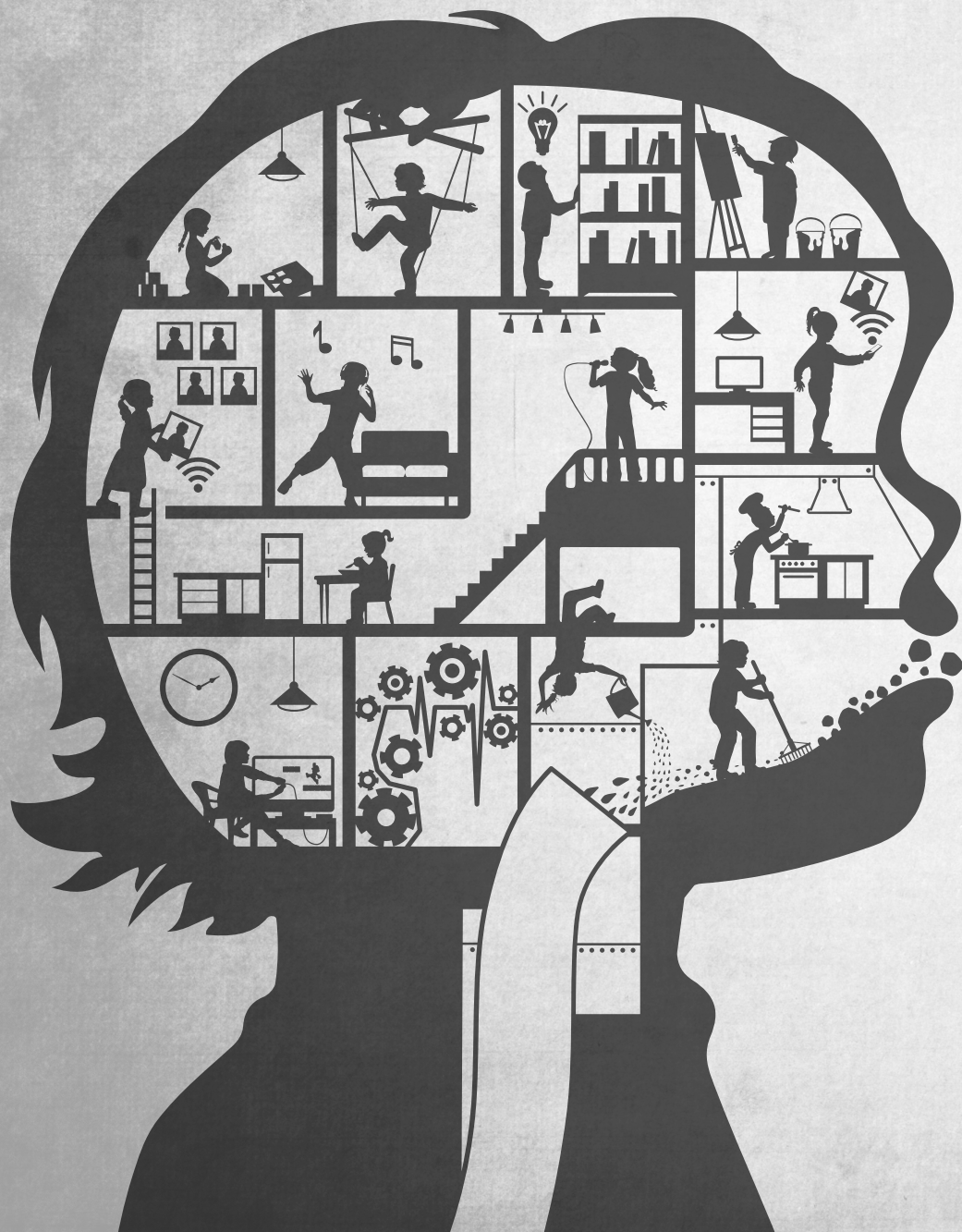
- Blanken, L. M., S. E. Mous, A. Ghassabian, R. L. Muetzel, N. K. Schoemaker, H. El Marroun, A. van der Lugt, V. W. Jaddoe, A. Hofman, F. C. Verhulst, H. Tiemeier and T. White (2015). Cortical morphology in 6- to 10-year old children with autistic traits: a population-based neuroimaging study. *Am J Psychiatry* **172**(5): 479-486.
- Button, K. S., J. P. Ioannidis, C. Mokrysz, B. A. Nosek, J. Flint, E. S. Robinson and M. R. Munafò (2013). Power failure: why small sample size undermines the reliability of neuroscience. *Nat Rev Neurosci* **14**(5): 365-376.
- Calhoun, V. D., T. Adali, G. D. Pearson and J. J. Pekar (2001). A method for making group inferences from functional MRI data using independent component analysis. *Human brain mapping* **14**(3): 140-151.
- Chen, J., J. Liu, V. D. Calhoun, A. Arias-Vasquez, M. P. Zwiers, C. N. Gupta, B. Franke and J. A. Turner (2014). Exploration of scanning effects in multi-site structural MRI studies. *J Neurosci Methods* **230**: 37-50.
- Constantino, J. N. and R. D. Todd (2003). Autistic traits in the general population: a twin study. *Arch Gen Psychiatry* **60**(5): 524-530.
- Cullen, K. R., B. Klimes-Dougan, R. Muetzel, B. A. Mueller, J. Camchong, A. Hourii, S. Kurma and K. O. Lim (2010). Altered white matter microstructure in adolescents with major depression: a preliminary study. *J Am Acad Child Adolesc Psychiatry* **49**(2): 173-183 e171.
- Damaraju, E., E. A. Allen, A. Belger, J. M. Ford, S. McEwen, D. H. Mathalon, B. A. Mueller, G. D. Pearson, S. G. Potkin, A. Preda, J. A. Turner, J. G. Vaidya, T. G. van Erp and V. D. Calhoun (2014). Dynamic functional connectivity analysis reveals transient states of dysconnectivity in schizophrenia. *Neuroimage Clin* **5**: 298-308.
- de Bie, H. M., M. Boersma, S. Adriaanse, D. J. Veltman, A. M. Wink, S. D. Roosendaal, F. Barkhof, C. J. Stam, K. J. Oostrom, H. A. Delemarre-van de Waal and E. J. Sanz-Arigita (2012). Resting-state networks in awake five- to eight-year old children. *Human brain mapping* **33**(5): 1189-1201.
- Di Martino, A., D. A. Fair, C. Kelly, T. D. Satterthwaite, F. X. Castellanos, M. E. Thomason, R. C. Craddock, B. Luna, B. L. Leventhal, X. N. Zuo and M. P. Milham (2014). Unraveling the miswired connectome: a developmental perspective. *Neuron* **83**(6): 1335-1353.
- Di Martino, A., C. G. Yan, Q. Li, E. Denio, F. X. Castellanos, K. Alaerts, J. S. Anderson, M. Assaf, S. Y. Bookheimer, M. Dapretto, B. Deen, S. Delmonte, I. Dinstein, B. Ertl-Wagner, D. A. Fair, L. Gallagher, D. P. Kennedy, C. L. Keown, C. Keyzers, J. E. Lainhart, C. Lord, B. Luna, V. Menon, N. J. Minshew, C. S. Monk, S. Mueller, R. A. Muller, M. B. Nebel, J. T. Nigg, K. O'Hearn, K. A. Pelphrey, S. J. Peltier, J. D. Rudie, S. Sunaert, M. Thioux, J. M. Tyszka, L. Q. Uddin, J. S. Verhoeven, N. Wenderoth, J. L. Wiggins, S. H. Mostofsky and M. P. Milham (2014). The autism brain imaging data exchange: towards a large-scale evaluation of the intrinsic brain architecture in autism. *Mol Psychiatry* **19**(6): 659-667.
- Ducharme, S., M. D. Albaugh, J. J. Hudziak, K. N. Botteron, T. V. Nguyen, C. Truong, A. C. Evans, S. Karama and G. Brain Development Cooperative (2014). Anxious/depressed symptoms are linked to right ventromedial prefrontal cortical thickness maturation in healthy children and young adults. *Cereb Cortex* **24**(11): 2941-2950.
- Dudbridge, F. and A. Gusnanto (2008). Estimation of significance thresholds for genomewide association scans. *Genet Epidemiol* **32**(3): 227-234.
- Dunlop, B. W. and H. S. Mayberg (2014). Neuroimaging-based biomarkers for treatment selection in major depressive disorder. *Dialogues Clin Neurosci* **16**(4): 479-490.
- Edelstein, W. A., G. H. Glover, C. J. Hardy and R. W. Redington (1986). The intrinsic signal-to-noise ratio in NMR imaging. *Magn Reson Med* **3**(4): 604-618.
- Franco, A. R., M. V. Mannell, V. D. Calhoun and A. R. Mayer (2013). Impact of analysis methods on the reproducibility and reliability of resting-state networks. *Brain connectivity* **3**(4): 363-374.

- Friedman, L., H. Stern, G. G. Brown, D. H. Mathalon, J. Turner, G. H. Glover, R. L. Gollub, J. Lauriello, K. O. Lim, T. Cannon, D. N. Greve, H. J. Bockholt, A. Belger, B. Mueller, M. J. Doty, J. He, W. Wells, P. Smyth, S. Pieper, S. Kim, M. Kubicki, M. Vangel and S. G. Potkin (2008). Test-retest and between-site reliability in a multicenter fMRI study. *Hum Brain Mapp* **29**(8): 958-972.
- Gallichan, D., J. Scholz, A. Bartsch, T. E. Behrens, M. D. Robson and K. L. Miller (2010). Addressing a systematic vibration artifact in diffusion-weighted MRI. *Hum Brain Mapp* **31**(2): 193-202.
- Galwey, N. W. (2009). A new measure of the effective number of tests, a practical tool for comparing families of non-independent significance tests. *Genet Epidemiol* **33**(7): 559-568.
- Giedd, J. N., J. M. Rumsey, F. X. Castellanos, J. C. Rajapakse, D. Kaysen, A. C. Vaituzis, Y. C. Vauss, S. D. Hamburger and J. L. Rapoport (1996). A quantitative MRI study of the corpus callosum in children and adolescents. *Brain Res Dev Brain Res* **91**(2): 274-280.
- Glover, G. H., B. A. Mueller, J. A. Turner, T. G. van Erp, T. T. Liu, D. N. Greve, J. T. Voyvodic, J. Rasmussen, G. G. Brown, D. B. Keator, V. D. Calhoun, H. J. Lee, J. M. Ford, D. H. Mathalon, M. Diaz, D. S. O'Leary, S. Gadde, A. Preda, K. O. Lim, C. G. Wible, H. S. Stern, A. Belger, G. McCarthy, B. Ozyurt and S. G. Potkin (2012). Function biomedical informatics research network recommendations for prospective multicenter functional MRI studies. *J Magn Reson Imaging* **36**(1): 39-54.
- Gogtay, N., J. N. Giedd, L. Lusk, K. M. Hayashi, D. Greenstein, A. C. Vaituzis, T. F. Nugent, 3rd, D. H. Herman, L. S. Clasen, A. W. Toga, J. L. Rapoport and P. M. Thompson (2004). Dynamic mapping of human cortical development during childhood through early adulthood. *Proc Natl Acad Sci U S A* **101**(21): 8174-8179.
- Golland, P. and B. Fischl (2003). Permutation tests for classification: towards statistical significance in image-based studies. *Inf Process Med Imaging* **18**: 330-341.
- Greene, D. J., K. J. Black and B. L. Schlaggar (2016). Considerations for MRI study design and implementation in pediatric and clinical populations. *Dev Cogn Neurosci* **18**: 101-112.
- Gronenschild, E. H., P. Habets, H. I. Jacobs, R. Mengelers, N. Rozenaal, J. van Os and M. Marcelis (2012). The effects of FreeSurfer version, workstation type, and Macintosh operating system version on anatomical volume and cortical thickness measurements. *PLoS One* **7**(6): e38234.
- Hathaway, S. R. and J. C. McKinley (1943). *Manual for the Minnesota Multiphasic Personality Inventory*. New York, Psychological Cooperation.
- Hayasaka, S. and T. E. Nichols (2003). Validating cluster size inference: random field and permutation methods. *Neuroimage* **20**(4): 2343-2356.
- Himberg, J., A. Hyvarinen and F. Esposito (2004). Validating the independent components of neuroimaging time series via clustering and visualization. *Neuroimage* **22**(3): 1214-1222.
- Hoening, K., C. K. Kuhl and L. Scheef (2005). Functional 3.0-T MR assessment of higher cognitive function: are there advantages over 1.5-T imaging? *Radiology* **234**(3): 860-868.
- Hofstra, M. B., J. van der Ende and F. C. Verhulst (2002). Child and adolescent problems predict DSM-IV disorders in adulthood: a 14-year follow-up of a Dutch epidemiological sample. *J Am Acad Child Adolesc Psychiatry* **41**(2): 182-189.
- Hudziak, J. J., T. M. Achenbach, R. R. Althoff and D. S. Pine (2007). A dimensional approach to developmental psychopathology. *Int J Methods Psychiatr Res* **16 Suppl 1**: S16-23.
- Huibers, M. J., Z. D. Cohen, L. H. Lemmens, A. Arntz, F. P. Peeters, P. Cuijpers and R. J. DeRubeis (2015). Predicting Optimal Outcomes in Cognitive Therapy or Interpersonal Psychotherapy for Depressed Individuals Using the Personalized Advantage Index Approach. *PLoS One* **10**(11): e0140771.
- Ikram, M. A., A. van der Lugt, W. J. Niessen, P. J. Koudstaal, G. P. Krestin, A. Hofman, D. Bos and M. W. Vernooij (2015). The Rotterdam Scan Study: design update 2016 and main findings. *Eur J Epidemiol* **30**(12): 1299-1315.
- Insel, T., B. Cuthbert, M. Garvey, R. Heinssen, D. S. Pine, K. Quinn, C. Sanislow and P. Wang (2010). Research domain criteria (RDoC): toward a new classification framework for research on mental disorders. *Am J Psychiatry* **167**(7): 748-751.

- Jones, D. K. and M. Cercignani (2010). Twenty-five pitfalls in the analysis of diffusion MRI data. *NMR Biomed* **23**(7): 803-820.
- Jones, T. B., P. A. Bandettini, L. Kenworthy, L. K. Case, S. C. Milleville, A. Martin and R. M. Birn (2010). Sources of group differences in functional connectivity: an investigation applied to autism spectrum disorder. *Neuroimage* **49**(1): 401-414.
- Jovicich, J., S. Czanner, D. Greve, E. Haley, A. van der Kouwe, R. Gollub, D. Kennedy, F. Schmitt, G. Brown, J. Macfall, B. Fischl and A. Dale (2006). Reliability in multi-site structural MRI studies: effects of gradient non-linearity correction on phantom and human data. *Neuroimage* **30**(2): 436-443.
- Klein, A., J. Andersson, B. A. Ardekani, J. Ashburner, B. Avants, M. C. Chiang, G. E. Christensen, D. L. Collins, J. Gee, P. Hellier, J. H. Song, M. Jenkinson, C. Lepage, D. Rueckert, P. Thompson, T. Vercauteren, R. P. Woods, J. J. Mann and R. V. Parsey (2009). Evaluation of 14 nonlinear deformation algorithms applied to human brain MRI registration. *Neuroimage* **46**(3): 786-802.
- Lebel, C., C. Rasmussen, K. Wyper, G. Andrew and C. Beaulieu (2010). Brain microstructure is related to math ability in children with fetal alcohol spectrum disorder. *Alcohol Clin Exp Res* **34**(2): 354-363.
- Leemans, A. and D. K. Jones (2009). The B-matrix must be rotated when correcting for subject motion in DTI data. *Magn Reson Med* **61**(6): 1336-1349.
- Lenroot, R. K. and J. N. Giedd (2006). Brain development in children and adolescents: insights from anatomical magnetic resonance imaging. *Neurosci Biobehav Rev* **30**(6): 718-729.
- LeWinn, K. Z., C. G. Connolly, J. Wu, M. Drahos, F. Hoeft, T. C. Ho, A. N. Simmons and T. T. Yang (2014). White matter correlates of adolescent depression: structural evidence for frontolimbic disconnectivity. *J Am Acad Child Adolesc Psychiatry* **53**(8): 899-909, 909 e891-897.
- Magioncalda, P., M. Martino, B. Conio, N. Piaggio, R. Teodorescu, A. Escelsior, V. Marozzi, G. Rocchi, L. Roccatagliata, G. Northoff, M. Inglese and M. Amore (2016). Patterns of microstructural white matter abnormalities and their impact on cognitive dysfunction in the various phases of type I bipolar disorder. *J Affect Disord* **193**: 39-50.
- McArdle, J. J. (2009). Latent variable modeling of differences and changes with longitudinal data. *Annu Rev Psychol* **60**: 577-605.
- Moeller, S., E. Yacoub, C. A. Olman, E. Auerbach, J. Strupp, N. Harel and K. Ugurbil (2010). Multiband multislice GE-EPI at 7 tesla, with 16-fold acceleration using partial parallel imaging with application to high spatial and temporal whole-brain fMRI. *Magn Reson Med* **63**(5): 1144-1153.
- Muetzel, R. L., P. F. Collins, B. A. Mueller, K. O. Lim and M. Luciana (2009). Fiber tractography in healthy adolescents: An automated approach. International Society for Magnetic Resonance in Medicine. Honolulu, HI, USA.
- Murphy, M. L. and T. Frodl (2011). Meta-analysis of diffusion tensor imaging studies shows altered fractional anisotropy occurring in distinct brain areas in association with depression. *Biol Mood Anxiety Disord* **1**(1): 3.
- Nichols, T. E., S. Das, S. B. Eickhoff, A. C. Evans, T. Glatard, M. Hanke, N. Kriegeskorte, M. P. Milham, R. A. Poldrack, J.-B. Poline, E. Proal, B. Thirion, D. C. Van Essen, T. White and B. T. T. Yeo (2016). Best Practices in Data Analysis and Sharing in Neuroimaging using MRI. *bioRxiv*.
- Pe'er, I., R. Yelensky, D. Altshuler and M. J. Daly (2008). Estimation of the multiple testing burden for genome-wide association studies of nearly all common variants. *Genet Epidemiol* **32**(4): 381-385.
- Peters, B. D., P. R. Szeszko, J. Radua, T. Ikuta, P. Gruner, P. DeRosse, J. P. Zhang, A. Giorgio, D. Qiu, S. F. Tapert, J. Brauer, M. R. Asato, P. L. Khong, A. C. James, J. A. Gallego and A. K. Malhotra (2012). White matter development in adolescence: diffusion tensor imaging and meta-analytic results. *Schizophr Bull* **38**(6): 1308-1317.
- Pine, D. S., E. Cohen, P. Cohen and J. Brook (1999). Adolescent depressive symptoms as predictors of adult depression: moodiness or mood disorder? *Am J Psychiatry* **156**(1): 133-135.

- Poline, J. B., S. C. Strother, G. Dehaene-Lambertz, G. F. Egan and J. L. Lancaster (2006). Motivation and synthesis of the FIAC experiment: Reproducibility of fMRI results across expert analyses. *Hum Brain Mapp* **27**(5): 351-359.
- Reuter, M. and B. Fischl (2011). Avoiding asymmetry-induced bias in longitudinal image processing. *Neuroimage* **57**(1): 19-21.
- Reuter, M., N. J. Schmansky, H. D. Rosas and B. Fischl (2012). Within-subject template estimation for unbiased longitudinal image analysis. *Neuroimage* **61**(4): 1402-1418.
- Sanchez, C. E., J. E. Richards and C. R. Almlil (2012). Age-specific MRI templates for pediatric neuroimaging. *Developmental neuropsychology* **37**(5): 379-399.
- Schmahmann, J. D., D. N. Pandya, R. Wang, G. Dai, H. E. D'Arceuil, A. J. de Crespigny and V. J. Wedeen (2007). Association fibre pathways of the brain: parallel observations from diffusion spectrum imaging and autoradiography. *Brain* **130**(Pt 3): 630-653.
- Schmithorst, V. J. and W. Yuan (2010). White matter development during adolescence as shown by diffusion MRI. *Brain Cogn* **72**(1): 16-25.
- Schnack, H. G. and R. S. Kahn (2016). Detecting Neuroimaging Biomarkers for Psychiatric Disorders: Sample Size Matters. *Front Psychiatry* **7**: 50.
- Schwartz, S. and E. Susser (2011). The use of well controls: an unhealthy practice in psychiatric research. *Psychol Med* **41**(6): 1127-1131.
- Segall, J. M., J. A. Turner, T. G. van Erp, T. White, H. J. Bockholt, R. L. Gollub, B. C. Ho, V. Magnotta, R. E. Jung, R. W. McCarley, S. C. Schulz, J. Lauriello, V. P. Clark, J. T. Voyvodic, M. T. Diaz and V. D. Calhoun (2009). Voxel-based morphometric multisite collaborative study on schizophrenia. *Schizophr Bull* **35**(1): 82-95.
- Shaw, P., K. Eckstrand, M. Sharp, J. Blumenthal, J. P. Lerch, D. Greenstein, L. Clasen, A. Evans, J. Giedd and J. L. Rapoport (2007). Attention-deficit/hyperactivity disorder is characterized by a delay in cortical maturation. *Proceedings of the National Academy of Sciences of the United States of America* **104**(49): 19649-19654.
- Smith, S. M., P. T. Fox, K. L. Miller, D. C. Glahn, P. M. Fox, C. E. Mackay, N. Filippini, K. E. Watkins, R. Toro, A. R. Laird and C. F. Beckmann (2009). Correspondence of the brain's functional architecture during activation and rest. *Proceedings of the National Academy of Sciences of the United States of America* **106**(31): 13040-13045.
- Smith, S. M. and T. E. Nichols (2009). Threshold-free cluster enhancement: addressing problems of smoothing, threshold dependence and localisation in cluster inference. *Neuroimage* **44**(1): 83-98.
- Smith, S. M., Y. Zhang, M. Jenkinson, J. Chen, P. M. Matthews, A. Federico and N. De Stefano (2002). Accurate, robust, and automated longitudinal and cross-sectional brain change analysis. *Neuroimage* **17**(1): 479-489.
- Strother, S., S. La Conte, L. Kai Hansen, J. Anderson, J. Zhang, S. Pulapura and D. Rottenberg (2004). Optimizing the fMRI data-processing pipeline using prediction and reproducibility performance metrics: I. A preliminary group analysis. *Neuroimage* **23 Suppl 1**: S196-207.
- Sui, J., T. Adali, Q. Yu, J. Chen and V. D. Calhoun (2012). A review of multivariate methods for multimodal fusion of brain imaging data. *J Neurosci Methods* **204**(1): 68-81.
- Uddin, L. Q., K. Supekar and V. Menon (2013). Reconceptualizing functional brain connectivity in autism from a developmental perspective. *Front Hum Neurosci* **7**: 458.
- van der Kouwe, A. J., T. Benner, B. Fischl, F. Schmitt, D. H. Salat, M. Harder, A. G. Sorensen and A. M. Dale (2005). On-line automatic slice positioning for brain MR imaging. *Neuroimage* **27**(1): 222-230.
- White, T., M. Nelson and K. O. Lim (2008). Diffusion tensor imaging in psychiatric disorders. *Top Magn Reson Imaging* **19**(2): 97-109.

- White, T., D. O’Leary, V. Magnotta, S. Arndt, M. Flaum and N. C. Andreasen (2001). Anatomic and functional variability: the effects of filter size in group fMRI data analysis. *Neuroimage* **13**(4): 577-588.
- White, T., M. Schmidt and C. Karatekin (2009). White matter ‘potholes’ in early-onset schizophrenia: a new approach to evaluate white matter microstructure using diffusion tensor imaging. *Psychiatry Res* **174**(2): 110-115.
- Winkler, A. M., G. R. Ridgway, M. A. Webster, S. M. Smith and T. E. Nichols (2014). Permutation inference for the general linear model. *Neuroimage* **92**: 381-397.
- Wonderlick, J. S., D. A. Ziegler, P. Hosseini-Varnamkhasti, J. J. Locascio, A. Bakkour, A. van der Kouwe, C. Triantafyllou, S. Corkin and B. C. Dickerson (2009). Reliability of MRI-derived cortical and subcortical morphometric measures: effects of pulse sequence, voxel geometry, and parallel imaging. *Neuroimage* **44**(4): 1324-1333.
- Worsley, K. J., S. Marrett, P. Neelin, A. C. Vandal, K. J. Friston and A. C. Evans (1996). A unified statistical approach for determining significant signals in images of cerebral activation. *Hum Brain Mapp* **4**(1): 58-73.
- Wozniak, J. R., B. A. Mueller, R. L. Muetzel, C. J. Bell, H. L. Hoecker, M. L. Nelson, P. N. Chang and K. O. Lim (2011). Inter-hemispheric functional connectivity disruption in children with prenatal alcohol exposure. *Alcohol Clin Exp Res* **35**(5): 849-861.
- Zhang, H., X. N. Zuo, S. Y. Ma, Y. F. Zang, M. P. Milham and C. Z. Zhu (2010). Subject order-independent group ICA (SOI-GICA) for functional MRI data analysis. *Neuroimage* **51**(4): 1414-1424.



CHAPTER

9

Summary/Samenvatting

SUMMARY

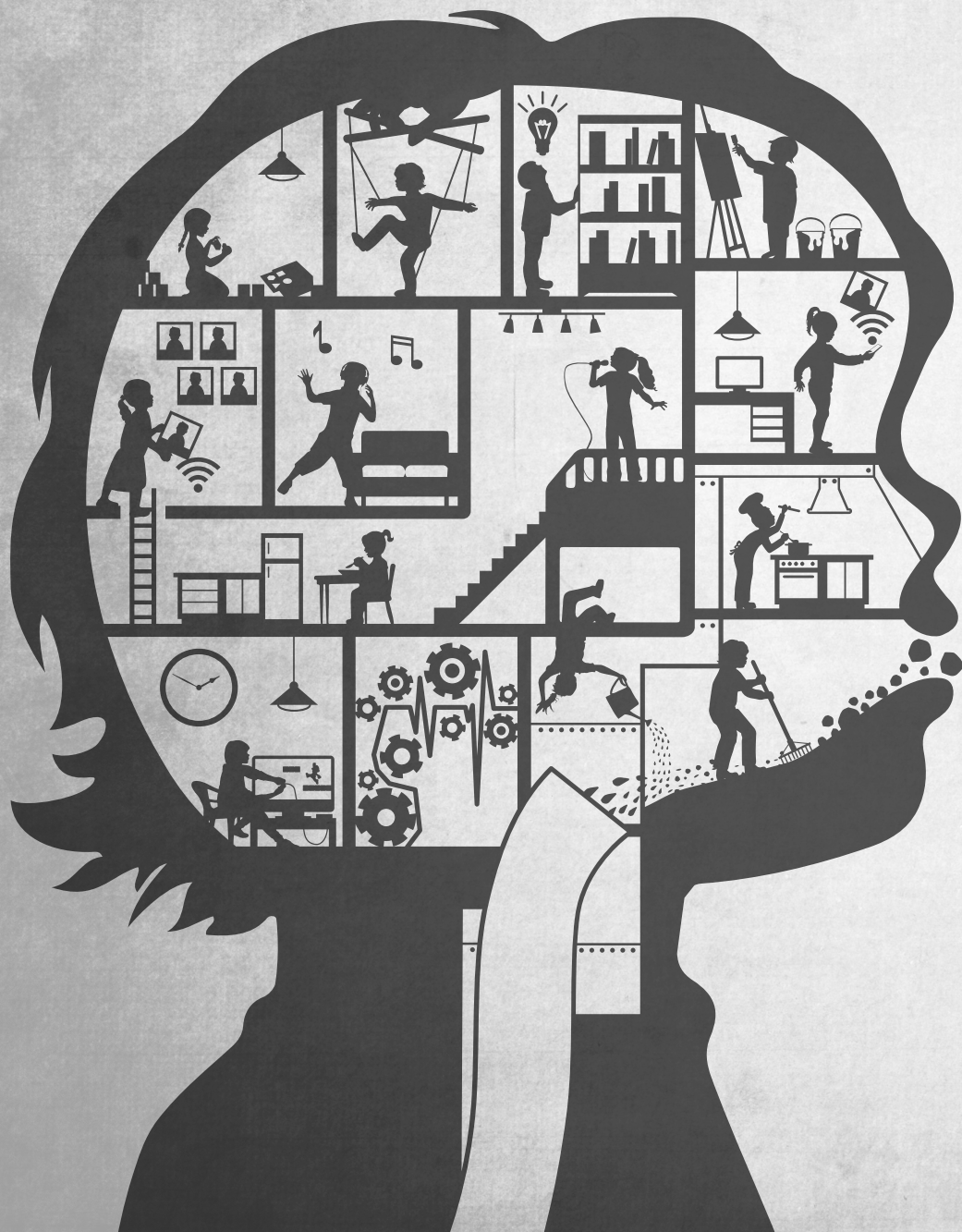
Over the past two decades, magnetic resonance imaging (MRI) has transformed the field of neuroscience, offering a unique and *in vivo* window into the developing brain. Sophisticated neuroimaging techniques, such as diffusion tensor imaging and resting-state functional MRI, have allowed for the precise quantification of numerous neurobiological features. In this thesis, both diffusion imaging and resting-state functional imaging are used to explore these features in both typical development and psychopathology in children. As a thorough understanding of the typically developing brain is essential for accurately characterizing disrupted features in children with psychopathology, the first aim of this thesis was to study structural and functional connectivity in children from the general population. The second aim of this thesis was to study how subclinical psychopathology in the general population is related to structural and functional connectivity. These aims are addressed using data from two large studies of children and are organized into two parts, with **Part I** examining structural connectivity, specifically structure-function associations in typical development and white matter microstructural features of psychopathology. **Chapter 2** uses a large sample of typically developing children, adolescents and young adults to study the corpus callosum, which is the primary interconnecting bridge between the right and left hemispheres of the brain. In this chapter, white matter microstructural integrity in the corpus callosum was related to age, suggesting continued development from childhood into young adulthood. Further, independent of age, metrics of white matter microstructure in the corpus callosum were related to performance on a motor task, demonstrating that structural features of the brain measured with MRI are related to motor performance. **Chapter 3** expands upon this, examining structure-function associations across a battery of neuropsychological tests in a large sample of children recruited from the general population. Global metrics of white matter microstructure across the brain were related to both general intellectual functioning (i.e., IQ), as well as spatial ability. In **Chapter 4**, a transition is made to studying structural connectivity in sub-clinical psychopathology using a dimensional approach. Autistic traits measured along a continuum in the general population were associated with lower fractional anisotropy (a measure of white matter microstructure) in the superior longitudinal fasciculus, a region previously implicated in clinical autism spectrum disorder. Thus, autistic traits in a non-clinical sample are related to features of white matter integrity, suggesting neurobiological features covary with the severity of the behavioral phenotype and extend to the general population. Concluding **Part I**, **Chapter 5** utilizes a longitudinal design to explore sub-clinical psychiatric symptoms in relation to trajectories of white matter maturation. Global white matter maturation was significantly attenuated in children with higher levels of affective (depressive) problems, lending additional support to the notion that dimensional psychiatric problems covary with detectable neurobiological features outside of clinical samples.

Part II examines functional connectivity in both typical development and in children with traits of autism spectrum disorder. **Chapter 6** uses a data-driven approach to identify and categorize resting-state functional connectivity networks in typically developing children. Networks previously identified in adults were also present in children, and these networks were highly robust after repeated subsampling, with many common networks present in over 95% of the resamples. Further, some of the networks showed evidence of continued maturation through age-related associations. Finally, **Chapter 7** utilizes a cutting-edge data analysis technique in resting-state MRI, examining transient states of functional connectivity in children in relation to age and autistic traits along a continuum. Both younger children and children with higher levels of autistic traits spent more time in disconnected transient states and less time in a transient state characterized by the default mode network, suggesting a less mature pattern of connectivity in children with high levels of autistic traits. This thesis is concluded with **Chapter 8**: a general discussion of these findings in the context of the literature, a look at important methodological considerations for the field, clinical implications of this work, and proposed future directions for the study of typical and atypical brain development in child psychiatry.

SAMENVATTING

Magnetic resonance imaging (MRI) heeft de laatste 20 jaar grote veranderingen teweeggebracht op het gebied van neurowetenschappelijk onderzoek, en geeft inzicht in het ontwikkelende brein *in vivo*. Geavanceerde beeldvormende technieken, zoals “diffusion tensor imaging” en “resting-state functionele MRI”, hebben het mogelijk gemaakt om verschillende neurobiologische parameters te kwantificeren. In dit proefschrift wordt gebruik gemaakt van diffusion tensor imaging en resting-state functionele MRI om deze eigenschappen van het brein te onderzoeken, zowel wanneer het brein zich normaal ontwikkelt als bij kinderen met psychopathologie. Nauwkeurige kennis over de normale ontwikkeling van het brein is belangrijk om verstoorde functies te kunnen begrijpen; de eerste doelstelling van dit proefschrift is dan ook om structurele en functionele verbindingen in de algemene bevolking te onderzoeken. De tweede doelstelling van dit proefschrift is het bestuderen van subklinische psychopathologie in de algemene populatie, in relatie tot structurele en functionele connectiviteit van de hersenen. Deze doelstellingen worden onderzocht in twee grote kindercohorten. Dit proefschrift is opgedeeld in twee delen. In **Deel I** richtten we ons op structurele connectiviteit, in het bijzonder op structuur-functie associaties bij normale ontwikkeling en witte stof eigenschappen bij kinderen met kenmerken van psychopathologie. In **Hoofdstuk 2** bestudeerden we het corpus callosum, de primaire verbinding tussen de linker- en rechterhersenhalfrand, in een grote groep normaal ontwikkelende kinderen, adolescenten en jongvolwassenen. In dit hoofdstuk zagen we dat de witte stof integriteit in het corpus callosum gerelateerd was aan leeftijd, wat erop wijst dat er een doorlopende ontwikkeling plaatsvindt tussen de kindertijd en jongvolwassenheid. Daarnaast waren metingen van de witte stof microstructuur in het corpus callosum, onafhankelijk van leeftijd, gerelateerd aan de prestatie in motorische taken, wat laat zien dat structurele eigenschappen van het brein, die gekwantificeerd kunnen worden met MRI, gerelateerd zijn aan motorische vaardigheden. **Hoofdstuk 3** gaat hier verder op in, en in dit hoofdstuk werden structuur-functie associaties bestudeerd aan de hand van een aantal neuropsychologische testen in een groot cohort van kinderen uit de algemene populatie. Globale parameters van de witte stof microstructuur in het brein waren gerelateerd aan zowel het algemene intellectuele functioneren als aan ruimtelijk inzicht. In **Hoofdstuk 4** wordt een overgang gemaakt naar het bestuderen van structurele connectiviteit in relatie tot subklinische psychopathologie, waarbij gebruikt wordt van een dimensionele benadering voor het kwantificeren van de psychopathologie. Autistische kenmerken, gemeten op een continue schaal in de algemene populatie, waren geassocieerd met lagere “fractional anisotropy” (een maat voor witte stof integriteit) in de superieure longitudinale fasciculus, een structuur die al eerder in verband werd gebracht met autisme spectrum stoornissen. Autistische kenmerken zijn dus ook in een niet-klinische

populatie gerelateerd aan witte stof integriteit, hetgeen suggereert dat neurobiologische kenmerken van autisme variëren naargelang de ernst van de symptomen en ook voorkomen in de algemene bevolking. **Hoofdstuk 5** sluit **Deel I** af en in dit hoofdstuk maakten we gebruik van een longitudinale studie-opzet om de relatie tussen subklinische psychiatrische symptomen en rijping van de witte stof banen te bestuderen. Globale witte stof maturatie was significant verminderd in kinderen met meer affectieve (depressieve) symptomen, hetgeen extra steun geeft aan het inzicht dat er meetbare neurobiologische verschillen zijn in relatie tot dimensionele psychiatrische problemen, ook buiten de klinisch-psychiatrische populatie. In **Deel II** behandelden we functionele connectiviteit, zowel in kinderen die zich normaal ontwikkelen, als in kinderen met kenmerken van autisme spectrum stoornissen. In **Hoofdstuk 6** maakten we gebruik van een data-gedreven benadering om resting-state netwerken te identificeren en te categoriseren in kinderen die zich normaal ontwikkelen. Netwerken die eerder geïdentificeerd waren in volwassenen bleken ook aanwezig te zijn in kinderen, en deze netwerken waren zeer robuust; wanneer de analyses volgens een iteratief proces herhaald werden in kleinere subgroepen waren de veelvoorkomende netwerken aanwezig in 95% van de steekproeven. Daarnaast vertoonden een aantal netwerken kenmerken van doorlopende ontwikkeling, die werden geïdentificeerd door middel van leeftijds- associaties. Tenslotte maken we in **Hoofdstuk 7** gebruik van innovatieve analysetechnieken voor resting-state MRI-data om dynamische kenmerken van functionele connectiviteit in kinderen te bestuderen, in relatie tot leeftijd en autistische kenmerken, gemeten op een continue schaal. De patronen in de hersenen van jongere kinderen, evenals die van kinderen met veel autistische kenmerken, wijzen erop dat zij meer tijd doorbrengen in een staat die gekenmerkt wordt door verminderde connectiviteit en minder tijd in een staat waarin het “default mode netwerk” prominent was. Dit suggereert dat kinderen met autistische trekken wellicht vertraagde ontwikkeling van connectiviteit in de hersenen laten zien. Tenslotte wordt dit proefschrift afgerond met **Hoofdstuk 8**: een algemene discussie van de bevindingen in de context van de bestaande literatuur, een blik op de belangrijke methodologische overwegingen voor dit onderzoeksgebied, klinische implicaties van deze bevindingen, en mogelijkheden voor toekomstig onderzoek naar typische- en atypische hersenontwikkeling.



APPENDIX

A

Acknowledgements

Author Affiliations

Publications

Portfolio

Words of Gratitude / Dankwoord

ACKNOWLEDGEMENTS

The Generation R Study is conducted by the Erasmus Medical Centre Rotterdam in close collaboration with the Faculty of Social Sciences of the Erasmus University Rotterdam, the Municipal Health Service Rotterdam, and the Stichting Trombosedienst & Artsenlaboratorium Rijnmond (STAR), Rotterdam. We gratefully acknowledge the contribution of all participating children and their families, general practitioners, hospitals, midwives, and pharmacies in Rotterdam. The general design of the Generation R Study is made possible by the Erasmus Medical Centre Rotterdam, the Erasmus University Rotterdam, the Netherlands Organisation for Health Research and Development (ZonMw), the Netherlands Organisation for Scientific Research (NWO), the Ministry of Health, Welfare and Sport, and the Ministry of Youth and Families.

The work presented in this thesis was conducted at the Department of Child and Adolescent Psychiatry/Psychology of the Erasmus Medical Centre – Sophia's Children Hospital in Rotterdam, the Netherlands. Studies were financially supported by grants from, NWO/ZonMw (TOP, 91211021), the Sophia Children's Hospital Research Foundation (SSWO) (project 639 and 677) and the and the Simons Foundation Autism Research Initiative (SFARI - 307280). Supercomputing resources were supported by the NWO Physical Sciences Division (Exacte Wetenschappen) and SURFsara (Lisa compute cluster, www.surfsara.nl). Financial support for the publication of this thesis was provided by the Department of Child and Adolescent Psychiatry/Psychology, the Generation R Study, and the Erasmus Medical Centre.

AUTHOR AFFILIATIONS

Center for Child and Family Studies, Leiden University, Leiden, the Netherlands

Sandra Thijssen

Department of Child and Adolescent Psychiatry, Erasmus MC –Sophia Children’s Hospital, Rotterdam, the Netherlands.

Laura Blanken, Hanan El Marroun, Jan van der Ende, Sabine Mous, Ryan Muetzel, Henning Tiemeier, Frank Verhulst, Tonya White

Department of Electrical and Computer Engineering, University of New Mexico, USA

Vince Calhoun, Eswar Damaraju, Barnaly Rashid

Department of Epidemiology, Erasmus MC, Rotterdam, the Netherlands

Vincent Jaddoe, Henning Tiemeier

Department of Mathematics and Statistics, University of New Mexico, USA

Erik Erhardt

Department of Pediatrics, Erasmus MC – Sophia Children’s Hospital, Rotterdam, the Netherlands.

Vincent Jaddoe

Department of Psychiatry, Erasmus MC, Rotterdam, the Netherlands.

Henning Tiemeier

Department of Psychiatry, University of Minnesota, Minneapolis, MN, USA.

Kelvin Lim, Bryon Mueller

Department of Psychology, University of Minnesota, Minneapolis, MN, USA.

Paul Collins, Monica Luciana, Ryan Muetzel, Ann Schissel

Department of Radiology, Erasmus MC, Rotterdam, the Netherlands

Aad van der Lugt, Tonya White

The Generation R Study Group, Erasmus MC – Sophia Children’s Hospital, Rotterdam, the Netherlands.

Laura Blanken, Hanan El Marroun, Vincent Jaddoe, Sabine Mous, Ryan Muetzel, Sandra Thijssen

The Mind Research Network & LBERI, USA

Mohammad Arbabshirani, Vince Calhoun, Eswar Damaraju, Robyn Miller, Barnaly Rashid

School of Pedagogical and Educational Sciences, Erasmus University, Rotterdam, The Netherlands

Sandra Thijssen

PUBLICATIONS

Admas, H., Hibar, D., Chouraki, V., Stein, J., ... **Muetzel, R.L.**, ... Debette, S., Medland, S., Ikram, A., Thompson, P. (2016). Novel genetic loci underlying human intracranial volume identified through genome-wide association. *Nature Neuroscience*. (*in press*).

Ars, C.L., Nijs, I.M., Marroun, H.E., **Muetzel, R.**, Schmidt, M., Steenweg-de Graaff, J., van der Lugt, A., Jaddoe, V.W., Hofman, A., Steegers, E.A., Verhulst, F.C., Tiemeier, H., White, T. (2016) Prenatal folate, homocysteine and vitamin B12 levels and child brain volumes, cognitive development and psychological functioning: the Generation R Study. *Br J Nutr*:1-9.

Becker, M.P., Collins, P.F., Lim, K.O., **Muetzel, R.L.**, Luciana, M. (2015) Longitudinal changes in white matter microstructure after heavy cannabis use. *Dev Cogn Neurosci*, 16:23-35.

Blanken, L.M., Mous, S.E., Ghassabian, A., **Muetzel, R.L.**, Schoemaker, N.K., El Marroun, H., van der Lugt, A., Jaddoe, V.W., Hofman, A., Verhulst, F.C., Tiemeier, H., White, T. (2015) Cortical morphology in 6- to 10-year old children with autistic traits: a population-based neuroimaging study. *Am J Psychiatry*, 172:479-86.

Blanken, L.M.E., White, T., Mous, S.E., Basten, M., **Muetzel, R.L.**, Jaddoe, V.W.V., Wals, M., van der Ende, J., Verhulst, F.C., Tiemeier, H. (2016) Cognitive functioning in children with internalising, externalising and dysregulation problems: a population-based study. *European Journal of Child and Adolescent Psychiatry*, *in press*.

Chen, R., **Muetzel, R.L.**, El Marroun, H., Noppe, G., van Rossum, E.F., Jaddoe, V.W., Verhulst, F.C., White, T., Fang, F., Tiemeier, H. (2016) No association between hair cortisol or cortisone and brain morphology in children. *Psychoneuroendocrinology*, 74:101-110.

Cullen, K.R., Klimes-Dougan, B., **Muetzel, R.**, Mueller, B.A., Camchong, J., Houri, A., Kurma, S., Lim, K.O. (2010) Altered white matter microstructure in adolescents with major depression: a preliminary study. *J Am Acad Child Adolesc Psychiatry*, 49:173-83 e1.

El Marroun, H., Tiemeier, H., **Muetzel, R.L.**, Thijssen, S., van der Knaap, N.J., Jaddoe, V.W., Fernandez, G., Verhulst, F.C., White, T.J. (2016) Prenatal Exposure to Maternal and Paternal Depressive Symptoms and Brain Morphology: A Population-Based Prospective Neuroimaging Study in Young Children. *Depress Anxiety*, 33:658-66.

Franc, D.T., Kodl, C.T., Mueller, B.A., **Muetzel, R.L.**, Lim, K.O., Seaquist, E.R. (2011) High connectivity between reduced cortical thickness and disrupted white matter tracts in long-standing type 1 diabetes. *Diabetes*, 60:315-9.

Franc, D.T., **Muetzel, R.L.**, Robinson, P.R., Rodriguez, C.P., Dalton, J.C., Naughton, C.E., Mueller, B.A., Wozniak, J.R., Lim, K.O., Day, J.W. (2012) Cerebral and muscle MRI abnormalities in myotonic dystrophy. *Neuromuscul Disord*, 22:483-91.

Kennedy, M.R., Wozniak, J.R., **Muetzel, R.L.**, Mueller, B.A., Chiou, H.H., Pantekoek, K., Lim, K.O. (2009) White matter and neurocognitive changes in adults with chronic traumatic brain injury. *J Int Neuropsychol Soc*, 15:130-6.

Kocevska, D., **Muetzel, R.L.**, Luik, A.I., Jaddoe, V.W.V., Verhulst, F.C., White, T., Tiemeier, H. The developmental course of sleep disturbances across childhood relates to brain morphology at age seven. *The Generation R Study. Sleep. (in press.)*

Korevaar, T.I., **Muetzel, R.**, Medici, M., Chaker, L., Jaddoe, V.W., de Rijke, Y.B., Steegers, E.A., Visser, T.J., White, T., Tiemeier, H., Peeters, R.P. (2016a) Association of maternal thyroid function during early pregnancy with offspring IQ and brain morphology in childhood: a population-based prospective cohort study. *Lancet Diabetes Endocrinol*, 4:35-43.

Korevaar, T.I., **Muetzel, R.**, Tiemeier, H., Peeters, R.P. (2016b) Maternal thyroid function and child IQ - Authors' reply. *Lancet Diabetes Endocrinol*, 4:18.

Luciana, M., Collins, P.F., **Muetzel, R.L.**, Lim, K.O. (2013) Effects of alcohol use initiation on brain structure in typically developing adolescents. *Am J Drug Alcohol Abuse*, 39:345-55.

Menary, K., Collins, P.F., Porter, J.N., **Muetzel, R.**, Olson, E.A., Kumar, V., Steinbach, M., Lim, K.O., Luciana, M. (2013) Associations between cortical thickness and general intelligence in children, adolescents and young adults. *Intelligence*, 41:597-606.

Mous, S.E., **Muetzel, R.L.**, El Marroun, H., Polderman, T.J., van der Lugt, A., Jaddoe, V.W., Hofman, A., Verhulst, F.C., Tiemeier, H., Posthuma, D., White, T. (2014) Cortical thickness and inattention/hyperactivity symptoms in young children: a population-based study. *Psychol Med*, 44:3203-13.

Muetzel, R.L., Blanken, L.M., Thijssen, S., van der Lugt, A., Jaddoe, V.W., Verhulst, F.C., Tiemeier, H., White, T. (2016) Resting-state networks in 6-to-10 year old children. *Hum Brain Mapp*.

Muetzel, R.L., Collins, P.F., Mueller, B.A., A, M.S., Lim, K.O., Luciana, M. (2008) The development of corpus callosum microstructure and associations with bimanual task performance in healthy adolescents. *Neuroimage*, 39:1918-25.

Muetzel, R.L., Marjanska, M., Collins, P.F., Becker, M.P., Valabregue, R., Auerbach, E.J., Lim, K.O., Luciana, M. (2013) In vivo 1H magnetic resonance spectroscopy in young-adult daily marijuana users. *Neuroimage Clin*, 2:581-589.

Muetzel, R.L., Mous, S.E., van der Ende, J., Blanken, L.M., van der Lugt, A., Jaddoe, V.W., Verhulst, F.C., Tiemeier, H., White, T. (2015) White matter integrity and cognitive performance in school-age children: A population-based neuroimaging study. *Neuroimage*, 119:119-28.

Olson, E.A., Collins, P.F., Hooper, C.J., **Muetzel, R.,** Lim, K.O., Luciana, M. (2009) White matter integrity predicts delay discounting behavior in 9- to 23-year-olds: a diffusion tensor imaging study. *J Cogn Neurosci*, 21:1406-21.

Porter, J.N., Collins, P.F., **Muetzel, R.L.,** Lim, K.O., Luciana, M. (2011) Associations between cortical thickness and verbal fluency in childhood, adolescence, and young adulthood. *Neuroimage*, 55:1865-77.

Thijssen, S., Wildeboer, A., **Muetzel, R.L.,** Bakermans-Kranenburg, M.J., El Marroun, H., Hofman, A., Jaddoe, V.W., van der Lugt, A., Verhulst, F.C., Tiemeier, H., van, I.M.H., White, T. (2015) Cortical thickness and prosocial behavior in school-age children: A population-based MRI study. *Soc Neurosci*, 10:571-82.

Urošević, S., Collins, P., **Muetzel, R.,** Lim, K., Luciana, M. (2012) Longitudinal changes in behavioral approach system sensitivity and brain structures involved in reward processing during adolescence. *Dev Psychol*, 48:1488-500.

Urošević, S., Collins, P., **Muetzel, R.,** Lim, K.O., Luciana, M. (2014) Pubertal status associations with reward and threat sensitivities and subcortical brain volumes during adolescence. *Brain Cogn*, 89:15-26.

Urošević, S., Collins, P., **Muetzel, R.,** Schissel, A., Lim, K.O., Luciana, M. (2015) Effects of reward sensitivity and regional brain volumes on substance use initiation in adolescence. *Soc Cogn Affect Neurosci*, 10:106-13.

White, T., **Muetzel, R.**, Schmidt, M., Langeslag, S.J., Jaddoe, V., Hofman, A., Calhoun, V.D., Verhulst, F.C., Tiemeier, H. (2014) Time of acquisition and network stability in pediatric resting-state functional magnetic resonance imaging. *Brain Connect*, 4:417-27.

Wozniak, J.R., Krach, L., Ward, E., Mueller, B.A., **Muetzel, R.**, Schnoebelen, S., Kiragu, A., Lim, K.O. (2007) Neurocognitive and neuroimaging correlates of pediatric traumatic brain injury: a diffusion tensor imaging (DTI) study. *Arch Clin Neuropsychol*, 22:555-68.

Wozniak, J.R., Mueller, B.A., Bell, C.J., **Muetzel, R.L.**, Hoecker, H.L., Boys, C.J., Lim, K.O. (2013a) Global functional connectivity abnormalities in children with fetal alcohol spectrum disorders. *Alcohol Clin Exp Res*, 37:748-56.

Wozniak, J.R., Mueller, B.A., Bell, C.J., **Muetzel, R.L.**, Lim, K.O., Day, J.W. (2013b) Diffusion tensor imaging reveals widespread white matter abnormalities in children and adolescents with myotonic dystrophy type 1. *J Neurol*, 260:1122-31.

Wozniak, J.R., Mueller, B.A., Chang, P.N., **Muetzel, R.L.**, Caros, L., Lim, K.O. (2006) Diffusion tensor imaging in children with fetal alcohol spectrum disorders. *Alcohol Clin Exp Res*, 30:1799-806.

Wozniak, J.R., Mueller, B.A., **Muetzel, R.L.**, Bell, C.J., Hoecker, H.L., Nelson, M.L., Chang, P.N., Lim, K.O. (2011) Inter-hemispheric functional connectivity disruption in children with prenatal alcohol exposure. *Alcohol Clin Exp Res*, 35:849-61.

Wozniak, J.R., **Muetzel, R.L.** (2011) What does diffusion tensor imaging reveal about the brain and cognition in fetal alcohol spectrum disorders? *Neuropsychol Rev*, 21:133-47.

Wozniak, J.R., **Muetzel, R.L.**, Mueller, B.A., McGee, C.L., Freerks, M.A., Ward, E.E., Nelson, M.L., Chang, P.N., Lim, K.O. (2009) Microstructural corpus callosum anomalies in children with prenatal alcohol exposure: an extension of previous diffusion tensor imaging findings. *Alcohol Clin Exp Res*, 33:1825-35.

SUBMITTED MANUSCRIPTS

Blanken, L.M.E., **Muetzel, R.L.**, Jaddoe, V.W.V., Verhulst, F.C., van der Lugt, A., Tiemeier, H., White, T. White matter microstructure in children with autistic traits.

Ghassabian, A., Blanken, L.M.E., **Muetzel, R.L.**, Basten, M.G.J., Verhulst, F.C., El Marroun, H., Yeung, E., Jaddoe, V.W.V., White, T., Tiemeier, H. Brain morphology and internalizing problems in young children: a population based study.

Guxens, M., Lubczynska, M., **Muetzel, R.**, Dalmau, A., Jaddoe, V.W.V., Hoek, G., Verhulst, F.C., White, T., Brunekreef, B., Tiemeier, H., El Marroun, H. Air pollution exposure during pregnancy and brain morphology in young children: a population-based prospective birth cohort study.

Lopez, M., Wildeboer, A., **Muetzel, R.L.**, Verhulst, F.C., Jaddoe, V.W.V., Sunyer, J., Tiemeier, H., White, T. Cortical structures associated with sports participation in children: a population-based study.

Muetzel, R.L., Blanken, L.M.E., van der Ende, J., El Marroun, H., van der Lugt, A., Jaddoe, V., Verhulst, F.C., Tiemeier, H., White, T. Childhood psychiatric symptoms and white matter development: A longitudinal population-based neuroimaging study.

Muetzel, R.L.*, Blanken, L.M.E.*, Rashid, B.*, Miller, R., Damaraju, E., Arbabshirani, M.R., Erhardt, E.B., Verhulst, F.C., van der Lugt, A., Jaddoe, V.W.V., Tiemeier, H., White, T., Calhoun, V. From Chronnectivity To Chronnectopathy: Connectivity Dynamics of Typical Development And Autistic Traits

Schiller, R.M., van den Bosch, G.E., **Muetzel, R.L.**, Smits, M., Dudink, J., Tibboel, D., Ijsselstijn, H., White, T. Neonatal critical illness and development: White matter alterations and lower hippocampal volume in school-age neonatal ECMO survivors.

Thijssen, S., Wildeboer, A., **Muetzel, R.L.**, Langeslag, S.J.E., Bakermans-Kranenburg, M.J., Jaddoe, V.W.V., Verhulst, F. C., Tiemeier, H., Van IJzendoorn, M.H., & White, T. The honest truth about lying: demographic, cognitive and neurobiological correlates of typical and persistent lie-telling

Wildeboer, A., Thijssen, S., **Muetzel, R.L.**, Bakermans-Kranenburg, M.J., Tiemeier, H., Verhulst, F.C., Jaddoe, V.W.V., White, T., van IJzendoorn, M.H. Neuroanatomical correlates of donating behavior in middle childhood.

PORTFOLIO

Name PhD student:	Ryan Muetzel
Research School:	Netherlands Institute for Health Sciences (NIHES)
Erasmus MC Department:	Child- and Adolescent Psychiatry
PhD period:	January 2012 – April 2016
Promotor(s):	Prof.dr. H. Tiemeier, Prof.dr. F.C. Verhulst
Copromotor(s):	Dr. T. White

	Year	Workload
1. PhD Training		
Master of Sciences Degree, Epidemiology, Erasmus University, Rotterdam the Netherlands		
Erasmus Summer Program		
Principles of Research in Medicine	2012	0.7
Methods of Clinical Research	2013	0.7
Methods of Public Health Research	2012	0.7
Topics in Meta-analysis	2013	0.7
Genome-wide association analysis	2013	1.4
Introduction to global public health	2012	0.7
Principles of Genetic Epidemiology	2013	0.7
Social Epidemiology	2012	0.7
Markers of Prognostic Research	2012	0.7
Core Curriculum		
Study Design	2012	4.3
Biostatistical Methods I	2012	5.7
Clinical Epidemiology	2013	5.7
Methodological Topics in Epidemiological Research	2013	1.4
Biostatistical Methods II	2013	4.3
Advanced Courses		
Repeated Measurements in Clinical Studies	2013	1.4
Psychiatric Epidemiology	2013	1.1
Missing Values in Clinical Research	2013	0.7
Diagnostic Research	2012	0.9
Advanced Analysis of Prognostic Studies	2012	0.9
Prognosis Research	2012	0.9
Principles of Epidemiological Data Analysis	2012	0.7

Skills Courses

Courses for the Quantitative Researcher	2012	1.4
---	------	-----

Other Courses

MRI Safety course, Erasmus MC, Rotterdam, the Netherlands	2012	0.3
The art and pitfalls of fMRI preprocessing	2015	0.3
Reproducible neuroimaging	2015	0.3
Pattern recognition for neuroimaging	2016	0.6

International Conferences

Organization for Human Brain Mapping (Hamburg, Germany)	2014	1.2
Organization for Human Brain Mapping (Honolulu, HI, USA)	2015	1.2
Organization for Human Brain Mapping (Geneva, Switzerland)	2016	1.2
International Meeting for Autism Research (Baltimore, MD, USA)	2016	0.9

Workshops, Meetings, and Symposia

Generation R Research Meetings	2012-2016	1.0
Child Psychiatry Colloquium (1 oral presentation)	2012-2016	1.0
Sophia Research Day (poster session)	2013-2016	0.6
Symposium 'Brain Development and Developmental Disorders', Utrecht, the Netherlands	2012	0.3
Workshop: Share and Flourish: New Standards for Data Sharing in the Neurosciences, Leiden, the Netherlands	2014	1.5

2. Teaching Activities**Supervising Master's Theses**

Marloes Devries: <i>Does prenatal cannabis exposure affect white matter development in young children?</i>	2013	3.0
Kirsten Ellens: <i>White matter integrity and anxiety symptoms in a pediatric population</i>	2014	3.0
Luna Vesseur: <i>Stress and ostracism: a diffusion tensor imaging study</i>	2015	3.0

Other Teaching Activities

Teaching Assistant, Biostatistical Methods	2013-2015	0.3
Child Psychiatry Lectures for Medical Students	2012-2014	0.3

3. Other Activities

Generation R MRI Image Analysis	2012-2016	6.0
Generation R Neuroinformatics	2012-2016	6.0
Peer Review, OHBM, NeuroImage, PLOS One, Psychopharmacology	2012-2016	0.5

1 ECTS (European Credit Transfer System) is equal to a workload of 28 hours

WORDS OF GRATITUDE / DANKWOORD

With a sole author listed on the cover, preparing and finalizing a dissertation may at a glance seem like a largely independent process that lasts four years; the reality could not be further from this. Through the various peaks and valleys of PhD student life, I have been continually humbled by overflowing support, friendship and love from those near and far, and wish to take this opportunity to express my most sincere gratitude. Without these people, this dissertation would not have been possible.

The Generation R Study would not be feasible without the vision of the architects of the project, and certainly not without the families and children who participate. Aan de families die deelnemen aan Generation R: Dank voor uw tijd en uw bereidheid mee te doen aan dit onderzoeksproject. Uw bijdrage maakt een wezenlijk verschil in de wetenschap en geneeskunde, en zal ook in de toekomst onze visie op de gezondheid en ontwikkeling van kinderen mede bepalen.

To my mentors, Professor Tiemeier, Professor Verhulst and Dr. White. Henning, one of my earliest recollections with you and a perfect illustrations of your mentoring and teaching abilities is from “Study Design”; without a visual aid or single slide, you were able to capture the attention and interest of an auditorium full of students for hours on end. I envy your deep passion and excitement for research, and am grateful for all of your teachings and feedback. Frank, as the chair of the department, you somehow still find the time to meet with your students and provide us with thoughtful and useful feedback on our progress, projects and manuscripts. I’m very grateful to have you as a Promoter, and for all I’ve learned from you not only about research, but also about academia in general. Tonya, thank you for this wonderful opportunity to join the amazing ‘KNICR’ group you’ve developed here in Rotterdam. It has been a life-changing experience for me. I’m grateful for the freedom you’ve given me to tackle this project in my own way, and also for being there to keep me on track when needed. I’ve learned a tremendous amount, in science, academia and life working in your lab, and am looking forward to seeing your group continue to build upon this unparalleled initiative of pediatric neuroimaging that I’m proud to say I was a part of.

To the inner committee members, Professor Niessen, Professor Crone, and Dr. Shaw. Wiro, thank you for agreeing to not only review and critique my dissertation, but to also serve as the secretary of the committee. Professor Crone, thank you for agreeing to review my thesis --- I still remember reading papers from your group as an undergraduate student, and am honored to have you as part of this committee. Philip, I likewise still recall reading your seminal papers on ADHD and brain development while working as a research assistant in

Minnesota, and couldn't be more excited for you to be part of this committee. I've sincerely enjoyed the GenR-NHGRI collaborations so far, and am looking forward to all of the exciting work that will come out of these two amazing datasets in the future. Professor van den Heuvel, Professor van der Lugt, and Dr. Ikram, thank you for agreeing to participate in the committee – I'm grateful to have the opportunity to discuss my work with each of you.

To the Generation R team, Claudia, Marjolein, Patricia, Rose, Ronald, Janine, Vincent and all of the 'focus dames': You do the work of a team twice as large. What you've accomplished is remarkable, and none of the researchers at Generation R would be where they are today without your efforts – daily, monthly, yearly – that keep this study moving forward at such an impressive level and pace. Claudia, you were one of the first faces I met at GenR, and I'm really glad that you got stuck with me for my 'algemene taken'. It was a pleasure working together for those first couple of years, and I'm glad we've been able to continue to work together on MRI data since then. Aan de dames van het focus centrum, en in het bijzonder Anneke, Ineke, Rukiye en Sabah van de gedragsgroep: dank voor alle tijd en moeite die jullie steken in ons onderzoek!

To my colleagues, the Generation R PhD students, post-docs and faculty: Agnes Akhgar, Aleksandra, Alex, Andrea C., Andrea W., Ank, Anne, Ayesha, Bruna, Carlijn, Carolina, Charlotte, Claire, Claudia, Dafna, Denise, Desi, Edith, Eirini, Elise, Elize, Evelien, Florianne, Gavro, Gerard, Gijs, Guannan, Hanneke, Ilse, Ivonne, Jessica, Jia-Lian, Jolien R., Jolien S., Junwen, Koen, Kozeta, Laura Benschop, Laura Blanken, Layla, Lea, Lisan, Lisanne, Liza, Maartje B., Maartje L., Marieke, Marina, Marleen, Martijn, Michelle, Michiel, Mirjana, Monica, Myrte, Nienke, Niels, Nina, Olta, Pauline, Philip, Ralf, Rianne, Rob, Rolieke, Romy, Rosa, Sabine, Sander, Sandra, Sanne, Selma, Simone, Strahinja, Suzanne, Tamara, Tim, Trudy, Viara, Willem, Zoe. You have all played a crucial role in ensuring the Generation R study continues on, through data collection, phase planning, and publishing. It has been a pleasure learning from you, and watching each of you grow as scientists over the past four years. The work in this thesis has without question benefitted from interactions with many of you, both informally at the coffee machine and more formally during our scientific discussions. A special thank you to a few people in particular, Akhgar, Anne, Bruna, Hanneke, Desi, Koen, Olta and Rosa, for all of the fun conversations and 'gezelligheid'.

To the BGR and AMBER groups: It has been wonderful working together, and joining in on your imaging meetings. Hakim and Marcel, I've learned a lot from you guys about informatics – thanks for all of the interesting discussions. Rozanna, it was a lot of fun attending OHBM Hamburg and Geneva with you!

To the great people at KJPP: While my time at GenR has been largely separate from the other amazing research activities going on within the department, it has been wonderful getting to know all of you. Vandhana, I think the New Years borrel has been a big success, and it was fun planning it together with you! Speaking of, maybe we need to start planning again for this year??? Laureen, thank you for all of your help over the past 4+ years – we’d be lost without you! Jan, I can’t express enough how grateful I am for your crucial expertise, genuine interest in our projects, and your unending willingness to help. The department leans on you immensely, and your contributions help to propel our work to a higher level.

To our collaborators and friends at the Mind Research Network: It has been a true pleasure working together over the past year. This collaboration is a fundamental example of multidisciplinary research at its best, and I’m positive more great work will follow. Barnaly, I’m glad you had the opportunity to join us in Rotterdam! Not only did it give the project a helpful ‘push’, it was also, as they say here, ‘gezellig’ to have you in our group and to take the much-deserved day trip to Belgium.

To the KNICR group, Akvile, Andrea, Carolyn, Desi, Gerbrich, Hanan, Ilse, Koen, Laura, Marcus, Nikita, Philip, Raisa, Rosa, Sabine, Sander, Sandra --- What we’ve accomplished as such a small group is nothing short of remarkable. Over one thousand MRI scans as part of our ‘pilot’ study and now over four thousand more; easily the most impressive pediatric neuroimaging study in the world. But the great thing about this group isn’t just what we’ve accomplished, but also the amazing individuals who I’m humbled to call my friends. Marcus, we first met in Minnesota, and then again here in Rotterdam. Thanks for being not only an outstanding colleague, but also a good friend. You made my transition to life in Europe incredibly enjoyable and easy, and we miss you here! Hanan, I still recall a skype call with you and Marcus about FreeSurfer while I was in Minnesota...I had no clue a few years later I’d be your colleague here in Holland! You’re a fantastic colleague and friend, and I’m glad we’ll get to continue working together. Andrea, you are the person that everyone simply likes to be around; along with your contagious smile comes an incredibly bright, critically thinking, honest, and genuine person. I’m very much looking forward to your defense, and to another...contest. Even though you don’t play fair, I will still win! Sandra, though we learned that we both were intimidated by each other when we first met, this quickly faded and working together has been a true pleasure. I’m elated you’ve elected to stay in (imaging) research – not only did you quickly pick up the technical aspects needed to be successful in imaging research, but you also write beautifully and think critically.

While my research career has continued in Holland, it began in Minnesota with a group of amazing people: Monica Luciana, Bryon Mueller, Paul Collins, Jeff Wozniak, and Kelvin Lim. Though I love my life in Holland, it would be impossible to say that I don't miss working with you all. The content of this thesis without question benefited immensely from our interactions. Monica, you've been an incredible and inspirational mentor. Thank you for giving me the opportunity to work in your group, and for believing in me. Though it was my first 'real job', it never felt like 'work'. I was always learning, and it was a truly enjoyable experience working with you and the wonderful team you surround yourself with. Bryon, you've been a great mentor, colleague and friend. Even as a Cal-Tech physicist, you patiently helped this psychology undergrad learn about MR-physics and image processing. I'm very grateful our paths crossed. Paul, you are without a doubt one of the reasons working in Minnesota never felt like 'work'. Your jovial spirit makes science fun, and some of our greatest ideas came from the weekly imaging brainstorm sessions. The folks here in Rotterdam will recognize this, as I've tried my best to borrow this style and bring it with me to Holland. Kelvin, thank you for all of the opportunities you've provided me with, from starting in your group as an RA and helping with data collection, to presenting my work at a conference. I've learned a lot not only from you, but also the great LNPI group that you lead in Minnesota. Jeff, early on during my time in the LNPI, you helped guide me through the basics of data analysis and statistics. Thanks for joining me on the trip to Lexington for the undergraduate research conference, and for all of your help and advice. I'm grateful you included me on what turns out to be my very first scientific publication, and know without a doubt your guidance and insight helped prepare me for taking on this thesis.

Linda --- heel erg bedankt voor je echt leuke Nederlandse les. Je bent een van de aardigste mensen dat ik ken....echt een goed mens....en een toffe lerares. Ik kijk uit naar meer lessen met je in de toekomst. Excuses mijn Nederlands zo slecht is...dit is niet jouw schuld, maar omdat ik een luie student ben! Punya and Sungho, thanks for helping me find my way the first year in Holland! Lis, thank you for all of your support! To the "Zalmhaven" ladies, Adriana, Dina and Claudia --- Thanks for having me over for your delicious dinners, holiday parties, and just to chill. Adriana, Tenerife was a much needed, fun week away (vale, vale)!

To the GenR guys, Gerard, Gijs, Martijn, Philip, Ronald, Strahinja, Tim, Willem: It's been great having such fun and interesting colleagues. Work would not be as enjoyable as it is without the spirit you bring each day. The highlights are clear: the football table, Serbia, Oktoberfest, Efteling, BBQs, Onbeperkt Sparerib Avonds, Borrels, coffee breaks, and more. Thanks for being such great colleagues and friends. A special thanks to the 'kapsalon' crew, Philip, Ronald and Strahinja – it has been a huge support and a lot of fun having you guys around (Willem, if you had Whatsapp, you would be in this group). Looking forward to the next adventure.

To the amazing ‘kamergenooten’, Sabine Jolien, Hieab, Vincent, Tavia and Daniel, with whom I’ve spent the majority of my working hours with over the last four years. Sabine and Jolien, I couldn’t have asked for kinder, more helpful officemates my first two years here. Though my new home is in the Na building, I have extremely fond memories of AE005 with both of you. You helped me more than I can describe with my transition to life in Rotterdam, and with getting settled in Generation R. Navigating such a massive project without your experience and expertise would have been impossible. What’s even more special is that I made two incredible friends. Thank you for everything. Vincent, though it was only for a limited time, it was great sharing an office with you, and learning about the Rotterdam Study. We had numerous interesting scientific discussions, but also got side-tracked often with other equally interesting conversation. Daniel, though you’ve been away at Harvard for a while, I look forward to the perfect blend of fun and seriousness you bring to the office. Tavia, we already miss you! It’s been fun having another expat around, and I’m doing my best to make my accent a bit more proper (by copying yours, but clearly not going well). Thanks for the nice conversations, coffee breaks, borrels, Pathé nights and training sessions! Hieab, you are without question one of the most talented PhD students I have ever met, and I’m lucky to share an office with you. In addition to the scientific expertise you possess, you are an incredibly down-to-earth, kind, and genuine person. Thanks for all of the help and useful advice you continuously provide.

To my incredible friends back in Minnesota. Shane, Matt, Tracie, Travis, Colt, Frieda, Ana, Meg, and Emily. Thank you all for your continued support in my move away from home, and throughout this whole process. Your calls, texts emails, cards and visits to Europe have always come when I needed them the most, and gave me the extra push I needed to finish this thesis. Shane, thanks for everything and especially for traveling around Europe with me. Matt, thanks for all of the support over the years, and for making sure to keep in touch, even when I was busy and letting things slip.

Raisa, it was easy to see that we were going to get along from the beginning! Thank you for all of your support, encouragement, and advice (and for so patiently reading through this dreadful book). I’m lucky to have such a great friend, both at and away from the office. Also, thanks for showing me around the ‘disco’, and proving there are some decent hamburgers in Holland. Strahinja, I still remember your early days at the AE building, in particular when you commandeered a cup of tea Eirini just prepared! Thank you (and your incredible family and friends) for opening your home Serbia and showing us the wonderful country you come from. You are an all-around good person who I look up to and admire, and I’m grateful to have as a friend.

To the amazing people who agreed to join me as paranymphs on this special occasion: Eirini and Laura. Eirini, you have been with me at GenR from the start, and I'm grateful for all of your help, advice, and support, and most of all for your friendship. Your positive and caring attitude comes with you everyday, spreading to those around you. Laura, simply put, it's difficult to imagine getting through this without your help and support. From the first KNICR dinner at Sumo, all the way to today. Not only have you influenced the content and quality of this thesis immensely as a scientist, colleague and coauthor, you have also been an inspirational person outside of the office, and one of my closest friends. Thank you for everything. Though the clinical world will benefit greatly with you beginning your residency, the research world will be losing a valuable asset; I'm hopeful your talents will occupy both worlds eventually. Tenslotte van harte gefeliciteerd met je proefschrift, Lau! Het is echt gezellig dat we op dezelfde dag promoveren. We made it.

Lastly, to my incredible family, Mom, Dad, Kel, Kase and Tay. Thank you for supporting me from the beginning with this endeavor. Being so far away has been difficult at times – both for me in Holland and for you in the US – and I'm grateful for the love, support and patience you've given me these past four years while I experienced this new part of my life. You always help keep me focused on what is most important.

